Mediterranean Science Commission CIESM

An intergovernmental organization
- 23 Member states - promoting since 1910 research cooperations in the Mediterranean and Black Seas in the many sectors of oceanographic and coastal sciences as well as marine policy. Supported by a large pluridisciplinary network: more than 500 institutes and 10 000 researchers.

Une organisation intergouvernementale - 23 Etats membres - intervenant dans les domaines de la recherche océanographique pour favoriser les coopérations entre scientifiques ainsi qu'entre chercheurs et décideurs. Avec le concours d'un vaste réseau pluridisciplinaire : plus de 500 instituts spécialisés et de 10 000 chercheurs.

www.ciesm.org

** CIESM Workshop volumes have been published since 1997 as such under:*
- CIESM Workshop Series, n°1-18
- CIESM Workshop Monographs, n° 19-onward

The full list is available on our website as well as an order form.

*Already published **

*Déjà parus **

33
The Messinian Salinity Crisis from mega-deposits to microbiology - A consensus report
Almeria (Spain), 7-10 November 2007

34
Towards an integrated system of Mediterranean marine observatories
La Spezia (Italy), 16-19 January 2008

35
Climate warming and related changes in Mediterranean marine biota
Helgoland (Germany), 27-31 May 2008

36
Impacts of acidification on biological, chemical and physical systems in the Mediterranean and Black Seas
Menton (France), 1-4 October 2008

37
Economic valuation of natural coastal and marine ecosystems
Bodrum (Turkey), 22-25 October 2008

38
Dynamics of Mediterranean deep waters
Malta, 27-30 May 2009

39
Climate forcing and its impacts on the Black Sea marine biota
Trabzon (Turkey), 3-6 June 2009

40
Phytoplankton responses to Mediterranean environmental changes
Tunis (Tunisia), 7-10 October 2009

41
Marine Peace Parks in the Mediterranean - a CIESM proposal
Syracuse (Italy), 18-20 November 2010

42
Marine geo-hazards in the Mediterranean
Nicosia (Cyprus), 2-5 February 2011

43
Designing Med-SHIP: a Program for repeated oceanographic surveys
Supetar, Brac Island (Croatia), 11-14 May 2011

44
Molecular adaptations of marine microbial life to extreme environments - Mediterranean opportunities
Island of Samos (Greece), 12-15 October 2011

45
Marine extinctions - patterns and processes
Valencia (Spain), 10-13 October 2012

46
Marine litter in the Mediterranean and Black Seas
Tirana (Albania), 18-21 June 2014

47
Submarine canyon dynamics in the Mediterranean and tributary seas - An integrated geological, oceanographic and biological perspective
Sorrento (Italy), 15-18 April 2015

48
Marine connectivity - migration and larval dispersal
Sòller (Spain), 9-12 March 2016

49
Searching for bacterial pathogens in the Digital Ocean
Paris (France), 27-30 September 2017

50
Engaging marine scientists and fishers to share knowledge and perceptions - Early lessons
Paris (France), 18-21 April 2018

51
Marine heatwaves in the Mediterranean Sea and beyond -
Paris (France), 27-30 November 2023

CIESM WORKSHOP MONOGRAPHS

ISSN 1726-5886

52

Marine hazards, coastal vulnerability, risk (mis)perceptions – a Mediterranean perspective

The Mediterranean Science Commission

Cover: 19th century illustration of the earthquake and tsunami which destroyed Lisbon almost completely on 1st November 1755.

CIESM Workshop Monographs

Marine hazards, coastal vulnerability, risk (mis)perceptions – a Mediterranean perspective

CIESM Workshop Monographs ◊ 52.

This collection offers a broad range of titles in the marine sciences, with a particular focus on emerging issues. CIESM Monographs do not aim to present state-of-the-art reviews; they reflect the latest thinking of researchers gathered at CIESM invitation to assess existing knowledge, confront their hypotheses and perspectives, and to identify the most interesting paths for future action.

A collection founded and edited by Frédéric Briand.

CONTENTS

Marine hazards and coastal vulnerabilities in the Mediterranean – realities and misperceptions

[1] to be cited as: Chiocci F.L., Brückner H., Briand F., Bertoldo R., Urgeles R., Mohamed R.E., Međugorac I., Baptista M.A., Ozeren M.S., Mhammdi N., Monioudi I. and L. Pinheiro. 2024. Marine hazards and coastal vulnerabilities in the Mediterranean - realities and misperceptions. pp 5 – 26 In CIESM Monograph 52 [F. Briand, ed.] CIESM Publisher, Paris, Monaco, 182 p.

This article was first sketched during the course of an immersive CIESM Workshop that took place in Istanbul in early December 2023. Developed in the months thereafter on the basis of written exchanges among the participants, it carefully synthesises the main lessons derived from this stimulating exercise and serves as the opening chapter of volume 52 of the CIESM Monographs Series. The authors are grateful to Annelyse Gastaldi for carefully and patiently overseeing the physical production of the Monograph at CIESM headquarters.

1. BACKGROUND

The Mediterranean is the most geologically active maritime region of Europe, sitting on a complex tectonic boundary zone between the European and African plates, and hosting an array of environmental processes that give rise to marine geohazards. While the geology of the region – with the presence of plate boundaries and active faults – makes it prone to relatively frequent earthquakes, tsunamis and submarine landslides, climate change intensifies the frequency and impacts of storm surges and coastal flooding (IPCC 2023).

The Mediterranean Basin is also a densely populated region that operates within multiple national jurisdictions without much regional coordination, with a wide range of coastal and offshore infrastructure developments. Such a context makes Mediterranean shores particularly vulnerable to natural hazards, putting human lives and property at risk.

Curiously, despite a very long history of devastating events (see *Brückner 2024), most notably from tsunamis generated by earthquakes, volcanic eruptions or submarine landslides, the impacts of marine geohazards remain widely underestimated in the Mediterranean. Yet seafloor ruptures due to recent faults, active volcanoes, landslides on steep continental slopes, retrogressive erosion at submarine canyon heads are common features along the Levantine, Aegean, Ionian, Tyrrhenian, Ligurian shores (*Chiocci 2024; *Urgeles 2024) – a coastal landscape complicated by increasingly severe storm surges and river flooding from the hinterland (*Međugorac and Pasarić 2024).

While local communities have learned from the past to build resilience in an environment to which they have adapted over generations (*Bertoldo 2024), this delicate balance is now threatened by significant demographic and economic pressures. The intense coastal urbanization, growing maritime traffic, unceasing touristic developments are of particular concern: they do lead to significant, lasting changes in the coastline such as accelerated coastal erosion that require urgent but adapted management measures (*Mohamed 2024).

**the asterisk refers to a distinct chapter in this Monograph*

According to the IPCC 2021 scenarios, accelerated sea-level rise and more frequent storminess, both projected to increase in the future, are now the main drivers of coastal erosion and flooding of low-lying coastal areas. In densely populated coastal areas, groundwater extraction, sediment compaction and land subsidence due to infrastructure construction do constitute additional threats.

Box 1: Definitions of key terms

HAZARD[1]: A process, phenomenon or human activity that, in a given span of time, may cause loss of life, injury or other health impacts, property damage, social and economic disruption or environmental degradation. Hazards may be natural, anthropogenic or socionatural in origin. 'Natech' qualifies a natural hazard whose effect is amplified by technological infrastructures (e.g., flooding of power and chemical plant).

RISK[2]: The natural scientific and actuarial concept of risk is based on the coupling of natural hazard and vulnerability in the form "risk = hazard x vulnerability x exposure". Accordingly, risk is understood as the probability of damage to vulnerable people and their property (fatalities, injuries, property damage, economic losses, environmental damage) resulting from an event.

DISASTER[1]: A serious disruption of the functioning of a community or a society at any scale due to hazardous events interacting with conditions of exposure, vulnerability and capacity, leading to one or more of the following: human, material, economic and environmental losses and impacts. Annotation: the effect of the disaster can be immediate and localized, but is often widespread and could last for a long period of time.

DISASTER RISK[1]: The potential loss of life, injury, or destroyed or damaged assets which could occur to a system, society or a community in a specific period of time, determined probabilistically as a function of hazard, exposure, vulnerability and capacity. Annotation: the definition of disaster risk reflects the concept of hazardous events and disasters as the outcome of continuously present conditions of risk.

NATURAL CATASTROPHE[2]: A serious disruption and severe change in the activities, tasks and objectives of a society due to the actual occurrence of an 'extreme' natural process. The effects lead to extensive material, economic or environmental damage with massive social consequences. The decisive factor in natural catastrophes is that the affected society is no longer able to overcome the crisis with its own resources and outside help is required. The term 'extreme' refers of course only to the human viewpoint.

VULNERABILITY[1]: The conditions determined by physical, social, economic and environmental factors or processes which define the susceptibility of an individual, a community, assets or systems to the impacts of hazards.

N.B. A natural hazard can be differentiated according to the following factors: frequency (temporal frequency, low-high), magnitude (mass or energy transfer, low-high), duration (short-long), spatial extent (limited-large), speed of process build-up (slow-fast), spatial distribution (distribution pattern, punctual-diffuse), and temporal variation (cyclical-stochastic).

[1] Source: UNDRR - United Nations Office for Disaster Risk Reduction, https://www.undrr.org/terminology (accessed: 12 Jan 2024)

[2] Source: Dikau *et al.* 2009

2. THE MEDITERRANEAN CONTEXT OF GEOHAZARDS

As expressed in Figure 1, the active geology and the high density of coastal human settlements and infrastructures make the Mediterranean region very vulnerable to marine geohazards. No surprise then if this semi-enclosed basin has the longest historical record of devastating events linked to earthquakes, tsunamis, eruptions and submarine landslides.

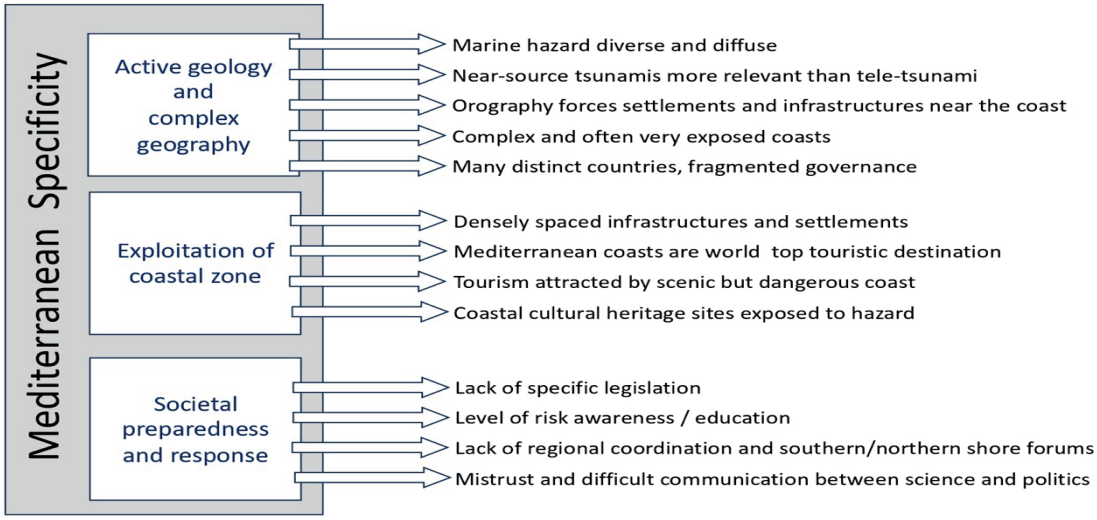

Figure 1. Main markers of marine geohazards in the Mediterranean region.

2.1. Geology and geomorphology

Given its very active geodynamic setting, the Mediterranean region is characterized by high seismicity, volcanism, tectonic seafloor deformation and uplift, plus a range of seafloor sedimentary processes that over historical timescales have repeatedly demonstrated their capacity to generate catastrophic marine events.

Seismicity and volcanism have well-known direct consequences on land and are equally devastating offshore, where they may easily trigger slope failures. In the oceanic domain, these failures may take place on negligible slopes (<1˚) and affect vast seabed areas; moreover, they usually retrograde upslope to affect the coastal zone. In addition, rapid seafloor deformation, induced by faulting, volcanic activity and/or slope failure may generate tsunami waves, which can travel great distances and have catastrophic consequences for coastal zones (e.g. the 1908 events in the Messina Strait that together caused over 70,000 casualties). Most tsunamis in the Mediterranean are triggered by earthquakes, submarine landslides, volcanic eruptions and the collapse of coastal cliffs or volcanic flanks (see *Chiocci 2024; *Urgeles 2024; *Brückner 2024). After the Pacific Ocean, the Mediterranean constitutes the second highest source of tsunamis in the world, with 98 large tsunamis observed in historical times. Every century on average a tsunami of disastrous proportions takes place in the Mediterranean Sea (Papadopoulos 2016). Smaller tsunamis such as those generated by landslides are common and often escape historical reports: such is the case of Stromboli (one of many small Mediterranean islands) where recent analyses point to several tsunamis over the 20th century (Maramai *et al.* 2005). On a longer time scale, sedimentary records indicate that the Mediterranean region has experienced many large catastrophic events involving tsunamis, volcanism, and cliff failures (Papadopoulos *et al.* 2014; Urgeles and Camerlinghi 2013).

While seismicity is widespread in the Mediterranean region, the eastern Mediterranean and in particular the Aegean and Marmara seas are most active in that regard (for details see the map in *Brückner 2024 which illustrates the historical distribution of significant earthquake-triggered tsunamis in the broad Mediterranean Basin).

2.2. Marine climate and oceanography

The Mediterranean Sea generally has a mild climate, though marked winter storms often occur. The maximum recorded significant wave height reaches 10 m, with estimates suggesting even larger values for some undocumented storms. The winter mean significant wave height ranges from approximately 0.8 to 2 m, with the Gulf of Lion in the Western Mediterranean experiencing the largest values (Cavaleri 2005). Wave dynamics in the Mediterranean is primarily influenced by regional orographic conformation and fetch (Lionello and Sanna 2005). Tidal currents are only significant near major passages (e.g., Strait of Gibraltar, Sicily Channel), some smaller passages (e.g., Strait of Messina) and in the Adriatic Sea (Janeković and Kuzmić 2005). Elsewhere, tidal currents are generally just a few mm per second (Albérola *et al.* 1995). Tidal amplitude rarely exceeds 0.5 m, except in the Gulf of Gabes (up to 1.5 m) and in the northern Adriatic (~0.6 m) due to the interaction of tidal wave and bathymetry (Tsimplis *et al*. 1995).
The semi-enclosed Mediterranean Sea is characterized by evaporation exceeding precipitation and river runoff (Millot and Taupier-Letage 2005a). This imbalance causes a difference in water level between the Mediterranean Sea and the Atlantic Ocean, leading to a surface inflow of Atlantic Water into the Mediterranean. The incoming Atlantic Water is continuously modified through interactions with the atmosphere and mixing with older surface Atlantic Water and underlying waters. Sinking and deep-water formation occur in specific zones, typically in the northern parts of the basins, where deep dense water convection takes place. Due to the Coriolis Effect, waters circulating at basin scale (at all depths) tend to follow the isobaths corresponding to their density level in a counterclockwise direction (Millot and Taupier-Letage 2005b). On the northern Mediterranean continental shelves (e.g., Gulf of Lion, northern Adriatic, northern Aegean), waters are significantly cooled during winter as the reduced depth limits heat retention. Despite the buoyancy increase from freshwater inputs via river runoff, dense waters are generated on these northern shelves. These dense waters travel along the shelf and cascade to greater depths, primarily through submarine canyons, until they reach their density equilibrium level (Durrieu de Madron *et al.* 2005).

2.3. Coastal / island populations at risk

According to the records kept by the UN Office for Disaster Risk Reduction (see CRED / UNISDR 2020), human fatalities and serious injuries due to geophysical events (mostly earthquakes and associated tsunamis), or to climate-related disasters (mostly storms, floods, droughts) are now counted in millions every year, while economic losses reach billions of dollars. The Mediterranean population, which lives for a large part in coastal areas at increasing risk of flooding from storm surges, high river discharge, or even tsunamis, is obviously concerned (see Vousdoukas *et al*. 2017).

The Mediterranean region boasts 46,000 km of densely populated shores. At the crossroad of three continents, Mediterranean trade and demographic trends drive increased maritime transport, leading to heightened use of harbors, coastal facilities, and associated developments.

With a rich, long history of human settlement, the region is dotted with numerous coastal towns and villages, and some 200 inhabited islands, together home to almost 9 million islanders.
By recent estimates, in the Mediterranean Basin some 100 million people live close to the coast all year around - a number that is at least multiplied by four in the summer months as the Mediterranean remains the world' largest tourist destination. During the summer season, crowded beaches, cruise liners, and private yachts are ubiquitous along the shores. In 2019, just prior to the Covid pandemic, the Mediterranean region received 386 million international tourist arrivals according to UNWTO- the World Tourism Organization. More recent numbers indicate a return to pre-pandemic levels, with continuing increases driven by improved travel infrastructure and a growing middle class.

2.4. Infrastructures at risk

Coastal zones are prime areas for the development of civil infrastructure and large industrial plants in need of maritime access and cooling water. In regions where mountain ranges meet the sea, transport infrastructure like railways, highways, and even airports are often constructed close to the coast. In addition, the region hosts a variety of offshore industries, leading to a growing number of seafloor installations from coastal areas to deep waters. The expansion of trade between Europe, Asia, and Africa causes increasing maritime traffic in the Mediterranean Sea. This maritime transport necessitates secure routes, harbors and associated coastal infrastructure such as shipyards, maritime terminals, storage facilities, piers and jetties.

As of 2010, almost 65,000 km of submarine cables were operational in the Mediterranean Sea. While fiber optic cables exchange data among countries and continents, power cables transfer electricity from the mainland to islands like Sardinia, Corsica, and Mallorca, and connect Albania to Italy. Long distance pipelines also connect different Mediterranean shores. They are all vulnerable to undersea earthquakes and to submarine landslides that can break or damage them.

The offshore exploration of mineral resources on or below the sea floor is another cause for concern. The Mediterranean offshore hydrocarbon production contributes nearly 5% of global oil reserves. While current production and development contracts cover only 1% of the Mediterranean sea bottom - mainly concentrated in the Adriatic Sea, Sicily Channel, Nile Delta, and off Cyprus - oil and gas exploration contracts encompass 23% of the sea floor, and areas designated by governments as open for tenders add another 21%.

Field tests in the Mediterranean Sea, specifically in the Tyrrhenian and Aegean seas, have investigated ore-bearing deposits from submarine volcanic activity. Additionally, marine aggregate extraction on continental shelves is increasing, particularly for relict sand deposits used in beach nourishment for retreating coasts.

2.5. A vulnerable cultural heritage

The Mediterranean is one of the few regions in the world with a long and continuous historical/ geographical record, that has been documented since ancient times by prominent authors such as Herodotus, Strabo and Pliny the Elder. From an historical perspective, a major, long-term natural hazard that led to the demise of many former ports (Ephesus, Carthage, Ostia antica) is siltation (*Brückner 2024). In most cases their fate was sealed when the delta of the river

bypassed them and the harbours silted up. Despite desperate attempts not to lose contact with the sea, the harbours had to be abandoned in the end.
Now that sea levels are rising at a rate faster than in the 20th century and that changing weather patterns enhance the probability of coastal flooding (Bevacqua *et al.* 2020) and extreme wave events (Meucci *et al.* 2020), growing attention is given to the near-term fate of coastal cities dating from the Greek and Roman empires, often located within a few meters of the current coastline.

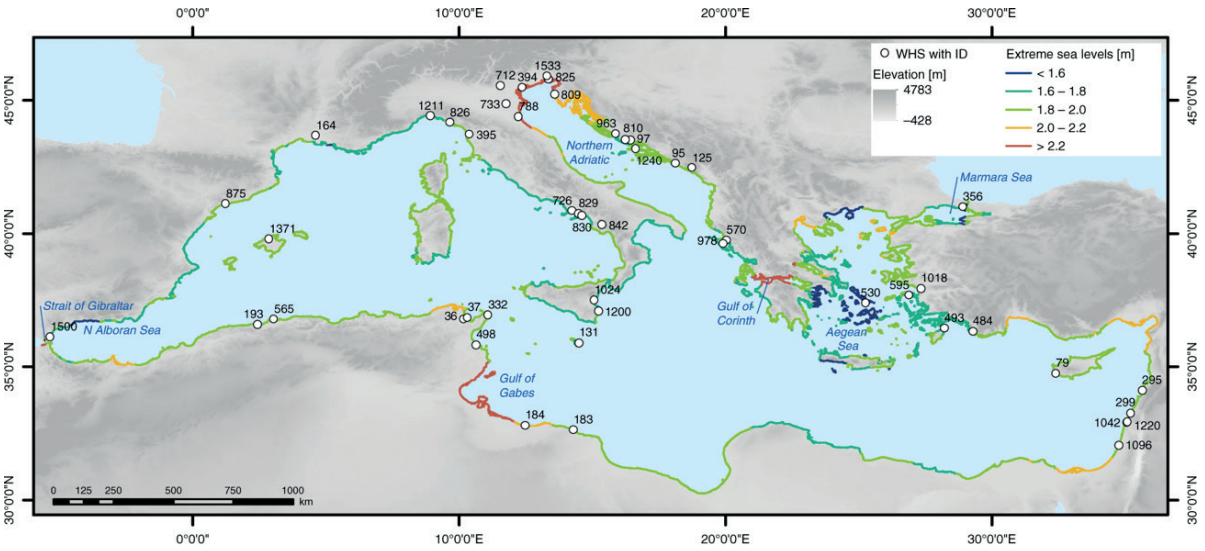

36	Medina of Tunis	493	Medieval City of Rhodes	842	Cilento and Vallo di Diano National Park with the Archeological Sites of Paestum and Velia, and the Certosa di Padula
37	Archaeological Site of Carthage	498	Medina of Sousse	875	Archaeological Ensemble of Tárraco
79	Paphos	530	Delos	963	The Cathedral of St James in Šibenik
95	Old City of Dubrovnik	565	Kasbah of Algiers	978	Old Town of Corfu
97	Historical Complex of Split with the Palace of Diocletian	570	Butrint	1018	Ephesus
125	Natural and Culturo-Historical Region of Kotor	595	Pythagoreion and Heraion of Samos	1024	Late Baroque Towns of the Val di Noto (South -Eastern Sicily)
131	City of Valletta	712	City of Vicenza and the Palladian Villas of the Veneto	1042	Old City of Acre
164	Arles, Roman and Romanesque Monuments	726	Historic Centre of Naples	1096	White City of Tel-Aviv --the Modern Movement
183	Archaeological Site of Leptis Magna	733	Ferrara, City of the Renaissance, and its Po Delta	1200	Syracuse and the Rocky Necropolis of Pantalica
184	Archaeological Site of Sabratha	788	Early Christian Monuments of Ravenna	1211	Genoa: Le Strade Nuove and the system of the Palazzi dei Rolli
193	Tipasa	809	Episcopal Complex of the Euphrasian Basilica in the Historic Centre of Poreč	1220	Bahá'í Holy Places in Haifa and the Western Galilee
295	Byblos	810	Historic City of Trogir	1240	Stari Grad Plain
299	Tyre	825	Archaeological Area and the Patriarchal Basilica of Aqui leia	1371	Cultural Landscape of the Serra de Tramuntana
332	Punic Town of Kerkuane and its Necropolis	826	Portovenere, Cinque Terre, and the Islands (Palmaria, Tino and Tinetto)	1500	Gorham's Cave Complex
356	Historic Areas of Istanbul	829	Archaeological Areas of Pompei, Herculaneum and Torre Annunziata	1533	Venetian Works of Defence between 15th and 17th centuries: Stato da Terra – western Stato da Mar
394	Venice and its Lagoon	830	Costiera Amalfitana		
395	Piazza del Duomo, Pisa				
484	Xanthos-Letoon				

Figure 2. UNESCO cultural World Heritage sites located in the Mediterranean Low Elevation Coastal Zone. All 49 sites are shown with their official UNESCO ID and name. The map shows extreme sea levels per coastal segment under the high-end sea-level rise scenario in 2100. [source: Reimann *et al*. 2018]

Mediterranean shores host many sites considered of 'outstanding universal value' that are listed by UNESCO as World Heritage Sites (WHS). A number of them (49) – mapped on Figure 2 - are situated in the Low Elevation Coastal Zone, with limited protection from rising sea level and flooding hazards. Out of this total, under current conditions (base year 2000), 37 Mediterranean WHS are projected in coming decades to be at risk from flooding - defined as the 100-year storm surge (including tides) - while 42 WHS face a risk of erosion in view of their close proximity to the coastline and of the nature of the sediments (Reimann *et al*. 2018). In the same vein a future scenario integrating projected rises in sea level and increases in storm surges based on IPCC 2021 has been developed for the city of Ampurias - founded around 575 BC by Greeks in what is now northern Catalonia (see *Brückner 2024).

2.6. A fragmented governance

Mediterranean countries display much cultural, linguistic heterogeneity, plus a high level of administrative fragmentation. As a result, communication among neighboring governments, public authorities, industry and research is rarely fluid, with a notable lack of collaboration. For instance, administrative responsibilities for the marine environment are usually divided between regional and national agencies, and often fragmented among various ministries. This division of competencies, compounded by a difficult dialogue between scientists and political level (Briand 2012), unavoidably leads to inefficiencies and difficulties in addressing marine issues comprehensively.

3. GEOHAZARD FREQUENCY vs MAGNITUDE – AN INVERSE RELATION

There is typically an inverse relation between the frequency and the magnitude of geohazards. Thus, events of low intensity (such as minor earthquakes, small landslides, low-level flooding) occur more frequently. For example, small earthquakes can happen hundreds of times a year in a given region. Conversely major earthquakes, large tsunamis, volcanic eruptions occur far less frequently. Understanding this relation is fundamental for risk assessment and preparedness planning, given that rare events will often have catastrophic impacts and that minor but frequent events can have cumulative effects comparable in certain cases to those of major events.

Earthquakes are relatively frequent events in the Mediterranean region (see Fig. 3). They rank among the most damaging geohazards, frequently causing large losses of lives, assets and infrastructure. A most destructive one was the Crete earthquake, with Mw>8, of AD 365 (Ott *et al*. 2021; Shaw *et al*. 2008) which raised the western part of the island by up to 9 m, uplifted and drained the port of Falasarna, and caused a mega-tsunami that destroyed many harbors in the eastern sub-basin. Earthquakes in the Mediterranean region occur not only in compressional settings, but also in extensional settings (e.g., the Gulf of Corinth - one of the fastest spreading rifts in the world) and strike slip settings, with extraordinary evidence of neo-tectonic activity and fluid expulsion at the seafloor in the Marmara Sea (Tryon *et al.* 2012).

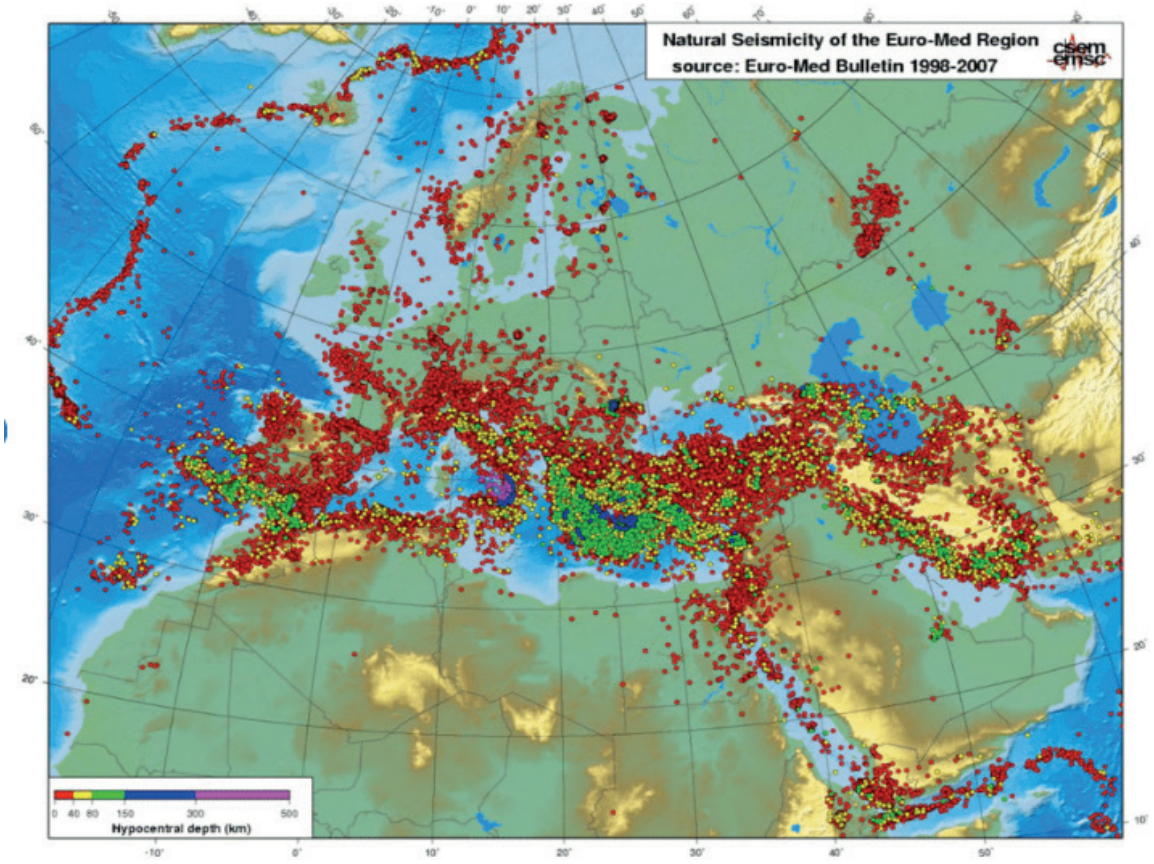

Figure 3. Seismicity in the Mediterranean and adjacent regions (1998-2007). Source: Euro-Med Bulletin.

Submarine landslides do occur in the Mediterranean Sea on magnitude-scales ranging from several 100 km^3 to a few 100 m^3, despite large observational bias towards the smaller events (*Urgeles 2024). Their frequency may vary from several thousand years to a few years respectively. Recent examples of submarine landslides in the Mediterranean Sea, with cascading effects in the form of tsunamis, include the 1954 Algerian margin event (El-Robrini *et al.* 1985), the 1979 event off Nice (Ioualalen *et al*. 2010; Dan *et al*. 2007), the 1977 event at Gioia Tauro (Colantoni *et al.* 1992) and the Stromboli collapse of 2002 (Fornaciai *et al.* 2019; Chiocci *et al*. 2008). None of these landslides exceeded 0.2 km^3 and they can be considered relatively frequent. Much larger events are found in the late Quaternary record.

Volcanic eruptions are not uncommon in the Mediterranean region and have left their mark in historical and archaeological records. The largest include the Thera eruption around 1600 BC, the 217 BC Vesuvius, 44 BC Etna, AD 79 and AD 472 Vesuvius (Stothers and Rampino 1983). Multiple tephra layers have been identified earlier in the upper Quaternary sequence of deep-sea cores from the eastern Mediterranean. These tephra layers appear to be correlated with major source volcanoes such as the Somma-Vesuvius, the Phlegraean Fields, Ischia, Pantelleria, the Aeolian Islands, Mount Etna, and the Aegean arc (Keller *et al.* 1978). The Phlegraean Fields in particular, located near Naples, constitute one of the most significant volcanic systems in the world, with massive eruptions that seem to recur at rates of 10-15 kyrs/event (Sawyer *et al.*

2023), causing widespread devastation and changes to the landscape. In the same sub-basin, volcanoes like Mt. Etna and Stromboli are considered in a state of permanent activity, with frequent eruptions and lava emissions (see Barberi *et al*. 1993) through the past 1500 years.

Tsunamis are usually triggered by earthquakes, volcanic eruptions and submarine landslides (see *Chiocci *et al*. 2024; *Urgeles *et al.* 2024). The zone where the African plate subducts beneath the Eurasian plate, especially near the Hellenic Arc, is a frequent source (Sørensen *et al*. 2012; Tinti *et al*. 2001). The Mediterranean region has experienced several catastrophic tsunamis in the past 2500 years, most of them generated by strong earthquakes (Papadopoulos and Fokaefs 2005). Documented historical examples include the 365 and 1303 tsunamis caused by earthquakes in the Hellenic Arc, and the disastrous 1908 event that destroyed the cities of Messina and Reggio Calabria. Other devastating events occurred in 373 BC and 1748 in the Gulf of Corinth. More recently destructive tsunamis have occurred in the Aegean Sea in 1956 with runup heights reaching 25 m (Papazachos *et al.* 1985) and off the Algerian margin in 2003 (Alasset *et al.* 2006).
There are historical examples of landslide-generated tsunamis in the Mediterranean Sea such as the 1783 Scilla tsunami in the Messina strait (Wang *et al.* 2019; Mazzanti and Bozzano 2011) or, more recently, the 1954 Algerian margin event (El-Robrini *et al.* 1985), the 1979 event off Nice (Ioualalen *et al.* 2010) and the Stromboli collapse of December 2002 (Fornaciai *et al.* 2019). Large tsunamis can also be generated by caldera-forming volcanic eruptions, such as the massive tsunami caused by the eruption of Thera (Santorini) volcano in the southern Aegean Sea around 1600 BC (Friedrich *et al.* 2006) which is widely cited (see Soloviev 1990) as ultimately driving the destruction of the Minoan civilization.

Storm surges, caused by air pressure gradient and wind forcing, may last from several hours to several days. They are more likely to occur in regions with wide continental shelves where winds play a major role in their formation (Toomey *et al.* 2022), and in areas with an extended fetch where wind can considerably build up. In the Mediterranean, they are a major contributor to coastal sea-level extremes, with frequent occurrences along the northern Adriatic, the Aegean coasts and in the Gulf of Gabes (Cid *et al*. 2016; Pérez Gómez *et al*. 2022). There are historical, famous examples of storms which determined the course of naval battles, such as the confrontation between the Persian and Greek fleets in 480 BC, when two storms largely destroyed the Persian fleet (Herodotus 8.1-39).
Other sectors of the Mediterranean coast are less prone to storm surges, but certain areas with low-laying terrain (e.g., the Nile Delta in Egypt, the Ebro Delta in Spain; Hereher 2015; Grases *et al.* 2020) are vulnerable to high flood risk during extreme events. In the northern Adriatic, where storm surges can be superimposed on other sea-level processes, total sea levels can be particularly pronounced, up to nearly 2 m (Marcos *et al*. 2009; Lionello *et al*. 2021).

Meteotsunamis generate waves that can travel at high speeds due to high frequency atmospheric disturbances but are limited to shallower water bodies than standard tsunamis. This phenomenon can be quite sudden, often with little warning, occurring unfrequently (ca. once in a decade) and at specific sites, notably on the eastern Adriatic coast (see Šepić and Orlić 2024). They are localized events that typically arise during the summer months due to specific resonance conditions which involve the coupling of atmospheric forcing with the geomorphological properties of certain bays and harbors. They last from several minutes to an hour, and their amplitudes can attain several meters (Vilibić *et al.* 2021). From 23 to 27 June 2014 a series of meteotsunami waves of long period, up to 2-3 m high, generated by intense small-scale air pressure disturbances and propagating eastward, caused considerable damage from the

Balearic Islands to Odessa (Šepić *et al*. 2015). That was the first documented case of a chain of destructive meteorological tsunamis occurring over a distance of thousands of kilometres. Mediterranean meteotsunamis are events out of the ordinary, at least enough to receive local names- *rissaga* (Balearic Islands), *marrobbio/ marrubbio* (Strait of Sicily), *milghuba* (Maltese Islands), and *šćiga/ štiga* (Adriatic Sea).

Coastal erosion is a significant concern in the Mediterranean Basin, carrying large economic costs. It is the outcome of continuous, complex interactions between natural processes and human activities. Natural processes encompass local conditions (topography, wave dynamics), shoreline dynamics driven by long-term hydrodynamic and geological factors (e.g., loosely consolidated substratum), shoreline retreat due to relative sea-level rise, and episodic erosion during more frequent storms (Pang *et al.* 2023) with intense wind-wave action and higher sediment instability. Human activities (such as construction of harbors, recurrent dredging operations in port areas, coastal infrastructures like seawalls and jetties, flood control works, sand mining) will often disrupt the delivery of sand to the coast and contribute to beach erosion, especially in low-lying, flat coastal areas. Furthermore, all Mediterranean deltas are 'undernourished' and therefore impacted by erosion, as the river sediment is trapped in reservoirs while the river water is extracted for human purposes (drinking water, irrigation of fields).

4. FROM RISK PERCEPTION TO PREPAREDNESS

Risk is mainly the possibility that a hazard is made real. Individuals alone or in communities can shape how they view these possibilities to be able to go about their lives. Risk preparedness is a function of knowledge, experience and perception of such events. As one of the regions with high geohazard potential and most exposed to global warming, with a forecast rise in temperature of 2-3°C by 2050, the Mediterranean Basin is projected to experience an unparallel increase in the frequency of extreme weather events (Vousdoukas *et al.* 2017). An open, important question is whether Mediterranean populations are aware of such imminent risks.

Over generations Mediterranean communities have dealt with painful memories of catastrophic events which still nourish social memories, instead of being forgotten. These social memories contribute to communities' resilience, through increased risk perception and adaptation.

4.1. The memory loss of catastrophic events

In the aftermath of a major natural disaster, the memory of the horror gradually fades and other aspects come to the fore. This applies as well to coastal disasters in the Mediterranean. Take the island of Santorini that is thriving with people today and ranks as a major touristic destination, despite the devastating 'Minoan' eruption around 1600 BC that blew up most of the Thera volcano. Or the Crete earthquake in AD 365 when the tsunami waves that followed destroyed many harbors and coastlines in the eastern Mediterranean. The areas were soon resettled and nowadays hundreds of thousands of tourists enjoy the Cretan beaches every year.

Eruptions of Mt. Vesuvius have been reported on several occasions throughout history, with a major one in 1944 during WWII. The most famous no doubt is that of AD 79 which entirely destroyed the wealthy towns of Pompeii and Herculaneum and passed on to posterity through the letters of Pliny the Younger who lost his illustrious uncle in the tragedy. Yet, despite the destruction and large loss of lives, people later returned to the area and resettled the flanks of the

volcano, attracted by the favourable conditions for agriculture. Eventually human memory lost track of the massive eruption and it was not until many centuries later that the well-preserved ruins of Pompei were 'rediscovered' fortuitously under thick layers of ashes and soil by a farmer in the late 16th century.

4.2. Social perception of hazards

Cultures around the Mediterranean deal differently with social memories of past disasters (see *Bertoldo 2024). While some cultures deal with the anxiety created by past events by remembering and planning, others are more comfortable with collective efforts to 'forget'. When public management downplays the possibility of a catastrophic event despite the local knowledge of a risk, a number of studies have described signs of collective anxiety and fatalism (Joffe *et al*. 2013).

It is of course important to make a distinction between low impact / high frequency risks such as storms – that tend to be 'normalized' (see Luís *et al.* 2016) – and risks with high impact / low frequency as tsunamis – which tend to be amplified in social memory.

Therefore, the preservation of social memory - through memorial sites, celebrations, teaching and informative risk awareness sessions - fills an important role in keeping alive risk perception and, at the same time, it reassures communities that they can cope with these risks if/ when they will be hit again.

The societal acceptance of natural hazards and, most importantly, the degree of human preparedness will be much enhanced as more is known about them, about their mechanisms, about their effects on landscapes and societies, and as more is shared among local communities. As a result, information transfer will be optimised and the risk management strategies will be better understood and accepted (Ivčević *et al*. 2021).

As a collective exercise, the workshop participants compared their perceptions of a variety of coastal hazards – from rare to recurrent – that were discussed during the course of this workshop. The subjective outcome, purely qualitative, is illustrated in Figure 4, in the form of a 3-D diagram and in Figures 5A and 5B, as 2-D diagrams, where geohazards are positioned as a function of their recurrence, perceived level of economic destruction, and their degree of public recognition/ perception.

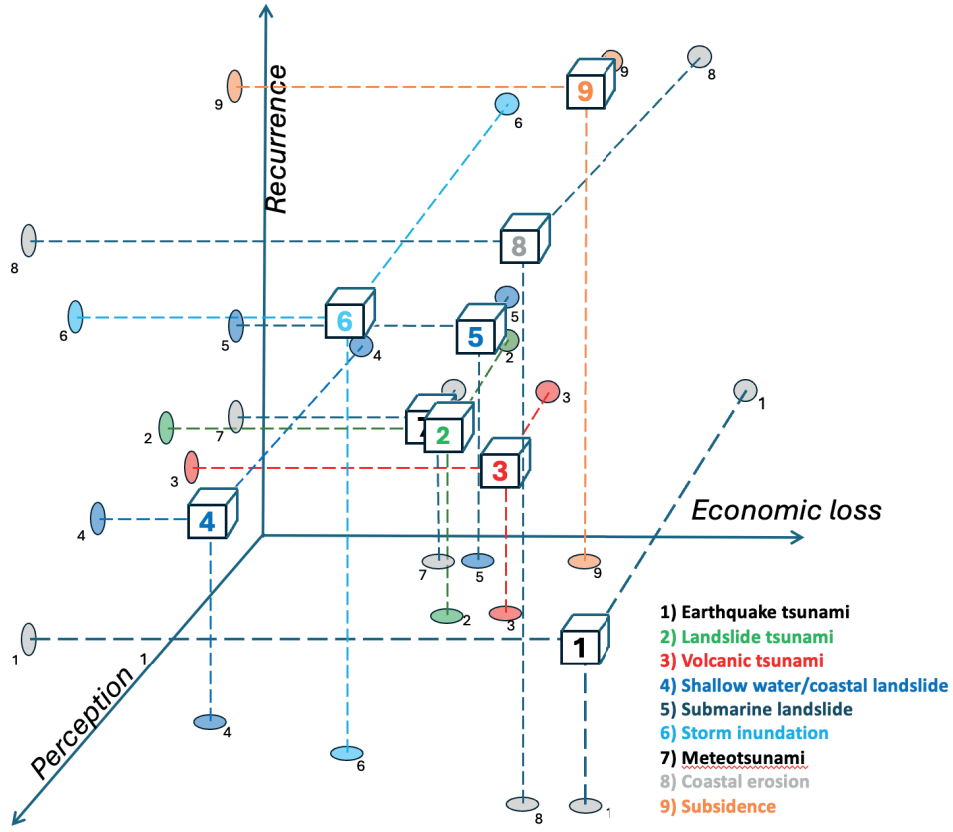

Figure 4. Level of perception of coastal geohazards, their economic impact, their frequency in 3D

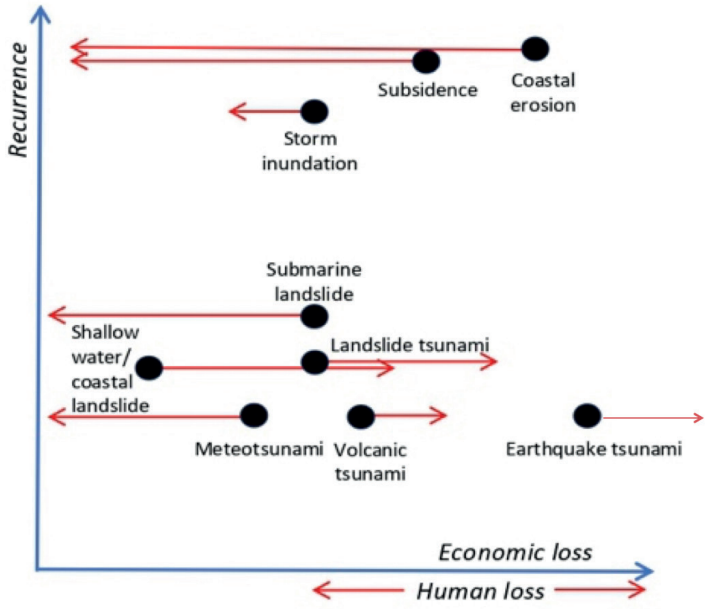

Figure 5A. XY diagram of Figure 4, which indicates the economic loss generated by geohazards of different frequency/ magnitude. The red arrows signal how the "damage" increases or decreases when human loss, instead of economic loss, is taken into account.

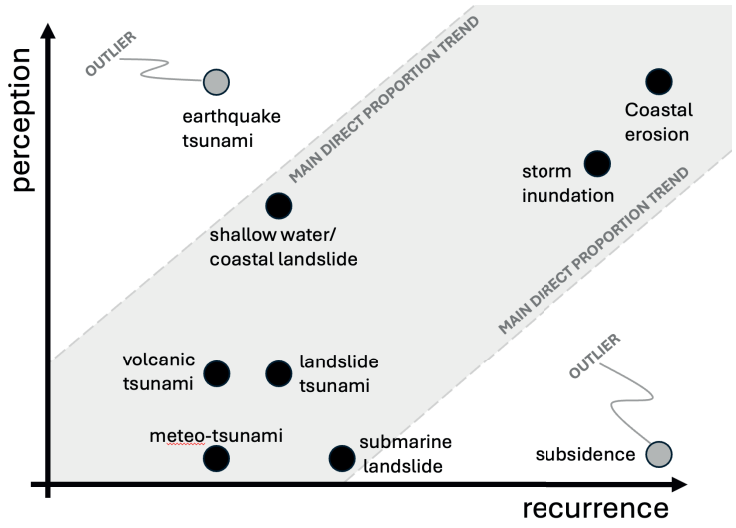

Figure 5B. YZ diagram of Figure 4, which illustrates the general relation between the level of perception of geohazards and their frequency.

The direct increase (shaded area) between perception and recurrence is not unexpected as the most frequent hazards are more easily recognized than rare ones, but there are two interesting outliers. The first is subsidence: while very frequent (in deltas, coastal plains, etc.), subsidence remains broadly ignored even if it drives coastal erosion, salinization of groundwater, and high risks for infrastructures. The other outlier - tsunami generated by earthquake – benefits from a high global recognition although it is a very rare event. Millions of people worldwide have seen on television the catastrophic images of the 2004 Indian Ocean tsunami and of the 2011 Tōhoku tsunami that devastated the eastern coast of Japan and the Fukushima nuclear plant.

4.3. Management / mitigation of coastal hazards

Distinct human societies face diverse risks and will not necessarily have the same level of local awareness about the potential natural disasters confronting them. But all deserve to receive the best possible information. The 2004 Indian Ocean tsunami suddenly raised awareness of the possibility of tsunamis in several Mediterranean countries. Countries with high seismicity, such as Greece and Turkey, were particularly alarmed. Subsequently tsunami warning signs and designated evacuation routes (see Figure 6) were erected in a number of vulnerable locations. But local tsunamis can also be triggered by submarine landslides, or collapses of volcano flanks which are much more difficult to foresee.

Figure 6. Tsunami warning signs: left in Stromboli Island (source: https://www.esvaso.it) - right : at a gate of the old city wall in Istanbul Fatih District (source: H. Brückner)

We have days of warning before a major storm surge, and so we can prepare and evacuate. Even volcanic eruptions have warning signs at least a few hours or even days in advance. Further, social media and mobile phone applications can relay such alerts fast and wide.

However, the same cannot be said for earthquakes and the tsunamis they may generate. We know that the Hellenic Arc and the North Anatolian Fault Zone can become active at any time, with devastating consequences. Cliff collapses and submarine landslides can also happen quickly. Even if a well-functioning early warning system were in place, the time required for tsunami waves to hit Mediterranean coasts would be short – in all cases less than one hour, and often much less.

On the other hand, there is a variety of solutions available to mitigate the effects of the anticipated sea-level rise and protect residents and socioeconomic activities in vulnerable coastal areas. They range, as seen in Figure 7, from coastline retreat, accommodation, advances into the sea, coastal protection, to ecosystem-based adaptation. The most appropriate strategy will depend of the local social and legal context which is often challenging.

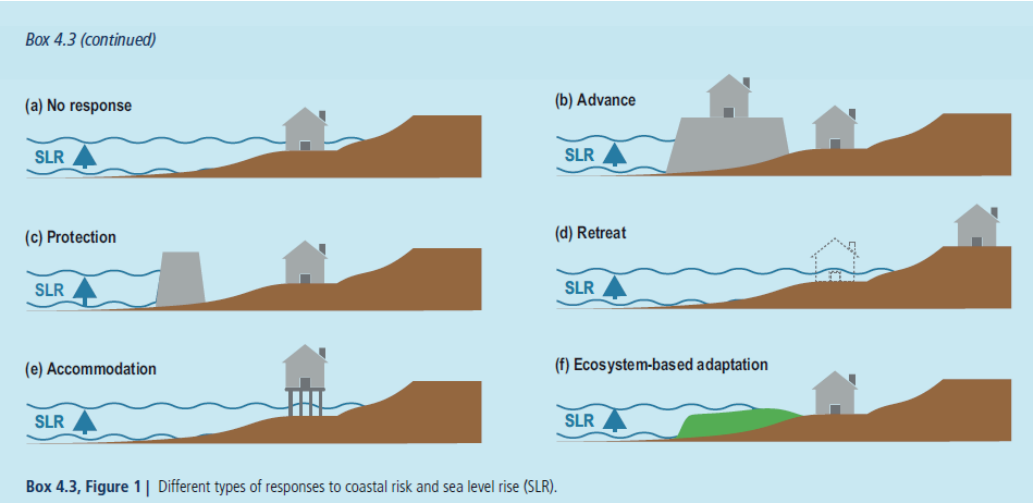

Figure 7. The various responses to risks associated with sea level rise. [Source: IPCC 2019]

When the *retreat option* is chosen, the coastal area does not receive marine protection. In the worst-case scenario, an entire coastal region can be destroyed. In highly populated areas hosting a range of socioeconomic activities, retreat is not an option and *accommodation* measures need to be implemented so as to reduce coastal risk and impacts on the residents, human activities, ecosystems, and the built-in environment. Measures will include building codes, elevation changes, land use changes, and institutional responses like Emergency Warning Systems, insurance schemes, and setback zones. Under the *protection option*, combined hard and soft stabilization measures are implemented: the shoreline is protected from the sea by the construction of solid structures including rock revetments, sea walls, and breakwaters, and dunes are used as soft solutions to stabilize the coast. The *ecosystem-based option* reduces coastal risks by creating new land by building seaward, reducing coastal risks. This includes land reclamation, landfilling, planting vegetation, and polarization, requiring drainage and pumping systems.

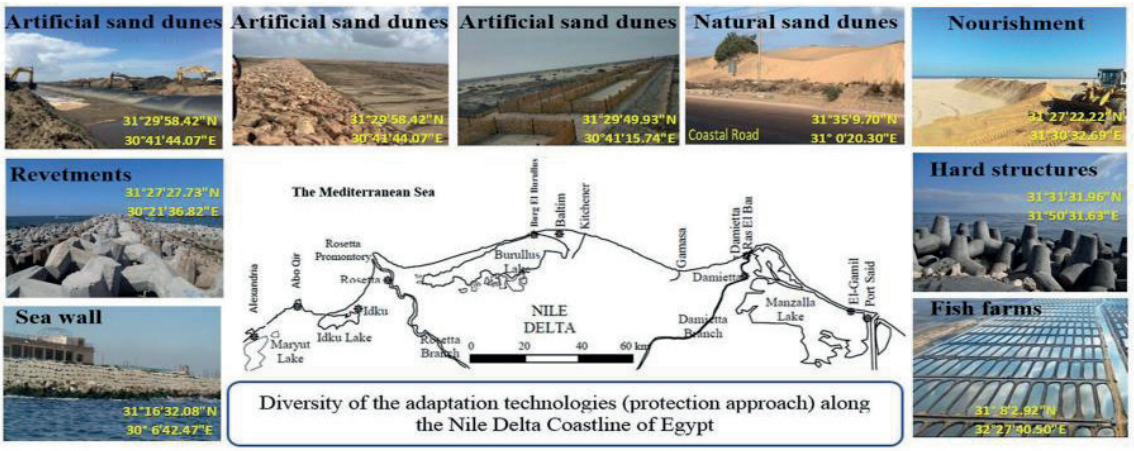

Figure 8. Adaptation technologies along the Nile Delta coastline (after Mohamed and Abd-El-Mooty, 2023).

The mitigation of coastal erosion will involve a combination of such natural and engineered solutions, from beach nourishment, dune restoration and the construction of coastal protection structures. In the highly impacted Nile Delta coastal zone (see Fig. 8), good practices and adaptation strategies include limiting construction in risky areas, rebuilding coastal sand belts and dunes, maintaining wetlands, modifying land use, shifting infrastructure, monitoring water extraction, together with monitoring programs and early warning systems.

4.4. Projected trends

With the projected increase in sea level (IPCC 2023) it is easy to predict an intensification of marine natural hazards and increasing coastal vulnerability in coming decades. Zones already affected by coastal storms, flooding, and erosion will be each year more impacted. As illustrated in Figure 9, climate change will be a significant actor indeed, but not necessarily the main one: as coastal urbanization will intensify, human pressure and demand for energy, groundwater, harbors, transport, etc. will only grow, making populations even more vulnerable and exposed to marine geohazards, with largely lagging legislation and rare mitigating measures.
The action of sea level rise (itself induced by human activities) will be compounded by direct human intervention. In recent decades already, the trend of continued delta progradation has been reversed: the construction of reservoirs and the extraction of water for drinking and irrigation have led to a significant transgression and ingression of the sea, resulting in further

coastal erosion and salinization of aquifers. The latter effects are exacerbated by sea-level rise and storminess. These two factors will only accelerate in the future, affecting all coasts worldwide and leading to increased coastal erosion. Low-lying coasts and areas undergoing tectonic subsidence are particularly at risk. Mediterranean deltas in particular will all suffer from erosion, subsidence and salinization.

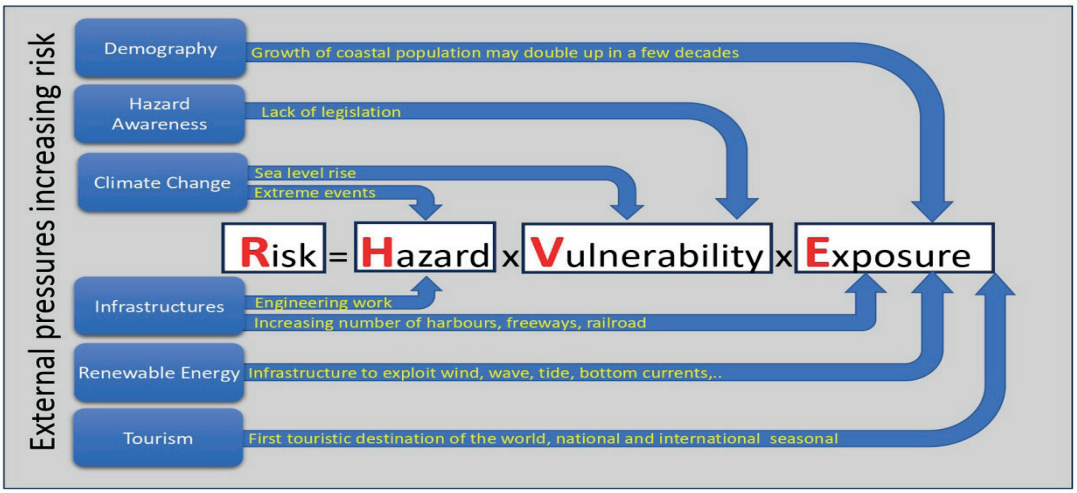

Figure 9. Synthetic diagram of why the risk for coastal communities and infrastructures is bound to increase in the near future, in response to different environmental/anthropic pressures**.**

On a longer time scale, the potential effects of major global climatic changes on rare events such as earthquakes, submarine landslides and tsunamis remain scientifically hard to determine and predict. Evidence from the geological record and numerical models suggests that on the short/medium term (100 years) significant deviations in the current seismicity rate due to flexural bending stresses (Brothers *et al.* 2013) from recent sea-level rise (estimated at 3.6 mm/yr for the period 2000-2018 (Calafat *et al*. 2022) are not expected.
Given earthquake occurrence rates and the downward propagation of thermal perturbations from global warming that could affect the few gas hydrate reservoirs in the shallow subsurface of the Mediterranean (Archer 2007), it is only in the long term that variations in the trends of submarine landslide occurrence may emerge. No changes are expected in earthquake rates from lithospheric-asthenospheric processes such as subduction earthquakes and derived tsunamis (Sallarès and Ranero 2019) as in the Hellenic Arc.

5. SELECTED PRIORITIES FOR RESEARCH

Here is a (non-exhaustive) list of research areas that were considered as priorities by the workshop participants:

- Assess the risk of natural hazards for densely populated coasts and for coastal heritage sites in the Mediterranean region.
- Identify Mediterranean coasts where sea level rise is amplified by land subsidence.
- Assess the potential of non-seismic tsunami sources: volcanoes, atmospheric disturbances and landslides.

- Develop probabilistic approaches to tsunami forecasting that include submarine landslides as a source mechanism.
- Explore further the continental margins of the southern Mediterranean in order to better understand the distribution and frequency of natural hazards.
- Analyse when and where do medicanes form. What are the triggering mechanisms?
- Compare the effectiveness of ecosystem-based coastal management strategies to mitigate coastal erosion and enhance resilience.
- Identify high population tsunami risk areas that feature bays of various scales.
- Improve the risk management of off-grid, cascading events: how are such risks anticipated, perceived and managed around the Mediterranean?
- Analyse the societal and cultural implications of natural hazards in coastal Mediterranean communities, in particular the impacts on traditional livelihoods, cultural heritage and community resilience.
- Integrate marine geohazards into land management policies at regional, national, and local levels.

References

Alasset P.J., Hébert H., Maouche S., Calbini V. and M. Meghraoui. 2006. The tsunami induced by the 2003 Zemmouri earthquake (Mw= 6.9, Algeria): modelling and results. *Geophysical Journal International* 166 (1): 213-226.

Albérola C., Rousseau S., Millot C., Astraldi M., Garcia-Lafuente J.J., Gasparini G.P., Send U. and A. Vangriesheim. 1995. Tidal currents in the Western Mediterranean Sea. *Oceanol. Acta* 18: 273–284.

Archer D. 2007. Methane hydrate stability and anthropogenic climate change. *Biogeosciences* 4: 521–544.

Barberi, F., M. Rosi, and A. Sodi. 1993. Volcanic hazard assessment at Stromboli based on review of historical data. *Acta Vulcanol.* 3: 173–187.

Bevacqua E., Vousdoukas M., Zappa G., Hodges K., Shepherd T., Maraun D., Mentaschi L. and L. Feyen. 2020. More meteorological events that drive compound coastal flooding are projected under climate change. *Commun. Earth Environ.* 1, 47.

Briand F. 2012. Making research count in marine governance – The communication challenge. *CIESM Marine Policy Series* 3, 36 pp.

Brothers D., Luttrell K. and J. Chaytor 2013. Sea-level–induced seismicity and submarine landslide occurrence. *Geology* 41: 979–982.

Calafat F., Frederikse T. and K. Horsburgh. 2022. The sources of sea-level changes in the Mediterranean Sea since 1960. *J. Geophys. Res.*: *Oceans* 127, e2022JC019061.

Cavaleri L. 2005. The wind and wave atlas of the Mediterranean sea - the calibration phase. *Adv. Geosci*. 2: 255–257

Chiocci F.L., Romagnoli C., Tommasi P. and A. Bosman. 2008. The Stromboli 2002 tsunamigenic submarine slide: characteristics and possible failure mechanisms. *J. Geophys. Res.: Solid Earth* 113 (B10).

Cid A., Menéndez M., Castanedo S., Abascal A., Méndez F. and R. Medina. 2016. Long-term changes in the frequency, intensity and duration of extreme storm surge events in southern Europe. *Climate Dynamics* 46: 1503–1516.

Colantoni P., Gennesseaux M., Vanney J., Ulzega A., Melegari G. and A. Trombetta. 1992. Processi dinamici del canyon sottomarinodi Gioia Tauro (Mare Tirreno). *Giornale di Geologia* 54: 199–213.

CRED /UNISDR. 2020. Economic Losses, Poverty and Disasters: 1998-2017. [http://www.unisdr.org/files/61119_credeconomiclosses.pdf]

Dan G., Sultan N. and B. Savoye. 2007. The 1979 Nice harbour catastrophe revisited: trigger mechanism inferred from geotechnical measurements and numerical modelling. *Marine Geology* 245: 40–64.

Dikau R., Meyer N. and J. Bedehäsing. 2009. Naturgefahren – gefährliche Erdoberflächenprozesse. In: Deutscher Arbeitskreis für Geomorphologie (Hrsg.). *Zeitschrift für Geomorphologie, N. F., Suppl.-Vol.* 148: 29-46.

Durrieu de Madron X., Zervakis V., Theocharis A. and D. Georgopoulos. 2005. Comments to "Cascades of dense water around the world ocean". *Progr. Oceanogr*. 64: 83–90

El-Robrini M., Gennesseaux M. and A. Mauffret. 1985. Consequences of the El-Asnam earthquakes: Turbidity currents and slumps on the Algerian margin (Western Mediterranean). *Geo-Marine Letters* 5: 171–176.

Fornaciai A., Favalli M. and L. Nannipieri. 2019. Numerical simulation of the tsunamis generated by the Sciara del Fuoco landslides (Stromboli Island, Italy). *Sci. Rep.* 9: 18542.

Friedrich W.L., Kromer B., Friedrich M., Heinemeier J., Pfeiffer T. and S. Talamo. 2006. Santorini eruption radiocarbon dated to 1627-1600 BC. *Science* 312 (5773): 548-548.

Grases A., Gracia V., García-León M., Lin-Ye J. and JP. Sierra. 2020. Coastal flooding and erosion under a changing climate: Implications at a low-lying coast (Ebro Delta). *Water* 12: 346.

Hereher M. 2015. Coastal vulnerability assessment for Egypt's Mediterranean coast. *Geomatics, Natural Hazards and Risk* 6: 342–355.

Ioualalen M., Migeon S. and O. Sardoux. 2010. Landslide tsunami vulnerability in the Ligurian Sea: case study of the 1979 October 16 Nice international airport submarine landslide and of identified geological mass failures. *Geophysical Journal International* 181: 724–740.

IPCC 2019. Land degradation. pp 345-436 *In* Climate Change and Land. Special Report of the Intergovernmental Panel on Climate Change. Cambridge University Press.

IPCC 2021. Climate Change, 2021. The Physical Science Basis. Working Group I Contribution to IPCC Sixth Assessment Report. [https://doi.org/10.1017/9781009157896]

IPCC 2022. Sea Level Rise and Implications for Low-Lying Islands, Coasts and Communities. pp. 321-446 In: The Ocean and Cryosphere in a Changing Climate: Special Report of the Intergovernmental Panel on Climate Change. Cambridge Univ. Press, UK.

IPCC 2023. Climate Change, 2023. Synthesis Report. Contribution of Working Groups I, II and III to the Sixth Assessment Report of the Intergovernmental Panel on Climate Change. [https://doi.org/10.59327/IPCC/AR6-9789291691647] Geneva, Switzerland.

Ivčević A., Mazurek H., Siame L., Bertoldo R., Statzu V., Agharroud K., Rego I.E., Mukherjee N., Kervyn M. and O. Bellier. 2021. The importance of raising risk awareness: lessons learned about risk awareness sessions from the Mediterranean region (North Morocco and West Sardinia, Italy). *Natural Hazards & Earth System Sciences Discussions*: 3749–3765. [https://doi.org/10.5194/nhess-2021-159]

Janeković I. and M. Kuzmić. 2005. Numerical simulation of the Adriatic Sea principal tidal constituents. *Annales Geophysicae* 23: 3207–3218.

Joffe H., Rossetto T., Solberg C. and C. O'Connor. 2013. Social representations of earthquakes: a study of people living in three highly seismic areas. *Earthquake Spectra* 29(2): 367–397.

Keller J., Ryan W.B., Ninkovich D. and R. Altherr. 1978. Explosive volcanic activity in the Mediterranean over the past 200000 years as recorded in deep-sea sediments. *Geol. Soc. America Bull.* 89 (4):591-604.

Lionello P., Barriopedro D., Ferrarin C., Nicholls R.J., Orlić M., Raicich F., Reale M., Umgiesser G., Vousdoukas M. and D. Zanchettin. 2021. Extreme floods of Venice: characteristics, dynamics, past and future evolution (review article). *Natural Hazards and Earth System Sciences* 21: 2705–2731.

Lionello P. and A. Sanna. 2005. Mediterranean wave climate variability and its links with NAO and Indian monsoon. *Clim. Dyn*. 25: 611–623

Luís S., Lima ML., Roseta-Palma C., Pinho L., Martins F. and A. Betâmio de Almeida. 2016. Is it all about awareness? The normalization of coastal risk. *J. Risk Research* 19 (6): 810–826.

Maramai A., Graziani L. and S. Tinti. 2005. Tsunamis in the Aeolian Islands (southern Italy): a review. *Mar. Geol.* 215 (1-2): 11-21

Marcos M., Tsimplis M. and A.G. Shaw. 2009. Sea level extremes in southern Europe. *J. Geophys. Res. Oceans* 114, C01007.

Mazzanti P. and F. Bozzano. 2011. Revisiting the February 6th 1783 Scilla (Calabria, Italy) landslide and tsunami by numerical simulation. *Mar. Geophys. Res*. 32: 273–286.

Meucci A., Young I., Hemer M., Kirezci E. and R. Ranasinghe. 2020. Projected 21st century changes in extreme wind-wave events. *Sci. Adv.* 6, eaaz7295.

Millot C. and I. Taupier-Letage. 2005a. Additional evidence of LIW entrainment across the Algerian Basin by mesoscale eddies and not by a permanent westward-flowing vein. *Prog. Oceanogr*. 66: 231–250

Millot C. and I. Taupier-Letage. 2005b. Circulation in the Mediterranean Sea. *Env. Chem.* 5: 29–66

Mohamed, R. and M. Abd-El-Mooty. 2023. Sustainable environmental coastal development of the surf zone of Alexandria. Proc. of 4th Intl Conf. of Chemical, Energy and Env. Engineering (ICCEE, 2023), Egypt Japan Univ. Sci. Tech., Alexandria, Egypt.

Ott R.F., Wegmann, K., Gallen, S., Pazzaglia, J., Brandon, M., Ueda, K. & C. Fassoulas. 2021. Reassessing Eastern Mediterranean tectonics and earthquake hazard from the 365 CE earthquake. *AGU Advances* 2 [https://doi.org/10.1029/2020AV000315]

Pang T., Wang X., Nawaz R., Keefe G. and T. Adekanmbi. 2023. Coastal erosion and climate change: A review on coastal-change process and modeling. *Ambio* 52 (12): 2034-2052.

Papadopoulos G.A. and A. Fokaefs. 2005. Strong tsunamis in the Mediterranean Sea: a re-evaluation. *ISET Journal of Earthquake Technology* 42 (4): 159-170.

Papadopoulos G.A. *et al.* 2014. Historical and pre-historical tsunamis in the Mediterranean and its connected seas: geological signatures, generation mechanisms and coastal impacts. *Marine Geology* 354: 81–109.

Papadopoulos G.A. 2016. Historical and geological evidence of tsunamis in Europe and the Mediterranean. pp. 39-76 *In* Tsunamis in the European-Mediterranean Region: From Historical Record to Risk Mitigation. Elsevier Book Series, doi:10.1016/B978-0-12-420224-5.00002-8.

Papazachos B., Koutitas Ch., Hatzidimitriou P.M., Karacostas B. and Ch. Papaioannou. 1985. Source and short-distance propagation of the July 9, 1956 southern Aegean tsunami. *Mar. Geol*. 65: 343–351.

Pérez Gómez B., Vilibić I., Šepić J., Međugorac I. and 40 others. 2022. Coastal sea level monitoring in the Mediterranean and Black seas. *Ocean Science*, 18: 997–1053.

Reimann L., Vafeidis A., Brown S., Hinkel J. and R. Tol. 2018. Mediterranean UNESCO World Heritage at risk from coastal flooding and erosion due to sea-level rise. *Nature Comm.* 9: 4161.

Sallarès V. and C.R. Ranero. 2019. Upper-plate rigidity determines depth-varying rupture behaviour of megathrust earthquakes. *Nature* 576: 96–101.

Sawyer D.E., Urgeles R. and C. Lo Iacono. 2023. 50,000 yrs of recurrent volcaniclastic megabed deposition in the Marsili Basin, Tyrrhenian Sea. *Geology* 51 (11): 1001–1006.

Šepić J., Vilibić I., Rabinovich A. and S. Monserrat. 2015. Widespread tsunami-like waves of 23-27 June in the Mediterranean and Black Seas generated by high-altitude atmospheric forcing. *Scientific Reports* 5: 11682.

Šepić J. and M. Orlić. 2024. Meteorological tsunamis in the Adriatic Sea, https://projekti.pmfst.unist.hr/floods/meteotsunamis/, last accessed on 10 January 2024.

Shaw B., Ambraseys N., England P. *et al.* 2008. Eastern Mediterranean tectonics and tsunami hazard inferred from the AD 365 earthquake. *Nature Geoscience* 1: 268–276.

Soloviev S.L. 1990. Tsunamigenic zones in the Mediterranean Sea. *Natural Hazards* 3: 183-202.

Sørensen M.B., Spada M., Babeyko A., Wiemer S. and G. Grünthal. 2012. Probabilistic tsunami hazard in the Mediterranean Sea. *J. Geophys. Res*. 117: B01305.

Stothers R. and M. Rampino. 1983. Volcanic eruptions in the Mediterranean before AD 630 from written and archaeological sources. *J. Geophys. Res*. 88: 6357-6371.

Tinti S., Maramai A. and L. Grazziani. 2001. A new version of the European tsunami catalogue: updating and revision. *Natural Hazards & Earth System Sci.* 1: 255-262.

Toomey T., Amores A., Marcos M. and A. Orfila. 2022. Coastal sea levels and wind-waves in the Mediterranean Sea since 1950 from a high-resolution ocean reanalysis. *Front. Mar. Sci.* 9: 991504.

Tryon M., Henri P. and D. Hilton, D. 2012. Quantifying submarine fluid seep activity along the North Anatolian Fault Zone in the Sea of Marmara. *Marine Geol.* 315-318: 15-28.

Tsimplis M.N., Proctor R. and R.A. Flather. 1995. A two-dimensional tidal model for the Mediterranean Sea. *J. Geophys Res: Oceans* 100: 16223–16239

UNDRR 2024. United Nations Office for Disaster Risk Reduction (accessed: 12 Jan 2024).

UNWTO 2019**.** World Tourism Barometer and Statistical Annex.

Urgeles R. and A. Camerlenghi. 2013. Submarine landslides of the Mediterranean Sea: trigger mechanisms, dynamics and frequency-magnitude distribution. *J Geophys Res. Earth Surface* 118: 2600–2618.

Vilibić I., Denamiel C., Zemunik P. and S. Monserrat. 2021. The Mediterranean and Black Sea meteotsunamis: an overview. *Natural Hazards* 106: 1223–1267.

Vousdoukas M., Mentaschi L., Voukouvalas E., Verlaan M. and L. Feyen. 2017. Extreme sea levels on the rise along Europe's coasts. *Earth's Future* 5(3): 304-323.

Wang L., Zaniboni F., Tinti S. and X. Zhang. 2019. Reconstruction of the 1783 Scilla landslide, Italy: numerical investigations on the flow-like behaviour of landslides. *Landslides* 16: 1065–1076.

COMMUNICATIONS

Marine hazards and coastal vulnerabilities in the Mediterranean region – a historical and geoarchaeological perspective

Helmut Brückner

Institute of Geography, University of Cologne, Köln, Germany

with contributions from Piero Bellanova[1], Hanna Hadler[2], Dieter Kelletat[3], Dirce Marzoli[4], Simon Matthias May[5], Klaus Reicherter[1], Patrick Schielein[6], Friederike Stock[7] and Andreas Vött[2]

[1] Institute of Neotectonics and Natural Hazards, RWTH Aachen University, Aachen, Germany
[2] Natural Hazard Research and Geoarchaeology Group, Institute of Geography, Johannes Gutenberg-Universität Mainz, Mainz, Germany
[3] Retired from University of Duisburg-Essen (UDE), Essen Campus, Essen, Germany
[4] German Archaeological Institute, Madrid Department, Madrid, Spain
[5] Institute of Geography, University of Cologne, Köln, Germany
[6] Department of Physical Geography, University of Bamberg, Bamberg, Germany
[7] German Federal Institute of Hydrology, Koblenz, Germany

Abstract

Coastal hazards are presented from a historical and geoarchaeological perspective. There are short-term events that occur rapidly, lasting minutes or few days only, but may significantly change coastal areas. The most prominent ones are storm surges and tsunamis. Cliff failure and collapse of flanks of volcanoes are also short-term hazards. Historically, the most dangerous long-term hazard has been the siltation of harbours, especially in areas where port cities are adjacent to a river delta. Examples described in ancient literature or discovered in geo-archives are presented. In addition to these more local phenomena, the most dangerous coastal hazards of the future, termed as "the creeping hazards", are the continued and accelerated rise in sea level and the increase in storminess. These global phenomena will affect all of the Mediterranean coasts to a greater or lesser extent.

Keywords: storm surge, tsunami, flooding, history, archaeology, geo-archives

1. Introduction

The major hazards to coastal areas can be divided into two categories: (i) long-term hazards, such as delta progradation, harbour siltation and sea level rise; (ii) short-term hazards, such as extreme wave events (storm surge, tsunami) and cliff failure. For the latter, questions of frequency (how often) and magnitude (how large) are important. Especially for rare events, such as tsunamis, geo-archives can provide answers when historical sources cannot.

2. Long-term coastal hazards

Long-term coastal hazards with gradual coastline shifts result from eustasy and isostasy. There are sediment eustasy, glacio-eustasy and hydro-eustasy. The latter, also known as the steric effect (expansion of water due to warming), is one of the main sources of sea level rise due to global warming, along with melting glaciers. Long-term coastal hazards also result from isostasy, which can be caused by the loading and unloading of sediment, water and ice on the shelf.

2.1. Coastline shifts

2.1.1. Landward coastline shift – the postglacial transgression

After the low stand during the LGM ca. 20,000 years ago, sea level rose rapidly from 15 to 7 ka BP due to global warming. This transgression caused a major landward shift of coastlines across the globe. In the Mediterranean, large sea inlets were created, former peninsulas became islands (such as Samos) and new islands were created (such as Lade and Hybanda in the area of the later Maiandros valley). The diversity of reconstructed sea-level curves (Fig. 1a) is mainly due to the tectonically active nature of the Mediterranean basin, especially its eastern part. Therefore, there are only regionally valid sea level curves.

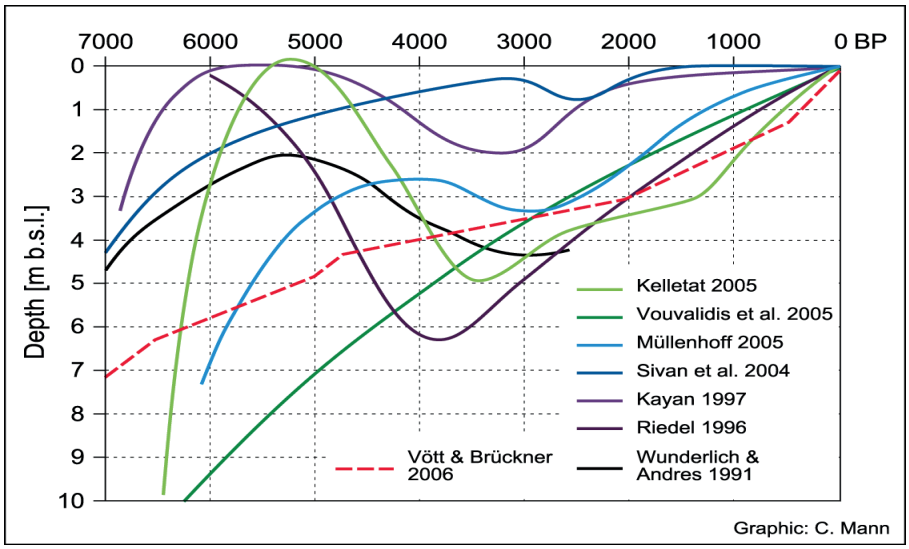

Figure 1a. Sea level evolution of the eastern Mediterranean. Source: Vött & Brückner 2006.

The reconstruction of a sea-level curve integrates natural features, such as sedimentological (transgression facies, beach ridges, foreset/topset contact), geomorphological (notches) and biological (salt marshes, paralic peat, biocrusts), as well as artificial (harbour installations such as jetties and moorings) ones. The curve for the area of Ainos (Enez) in Thrace (Fig. 1b) shows in its lower part the ^{14}C-dated transgression facies at different locations (green rectangles; vertical extent reflects the uncertainty of the elevation, horizontal extent the 2-sigma confidence interval of the ^{14}C age). The position of Greek Archaic graves from a necropolis, the entrance to a medieval coastal tower, and a freshwater spring in a Byzantine church provide constraints on the upper part of the curve.

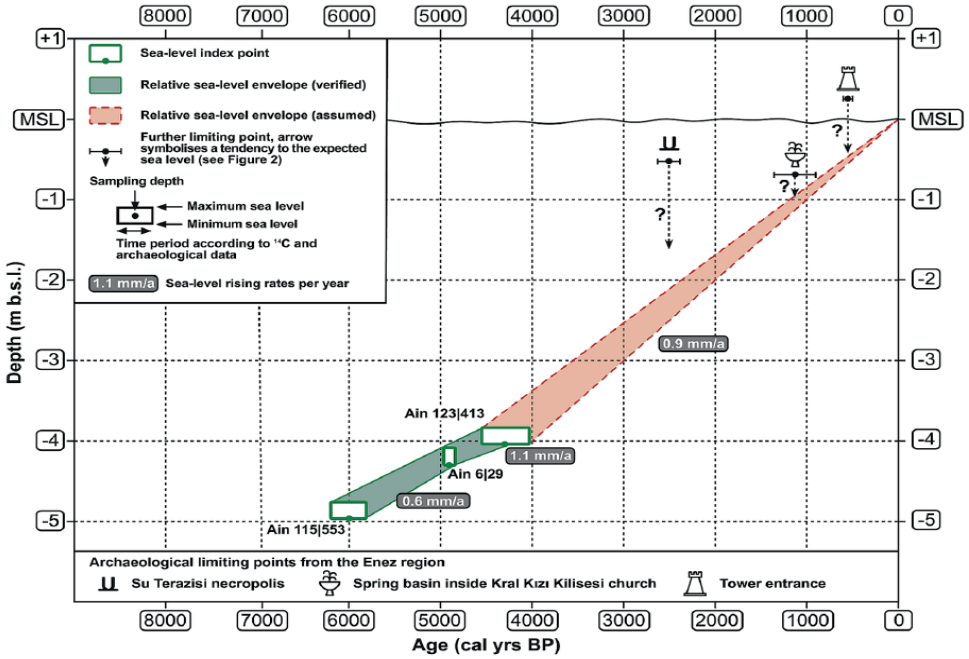

Figure 1b. Sea level evolution of the NE Aegean Sea in the area of Ainos (modern Enez) in Thrace. Source: Seeliger *et al.* 2021.

2.1.2. Seaward coastline shift – progradation of deltas and life cycle of islands

Seven to six millennia ago, the rate of sea-level rise slowed down, allowing deltas to form. With the ongoing advance of the deltas, several of the formerly 'born' islands were landlocked, turned into peninsulas and were finally totally integrated into the floodplains of the rivers. For the time span from the 'birth' to the 'death' of this kind of islands we coined the term: "life cycle of an estuarine island" (Brückner *et al.* 2017).

A perfect example of landlocking is the former island of Lade, which was the site of two naval (!) battles: In 494 BC the Persian fleet completely defeated the fleet of the Milesians and their Ionian allies (Herodotos 6.7-17); in 200 BC the Rhodians fought there at sea against Philip V (Polybios 16.15.6). Today, Lade is fully integrated into the Büyük Menderes (former Mainadros) delta plain. Dead sea cliffs can still be seen at the foot of its western slopes. More historical sources about delta advance and landlocked islands will be found in Appendix A.

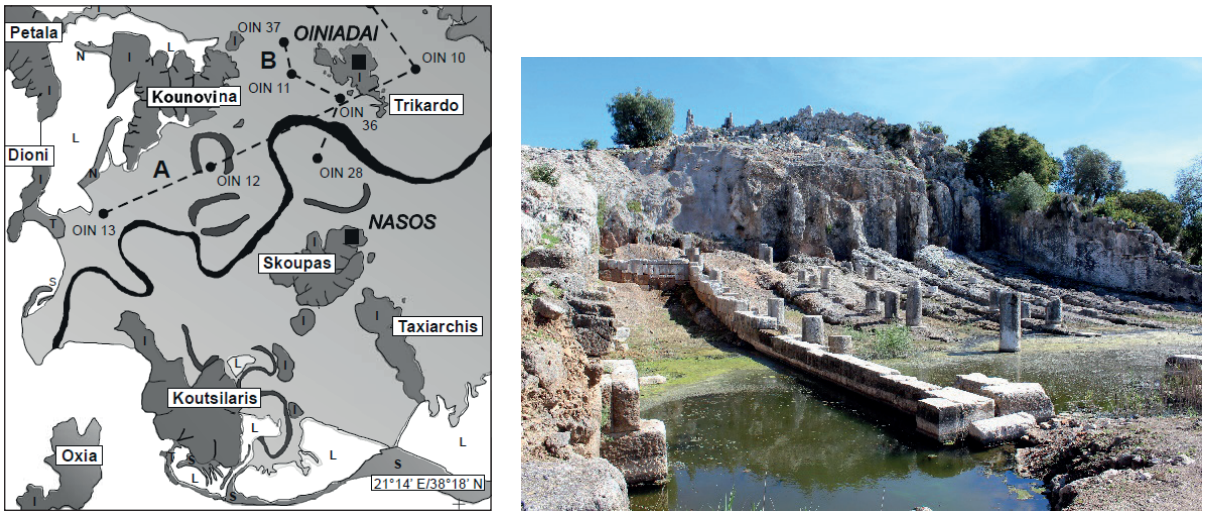

Figure 2. Left – Landlocked islands of the former Echinades archipelago due to the delta advance of the Acheloos (source: Vött *et al.*, 2004: fig. 1, extract). I: island, former island; L: lagoon, pond; S: beach ridge; N: spit; dot: coring site; dashed line: geological profile. Right – Ruins of the shipsheds of Oiniadai from the 5th to 3rd centuries BC (source: Wikipedia).

Another striking example comes from the delta plain of the Acheloos River (Fig. 2). The west-facing shipsheds of Oiniadai in Akarnania, NW Greece, are located on the north side of the former island of Tricardo; they date from the 5th to 3rd centuries BC. They are now about 9 km inland. Several of the former islands of the Echinades archipelago have been completely incorporated into the alluvial plain and the delta of the Acheloos (Skoupas, Taxiarchis) or have become peninsulas (Petala, Dioni, Kounovina, Koutsilaris). Herodotos, Thukydides (both 5th century B.C.) and Pausanias (2nd century A.D.) had already noticed that the Acheloos river had 'captured' the former Echinades islands with its sediments and connected them to the mainland (*cf.* Vött *et al.* 2004).

2.2 Long-term coastal hazard – siltation of harbours

One of the risks to maritime societies in ancient times was the silting up of their harbours. All ancient port cities lost access to the open sea when the delta of the river reached and eventually passed them, when coastal currents constantly accumulated sand and silt, and when material was washed in from the adjacent hills; another risk was the disposal of waste by the city's inhabitants. One can even speak of the life cycle of a port: its "birth" is the start of shipping, for private, commercial or military purposes; its "death" is total siltation.

A prominent example comes from the famous ancient city of Ephesos (Latin: Ephesus), once the capital of the Roman province of Asia. Its fate was strongly connected with the siltation of its harbour, for which the main factor was the continued progradation of the Kaystros (modern Küçük Menderes) river. The different harbour sites are depicted in Figure 3a. The most prominent one was the Roman – early Byzantine Harbour (no. 3; Fig. 3a, b). For details see Stock *et al.* 2013, 2014, 2016, 2019).

Harbours are excellent archives for archaeology, geology and biology. During the time of the intensive use of the Roman / early Byzantine harbour of Ephesos (1st cent. BC – 6th/7th cent. AD) pollution with the heavy metals lead (Pb) and copper (Cu) is evident (Delile *et al.* 2015). By then, also eggs of intestinal parasites, such as *Trichuris* sp., can be detected since this basin was the final sink of the city's waste (Ledger *et al.* 2018). Pollen of the thorny burnet (*Sarcopoterium spinosum*) shows its use as packaging material in ancient shipping (Stock *et al.* 2016). Organic contamination (polycyclical hydrocarbons, PAHs) is attested by high values of resins and essential oils (Schwarzbauer *et al.* 2018). The heavy mineral corundum (Al_2O_3, aluminium oxide), used as an abrasive for processing marble (Pliny, N.H., 37), is clearly present in the harbour sediments. The high amount of marble powder and emery (corundum) dumped into the harbour basin prompted the governor of the province of Asia to issue a decree that made this act a punishable offence.

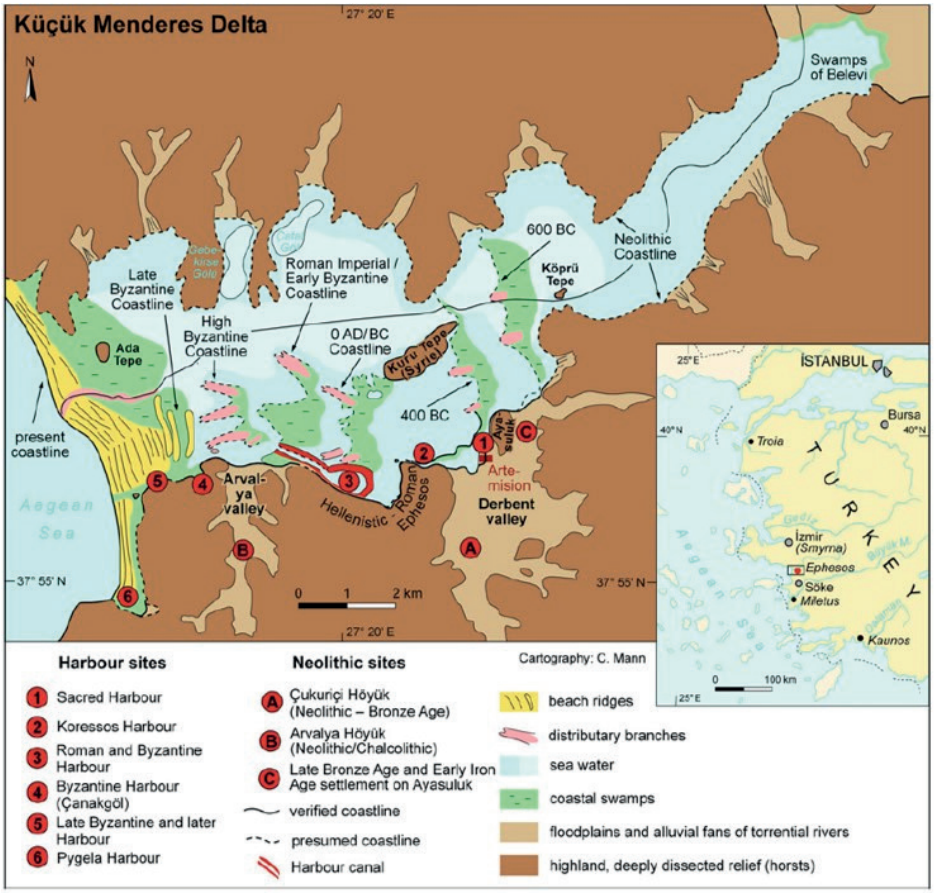

Figure 3a. Delta progradation scenario for the Kaystros (modern Küçük Menderes) after the maximum transgression about seven millennia ago. The ancient Ephesian Gulf was home to several islands, the most prominent of which was Syrie (now Korudağ or Kuru Tepe). The position of the shoreline is shown for different time periods. The harbour of the settlement had to be relocated several times due to the continuous advance of the delta.

Source: Brückner *et al.* 2017: fig. 10.

Figure 3b. The Roman Harbour and the harbour canal. With the ongoing delta advance a canal was built in order to keep the harbour's connection to the open sea. Harbour and harbour canal are easily recognisable throughout the year due to standing groundwater and green vegetation. They are good archives for archaeology, geology and biology. Oblique aerial view taken from a motor glider. Photo: H. Brückner, 09/2011.

A major measure to fight siltation was dredging. That the Romans knew how to carry out this kind of operation is attested with finds of dredging boats (Fig. 4). The sediment cores from Ephesus' Roman harbour show a clear erosional disconformity as evidence of dredging. During Roman times cleaning of the harbour basin is mentioned five times between the 1st and the 3rd centuries AD (Kraft *et al.* 2000, 2007). One of these operations occurred when the harbour was renewed: at the beginning of the 2nd century the high priest donated a huge amount of money to reconstruct and enlarge the harbour area. In order to keep it clean, the proconsul prohibited the disposal of waste, debris and construction rubble into the basin in the mid-2nd century (Kraft *et al.* 2000).

Figure 4. Dredging operations of Roman harbours as a measure to fight siltation. Left – Shipwreck Jules Verne 3, a Roman dredging boat unearthed in Marseilles' ancient harbour. The vessel dates from the 1st to 2nd centuries AD. The central opening measures 255 cm x 50 cm (Morhange & Marriner 2010: Fig. 8). Right – Traces of dredging on the seabed of the Late Roman port of Neapolis (Naples), unearthed during excavations in the Piazza Municipio in Naples (Carsana *et al.* 2009: fig. 3).

For Ephesos, another measure to cope with siltation was the construction of a canal (*cf.* Fig. 3b) to connect the harbour with the open sea. A transect through the canal showed that it was in full use during the 3rd to 5th centuries AD; in the 8th/9th century reeds grew at its fringes and only a narrow passage was left for navigation (Stock *et al.* 2016). Confirmation comes from archaeology: the canal was lined with necropolises on both sides which date from the first half of the 2nd century AD until the end of the 5th / beginning of the 6th century AD (Steskal 2017).

3. Short-term coastal hazards

Three main causes of short-term coastal hazards are presented below: extreme wave events (storm surges and tsunamis) and cliff failures. Extreme wave events are among the most dangerous coastal hazards, with severe storm surges far more common than tsunamis. Palaeo-events of these hazards can be detected in two different coastal settings: (i) as sand or pebble layers within fine-grained geo-archives (lagoons, coastal lakes, harbours); (ii) as massive boulders lying in the coastal zone. Criteria for distinguishing between the two hazards are challenging (*cf.* Engel and Brückner 2011): tsunamigenic boulders are often larger and further inland than storm boulders; tsunamigenic strata often show erosional disconformity at the base, a traction carpet, fining-upward sequences, closed bivalves within the sediment and a mud cap.

3.1. Storm surges

The main wind systems are shown in Figure 5. The Etesian, also known as the Meltemi, is a regularly recurring, dry north-westerly wind that blows very steadily in the Aegean and eastern Mediterranean from April to October; this has been an important factor for sailing. This wind can be fierce and dangerous. The typical Mediterranean climate is named after these winds: 'Etesian climate', characterised by hot & dry summers and mild & humid winters.

3.1.1. Storms in the Odyssey

Why deal with mythological accounts of extreme events? Because extensive and imaginative stories and legends often contain a 'true core', a condensed knowledge of natural hazards that has been passed down from generation to generation over centuries or even millennia. These narratives are often part of a society's collective memory (*cf.* Vött *et al.* 2017).

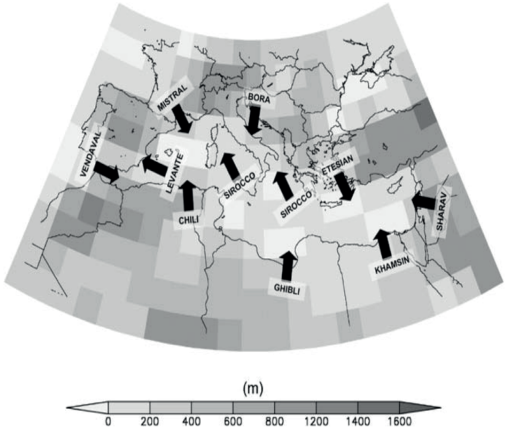

Figure 5. Major large-scale wind systems in the Mediterranean region (black arrows). Topography of the 2.5°×2.5° resolution ERA-40 reanalysis data set (shaded grid boxes). Source: Burlando 2009.

Homer's Odyssey[1] is the epic about the sea journey of Odysseus, king of Ithaca, from Troy (Troia) back to his homeland after winning the Trojan war. The narration about storms in the Odyssey reflects the dangers of seafaring in ancient times and presents particularly dangerous ship passages. Wolf's (last 2009) attempt to localise Odysseus' voyage helps to imagine the nautical dangers of this journey – from the side of the winds, the currents and the cliffs. See Appendix B for his map.

On their journey home Odysseus and his men fail to sail around Cape Malea, at the south-eastern tip of the Peloponnese, due to a strong, 9-day long northerly wind (Etesian!), which carries the fleet to the land of the Lotophagi (often identified with the North African coast, possibly the island of Djerba). Odysseus then sails to Aiolia, the island of the wind god Aiolos, probably the Aeolian Islands. In order to allow the sailors to return home quickly, Aiolos gives them all the unfavourable winds in hoses, except the west wind. When the men curiously open the hoses, the winds escape and the ships are carried back to Aiolia (Odyssey 10.1-79). Meteorological background: the Aeolian Islands are an archipelago with strong circulating winds which may rapidly change direction.

As the journey continues, Odysseus chooses to sail through the strait (usually identified as the Strait of Messina), with Charybdis and Scylla on either side. Charybdis was a dangerous whirlpool that sucked in and spat out water three times a day – an example of tides and dangerous currents. The hero keeps his ships close to the rock of Scylla, a six-headed monster – obviously several dangerous cliffs in the strait (Odyssey 12.201-259).

Due to unfavourable winds, Odysseus and his companions have to remain longer on the island of Thrinacia (Sicily) than expected. When they finally set sail again a gale-force wind destroys their ship. All drown; only Odysseus survives. More details in Wolf (2009).

3.1.2. Storm as an important war factor

In 480 BC, the Persians attacked the Greeks both on land and at sea. The land attack is known as Battle of Thermopylae; the sea attack as Naval Battle of Cape Artemision (Artemisium). This cape is the northern tip of the Greek island of Euboea. This is where the Persian and Greek fleets clashed. The reconstructions are based on Herodotus' account (Hdt. 8.1-39), discussed in detail, *e.g.*, by Hörhager (1973) and Green (1996).

The weather seems to have been the important factor: a severe summer storm off Magnisia, which lasted for three days, caused around a third of the Persians' ships to sink (Fig. 6, right). According to ancient tradition, Boreas, the personification of the wintry north wind, was held responsible. In order to hold their own against the numerically superior Persian fleet, the Greeks positioned themselves in a strait that was covered by the mainland to the west and the island of Euboea to the east. When some of the Persians ships tried to encircle the Greeks the weather intervened a second time: a storm almost completely wiped out this part of the Persian fleet. Although the Greeks were able to hold their own in the ensuing naval battle, they were ultimately forced to retreat after losing the Battle of Thermopylae. The battle of Artemision thus ended in a draw (*cf.* Appendix C2). Already during the first Persian invasion of Greece in 492 BC under Xerxes' father, Darius I, the Persian fleet was wrecked in a storm off the coast of Mt. Athos (*cf.* Appendix C3).

1 Together with the Iliad, the story of the battle of Troy, Homer's Odyssey is the first great epic in world literature. Homer probably lived in the second half of the 8th century and/or first half of the 7th century BC. If one wants to date the legendary fall of Troy, the best candidate is the end of the Bronze Age round 1200 BC.

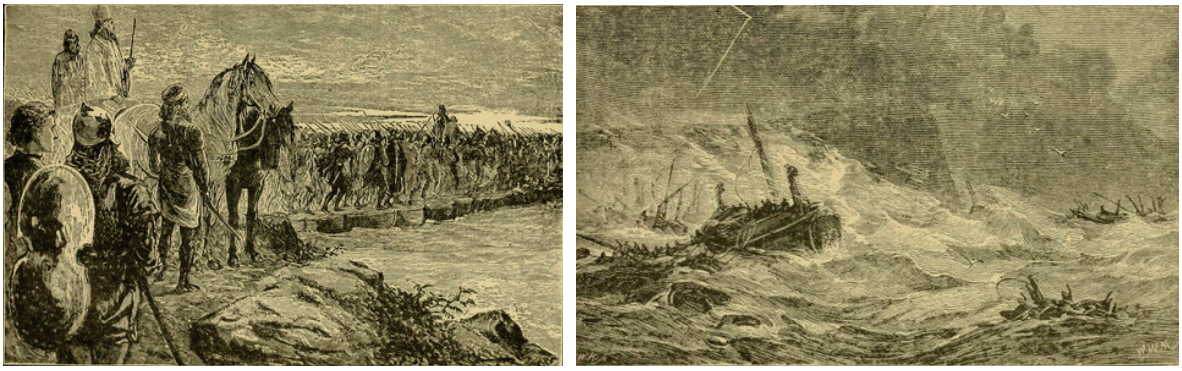

Figures 6. Left – The Persian Army crossing the Hellespont via a ship bridge. Xerxes I the Great had a ship bridge built across the Dardanelles in 480 BC. The endeavour only succeeded on the second attempt, since a violent storm tore apart the first bridge. Historical source: Hdt. 7,21.25 (cf. Appendix C1). Right – Disaster to the Persian Fleet at Cape Artemision (cf. Appendix C2). Both illustrations from Abbott 1900, p. 100 (left) and p. 168 (right).

3.1.3. Shipwrecks – evidence of the dangers of sailing

With its long seafaring tradition, the Mediterranean has been the grave of countless ships. The main causes of their drowning during storms consist of being overtaken by huge waves on the open sea or being smashed against cliffs near the coast.

The Apostle Paul's shipwreck

Famous is the Apostle Paul's shipwreck on Malta (Melite) (Acts of the Apostles 27-28). Paul, on his way to Rome as a prisoner, had come to the island of Crete, probably in AD 57. The month can be deduced from Acts 27:9: "...the voyage was now dangerous because the fast was already over"; "fast" refers to the Jewish Day of Atonement, Yom Kippur. It was already October and the dangerous winter winds were about to arrive. Since violent storms were not uncommon in the winter season, shipping had to be largely suspended between October and April (Der Neue Pauly 11, p. 162 "Schiffahrt").

The shipwreck was caused by long-lasting severe winds: "[14] Not long after this, a hurricane-force wind [a very violent wind like a typhoon or hurricane (τυφωνικός)] called the northeaster blew down from the island. [15] When the ship was caught in it and could not head into the wind, we gave way to it and were driven along..." (Acts 27:14-15; NET). The "northeaster" or Euraquilo is a sailor's term; according to Strabo (Geography 1.2.21) a violent northerly wind (*cf.* Appendices D1 and D2).

Shipwrecks in the Theodosian Harbour of Yenikapı

The Port of Theodosius was one of the ports of Constantinople, the capital of the Byzantine Empire. Built in the late 4th century, during the reign of Theodosius I (379-395 AD), it was the city's main trading venue in late antiquity. The port remained in use until the 11th century, when it silted up, probably due to sediments from the Lycus torrent.

The harbour was discovered in 2005 during work on the Bosphorus tunnel project in the Yenikapı district of Istanbul. More than 35 Byzantine ships dating from the 7th to the 10th/11th centuries were unearthed during the excavations (see Fig. 7a; further details in Pulak *et al.* 2015). The fact that some of them sank at the same time speaks for one (or several) extreme wave events, possibly triggered by severe storms. Another explanation for the massive destruction layer

visible in Figure 7b may be an exceptionally heavy flooding from the Lycus torrent. Thus, coastal sites in the Mediterranean – esp. those with a steep hinterland relief – may not only be endangered from the sea (storm surges, tsunamis), but also from the hinterland (severe flooding).

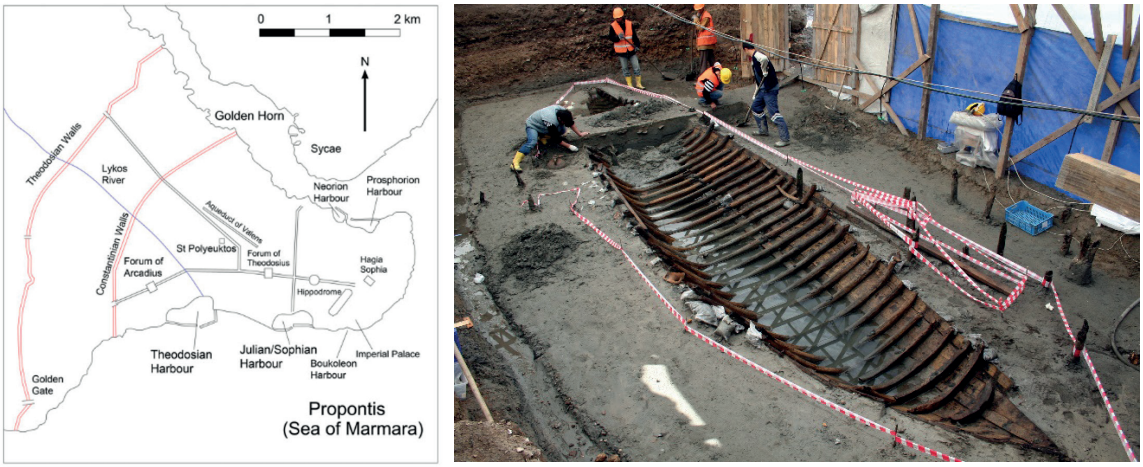

Figure 7a. Left – The Theodosian Harbour as one of Constantinople's harbours during the Byzantine period (cited from Pulak *et al.* 2015, fig. 1). Right – Late 9th or early 10th shipwreck YK 14 during excavation. Photo: Institute of Nautical Archaeology (INA), Ref. 4817; https://nauticalarch.org/projects/yenikapi-byzantine-shipwrecks-project/.

Figure 7b. Destruction layer in the former Theodosian harbour. Ceramics from the 5th – 7th centuries AD. Source: D. Perincek, transmitted by Ch. Morhange.

3.2. Tsunamis

The Mediterranean Sea has been affected by tsunamis throughout history. Of the 176 tsunamis since Minoan times listed by Schielein *et al.* (2007), more than 80 % were triggered by earthquakes. Tsunamigenic earthquakes occurred mainly along the North African margin in the western Mediterranean, along the Calabrian Arc, near the Hellenic Arc (Ionian Sea and Aegean Sea) and in the eastern Mediterranean (Fig. 8). These regions are tsunamigenic zones with a medium or high tsunami hazard potential; however, it has to be kept in mind that tsunami waves can also affect distant coastal areas.

Other tsunamis were generated by volcanic eruptions along the Hellenic and Calabrian arcs and further north in the Ligurian Sea. Failures of coastal cliffs and volcanic flanks, as well as

submarine slides, often with tectonic triggering mechanisms, produced sporadic tsunamis in different areas.

3.2.1. Tsunami evidence from fine-grained archives

After the 2004 Indian Ocean Tsunami, tsunami awareness was raised along the world's coastlines, as it was realised that a tsunami can be destructive not only in the region where the triggering mechanism, *e.g.* an earthquake, occurred, but also in very distant regions due to the high speed and energy of tsunami waves and the relatively long time and distance each of the waves (often 3-5 waves only) travel inland. Evidence of the tele-connection is often provided by sedimentary footprints: coarse-grained sand sheets in fine-grained coastal geo-archives (lagoons, beach lakes).

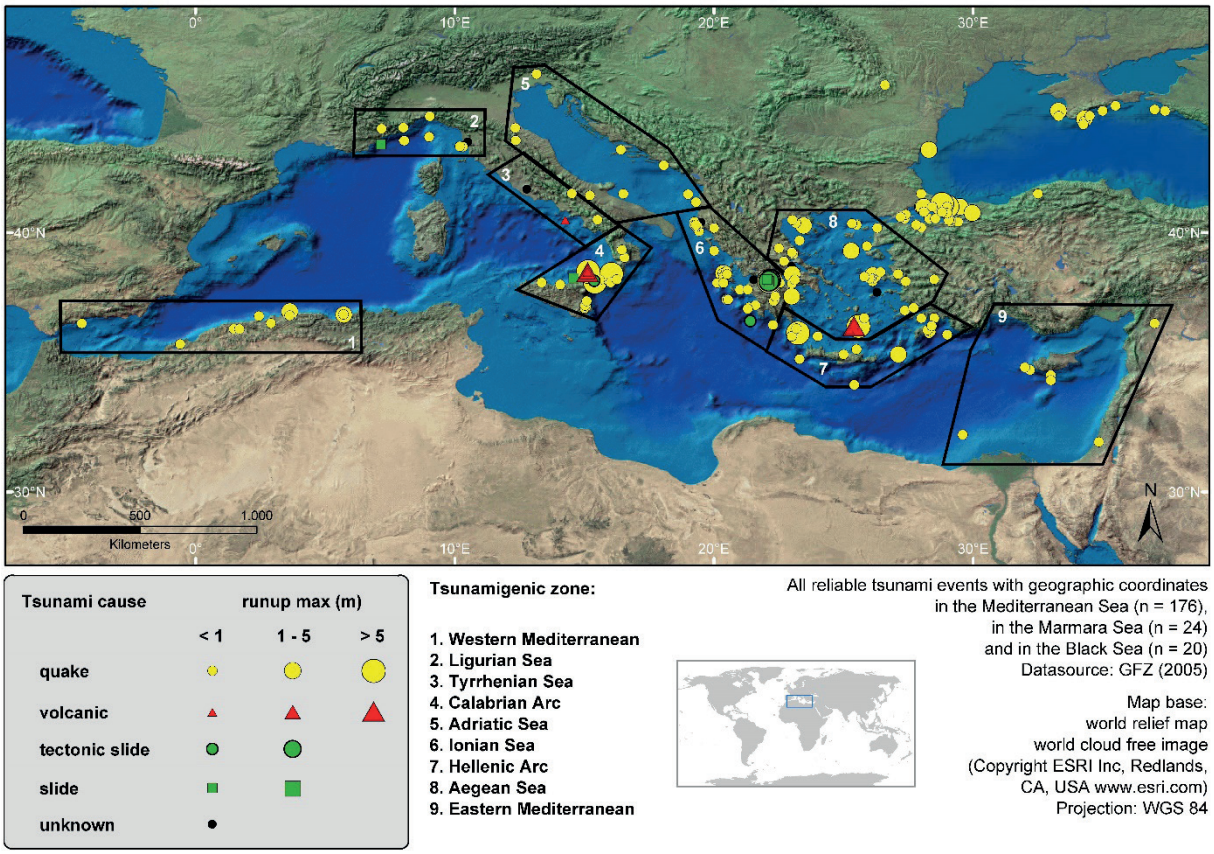

Figure 8. Tsunami sources in the Mediterranean Sea differentiated by cause and maximum run-up height. Source: Schielein *et al.*, 2007, fig. 5.

Earthquakes and tsunamis – the case of Baelo Claudia

The remains of the ancient Roman city of Baelo Claudia, located in southern Spain near the Strait of Gibraltar, provide a unique setting for the study of historical earthquakes and tsunamis in the Gulf of Cádiz. Baelo Claudia experienced two earthquakes during the Roman period, in the first and fourth centuries AD. The latter, coupled with a tsunami, led to the destruction of the city and its subsequent decline (Reicherter *et al.* 2022). In total, three tsunami deposits have been found at Baelo Claudia, dating from around 4000 cal BP (2000 BC), around 400 AD and 1755 AD (the Lisbon tsunami) (Silva *et al.* 2023). Interdisciplinary studies of the sedimentary, archaeological and palaeontological record have revealed deposits associated with these events,

as well as significant changes in the landscape around the bay following the earthquake and tsunami impacts (Reicherter *et al.* 2022).

The AD 365 Crete earthquake and tsunami

An event from Antiquity which triggered a major tsunami, was the earthquake of 21 July 365 AD. It strongly tilted the western part of Crete (maximum uplift: 9 m), while the island's eastern part was more or less unaffected. This can well be traced by the displacement of bioconstruction features like vermetid algal rims which are good sea-level indicators. The city of Phalasarna had an enclosed artificial war harbour measuring 100 m x 75 m, carved out of the coastal rocks (limestone). A canal connected it to the open sea. The earthquake uplifted the harbour for several metres, thus draining it (*cf.* Kelletat 1998).

There are numerous sites with evidence of tsunami boulders from this event, *e.g.* mega-clasts with imbrication bedding on the southern shores of the Peloponnese. But the AD 365 footprint is also detectable in fine-grained sedimentary archives, *e.g.*, the sandy-gravelly Gyrapetra washover fan in the Lefkada Lagoon in the northern part of the Ionian island of the same name in NW Greece (Fig. 9; May 2010; May *et al.* 2012). Arguments that it is the result of a tsunami rather than a mega-storm surge include: the washover fan's areal extent within the lagoon, its chevron-shaped wash over structure, stratigraphic architecture and microfaunal composition.

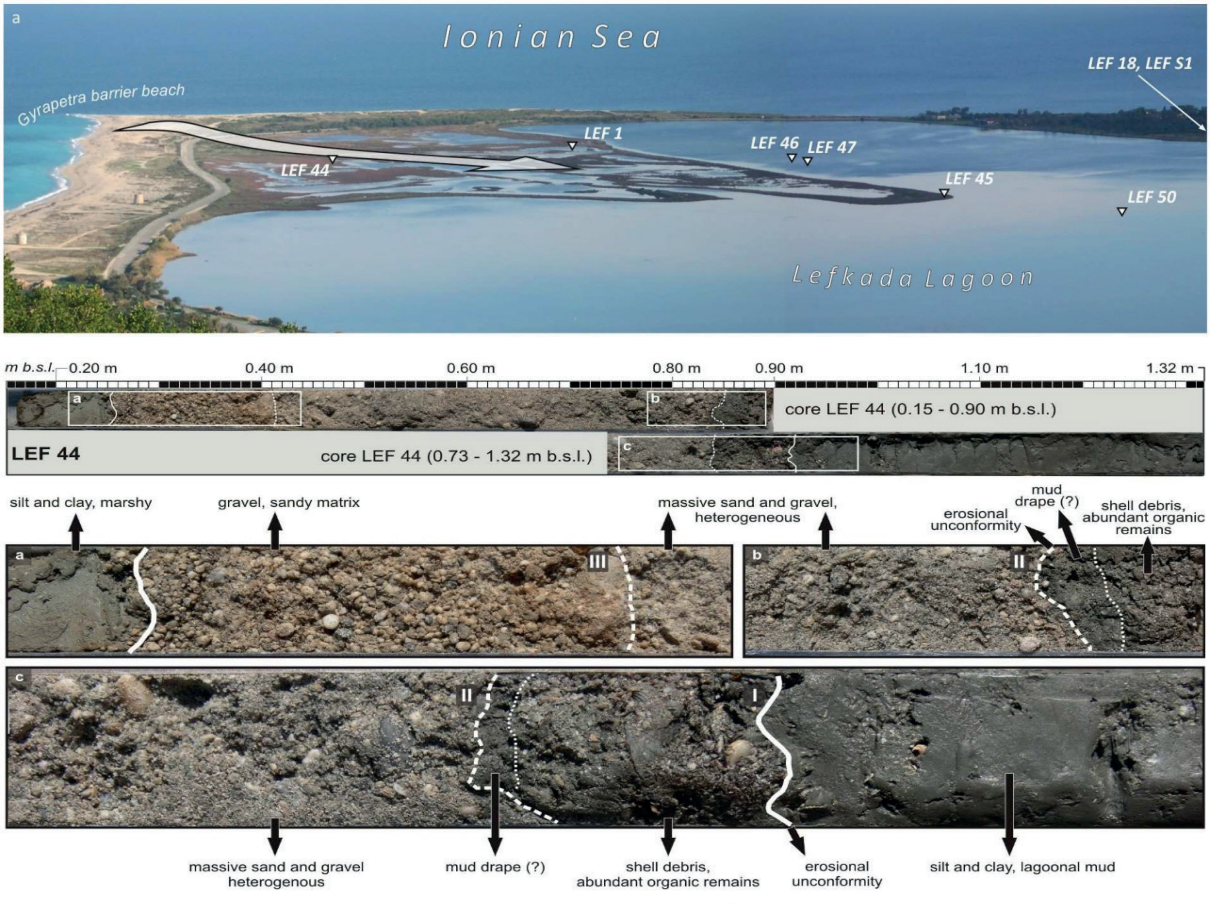

Figure 9. Gyrapetra washover fan in the Lefkada Lagoon with coring sites. Below: Details of vibracore Lef 44 (core section 1.32 – 0.15 m below sea level; important parts are enlarged and main sedimentary characteristics depicted). Sources: S.M. May 2010, figs. 4-2 & 4-3 (aerial photograph by A. Vött 2006).

The stratigraphy of vibracore Lev 44 (Fig. 9) can be explained as follows: on top of the lagoonal mud, a coarse-grained sedimentary sequence shows three distinct subunits starting with an erosional unconformity. Subunit I consists of shell debris and abundant organic remains; subunit II is a heterogeneous mixture of sand and gravel; subunit III is gravel in a sandy matrix. This is followed by fine-grained sediments, typical of a low-energy depositional environment, as expected in a lagoon. Units I to III, sandwiched between lagoonal silt and clay, are best interpreted as deposits from an extreme wave event, most likely a tsunami. The three subunits may reflect three successive waves. ^{14}C age estimates and ceramics point to the AD 365 earthquake and tsunami event as the cause (May 2010; May *et al.* 2012).

Tsunami impact in harbours

In several papers, Andreas Vött and his team have published evidence of deposits of extreme wave events in harbours in Greece, attributed to tsunamis: in the harbours of the ancient cities of Palairos-Pogonia (Akarnania), Lefkas/Leukas (Akarnania/Ionian Islands), Corfu/Kerkyra/Korkyra (Ionian Islands), Krane (modern Argostoli on Cephalonia, Ionian Islands), Corinth (Peloponnese) and Ostia (Italy). A prominent example is the Lechaion harbour of Corinth (Fig. 10a).

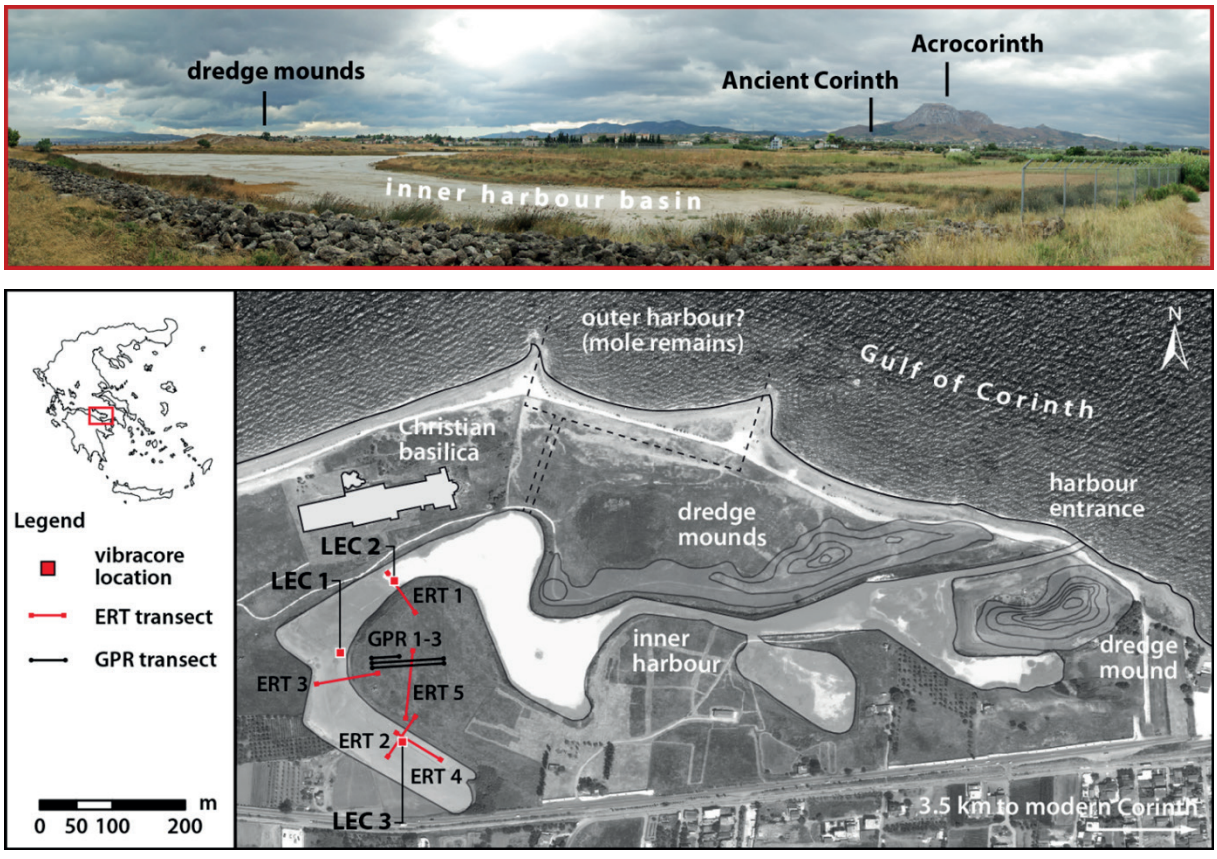

Figure 10a. Lechaion – the ancient harbour of Corinth. Overview of the general setting, the former harbour basin and field work locations (map modified after Google Earth images 2009). Source: Hadler *et al.* 2013.

In sediment cores and geophysical transects (GPR, ground-penetrating radar; ERT, earth resistivity tomography) from the harbour of ancient Corinth, Hadler *et al.* (2013) identified two distinct event layers, which they attribute to tsunami landfall (Fig. 10b). Their pro-tsunami and anti-storm arguments are: basal erosional unconformities, few abrupt facies changes, fining upward sequences, re-establishment of pre-event conditions, sheltered harbour basin, moderate winter storm activity, spatial dimensions of layers, as well as mixed microfauna. After criticism of the tsunami hypothesis by Kolaiti *et al.* (2017), Vött *et al.* (2018) emphasised once again the seismically-induced genesis of the event layers. Recalibrating the ^{14}C ages, the authors could narrow down the age estimates of the co-seismic tsunamis to the 770s BC, *i.e.* the early 8th cent. BC (Archaic period; event I), and to 69-79 AD (Roman Imperial period; event II) (Fig. 10b).

Whether tsunamites or temepestites, the layers show the vulnerability of the coasts of the eastern Gulf of Corinth to extreme wave events – coasts that are densely populated and annually visited by thousands of tourists.

3.2.2. Tsunami evidence from boulder archives

Mega-clasts are reported from numerous coasts around the world. They are evidence of extreme wave events. Again, there is a lively debate as to whether they are caused by severe storm surges or tsunamis. These boulders are sometimes arranged in imbricated bedding, reflecting the wave train during a tsunami event. We present two such examples, but there are many, many more.

Mega-clasts on Mallorca

Coastal boulders can be found along many of the rocky coasts of Mallorca (Roig-Munar *et al.* 2019). In eastern Mallorca, *e.g.*, boulder ridges are adjacent to semicircular erosional features (scars of former landslides?) that reach up to 16 m above sea level (Fig. 11a, b).

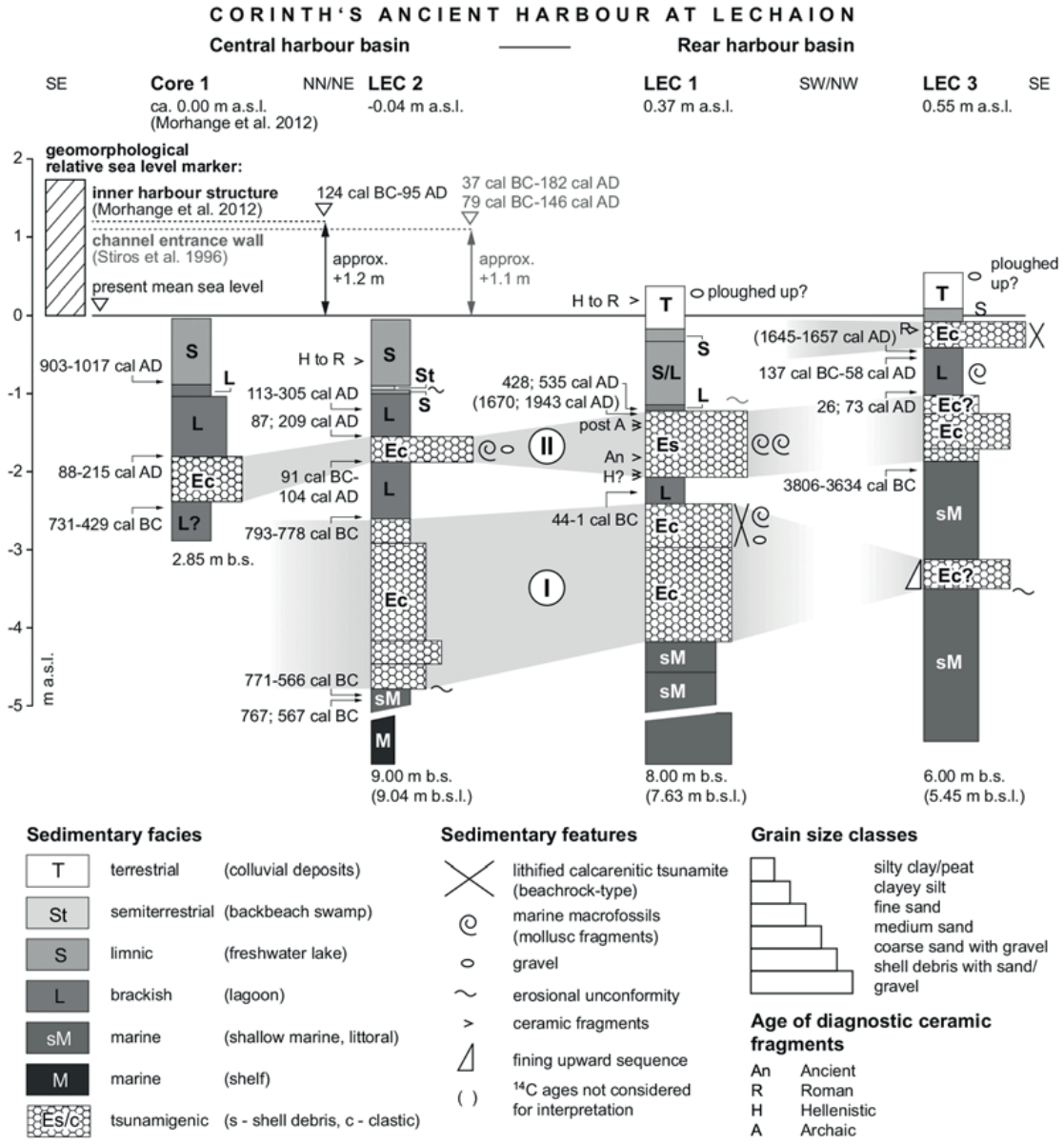

Figure 10b. Cross section through Corinth's ancient harbour at Lechaion. In this compilation of data from different sources, two prominent extreme wave events are depicted from the sediment columns. They are interpreted as co-seismic tsunami landfalls from the early 8th century BC and from 69–79 AD. Source: Vött *et al.* 2018, fig. 4.

Roig-Munar *et al.* (2023) discussed the origin of these coastal boulders and showed that they were displaced by tsunami waves generated by a seaquake at the North African margin. Dating the time of the boulder transport is always a problem, all the more since often a relocation in later times cannot be excluded. In the given case, one historical source describes an inundation of up to 2 km and a run-up of up to 45 m on the south coast of Mallorca in AD 1756 (apparently one year later than the well-known Lisbon tsunami of AD 1755). The growth rate of karst features (dissolution pans) on the calcareous cliff surface, from which the dislodged boulders originate, indicates an age between 1591 and 1894 AD (Roig-Munar *et al.* 2019). Radiocarbon data from marine fauna attached to other boulders in low-lying coastal areas to the east and south of Mallorca also yielded older depositional ages of around 1500 and 500 AD (Kelletat

et al. 2005). Future research will focus on the geomorphology and ages of boulder deposits in the Balearic Islands. In any case, these mega-boulders are an impressive sign of the hazards of these coasts, which are very popular with thousands of tourists.

Figure 11a. Boulders accumulated on a clifftop in eastern Mallorca. One site from where they originate can be recognised at the cliff face in the centre (Schielein, unpublished).

Figure 11b. Boulder deposits on the south coast of Mallorca. Dating the time of transport, i.e., the time of the extreme wave event, is challenging (Schielein, unpublished).

Mega-clasts on the island of Lefkada

Lefkada, the northernmost of the Ionian Islands, is connected to mainland Greece by a complex system of beach ridges and lagoons, including the Gyrapetra wash over fan (see Fig. 9 above).

The beachrock 'finger', locally called Plaka (Fig. 12, left), is the remnant of a former beach whose base had been cemented. The present beach ridge has shifted eastwards and is now separated from its original position marked by the beachrock (see May, 2010; May *et al.* 2012). On its top are mega-clasts (Fig. 12, right). These beachrock boulders, the stripping of the former beach and its eastward shift, as well as the existence of the Gyrapetra washover fan (*cf.* Fig. 9) have been attributed to (the same?) tsunami impact. However, this ensemble may also be explained by severe storm surges. Either way, both explanations demonstrate the exposure of the Western Greek coasts to extreme waves from the Ionian Sea.

Figure 12. Line of beachrock ('Plaka') as remnant of a former beach (left; photograph by H. Brückner, 2005). Displaced mega-boulders on the Plaka beach (right; source: Vött *et al.* 2006. Fig. 5).

3.2.3. Volcanogenic tsunamis

The link between volcanic island eruptions and tsunamis is well documented (*e.g.*, Krakatoa explosion in 1883: Mutaqin *et al.* 2019; Tonga volcano eruption in 2022: Zhou *et al.* 2023).

As far as the Mediterranean is concerned, it was the eruption of Santorini around 1600 BC that massively affected – but did not destroy – the Minoan culture. Its ash is widespread, especially in the eastern Mediterranean region. We discovered Santorini ash in Lake Belevi in the hinterland of Ephesus: about 3 cm of fallout tephra and on top at least 18 cm of tephra washed into the lake from the adjacent hills (Stock *et al.* 2020).

In their archaeological excavations at Palaikastro in north-eastern Crete, Bruins *et al.* (2008) provide field evidence for the Minoan tsunami deposits and reconstruct a tsunami wave of at least 9 m. There seems to be evidence that the Minoan tsunami wave even reached the coast of the Levant, leaving its sedimentary footprint on the continental shelf off Caesarea, in nowadays Israel: sediment cores from 10 to 20 m water depth revealed a sheet-like layer up to 40 cm thick, which Goodman-Tchernov *et al.* (2009) attribute to the Late Bronze Age Santorini eruption. Their arguments are based on grain size distribution, planar bedding, shell taphoecoensis, dating (radiocarbon, OSL, pottery) and comparison with storm deposits.

Tsunamis can be generated not only by the explosion of a volcanic island, but also by flank failure. Seismic data in the Ionian Sea reveal large submarine landslide deposits off the coast of Mt. Etna (Italy), apparently the correlative sediment for the collapse of part of a flank of this volcano around 8.3 ka BP (Pareschi *et al.* 2006). Pareschi *et al.* (2007) even suggest that there is a tele-connection between this event and the sudden destruction of the Neolithic village of Atlit-Yam on the Israeli coast. They support their hypothesis with field evidence of tsunami inundation at the mentioned site and by modelling a scenario of tsunami wave propagation from Mt. Etna to the Levantine coast. In any case, it shows that – other than a storm surge – such a mega-tsunami is not just a local phenomenon, but a major coastal hazard that can seriously affect a large part of the Mediterranean.

3.3. Short-term coastal hazard: cliff failure – the fate of Helike in 373 BC

The catastrophe in 373 BC destroyed one of the most important and oldest cities in the Achaia landscape, already mentioned by Homer in the Iliad: Helike on the southern shores of the Gulf of Corinth. The disaster occurred on a winter night in 373 BC. In the 1st century BC the Greek historian Diodoros (15.48-49) wrote: “Never before had Greek cities been struck by such a catastrophe, and never before had entire cities and their inhabitants disappeared.” What he describes can best be interpreted as a major earthquake. But the disaster continued: “Then a greater and more incredible catastrophe struck them. The sea rose to an immense height and a huge wave swamped them all, along with their hometown” (Diodoros 15.48-49). More ancient sources in Appendix E.

Dora Katsonopoulou and Steven Soter have been searching for Helike on land for many years. There have been finds of various settlements, but no definite remains of the Helike of 373 BC. We also participated for a few years with evidence from coring (Engel *et al.* 2016). For instance, coring Hel 8 (Fig. 13) shows an abrupt lithological change from coarse-grained lagoonal deposits to fine-grained limnic ones, suggesting the sudden formation of a lacustrine environment. Most likely, antithetic tilting of a block had caused the development of a lake which was later transformed into a moor. The age estimates point to a date of this earthquake before 1437-1634 AD, wherefore the best candidate is the AD 1402 earthquake.

In total, Engel *et al.* (2016) identified three major events: before 2550 BC, before 348 BC to 64 AD (probably 373 BC), and before 1437-1634 AD (probably AD 1402). The authors come to the conclusion: "Although the Helike Project reported possible tsunami evidence in earlier cores and trenches, no unequivocal sedimentary traces of a tsunami were identified in the Classical horizons of our cores" (Engel *et al.* 2016, p. 140).

Our research suggests that the earthquake caused fractures, faults and massive landslides. This is not surprising, as the landward side of Helike rises steeply to over 1000 metres, and the foreshore plunges deep into the Gulf of Corinth. Several prominent fault lines have been identified, and historic earthquakes, including that of 373 BC, have been reported from this region. The most plausible theory, therefore, is that the geological block, on which Helike once lay, slipped into the sea. A large tsunami would not be just a local phenomenon; it would have affected all the coastal towns on the gulf, which was not the case. That nothing has been found so far in the gulf, despite some underwater geophysical research, can be explained by the fact that in the almost 2,500 years since the catastrophe, rivers have washed a lot of sediment into the sea. These probably buried Helike.

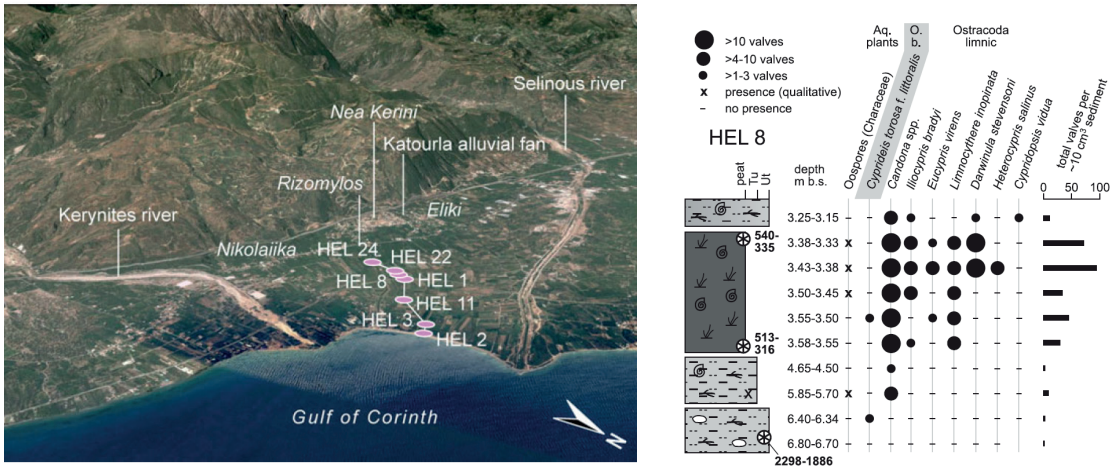

Figure 13. Left – Oblique view of the coalescing delta fans of the Kerynites and Selinous rivers forming the Helike delta plain (Google Earth). Right – Ostracods of sediment core Hel 8 (O. Ostracoda; b. brackish; Aq. aquatic). Radiocarbon ages are shown as cal. BP. Source: Engel *et al.* 2016, fig. 3 (left) and fig. 7 (right).

4. The creeping hazard: sea level rise and increased storminess

According to the IPCC 2021 scenarios, sea level will continue to rise worldwide and there will be an increase in storminess. Both phenomena will endanger coastal areas worldwide, including coastal heritage sites. This is exemplified by the ancient town of Ampurias (Empúries) on the Gulf of Rosas (NE Spain).

Ampurias was the westernmost settlement of the Greek colonisation, founded as a coastal trading settlement in 530/40 BC by the Phoceans of Massili (now Marseille) on the shores of what is now the Gulf of Rosas. Its ruins have been the subject of detailed archaeological excavations and historical studies. Knowledge of this famous site up to the early 2000s is excellently summarised in the comprehensive monograph of Marzoli (2005).

Based on the fact that the past is often the key to the future, a research project was carried out under the umbrella of the DAI Groundcheck programme. It was entitled "Ampurias' future – learning from the past"; the time period under consideration was from 5500 BC to AD 2100 (Marzoli *et al*. 2023). In a first step, the focus was put on the evolution of the landscape as well as the human-environment interaction from the maximum of the postglacial marine transgression during the 6th millennium BC until today. The interpretations were based on sediment columns of many already existing drillings in the ancient city and its surroundings for their sedimentological, geochemical, microfaunal and palynological contents. Thus, it was possible to differentiate the former depositional facies (shallow marine, littoral, lagoonal, limnic, fluvial) as well as the changes from the natural vegetation to the different stages of human-induced degradation. All of this was integrated into a holistic approach that also took into account the results of archaeological and historical research, as well as previous geoarchaeological studies; it was then visualised in an interactive 3D model (*cf.* Marzoli *et al.* 2023). Two scenarios are presented in Figure 14a.

But not only the most important historical-cultural phases of the last 7500 years were studied in retrospect. The second step – and this is of particular interest in the context of this CIESM workshop – was devoted to forecasting future developments. Two factors in particular had to be taken into account: the future rise in sea level and the expected increase in storm surges based on IPCC (2021).

As for the worst-case scenario, *i.e.*, the very high-emission scenario SSP5-8.5, sea level by 2100 could be more than 1 m higher than in 1971 (IPCC 2021, p. 1319). Until 2300, global mean sea level will rise between 0.3 m and 3.1 m or between 1.7 m and 6.8 m (worst-case scenario); even as much as 16 m is possible if the instability of marine ice cliffs is included – fortunately a scenario that is still considered with low confidence (IPCC 2021, p. 1217). In addition to that, "sea level rise will increase the frequency and severity of extreme sea level events at coasts" (IPCC 2021, p. 1318).

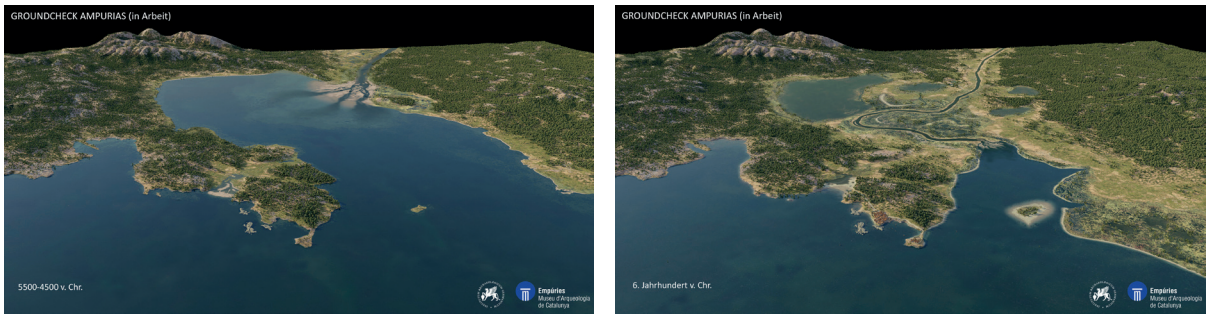

Figure 14a. Evolution of the Empordà (Spanish: Ampurdán), the area around the ancient Greek coastal city of Emporion, recent Empúries (Spanish: Ampurias). Scenario of the maximum marine transgression around 5000 BC (left) and at the time of the arrival of the first Greek settlers in 530/40 BC. Source: Marzoli *et al.* (2023). 3D model by Daniel Baños. © DAI Madrid and MAC (Museu d'Arqueologia de Catalunya) Empúries.

These global scenarios need to be broken down to the local setting. In mid-January 2020, the Catalan coast was severely affected by the storm "Gloria". Ampurias was hit by a storm surge with 7 m high waves. This is particularly disastrous because the earliest Greek settlement, dating from 530/540 BC, is on the present coast; it will be lost forever after a few more of such

catastrophic extreme waves (*cf.* Fig. 14b, left). Taking these aspects into account, we projected a scenario for Ampurias in 2100 with a sea level of +1 m compared to today and a storm surge with waves of 10 m. The areas of maximum inundation are well visible in Figure 14b (right).

Figure 14b. Left – Ampurias during a storm surge in November 2019. The outer wall of the Roman harbour acts as a wave breaker. At the time of this extreme wave event, rescue excavations were in progress, as the earliest settlement site is right next to this beach. Photo by Pere Castanyer, MAC Empúries. Right – Simulation of the flooding of the ruins of Ampurias, assuming a sea level of +1 m and a wave height of 10 m. The south is at the top. Source: J. Oetjen & W. Schüttrumpf, RWTH Aachen University. DEM by Daniel Baños, https://danielbanos.com/.

Summary

Coastal hazards are presented from a historical and geoarchaeological perspective. There are short-term events that occur rapidly, lasting minutes or few days only, but may significantly change coastal areas. The most prominent ones are storm surges and tsunamis. In the early 5th century BC, storms destroyed the Persian fleet on several occasions; some of the ships unearthed in the Theodosian harbour of Istanbul were sunk during storms. In several of the ancient coastal cities, esp. in their harbours, the footprint of extreme wave events are archived (*e.g.*, Baelo Claudia, Corinth). Traces of the tsunami waves that followed the AD 365 Crete earthquake can be seen in many parts of the Mediterranean; the earthquake uplifted Phalasarna by several metres, draining the city's harbour. Cliff failure and collapse of volcanic flanks are also short-term hazards.

Historically, the most dangerous long-term hazard has been the siltation of harbours, especially in areas where port cities are adjacent to a river delta. Prominent examples are Ephesus and Ostia antica. Finally, the future coastal hazards are described as 'the creeping hazards': the continued and accelerated rise in sea levels and the increase in storminess. This is illustrated by scenarios for the ruins of the ancient Graeco-Roman city of Ampurias in Catalonia (Catalunya).

To be cited as:

H. Brückner. 2024. Marine hazards and coastal vulnerabilities in the Mediterranean region – a historical and geoarchaeological perspective. p 29- 56. In CIESM Monograph 52 [F. Briand, Ed.] Marine hazards, coastal vulnerability, risk (mis)perceptions – a Mediterranean perspective. CIESM Publisher, Paris, Monaco, 182 p.

References

Abbott J. 1900. History of Xerxes the Great. Philadelphia; Henry Altemus Company [https://archive.org/details/historyofxerxesg02abbo/mode/2up]

Brückner H., Herda A., Kerschner M., Müllenhoff M. and F. Stock. 2017. Life cycle of estuarine islands – From the formation to the landlocking of former islands in the environs of Miletos and Ephesos in western Asia Minor (Turkey). *Journal of Archaeological Science: Reports*, 12: 876-894 [doi.org/10.1016/j.jasrep. 2016.11.024]

Bruins H.J., MacGillivray J.A., Synolakis C.E., Benjamini Ch., Keller J., Kisch H.J., Klügel A. and J. van der Plicht. 2008. Geoarchaeological tsunami deposits at Palaikastro (Crete) and the Late Minoan IA eruption of Santorini. *Journal of Archaeological Science* 35 (1): 191-212 [doi.org/10.1016/j.jas.2007.08.017]

Burlando M. 2009. The synoptic-scale surface wind climate regimes of the Mediterranean Sea according to the cluster analysis of ERA-40 wind fields. *Theor. Appl. Climatol*. 96: 69-83 [doi.org/10.1007/s00704-008-0033-5]

Carsana V., Febbraro St., Giampaola D., Guastaferro C., Irollo G. and M.R. Ruello. 2009. Evoluzione del paesaggio costiero tra Parthenope e Neapolis. *Méditerranée* 112: 14-22. [doi.org/10.4000/mediterranee.2943]

Delile H., Blichert-Toft J., Goiran J.-Ph., Stock F., Arnaud-Godet F., Bravard J.-P., Brückner H. and F. Albarède. 2015. Demise of a harbor: a geochemical chronicle from Ephesus. *Journal of Archaeological Science* 53: 202-213; doi.org/10.1016/j.jas.2014.10.002

Der Neue Pauly, vol. 11: Sam–Tal. 2001, 629 pages, edited by H. Cancik and H. Schneider. J.B. Metzler Verlag / Springer-Verlag GmbH.

Engel M. and H. Brückner. 2011. The identification of palaeo-tsunami deposits – A major challenge in coastal sedimentary research. *Coastline Reports* 17: 65-80. Rostock (http://www.eucc-d.de/).

Engel M., Jacobson K., Boldt K., Frenzel P., Katsonopoulou D., Soter S., Alvarez Zarikian C.A. and H. Brückner. 2016. New sediment cores reveal environmental changes driven by tectonic processes at ancient Helike, Greece. *Geoarchaeology* 31: 140-155.

Goodman-Tchernov B.N., Dey H.W., Reinhardt E., McCoy F. and Y. Mart. 2009. Tsunami waves generated by the Santorini eruption reached Eastern Mediterranean shores. *Geology* 37(10): 943-946 [doi: 10.1130/g25704a.1]

Green P. 1996. The Greco-Persian wars. University of California Press, Berkeley.

Hadler H., Vött A., Koster B., Mathes-Schmidt M., Mattern T., Ntageretzis K., Reicherter K. and T. Willershäuser. 2013. Multiple late-Holocene tsunami landfall in the eastern Gulf of Corinth recorded in the palaeotsunami geo-archive at Lechaion, harbour of ancient Corinth (Peloponnese, Greece). *Zeitschrift für Geomorphologie* N.F., Supplementary Issue 57/4: 139-180 [doi.org/10.1127/0372-8854/2013/S-00138]

Hörhager H. 1973: Zu den Flottenoperationen am Kap Artemision. Chiron, 3/1973: 43-60 [https://publications.dainst.org/journals/chiron/746/5115]

IPCC. 2021. Chapter 9. Ocean, Cryosphere and Sea Level Change. In: Climate Change 2021: The Physical Science Basis. Contribution of Working Group I to the Sixth Assessment Report of the Intergovernmental Panel on Climate Change, pp. 1211–1362 [doi:10.1017/9781009157896.011]

Kelletat D. 1998. Geologische Belege katastrophaler Erdkrustenbewegungen 365 AD im Raum Kreta. In: Olshausen, E., Sonnabend, H. (eds): Naturkatastrophen in der antiken Welt. Stuttgarter Kolloquium zur historischen Geographie des Altertums 6, 1996. *Geographica Historica* 10: 156-161.

Kelletat D., Whelan F., Bartel P. and A. Scheffers. 2005. New Tsunami evidences in Southern Spain Cabo de Trafalgar and Majorca Island. In: Sanjaume, E., Matheu, J.F. (Eds.), Geomorfologia Litoral I Quarternari. Homenatge al professor Vincenç M. Rosselló I Verger. Universitat de València, Spain, pp. 215-222.

Kolaiti E., Papadopoulos G.A., Morhange C., Vacchi M., Triantaphyllou I. and N.D. Mourtzas. 2017. Palaeoenvironmental evolution of the ancient harbor of Lechaion (Corinth Gulf, Greece): Were changes driven by human impacts and gradual coastal processes or catastrophic tsunamis? *Marine Geology* 392: 105–121 [doi.org/10.1016/j.margeo.2017.08.004]

Kraft J.C., Kayan I., Brückner H. and G. Rapp. 2000. A geological analysis of ancient landscapes and the harbors of Ephesus and the Artemision in Anatolia. Jahreshefte des Österreichischen Archäologischen Institutes, 69: 175-232; Wien.

Kraft J.C., Brückner H., Kayan I., Engelmann H. 2007. The geographies of ancient Ephesus and the Artemision in Anatolia. *Geoarchaeology* 22 (1): 121-149; doi.org/10.1002/gea.20151

Ledger M.L., Stock F., Schwaiger H., Knipping M., Brückner H., Ladstätter S. and P.D. Mitchell. 2018. Intestinal parasites from public and private latrines and the harbour canal in Roman Period Ephesus, Turkey (1st c. BCE to 6th c. CE). *Journal of Archaeological Science*: Reports, 21: 289-297; doi.org/10.1016/j.jasrep.2018.07.013

Marzoli D. 2005. Die Besiedlungs- und Landschaftsgeschichte im Empordà: von der Endbronzezeit bis zum Beginn der Romanisierung. Iberia Archaeologica 5, 423 pages; Mainz

Marzoli D., Baños Gómez D., Bouzas Sabater M., Brückner H., Castanyer Masoliver P., Hernández Pastor E., Julià Brugués R., Puig Griessenberger A.M., Santos Retolaza M. and J. Tremoleda Trilla. 2023. Excavaciones arqueológicas en la ciudad griega de Emporion (2018–2021) y el proyecto Groundcheck "Ampurias' Future – Learning from the Past. Sea Level Development and Climate Change from 5500 BC until AD 2100": Informe preliminar. Madrider Mitteilungen, 63/2022, 188–310 [doi.org/10.34780/6985-3kj6]

May S.M. 2010. Sedimentological, geomorphological and geochronological studies on Holocene tsunamis in the Lefkada – Preveza area (NW Greece) and their implications for coastal evolution. Inaugural-Dissertation, Köln (Cologne) [https://kups.ub.uni-koeln.de/3189/2/Dissertation_Simon_Matthias_May.pdf]

May S.M., Vött A., Brückner H. and A. Smedile. 2012. The Gyra wash over fan in the Lefkada Lagoon, NW Greece – possible evidence of the 365 AD Crete earthquake and tsunami. *Earth, Planets and Space* 64: 859-874.

Morhange, Ch.and N. Marriner. 2010. Mind the (stratigraphic) gap: Roman dredging in ancient Mediterranean harbours. Bollettino di Archeologia on line I 2010/ Volume speciale B / B7 / 4, pp. 23-32. https://www.ancientportsantiques.com/wp-content/uploads/Documents/AUTHORS/

Morhange-PublGenerales/Morhange&Marriner2010-Dragages.pdf

Mutaqin B.W., Lavigne F., Hadmoko D.S. and M.N. Ngalawani. 2019: Volcanic eruption-induced tsunami in Indonesia: *A review. IOP Conf. Series: Earth and Environmental Science* 256: 012023 [doi:10.1088/1755-1315/256/1/012023]

Pareschi M.T., Boschi E., Mazzarini F. and M. Favalli. 2006. Large submarine landslides offshore Mt. Etna. *Geophys. Res. Lett*. 33: L13302 [doi:10.1029/2006GL026064]

Pareschi M. T., Boschi E. and M. Favalli. 2007. Holocene tsunamis from Mount Etna and the fate of Israeli Neolithic communities. *Geophys. Res. Lett*. 34: L16317 [doi:10.1029/2007GL030717]

Pulak C., Ingram R. and M.R. Jones. 2015: Eight Byzantine shipwrecks from the Theodosian harbour excavations at Yenikapı in Istanbul, Turkey: an introduction. *The International Journal of Nautical Archaeology* (2015) 44.1: 39–73doi: 10.1111/1095-9270.12083

Reicherter K., Prados F., Jiménez-Vialás H., García-Jiménez I., Feist L., Val-Peón C., Höbig N., Mathes-Schmidt M., López-Sáez J.A., Röth J., Alexiou S., Silva Barroso P.G., Cämmerer C., Borau L., May S.M., Kraus W., Brückner H. and C. Grützner. 2022. The Baelo Claudia tsunami archive (SW Spain) – archaeological deposits of high energy events. In: Álvarez-Martí-Aguilar, M., Machuca Prieto, F. (eds.), Historical Earthquakes, Tsunamis and Archaeology in the Iberian Peninsula. Chapter 13, pp. 313-344. Natural Science in Archaeology. Springer Nature Singapore, Singapore [https://doi.org/10.1007/978-981-19-1979-4_13].

Roig-Munar F.X., Rodríguez-Perea A., Vilaplana J.M., Martín-Prieto J.A. and B. Gelabert. 2019. Tsunami boulders in Majorca Island (Balearic Islands, Spain). *Geomorphology* 334: 76-90.

Roig-Munar F.X., Gelabert B., Rodríguez-Perea, A., Martín-Prieto J.A. and J.M. Vilaplana. 2023. Storm or tsunamis: Boulder deposits on the rocky coasts of the Balearic Islands (Spain). Marine Geology 463, 107112 [doi.org/10.1016/j.margeo.2023.107112]

Schielein P., Zschau J., Woith H. and G. Schellmann. 2007. Tsunamigefährdung im Mittelmeer – Eine Analyse geomorphologischer und historischer Zeugnisse. *Bamberger Geogr. Schr*. 22: 153-199.

Schwarzbauer J., Stock F., Brückner H.,Dsikowitzky, L. and M. Krichel 2018 . Molecular organic indicators for human activities in the Roman harbor of Ephesus, Turkey. *Geoarchaeology* 33: 498-509; doi.org/10.1002/gea.21669

Seeliger M., Pint A., Frenzel P., Marriner N., Spada G., Vacchi M., Başaran S., Dan A., Seeger F., Seeger K., Schmidts T and H. Brückner. 2021. Mid- to late-Holocene sea-level evolution of the northeastern Aegean Sea. The Holocene, 31(10): 1621-1634 [doi.org/10.1177/09596836211025967]

Silva P.G., Reicherter K., García-Jiménez, I., Prados Martínez, F., Pérez-Tarruella, J. and Y. Sánchez-Sánchez. 2023. Geología y Arqueología del Terremoto-Tsunami de finales del Siglo IV d.C. que destruyó la ciudad Romana de Baelo Claudia (Cádiz, Sur España). Cuaternario y Geomorfología, 37: (3-4), 37-57 [https://doi.org/10.17735/cyg.v37i3-4.102693]

Steskal M. 2017. Reflections on the mortuary landscape of Ephesus: The archaeology of death in a Roman metropolis. In: Brandt, J.R., Hagelberg, E., Bjørnstad, G. & S. Ahrens (eds.): Life and death in Asia Minor in Hellenistic, Roman, and Byzantine times. Studies in *Archaeology* and Bioarchaeology, Studies in Funerary *Archaeology* 10: 176-187.

Stock F., Pint A., Horejs B., Ladstätter, S. and H. Brückner. 2013. In search of the harbours: New evidence of Late Roman and Byzantine harbours of Ephesus. Quaternary International, 312: 57-69; doi.org/10.1016/j.quaint.2013.03.002

Stock F., Kerschner M., Kraft J.C., Pint A., Frenzel P. and H. Brückner. 2014. The palaeogeographies of Ephesos (Turkey), its harbours, and the Artemision – a geoarchaeological reconstruction for the timespan 1500 – 300 BC. Zeitschrift für Geomorphologie, 58 (Suppl. 2): 33-66; doi.org/10.1127/0372-8854/2014/S-00166

Stock F., Knipping M., Pint A., Ladstätter S., Delile H., Heiss A.G., Laermanns H., Mitchell P.D., Ployer R., Steskal M., Thanheiser U., Urz R., Wennrich V. and H. Brückner. 2016. Human impact on Holocene sediment dynamics in the Eastern Mediterranean – the example of the Roman harbour of Ephesus. Earth Surface Processes and Landforms, 41: 980-996; doi.org/10.1002/esp.3914

Stock F., Halder St., Opitz St., Pint A., Seren S., Ladstätter S. and H. Brückner. 2019. Late Holocene coastline and landscape changes to the west of Ephesus, Turkey. *Quaternary International* 501: 349-363; doi.org/10.1016/j.quaint.2017.09.024

Stock F., Laermanns H., Pint A., Knipping M., Wulf S., Hassl A.R., Heiss A.G., Ladstätter S., Opitz St., Schwaiger H. and H. Brückner. 2020. Human-environment interaction in the hinterland of Ephesos – as deduced from an in-depth study of Lake Belevi, west Anatolia. *Quaternary Science Reviews* 244: 106418 [doi.org/10.1016/j.quascirev.2020.106418]

Vött A., Brückner H., Schriever A., Handl M., Besonen M. and K. van der Borg. 2004. Holocene coastal evolution around the ancient seaport of Oiniadai, Acheloos alluvial plain, NW Greece. In: G. Schernewski & T. Dolch (Hrsg.): Geographie der Meere und Küsten. *Coastline Reports* 1: 43-53; Warnemünde.

Vött A. and H. Brückner. 2006. Versunkene Häfen im Mittelmeerraum. Antike Küstenstädte als Archive für die geoarchäologische Forschung. *Geographische Rundschau* 58 (4): 12-21; Braunschweig.

Vött A., May M., Brückner H. and S. Brockmüller. 2006. Sedimentary evidence of Late Holocene Tsunami events near Lefkada Island (NW Greece). Zeitschrift für Geomorphologie N.F., Suppl.-Vol. 146: 139-172.

Vött A., Brückner H. and J.C. Kraft. 2017. Do mythological traditions reflect past geographies? The Acheloos delta (Greece) and the Artemision (Turkey) case studies. Zeitschrift für Geomorphologie, 61 (Suppl. 1): 203-221.

Vött A., Hadler H., Koster B., Mathes-Schmidt M., Röbke B.R., Willershäuser T. and K. Reicherter. 2018. Returning to the facts: Response to the refusal of tsunami traces in the ancient harbour of Lechaion (Gulf of Corinth, Greece) by 'non-catastrophists' – Reaffirmed evidence of harbour destruction by historical earthquakes and tsunamis in AD 69-79 and the 6th cent. AD and a preceding pre-historical event in the early 8th cent. BC. *Zeitschrift für Geomorphologie* N.F. 61/4: 275-302 [doi.org/10.1127/zfg/2018/0519]

Wolf A. 2009. Homers Reise: Auf den Spuren des Odysseus. 410 p., Köln.

Zhou Y., Niu X., Liu H., Zhao G. and X. Ye. 2023. Tsunami waves induced by the atmospheric pressure disturbance originating from the 2022 volcanic eruption in Tonga. *Applied Ocean Research*, vol. 130, 103447 [https://doi.org/10.1016/j.apor.2022.103447]

Appendices

Appendix A

Historical sources about delta advance and landlocking of islands

There are historical sources that well describe the process of delta progradation, with the effect of the islands becoming landlocked. Concerning the former islands of Hybanda in the hinterland of Miletus and of Syrie near Ephesos, Pliny the Elder (23/4 – 79 AD) writes c. 77 AD in his encyclopedic "Natural History": "Again she [natura, 'nature'] has taken islands from the sea and joined them to the land. .... Hybanda, once an Ionian island, is now 200 stadia from the sea, Ephesus has Syrie as part of the mainland... (Pliny, N.H. 2.204; trans. H. Rackham 1967). The distance Pliny gives (200 stadia, *i.e.* 36 km) is a rhetorical exaggeration; according to our research the maximum distance in the 1st century AD was only 112 stadia (about 20 km) (*cf.* Brückner 2020, footnote 14). Elsewhere he accurately describes the process of landlocking: "From these [rivers] comes a quantity of mud which advances the coastline and has now joined the island of Syrie on to the mainland by the flats interposed" (N.H. 5.115) (*cf.* Brückner 2020).

Appendix B

Possible route of Odysseus as interpreted from Homer's epic Odyssey

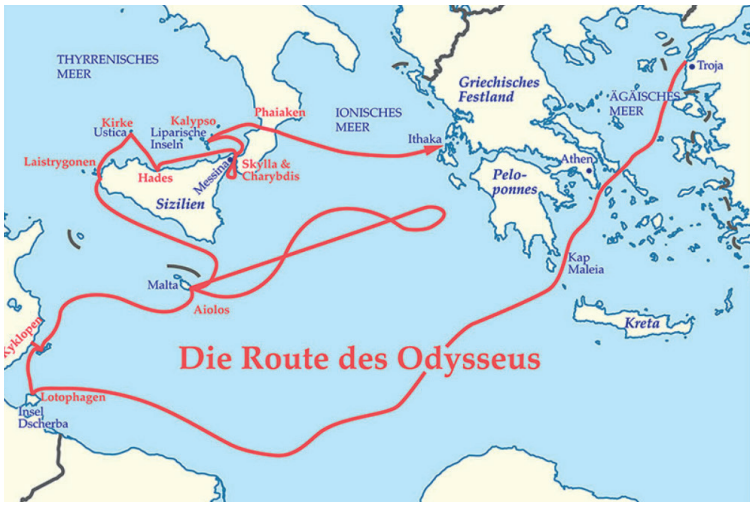

The attempt to reconstruct the route taken by Odysseus on his odyssey from Troy to Ithaca.
Source: Wolf (2009). Quoted from: https://jurclass.de/jurclass/ sachthemen/griechisch/homer/ odyssee/route-odysseus.html

Appendix C1

A storm destroys Xerxes' first ship bridge over the Hellespont (Dardanelles)

After the defeat at Marathon in 490 BC, Xerxes I (519 – 465 BC) launched a campaign of revenge against Greece in 480 BC. To cross the Hellespont, the strait separating Europe from Asia Minor at the northern end of the Aegean, he had built an extraordinary ship bridge, allegedly consisting of 700 ships. According to Herodotos (7,21.25), the first attempt went wrong. When the bridge was ready, a violent storm arose and tore everything apart. Xerxes had the unfortunate engineers beheaded. The building of the bridge then began anew under the direction of other master builders who were more fortunate (see Fig. 6 left above).

Appendix C2

Naval battle of Artemision between the Greek and Persian fleets (early September 480 BC)

"When darkness came, the season being midsummer, there was abundant rain all night and violent thunder from Pilion. … The crews of the ships that were there were dismayed at the noise of this, and, considering their present bad condition, expected to be utterly destroyed; for before they had recovered from the shipwreck and the storm off Pelion, they endured a fierce naval battle, and after the naval battle, rushing rains and mighty torrents pouring over the sea, and violent thunderings.

So the night dealt with them. But for those who sailed around Euboea, the same night was even crueler, for it caught them on the open sea. Their end was terrible, for when the storm and rain came upon them as they sailed from the caves of Euboea, they were driven by the wind in an unknown direction and struck the rocks."

Herodotus, Book 8, extract from chapters 12 and 13, transl. A.D. Godley. Cambridge. Harvard University Press. 1920; slightly modified.

Appendix C3

Sinking of the Persian fleet on the cliffs of the Athos peninsula (autumn 492 BC)

"Crossing over from Thasos, they [the Persian fleet] travelled close to the land as far as Acanthus, and from there they tried to encircle Athos. But a great and irresistible northerly wind came upon them as they passed, and dealt them very harshly, driving many of their ships into Athos. It is said that about three hundred ships and more than twenty thousand men were lost. As the coasts of Athos are full of wild beasts, some of the men were carried off by the beasts and thus perished; others were dashed against the rocks; those who could not swim perished by this, and still others by the cold."

Herodotus, Book 6, from Chapter 44; transl. A.D. Godley. Cambridge. Harvard University Press. 1920; slightly modified

Appendix D1

Extract from Acts of the Apostles, 27:13 – 28:1, New English Translation (NET)

13 When a gentle south wind sprang up, they weighed anchor and sailed close along the coast of Crete.
14 Not long after this, a hurricane-force wind[a] called the northeaster[b] blew down from the island.
15 When the ship was caught in it[c] and could not head into the wind, we gave way to it and were driven along... 27 When the fourteenth night had come, while we were being driven across the Adriatic Sea, about midnight the sailors suspected they were approaching some land… 39 When day came, they did not recognize the land, but they noticed a bay with a beach, where they decided to run the ship aground if they could. 41 But they encountered a patch of crosscurrents and ran the ship aground; the bow stuck fast and could not be moved, but the stern was being broken up by the force of the waves.
43 The centurion ordered those who could swim to jump overboard first and get to land, 44 and the rest were to follow, some on planks and some on pieces of the ship. And in this way all were brought safely to land. 1 After we had safely reached shore, we learned that the island was called Malta (Melite).

[a] "a wind like a typhoon". That is, a very violent wind like a typhoon or hurricane (τυφωνικός).

[b] Or called Euraquilo (the actual name of the wind, a sailor's term which was a combination of Greek and Latin). According to Strabo (Geography 1.2.21), this was a violent northern wind.

[c] Or "was forced off course".

Appendix D2

Reconstruction of the Apostle Paul's sea voyage to Rome according to Warnecke (2000).

Western section of the Apostle Paul's route on his way to Rome.

Heinz Warnecke argues that the apostle was not shipwrecked on the island that still today bears the name of Malta, but on the island of Cephalonia or Kefallinia (Greek: Κεφαλονιά), which in ancient times was also called "Melite".

Source: Warnecke, H. (2000): Paulus im Sturm, S. 89.

The ship was wrecked on a sandy coast of Malta (Melite). There is some disagreement as to where "Malta" or "Melite" was located. Based on historical sources, nautical (ocean currents) and meteorological (wind systems) data, Warnecke (2000) argues that the island of Paul's shipwreck was not the one still known today as Malta, but the island of Kefalonia or Cephalonia (Greek: Κεφαλονιά), the largest of the Ionian islands in western Greece, which in ancient times was also called "Melite".

Appendix E

The fate of Helike in ancient sources

In his chapter about Helike Holger Sonnabend (1999, 1-9) quotes and comments the ancient sources. The prominent one of the ancient Greek historian Diodoros (Latin: Diodorus) from the first half of the 1st century BC has already been mentioned above (*cf.* section 3.3). The following is taken from his book about perception and interpretation of natural disasters in Antiquity (Sonnabend 1999, excerpt from pages 1-9; translated from German and slightly modified).

According to the Greek historian and geographer Strabo, the city was twelve stadia (just over two kilometres) from the sea. And yet the whole area disappeared into the sea with the city. Strabo corrects Diodorus' version in one important detail: there was not one night between the earthquake and the tidal wave, but both events occurred simultaneously.

The Greek travel writer Pausanias (7,24,6.7,24,12.7,25,8-9) visited the area of the former Helike in the 2nd century AD. In his text, the earthquake and the sea wave are also contemporaneous events: The sea "washed Helike round about. And the waters also flooded the grove of Poseidon so high that only the tops of the trees were visible... The sea wave swallowed up Helike and its inhabitants".

It is interesting to note that Helike's neighbour city, Bura, which is situated in the mountains at an altitude of 500 metres, about seven kilometres from the sea, also disappeared in the same catastrophe. The naturalist Pliny (N.H. 2.206) noted in the 1st century AD: "Pyrrha and Antissa on the Mareotic Sea were swallowed by the Pontus, Helike and Bura by the Gulf of Corinth, the traces of which are still visible in the depths." Strabon (8,7,2) says that Bura "was swallowed

up by an earthquake". Pausanias confirms that Bura "was struck by a violent earthquake, so that not even the ancient statues in the sanctuaries remained". This argues against a tsunami and in favour of a massive landslide – triggered by the severe earthquake of 373 BC.

Additional References for the Appendices

Brückner H. 2020. Deltas, floodplains, and harbours as geo-bio-archives. Human-environment interactions in western Anatolia. *Göttinger Studien zur Mediterranen Archäologie*, 9: 37-50 + Tafeln 3-6; Verlag Marie Leidorf GmbH, Rahden/Westf.

Sonnabend H. 1999. Naturkatastrophen in der Antike: Wahrnehmung – Deutung – Management. Stuttgart & Weimar.

Warnecke, H. 2000. Paulus im Sturm. Über den Schiffbruch der Exegese und die Rettung des Apostels auf Kephallenia. Mit einem Geleitwort von Walther Hinz und einem Beitrag von Thomas Schirrmacher. Nürnberg.

Geohazard trends from submarine landslides and related tsunamis, a geological perspective and implications for present climate change.

R. Urgeles[1], S. Beyer[2], A. Cattaneo[3], M. de Gail[2], D. Gamboa[4], R. León[5], F. Løvholt[2], M. Vanneste[2], C. Vila[1]

[1]Institut de Ciències del Mar (CSIC), Barcelona, Spain (urgeles@icm.csic.es, carla.vila.f@gmail.com)
[2]Institut français de recherche pour l'exploitation de la mer (IFREMER), Brest, France (Antonio.Cattaneo@ifremer.fr)
[3]Universidade de Aveiro, Aveiro, Portugal (dgamboa@ua.pt)
[4]Instituto Geológico y Minero de España (CSIC), Madrid, Spain (r.leon@igme.es)
[5]Norges Geotekniske Institutt, Oslo, Norway (sjur.beyer@ngi.no, myriam.de.gail@ngi.no, Finn. Lovholt@ngi.no, Maarten.Vanneste@ngi.no)

Abstract

Analysis of the Euro-Mediterranean Submarine landSlide (EMSS) database in this study aims to review the role of past climate change in submarine landslide occurrence in the Mediterranean basin and reason how future trends may evolve given climate change. The development version of the catalogue includes polygons and polylines for the landslide deposits, landslide source areas and landslide scars. The catalogue shows that submarine landslides are widely present throughout the entire Mediterranean Sea, although tectonically active areas of the basin display smaller events. In the entire database, only few events (776) are reported with an age period and only 141 are reported with a numerical age. The trend that emerges when analyzing the number of landslides and flux of sediment from submarine landslides at various temporal scales is that of an increasing number and flux of sediment through time. We find that the database is biased towards younger and smaller landslides at different levels, which makes assessment of temporal trends difficult. Assuming the database is complete for the last 30 ka, particularly for events larger than 1 km^3, we find clustering during the Holocene. Onset of submarine slope failure during times of warming climate (and sea level rise) include gas hydrate dissociation and dissolution and increased seismicity from flexural bending stresses related to rising sea level. Despite present limited extent of gas hydrates in the Mediterranean basin, these are the mechanisms that are likely to function given anthropogenic global warming and further rise in sea level. Nevertheless, it is unlikely that any significant changes will be experienced in the short term given the rates of the various factors involved in these processes.

Keywords: *offshore geohazards, submarine landslides, tsunami, landslide catalog, hazard trends*, *global warming*

Introduction

Submarine landslides occur in all ocean basins (Hühnerbach and Masson 2004; Chaytor *et al.* 2009; Harders *et al.* 2011; Gamboa *et al.* 2022) and the Mediterranean Sea is no exception (Urgeles and Camerlenghi 2013). They are also capable of mobilizing hundreds of km^2 of seafloor while moving downslope hundreds of km (e.g., Masson *et al.* 1998; Chaytor *et al.* 2009) and may cause tsunami (Harbitz *et al.* 2006; Løvholt *et al.* 2015) with challenging early-warning potential (Baptista 2024). Therefore, they represent significant hazard. In fact, about

15% of all tsunamis worldwide are caused by submarine landslides or landslides entering a body of water (Harbitz *et al.* 2014), and the number may even be negatively biased due to the lack of reporting such events in the past. There are several examples of historical landslide generated tsunamis in the Mediterranean Sea such as the 1783 Scilla landslide tsunami (Wang *et al.* 2019), the 1954 Algerian margin event (El-Robrini *et al.* 1985), the catastrophic 1979 event off Nice, France (Ioualalen *et al.*, 2010) and the Stromboli collapse of 2003 (Fornaciai *et al.* 2019). The existence of significantly larger submarine landslides in the late Quaternary record of the Mediterranean Sea is a warning of the hazard and risk posed by such events. The sheer size implies that these events may potentially be catastrophic, yet the rarity of historical incidents means that risk perception and preparedness are rather reduced (Bertoldo 2024).

Submarine landslides occur due to both long-term and short-term factors. Some of these factors are essentially uncorrelated to climate change (e.g., earthquakes at subduction zones), while others are strongly correlated (e.g., sea level variation, precipitation, sedimentary supply) and may induce time-clustering of events at periods of rapidly changing environmental conditions. Possible controls on the timing of sediment failure, particularly on high latitude continental margins, include also climatically controlled processes such as glacial and/or groundwater loading. It should be noted, however, that submarine landslides most often occur due to a combination of factors (Løvholt *et al.* 2022).

As pointed by the Intergovernmental Panel On Climate Change (IPCC), global warming is unequivocal and its effects on the natural environment may be multiple but difficult to accurately determine. The six synthesis reports of the Intergovernmental Panel on Climate Change (Calvin *et al.* 2023) do not provide a global overview on landslides. Landslides (onshore) are considered in the IPCC special report on "Impacts, Adaptation and Vulnerability" (2023), which expresses medium confidence that, overall, landslides arising from heavy rainfall events will increasingly threaten infrastructure and agricultural production and high confidence that glacial retreat and heavy precipitation will affect landslides in mountain regions. However, there is not such assessment for submarine landslides.

Climate change also induces changes in sea level and the temperature of seafloor sediments; and their influence on slope stability and the occurrence of submarine landslides is still highly debated (e.g., Korup *et al.* 2012; Urlaub *et al.* 2013; Pope *et al.* 2015). The aim of this paper is therefore to review the role of past climate change in submarine landslide occurrence in the Mediterranean basin and to consider how geohazard from submarine landslides and related tsunamis could evolve in the future.

Data and methods

This study is based on the development version of the Euro-Mediterranean Submarine landSlide (EMSS) database, a catalogue of submarine landslides in the Mediterranean Sea and the European continental margins of the Atlantic and Arctic Oceans. The catalogue is compiled from data available in the literature as well as information collected from geophysical data and not published in the scientific literature. A first version of the catalogue has been recently made available online (https://ls3gp.icm.csic.es/?page_id=553) and delivered via OGC services through the EPOS data portal (https://www.ics-c.epos-eu.org/) in the frame of the EU-funded project Geo-Inquire. The version of the catalogue being developed improves areal coverage in the Atlantic Ocean and includes information relative to the source areas of such events (whereas only deposits and scars were considered in the previous version). The new catalogue includes polygons and polylines for the landslide deposits, landslide source areas and landslide scars as

well as information relative to age, volume, area, runout, thickness, typology, scar elevation, deposit thickness, relevant slopes and depths as well as related metadata. The database includes information for 4656 source areas and 1871 deposits of which 2870 and 956 respectively correspond to the Mediterranean-Black Sea basin and Atlantic adjacent areas.

Results

While submarine landslides are widely present throughout the entire Mediterranean Sea, the continental margins to the north of the basin have been more extensively studied and a higher amount of submarine landslides have been mapped there (Fig. 1).

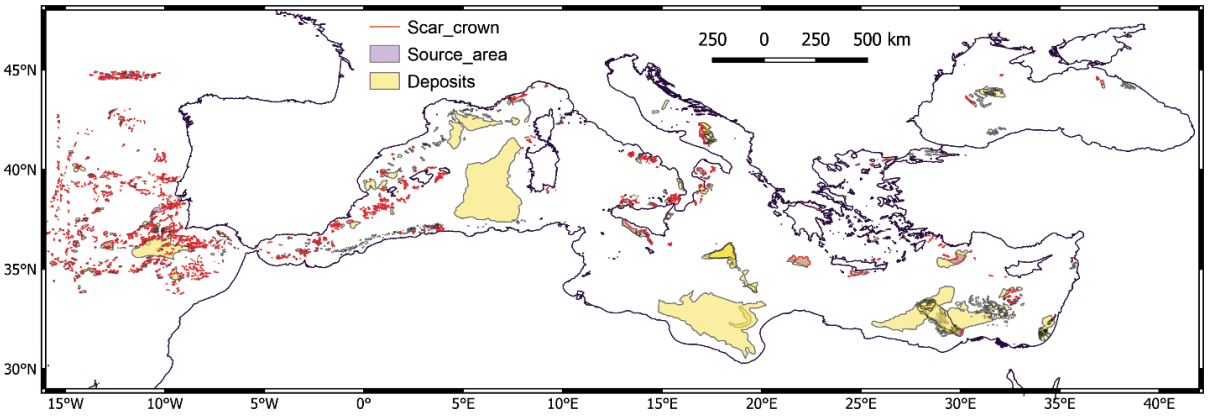

Figure 1. Landslides reported in the Mediterranean Sea and adjacent Atlantic region.

Exceptions to the rule include areas of the southern Mediterranean coast where significant oil exploration activity has taken place such as the Nile delta. Excluding the megabeds associated with extensive turbidite deposits on the abyssal plains, the largest submarine landslides in terms of areal extent and volume correspond to the major sedimentary depocenters such as the Ebro, Rhone, Po and Nile deltas (Fig. 1 and Fig. 2). The most tectonically active areas of the Mediterranean basin display no major landslide events (Fig. 1). The areas where most submarine landslides have been mapped include the Western Mediterranean basin (1603 in total) and the tectonically active areas to the south and east espousing the North Africa-Sicily-Calabria-Apennines thrust belt (1280), followed with one order of magnitude less submarine landslides, by the Mediterranean subduction (134)-Aegean Sea (138) regions (see Fig. 2 and Fig. 3).

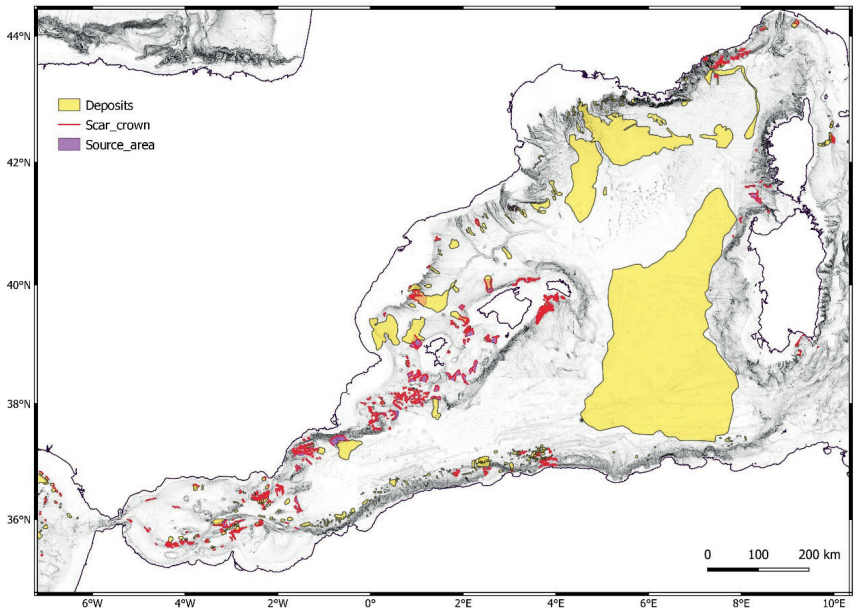

Figure 2. Detail of the EMSS24 in the Western Mediterranean.

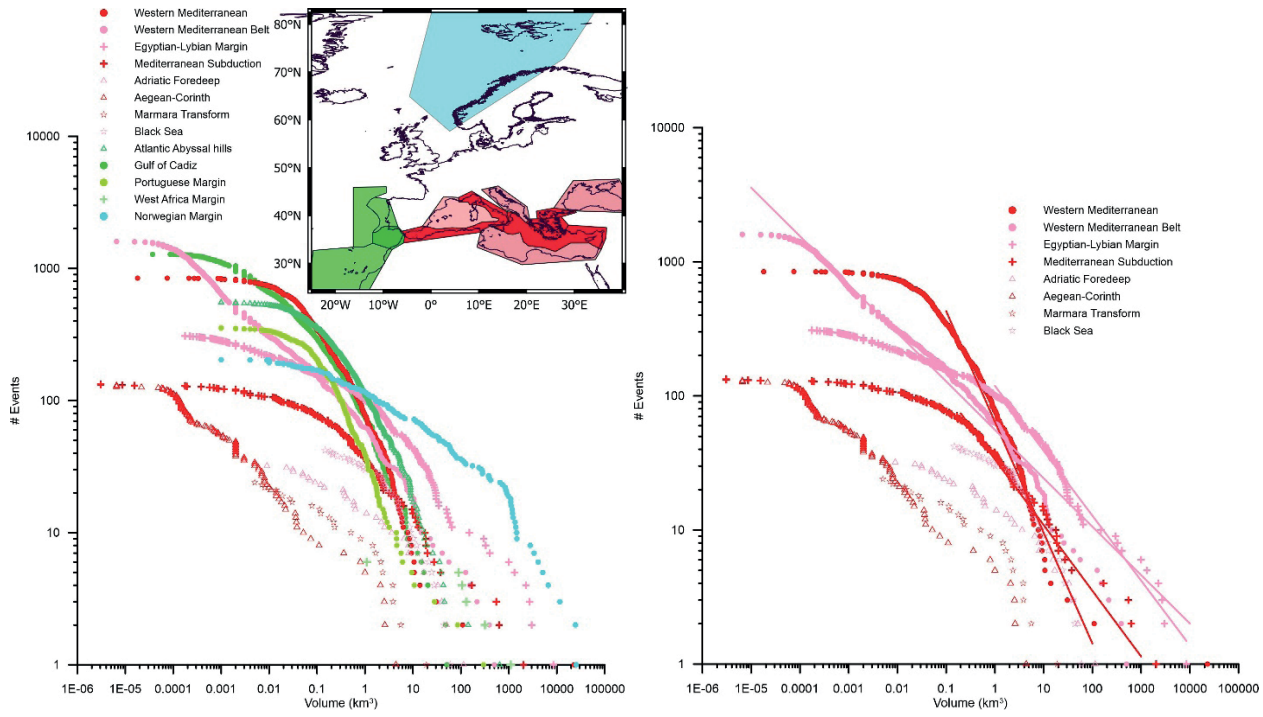

Figure 3. Frequency-magnitude distribution per EMSS24 region (left) and tectonic setting of the Mediterranean Sea (right). Tectonically active areas are shown in red and passive margins are shown in pink.

The frequency (number of events) – magnitude (volume of events) distribution of submarine landslides in the Mediterranean Sea typically displays power-law scaling behavior for the largest landslides and exhibits a roll-over point for smaller-landslides that is believed to result from observational bias (Fig.3). The passive margins generally display a gentler slope of the

frequency-magnitude relationship compared to active margins, which is explained by the paucity of larger submarine landslides and a higher weight from smaller landslides in the overall flux of sediment from smaller landslides in active margins. Power-law scaling relationships can be developed for smaller areas (or subsets of the EMSS) where high-resolution geophysical data is extensively available (Chiocci *et al*. 2024). In such instances, the roll-over point, and most often the entire frequency-magnitude relationship, displaces towards smaller volume landslides highlighting the lack of uniform data density in the database.

Submarine landslides excavate failure scars that may range from a few meters to several hundred meters (Fig. 4). The larger the landslides, the deeper is the excavation in the source area (Fig. 4). Similarly, the larger is the landslide, the thicker is the deposit, although the slope of the Area-to-Volume ratio is not as steep, suggesting also that the larger the landslides the longer the travel distance will be (Fig. 4).

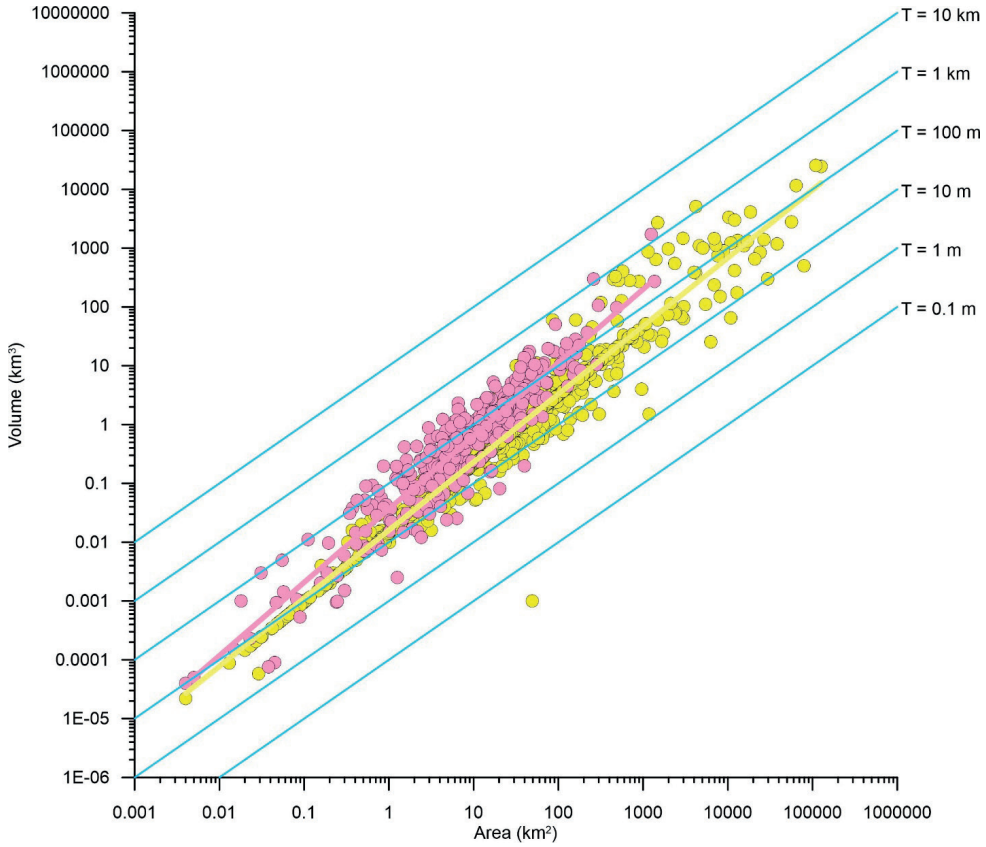

Figure 4. Area-Volume relationship for source areas (pink) and deposits (yellow) of submarine landslides in the EMSS24. Also shown in blue are iso-thickness area/volume relationships.

In terms of landslide distribution with time, few of the 5651 individual events mapped from both the source area and deposits include age information: in the entire database only 1156 events are reported with an age period and, out of these, only 512 are reported with a numerical age. For the Mediterranean Sea these numbers reduce to 776 and 141, respectively. The database includes events from the Miocene Epoch to Present (Fig.5). One notes a clear bias in the

database towards younger landslides. Smaller landslides are also misrepresented for the older geological periods, as these events are difficult to map/identify on lower resolution geophysical data sets typically collected in deep-water and large sub-surface depths. The trend that emerges when analyzing the flux of sediment from submarine landslides is that of an increasing flux of sediment through time from 0.015 km^3/kyr in the early Miocene to almost 10^3 km^3/kyr in the Holocene (Fig 5). Notable exceptions to this trend include the Messinian to Zanclean transition that records a peak at 9.6 km^3/kyr and a subsequent drop to 1.9 km^3/kyr in sediment flux from submarine landslides (Fig.5). This peak is entirely due to landslide activity in the Mediterranean region. An additional peak in Mediterranean landslide activity occurred in the Gelasian but does not translate in the general trend (Fig.5). Overall, the Arctic region displays one order of magnitude higher flux of sediment from submarine landslides, which is not a result of higher landslide activity but of significantly larger events.

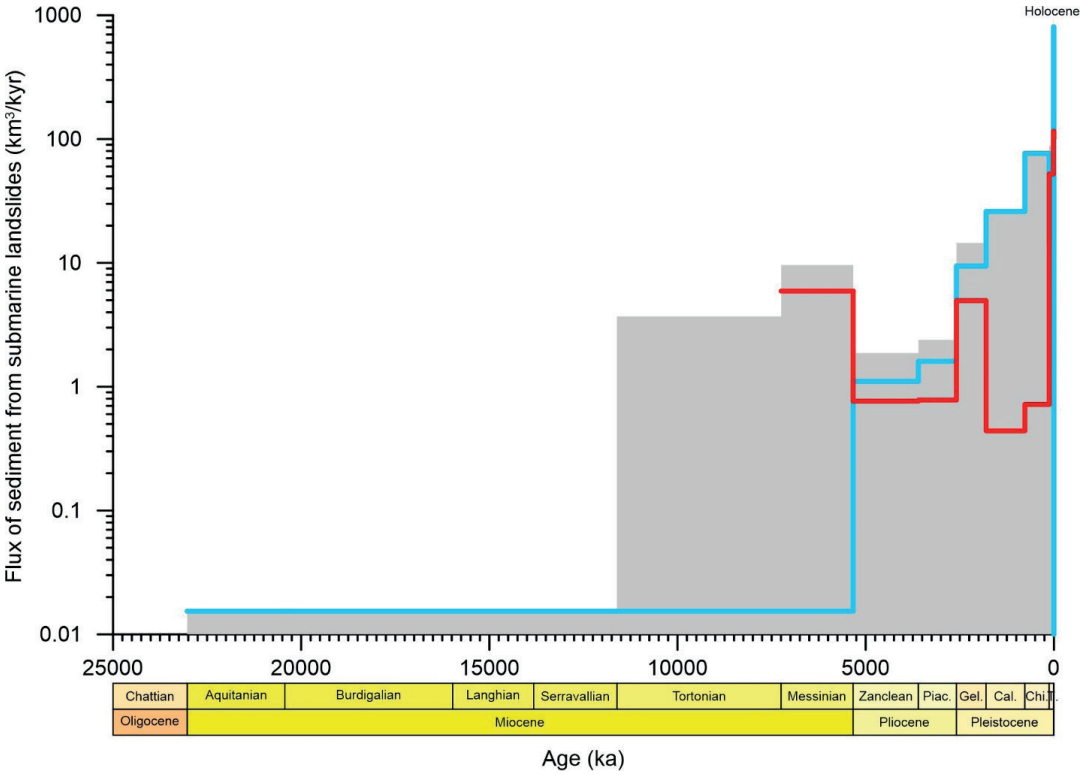

Figure 5. Flux of sediment from submarine landslides derived from the EuroMediterranean Submarine Landslide database (EMSS24) (grey) and separate fluxes for the Norwegian margin /Arctic region (blue) and Mediterranean Sea (red).

More accurate age information is, on most occasions, only available for late Pleistocene to Present submarine landslides (Fig. 6). Nevertheless, the age of these landslides reproduces the pattern displayed in Fig. 5, with younger landslides more frequent than older ones: the number of landslides as well as the flux of sediment from these dated submarine landslides displays significant increase in between 30 to 15 ka (MIS 2), during the latest lowstand period (Fig. 6). The number of events is higher in the Holocene and peaks between 6 and 4 ka, while the flux of sediment is higher during the MIS 2. The number of events reproduces the trend in the entire EMSS catalogue, but the sediment flux pattern is opposite to that displayed by major landslides in the Arctic region where most sediment flux appears during the late Pleistocene

sea level rise and initial Holocene highstand. The number of dated submarine landslides that exceed 1 km3 in volume (potentially less biased than smaller events) displays a similar trend to that of the Mediterranean set of dated events, while the peak in the Holocene is more subdued (Fig. 6). Note that submarine landslides in Fig. 5 and Fig. 6 include only the events that have the relevant age information, i.e., only ~ 1/5th of all events in Fig. 5 and ~1/25th in Fig. 6. In practice, most landslides that have no age information have been mapped from bathymetry data, implying that they have a late Pleistocene to Holocene age in most cases. The number of events in this time interval is therefore much larger than displayed in Fig. 6 and the cumulative flux distribution may also display significant variations, while the overall flux is, at least, one order of magnitude larger.

Submarine landslides in the Mediterranean Sea can be triggered by a number of reasons (Urgeles and Camerlenghi, 2013) that will act to increase the driving stress on the slope or reduce the shear resistance of the slope-forming materials. Most landslides in the Mediterranean Sea appear to occur due to earthquakes or slope erosion, such as in the development of submarine canyons. Indeed ground motions induced by earthquakes provide several historical examples of coastal and submarine slope failure in the Mediterranean (e.g., El-Robrini et al., 1985; Papatheodorou and Ferentinos, 1997; Hasiotis *et al,* 2002; Rathje *et al,* 2004; Chiocci *et al.* 2008; Stanley *et al.* 2014). Climate-controlled sediment deposition, related pore-pressure build-up, and gas hydrate / free gas phase changes may also play a role. Climate control over the occurrence of submarine landslides is also linked with the development of weak layers related to specific environmental and climatic conditions (e.g., the development of condensed sections during high-stand periods (Badhani *et al*. 2020).

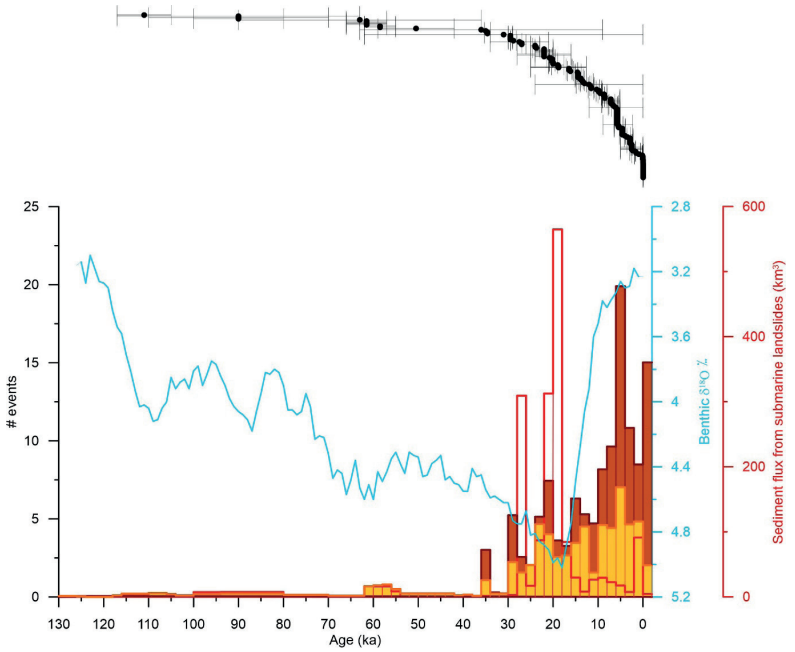

Figure 6. Number of submarine landslide events (brown bars) and events with volume > 1 km^3 (orange bars) binned at 2 kyr intervals. Also plotted is the flux of sediment from submarine landslides binned for the same interval (red empty bars). Submarine landslides refer to events of Pleistocene to Holocene age of the Mediterranean Sea containing age information beyond geological periods. Bins are constructed taking into account the uncertainty interval of ages so that number and volume for a particular event spans several bins with a weight proportional to the time overlap in that particular bin. It is assumed that the probability of the landslide is evenly distributed over the uncertainty interval. Also plotted for

reference is the stack of globally distributed benthic $\delta^{18}O$ records from Lisiecki and Raymo (2005). Top intervals shows individual landslide ages with available uncertainty information.

DISCUSSION

Do submarine landslides in the Mediterranean Sea occur randomly in time?

Analysis of the EMSS catalogue stresses how little we know about the time-distribution of submarine landslides as the catalogue displays clear indications of bias towards younger landslides and, yet, when considering the most recent time intervals (e.g., the Late Pleistocene-Holocene Periods) the bias persists. Similar problems and cautionary statements can be found in Korup *et al.* (2012) and Urlaub *et al.* (2013), based on the analysis of global submarine landslide catalogues.

The bias is apparent when considering the number of events, which significantly increases in MIS 2-1 and peaks in the mid-Holocene (Fig.6). Assuming, like Urlaub *et al.* (2013), that the number of events younger than 30 ka (117) reported in the catalogue is not biased, then we can apply a χ^2 test to assess the goodness of fit of the EMSS to the Poisson distribution, i.e. random occurrence through time. Pope *et al.* (2015) suggest that ~40 well-dated events from a specific environment is a minimum appropriate number to test such an hypothesis and/or links with sea level/climate. If the critical χ^2_{crit} value within a 5% or 10% level of significance exceeds the resulting χ^2 then the data set resembles a Poisson distribution. However, when compared to an artificially-generated Poisson model, the 2 ka binned submarine landslide data have a low correlation coefficient ($R^2 \sim 0$). The χ^2 test returns values of 126.2, which is well above the critical value of 5.991 (5% significance with two degrees of freedom) and 4.605 for a level of significance of 10%. Therefore, the time-distribution of landslides does not resemble a Poisson distribution, suggesting that bias still persists or that their occurrence over time is not randomly distributed (i.e., they cluster at specific intervals).

The above test gives equal weight to landslides of all volumes. A χ^2 test with landslides younger than 30 ka and exceeding volumes of 1 km^3 (n=57, Fig.6), which hold most tsunamigenic and hazard potential, returns values of 22.04 indicating lack of fit to a Poisson distribution as well. However, caution is needed when interpreting those results, as the catalogue suggests that the flux of sediment from submarine landslides, hence the larger events towards which the catalogues is potentially less biased, took place during MIS 2, the Last Glacial Maximum, as opposed to submarine landslides in high-latitude regions of Europe (Norwegian and Barents Sea Margin), where most sediment flux from submarine landslides appears to concentrate in the early Holocene. The Balearic (Rothwell *et al.* 1998; Cattaneo *et al.* 2020) and Herodotus (Reeder *et al.*, 2000) Abyssal Plain megaturbidites, as well as the major debris flows on the Rhone fan (Droz *et al.* 2006) and slope failures recorded in the SW Adriatic (Minisini *et al.* 2006) are the main contributors to such sediment flux in the Mediterranean Sea.

Potential mechanisms for the onset of submarine landslides during cold to warm climatic transitions

The time-distribution pattern of submarine landslides in the Mediterranean Sea, when compared to that of high-latitude margins, points to similar causal mechanisms. However climate likely has higher influence in high-latitude regions where sediment reaching the slope and the type of sediment are strongly controlled by ice-advance and retreat (Llopart *et al.* 2015; 2019). Indeed, one of the main conclusions of the Ormen Lange gas field development project, which happens

to be right in the middle of the giant Storegga Slide on the Norwegian continental margin, is that another glaciation is needed for a landslide volume of this order of magnitude to occur again (Bryn *et al.* 2005).

Because the Mediterranean Sea lacked major ice sheets over the continental shelf during glacial maxima, we need to find alternative factors for the potential submarine landslide cluster in the Holocene. Several papers emphasize that climate and sea level likely played a role in the generation of submarine landslides. Brothers *et al.* (2013) propose that eustatic sea-level rise has the potential to induce flexural bending stresses on the underlying plate that modulates seismicity, suggesting that rapid sea-level rise between ca. 15 and 8 ka promoted a rupture of passive margin fault systems, which in turn may have triggered landslides on the adjacent continental slopes and upper rises. Earthquakes are the most commonly cited mechanism for the initiation of slope failure in the Mediterranean Sea (Fig.7).
Urgeles and Camerlenghi (2013) proposed that relatively small earthquakes could trigger large-magnitude slope failures if the right conditions are set, advancing that a steady accumulation of sediments and buildup of specific slope conditions is a necessary prerequisite for large submarine landslides to occur. These conditions were likely found during cold low-stand periods, when depocenters shifted offshore and deposition rates were the highest.

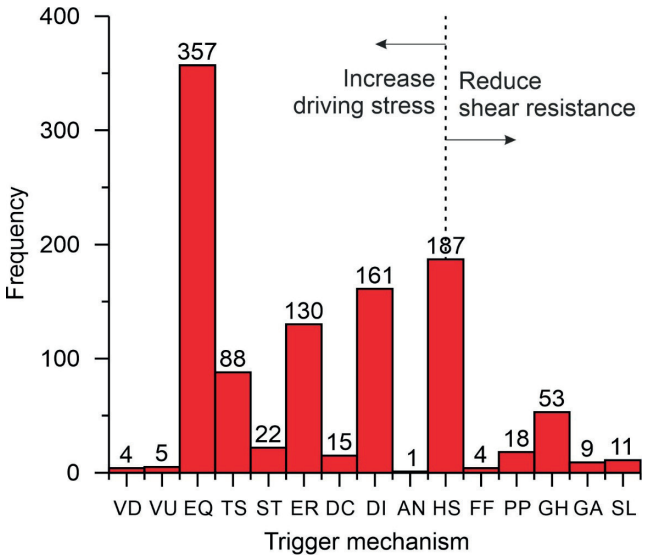

Figure 7. Factors cited to be involved in triggering offshore slope failures of the Mediterranean Sea (Urgeles and Camerlenghi, 2013) (VD: volcano development, VU: volcano uplift, EQ: earthquake, TS: Tectonic steepening, ST: Steepening, ER: Erosion, DC: differential compaction, DI: diapirism, AN: anthropic, HS: high sedimentation rates, FF: fluid flow, PP: pore pressure, GH: Gas hydrates, GA: Gas, SL: sea level).

Onset of submarine landslides may be influenced by past climate change through variations in sea level (stress) and near-seafloor temperature e.g., Sultan *et al.* 2004b when sediments bear gas hydrates (Brewer *et al.*, 1998). These changes in P-T can result in the dissociation and dissolution of the gas hydrates (Sultan *et al.* 2004b), or in gas exsolution and expansion in the case of free

gas (e.g., Lafuerza *et al.* 2012; Riboulot *et al.*, 2013; Gross *et al.* 2018). Such phase changes may induce excess pore pressure and/or degradation of sediment mechanical properties, leading to seafloor instability (Grozic 2010; Riboulot *et al.* 2013). In the context of current climate change, an increase in bottom water temperature, when propagated through the sedimentary column, will induce the dissociation of gas hydrates at the bottom of the gas hydrate stability zone (Nixon and Grozic, 2007), while rising sea level will cause the dissolution of gas hydrates at the top of the gas hydrate occurrence zone. Dissociation in turn will promote pore pressure build up at the base of the gas hydrate stability zone, while dissolution may induce a significantly weakened underconsolidated sediment due to the loss of hydrate cementation and pore pressure increase following soil structure collapse (Sultan *et al.* 2004a). Both mechanisms may contribute to a submarine slope failure. Nevertheless, occurrence of gas hydrates in the Mediterranean Sea is rather scarce and limited to the Black Sea, Marmara Sea and the eastern Mediterranean (León *et al.* 2021). It has been shown that a combination of geological (widespread interstitial brines and high heat flow) and oceanographic factors limits the theoretical stability field of methane in the subsurface of the Mediterranean Sea (Camerlenghi *et al.* 2022). Only the Black Sea, where evaporites did not form during the Messinian (Tari *et al.* 2015), displays significant potential for gas hydrate occurrence.

Cooler bottom water during MIS2 in the entire basin implied a higher potential for gas hydrate occurrence (Praeg *et al.* 2011) which could have vanished under present climatic conditions. During the passage from colder to warmer climatic conditions, trends in sediment deposition rates, migration of depocenters to the continental shelf, ground water flow and total stress changes in gassy sediments due to sea level rise, will likely stabilize the seafloor, as opposed to the above mechanisms.

How could submarine landslide trends evolve under current anthropogenic climate change?

The effects of global climatic changes on geohazards such as submarine landslides remain difficult to determine and to predict, but they can be pondered based on the geological record which displays conflicting evidence (given the many reservations regarding bias observed at different scales). The trends in the number of events point to potentially increasing rates of submarine landslide activity while the fluxes of sediment from submarine landslides support the occurrence of major events during low sea level. Analyzing the trends in landslides with $V > 1km^3$ balances out the two approaches supporting clustering in the Holocene. However, the rate at which such submarine landslides occur is rather low (minimum of one event of $V > 1km^3$ every 350 yrs, although 200 yrs is a more realistic approximation). On the short term (100s of years), it will be difficult to detect significant deviations from the current seismicity rate that point to increasing earthquake occurrence from flexural bending stresses, given the recent rates of sea level rise estimated at 3.6 mm/yr for the period 2000-2018 (Calafat *et al.* 2022). It is only in the long term (likely 1000s of yrs) that such a trend may emerge. Further, there is insufficient evidence that thermal perturbations may propagate rapidly enough in seafloor sediments to induce the pore pressure that promotes seafloor failure, as the scales of seafloor temperature and stress (sea level) variations have similar rates to that of pore pressure dissipation ensuing build-up from dissociation or dissolution of gas hydrates (Archer, 2007). Pore pressure influence on slope systems will be largely determined by local factors such as sediment hydromechanical properties and slope conditions. Also, such effects may only play a role in the eastern Mediterranean, Black and Marmara Seas, where those gas hydrates are present.

Conclusions

Analysis of the developing version of the EMSS submarine landslide database shows that submarine landslides are widely present in the Mediterranean Sea. In general, passive margins display fewer but larger landslides compared to tectonically active margins. Assuming that landslides are random in time, this translates in lower slope of the frequency-magnitude (volume) relationship for passive margins.

Assessing the time distribution of submarine landslides in more detail, we find that the database is biased towards younger and smaller landslides at different levels. It is more complete, however, for the last 30 ka, particularly for events larger than 1 km^3 which pose the largest tsunami threat. The number of events for that period is significantly higher for the last 15 kyrs, although the highest sediment flux from submarine landslides occurs during the 30-15 ka period during cold low-stand conditions. A χ^2 test to assess the goodness of fit to the Poisson distribution suggests that submarine landslides do not occur randomly in time but occur rather clustered (unless some bias still persists in the data).

The mechanisms likely involved in the onset of submarine slope failure during the passage of a cold to a warm period (sea level low-stand to high-stand) include gas hydrate dissociation and dissolution and increased seismicity from flexural bending stresses related to rising sea level (given that certain conditions were built in the previous low-stand sea level). These are the mechanisms that are likely to function under anthropogenic global warming and further rising sea level, although it appears unlikely that any significant changes will be experienced in the short term given the rates of the various factors involved in these processes.

More robust assessments of submarine landslide hazard driven by climate change will require more complete long-term records of previous events and additional studies (almost of exploratory nature) offshore developing countries to fill gaps in available catalogues. The developing EMSS may form the seed for the world ocean submarine landslide database and we encourage the offshore geohazards community to contribute to enlarge the database

Acknowledgements

The EMSS24 is developed in the frame of project Geo-INQUIRE, which is funded by the European Commission under project number 101058518 within the HORIZON-INFRA-2021-SERV-01 call.

To be cited as:

R. Urgeles, S. Beyer, A. Cattaneo, M. de Gail, D. Gamboa, R. León,, F. Løvholt, M. Vanneste, C. Vila. 2024. Geohazard trends from submarine landslides and related tsunamis, a geological perspective and implications for present climate change. p 57- 72. In CIESM Monograph 52 [F. Briand, Ed.] Marine hazards, coastal vulnerability, risk (mis)perceptions – a Mediterranean perspective. CIESM Publisher, Paris, Monaco, 182 p.

References

Archer D. 2007. Methane hydrate stability and anthropogenic climate change 2007. *Biogeosciences* 4: 521–544. doi:10.5194/bg-4-521-2007

Badhani S., Cattaneo A., Collico S., Urgeles R., Dennielou B., Leroux E., Colin F., Garziglia S., Rabineau M., Droz L. 2020. Integrated geophysical, sedimentological and geotechnical investigation of submarine landslides in the Gulf of Lions (Western Mediterranean). *Geological Society*, London, *Special Publications* 500: 359–376. doi:10.1144/SP500-2019-175

Baptista M.A. 2024. From Sumatra 2004 to Tonga 2022: Progress and Challenges of Tsunami Early Warning Systems. pp 89 - 96. In: Marine hazards, coastal vulnerability, risk (mis)perceptions – a Mediterranean perspective. CIESM Workshop Monograph n°52 [F. Briand, Ed.], 182 p., CIESM Publisher, Paris, Monaco.

Bertoldo R. 2024. Psychosocial factors around coastal risk management. pp 167 - 174. In: Marine hazards, coastal vulnerability, risk (mis)perceptions – a Mediterranean perspective. CIESM Workshop Monograph n°52 [F. Briand, Ed.], 182 p., CIESM Publisher, Paris, Monaco.

Brewer P.G., Orr Franklin M., Friederich G., Kvenvolden K.A., Orange D.L. 1998. Gas Hydrate Formation in the Deep Sea: In Situ Experiments with Controlled Release of Methane, Natural Gas, and Carbon Dioxide. *Energy & Fuels* 12: 183–188. doi:10.1021/ef970172q

Brothers D.S., Luttrell K.M., Chaytor J.D. 2013. Sea-level–induced seismicity and submarine landslide occurrence. *Geology* 41: 979–982. doi:10.1130/G34410.1

Bryn P., Berg K., Stoker M.S., Haflidason H., Solheim A. 2005. Contourites and their relevance for mass wasting along the Mid-Norwegian Margin. *Marine and Petroleum Geology* 22: 85–96. doi:10.1016/j.marpetgeo.2004.10.012

Calafat F.M., Frederikse T., Horsburgh K. 2022. The Sources of Sea-Level Changes in the Mediterranean Sea Since 1960. *Journal of Geophysical Research: Oceans* 127, e2022JC019061. doi:10.1029/2022JC019061

Calvin K., Dasgupta D., Krinner G., Mukherji A., Thorne P.W., Trisos C., Romero J., Aldunce P., Barrett K., Blanco G., Cheung W.W.L., Connors S. and 108 others. 2023. IPCC, 2023: Climate Change 2023: Synthesis Report. Contribution of Working Groups I, II and III to the Sixth Assessment Report of the Intergovernmental Panel on Climate Change [Core Writing Team, H. Lee and J. Romero (eds.)]. IPCC, Geneva, Switzerland. Intergovernmental Panel on Climate Change (IPCC). doi:10.59327/IPCC/AR6-9789291691647

Camerlenghi A., Corradin C., Tinivella U., Giustiniani M., Bertoni C. 2022. Subsurface heat and salts cause exceptionally limited methane hydrate stability in the Mediterranean Basin. *Geology* 51: 162–166. doi:10.1130/G50426.1

Cattaneo A., Badhani S., Caradonna C., Bellucci M., Leroux E., Babonneau N., Garziglia S., Poort J., Akhmanov G.G., Bayon G., Dennielou B., Jouet G., Migeon S., Rabineau M., Droz L., Clare M. 2020. The Last Glacial Maximum Balearic Abyssal Plain megabed revisited. Geological Society, London, Special Publications 500, 341–357. doi:10.1144/SP500-2019-188

Chaytor J.D., Brink U.S. ten., Solow A.R., Andrews B.D. 2009. Size distribution of submarine landslides along the U.S. Atlantic margin. *Marine Geology* 264: 16–27. doi:10.1016/j.margeo.2008.08.007

Chiocci F.L., Romagnoli C., Tommasi P., Bosman A. 2008. The Stromboli 2002 tsunamigenic submarine slide: Characteristics and possible failure mechanisms. *Journal of Geophysical Research* 113. doi:10.1029/2007JB005172

Chiocci F.L., Casalbore D., Falese F., Spatola D., Scacchia E., Bianchini. 2024. Marine Geohazards in Italy, their specificity and mitigation perspective. pp 73 - 84. In: Marine hazards, coastal vulnerability, risk (mis)perceptions – a Mediterranean perspective. CIESM Workshop Monograph n°52 [F. Briand, Ed.], 182 p., CIESM Publisher, Paris, Monaco.

Droz L., Reis A.T. dos., Rabineau M., Berné S., Bellaiche G. 2006. Quaternary turbidite systems on the northern margins of the Balearic Basin (Western Mediterranean): a synthesis. *Geo-Marine Letters* 26: 347–359. doi:10.1007/s00367-006-0044-0

El-Robrini M., Gennesseaux M., Mauffret A. 1985. Consequences of the El-Asnam earthquakes: Turbidity currents and slumps on the Algerian margin (Western Mediterranean). *Geo-Marine Letters* 5: 171–176. doi:10.1007/BF02281635

Fornaciai A., Favalli M., Nannipieri L. 2019. Numerical simulation of the tsunamis generated by the Sciara del Fuoco landslides (Stromboli Island, Italy). *Scientific Reports* 9: 18542. doi:10.1038/s41598-019-54949-7

Gamboa D., Omira R., Terrinha P. 2022. Spatial and morphometric relationships of submarine landslides offshore west and southwest Iberia. Landslides 19: 387–405. doi:10.1007/s10346-021-01786-3

Gross F., Mountjoy J.J., Crutchley G.J., Böttner C., Koch S., Bialas J., Pecher I., Woelz S., Dannowski A., Micallef A., Huhn K., Krastel S. 2018. Free gas distribution and basal shear zone development in a subaqueous landslide – Insight from 3D seismic imaging of the Tuaheni Landslide Complex, New Zealand. *Earth and Planetary Science Letters* 502: 231–243. doi:10.1016/j.epsl.2018.09.002

Grozic J.L.H. 2010. Interplay Between Gas Hydrates and Submarine Slope Failure. In: Mosher, D.C., Shipp, R.C., Moscardelli, L., Chaytor, J.D., Baxter, C.D.P., Lee, H.J., Urgeles, R. (Eds.), Submarine Mass Movements and Their Consequences, Advances in Natural and Technological Hazards Research. *Springer Netherlands*, pp. 11–30.

Harbitz C.B., Lovholt F., Pedersen G., Masson D.G. 2006. Mechanisms of tsunami generation by submarine landslides: a short review. *Norsk Geologisk Tidsskrift* 86: 255.

Harbitz C.B., Løvholt F., Bungum H. 2014. Submarine landslide tsunamis: how extreme and how likely? *Natural Hazards* 72: 1341–1374. doi:10.1007/s11069-013-0681-3

Harders R., Ranero C.R., Weinrebe W., Behrmann J.H. 2011. Submarine slope failures along the convergent continental margin of the Middle America Trench. *Geochemistry, Geophysics, Geosystems* 12, Q05S32. doi:10.1029/2010GC003401

Hasiotis T., Papatheodorou G., Bouckovalas G., Corbau C., Ferentinos G. 2002. Earthquake-induced coastal sediment instabilities in the western Gulf of Corinth, Greece. *Marine Geology* 186: 319–335. doi:10.1016/S0025-3227(02)00240-2

Hühnerbach V., Masson D.G. 2004. Landslides in the North Atlantic and its adjacent seas: an analysis of their morphology, setting and behaviour. Marine Geology, COSTA - Continental Slope Stability 213: 343–362. doi:10.1016/j.margeo.2004.10.013

Intergovernmental Panel On Climate Change (IPCC), 2023. Climate Change 2022 – Impacts, Adaptation and Vulnerability: Working Group II Contribution to the Sixth Assessment Report of the Intergovernmental Panel on Climate Change, 1st ed. Cambridge University Press. doi:10.1017/9781009325844

Ioualalen M., Migeon S., Sardoux O. 2010. Landslide tsunami vulnerability in the Ligurian Sea: case study of the 1979 October 16 Nice international airport submarine landslide and of identified geological mass failures. *Geophysical Journal International* 181: 724–740. doi:10.1111/j.1365-246X.2010.04572.x

Korup O., Görüm T., Hayakawa Y. 2012. Without power? Landslide inventories in the face of climate change. Earth Surface Processes and Landforms 37: 92–99. doi:10.1002/esp.2248

Lafuerza S., Sultan N., Canals M., Lastras G., Cattaneo A., Frigola J., Costa S., Berndt C. 2012. Failure mechanisms of Ana Slide from geotechnical evidence, Eivissa Channel, Western Mediterranean Sea. *Marine Geology* 307–310, 1–21. doi:10.1016/j.margeo.2012.02.010

León R., Llorente M., Giménez-Moreno C.J. 2021. Marine Gas Hydrate Geohazard Assessment on the European Continental Margins. The Impact of Critical Knowledge Gaps. *Applied Sciences* 11: 2865. doi:10.3390/app11062865

Lisiecki L.E., Raymo M.E. 2005. A Pliocene-Pleistocene stack of 57 globally distributed benthic δ18O records. *Paleoceanography* 20, PA1003. doi:10.1029/2004PA001071

Llopart J., Urgeles R., Camerlenghi A., Lucchi R.G., Rebesco M., De Mol B. 2015. Late Quaternary development of the Storfjorden and Kveithola Trough Mouth Fans, northwestern Barents Sea. Quaternary Science Reviews 129: 68–84. doi:10.1016/j.quascirev.2015.10.002

Llopart J., Urgeles R., Forsberg C.F., Camerlenghi A., Vanneste M., Rebesco M., Lucchi R.G., Rüther D.C., Lantzsch H. 2019. Fluid flow and pore pressure development throughout the evolution of a trough mouth fan, western Barents Sea. *Basin Research* 31: 487–513. doi:10.1111/bre.12331

Løvholt F., Pedersen G., Harbitz C.B., Glimsdal S., Kim J. 2015. On the characteristics of landslide tsunamis. *Phil. Trans. R. Soc.* A 373, 20140376. doi:10.1098/rsta.2014.0376

Løvholt F., Urgeles R., Harbitz C.B., Vanneste M., Carlton B. 2022. 8.34 - Submarine Landslides. In: Shroder, J. (Jack) F. (Ed.), Treatise on Geomorphology (Second Edition). Academic Press, Oxford, pp. 919–959. doi:10.1016/B978-0-12-818234-5.00139-5

Masson D., Canals M., Alonso B., Urgeles R., Huhnerbach V. 1998. The Canary Debris Flow: source area morphology and failure mechanisms. *Sedimentology* 45: 411–432.

Minisini D., Trincardi F., Asioli A. 2006. Evidence of slope instability in the Southwestern Adriatic Margin. *Natural Hazards and Earth System Science* 6: 1–20. doi:10.5194/nhess-6-1-2006

Nixon M.F., Grozic J.L. 2007. Submarine slope failure due to gas hydrate dissociation: a preliminary quantification. *Canadian Geotechnical Journal:* 44: 314–325. doi:10.1139/t06-121

Papatheodorou G., Ferentinos G. 1997. Submarine and coastal sediment failure triggered by the 1995, Ms = 6.1 R Aegion earthquake, Gulf of Corinth, Greece. *Marine Geology* 137: 287–304. doi:10.1016/S0025-3227(96)00089-8

Pope E.L., Talling P.J., Urlaub M., Hunt J.E., Clare M.A., Challenor P. 2015. Are large submarine landslides temporally random or do uncertainties in available age constraints make it impossible to tell? *Marine Geology* 369: 19–33. doi:10.1016/j.margeo.2015.07.002

Praeg D., Geletti R., Wardell N., Unnithan V., Mascle J., Migeon S., Camerlenghi A. 2011. The Mediterranean Sea: a natural laboratory to study gas hydrate dynamics? Presented at the 7th International Conference on Gas Hydrates (ICGH 2011), Edinburgh, UK, p. Full paper 322, 8 pp.

Rathje E.M., Karatas I., Wright S.G., Bachhuber J. 2004. Coastal failures during the 1999 Kocaeli earthquake in Turkey. *Soil Dynamics and Earthquake Engineering* 24: 699–712. doi:10.1016/j.soildyn.2004.06.003

Reeder M.S., Rothwell R.G., Stow D.A.V. 2000. Influence of sea level and basin physiography on emplacement of the late Pleistocene Herodotus Basin Megaturbidite, SE Mediterranean Sea. *Marine and Petroleum Geology* 17: 199–218. doi:10.1016/S0264-8172(99)00048-3

Riboulot V., Cattaneo A., Sultan N., Garziglia S., Ker S., Imbert P., Voisset M. 2013. Sea-level change and free gas occurrence influencing a submarine landslide and pockmark formation and distribution in deepwater Nigeria. *Earth and Planetary Science Letters* 375: 78–91. doi:10.1016/j.epsl.2013.05.013

Rothwell R.G., Thomson J., Kähler G. 1998. Low-sea-level emplacement of a very large Late Pleistocene 'megaturbidite' in the western Mediterranean Sea. *Nature* 392: 377–380. doi:10.1038/32871

Stanley J.-D., Bernasconi M.P., Nickerson G.A.J. 2014. Large Scarps and Massive Slide on the Briatico–Bivona Shelf, Calabria, Italy: Potential Link with the Destructive September 1905 Earthquake. *Journal of Coastal Research* 30: 215–227. doi:10.2112/JCOASTRES-D-13-00158.1

Sultan N., Cochonat P., Foucher J.-P., Mienert J., 2004a. Effect of gas hydrates melting on seafloor slope instability. *Marine Geology* 213: 379–401. doi:10.1016/j.margeo.2004.10.015

Sultan N., Cochonat P., Canals M., Cattaneo A., Dennielou B., Haflidason H., Laberg J.S., Long D., Mienert J., Trincardi F., Urgeles R., Vorren T.O., Wilson C. 2004b. Triggering mechanisms of slope instability processes and sediment failures on continental margins: a geotechnical approach. *Marine Geology* 213: 291–321. doi:10.1016/j.margeo.2004.10.011

Tari G., Fallah M., Kosi W., Floodpage J., Baur J., Bati Z., Sipahioğlu N.Ö. 2015. Is the impact of the Messinian Salinity Crisis in the Black Sea comparable to that of the Mediterranean?

Marine and Petroleum Geology, The Messinian events and hydrocarbon exploration in the Mediterranean 66, Part 1: 135–148. doi:10.1016/j.marpetgeo.2015.03.021

Urgeles R., Camerlenghi A. 2013. Submarine landslides of the Mediterranean Sea: Trigger mechanisms, dynamics, and frequency-magnitude distribution. *Journal of Geophysical Research*: Earth Surface 118, 2013JF002720. doi:10.1002/2013JF002720

Urlaub M., Talling P.J., Masson D.G. 2013. Timing and frequency of large submarine landslides: implications for understanding triggers and future geohazard. *Quaternary Science Reviews* 72: 63–82. doi:10.1016/j.quascirev.2013.04.020

Wang L., Zaniboni F., Tinti S., Zhang X. 2019. Reconstruction of the 1783 Scilla landslide, Italy: numerical investigations on the flow-like behaviour of landslides. *Landslides* 16: 1065–1076. doi:10.1007/s10346-019-01151-5

Marine geohazards in Italy, their specificity and mitigation perspective

F.L. Chiocci[1,2], D. Casalbore[1,2], F. Falese[2], D. Spatola[1], E. Scacchia[1], M. Bianchini[1,3]

[1]University of Rome Sapienza, Department of Earth Sciences; [2]National Research Council (CNR-IGAG); [3]National Institute of Oceanography and Applied Geophysics (OGS)

Introduction

Marine geohazards is one of the main topics where marine geology is called upon to make a significant contribution to society, responding to the demands of a future world in which economic and social development will have become increasingly sustainable and safe.

The two devastating tsunamis of 2004 in Indonesia and 2011 in Japan brought the issue of marine geohazards to the attention of the public and scientific research funding bodies. As often happens in geology, it is necessary to wait for tragic events to perceive the relevance of, and societal need for, deepeer knowledge of natural processes. The issue is not new however, and the solution has been known for a long time; going back half a millennium, Francis Bacon, the English philosopher and statesman, noted: "*Natura non nisi parendo vincitur*" (We cannot command Nature except by obeying her) (Bacon, 1620). Today, we certainly would not use the term "command nature", and Bacon's concept has somewhat triumphed : humans cannot simply manipulate or control nature as they would like to do; on the contrary, they need to understand and respect natural laws and processes. The quote highlights the importance of humility and the recognition that our power lies in the ability to adapt to nature, rather than oppose it. It involves adapting to natural processes, as in the case of submarine volcanic eruptions, seismogenic faults, the retrogressive evolution of canyon heads, the leakage of fluids from the seabed, and so on.

Absolutely catastrophic events such as the aforementioned 2004 and 2011 tsunamis are difficult to observe in Italy and commonly characterize areas of the world far away from the Mediterranean. However, the Mediterranean Basin is a geologically active region where seismicity, volcanism, faulting, fluid upwelling are very high, often resulting in relevant marine geohazards for offshore and coastal infrastructures.

This article describes, with references to specific cases, the marine geological hazards in the Italian seas, the research conducted and some perspectives for marine geohazard mitigation.

Relevance of marine geohazards

The "Blue Economy" is certainly one of the areas with the greatest potential development in the next decades. It includes the whole set of primary (fishing and extraction of raw materials), secondary (industry and infrastructures) and tertiary (tourism, data transmission) activities, representing 1.5% of the European economy and 2.2% of employments in 2018 (European Commission 2020). These figures can only increase because of the expansion of coastal settlements and infrastructures, the growth of the maritime industry, such as the transport of goods and people, and the increase in the production of renewable energy from wind, tides

and waves (Soukissian *et al*. 2017), not to mention the continued exploitation of marine, biotic and abiotic resources like raw minerals, aggregates for the nourishment of eroding coasts, or aquaculture, to cite only certain resources (OECD, 2016).

Unfortunately, many "blue" activities are exposed and vulnerable to marine geo-risks in relation to the high population density and tourist exploitation of the coasts and to the exponential emplacement of infrastructure in coastal and offshore regions.

To ensure safe and sustainable blue growth, the assessment of marine geological risks is therefore necessary. Yet this activity is not yet formally included in the numerous EU marine directives and initiatives such as the Maritime Spatial Planning Directive (MSP), Integrated Coastal Zone Management (ICZM) or the Marine Strategy Framework Directive (MSFD), despite initial European recommendations that go in this direction (Kopp *et al*. 2021).

The Italian seas and the marine geohazard

Italy has its own physiographic and geological specificity which makes marine geohazard a factor of even greater importance. From a physiographic point of view, the peninsular setting and the presence of numerous archipelagos make the coast/territory ratio very high; in addition, the widespread occurrence of mountain ranges close to the coast compels the development of settlements, industries, railways and roads at or close to the coast, thus exposed to marine geohazards, often with deleterious cascading effects and possible multiple natural/technological risks.

The geology of the Italian seas is rather complex in relation to the variability of the geodynamic domains that make up the country. The nature of the seas varies from a portion of the foredeep now almost filled with debris produced by the dismantling of the Alps, Apennines and Dinarides (Adriatic Sea, Syvitski and Kettner 2007), to a relict portion of oceanic crust (Ionian Sea) which was mostly destroyed by the collision between Africa and Europe, to a segment of the Apennine-Maghreb chain lowered by extension regime accompanied by submarine volcanic manifestations in historical times (Sicily Channel, Spatola *et al*. 2023a), to newly formed deep oceanic basins which make up the western Mediterranean (Cavazza *et al*. 2004). The most recent oceanic basin (the south-eastern Tyrrhenian Sea) hosts the largest submarine volcano in the Mediterranean, Mount Marsili, which is characterized by recent activity (Gamberi and Marani, 2011; Italiano *et al.* 2014).

Most parts of the continental slopes are affected by widespread mass-wasting processes occurring at different spatial and temporal scales (Chiocci and Casalbore, 2017). These processes include several submarine landslides (e.g, Casalbore *et al.* 2012; Rovere *et al*. 2014; Sammartini *et al.* 2019) together with systems of shelf-indenting submarine canyons occurring in the Ionian Sea (Micallef *et al.* 2019; Ceramicola *et al.* 2014), in the southern Tyrrhenian Sea (Gamberi *et al*. 2007), in the Ligurian Sea (Soulet *et al.* 2016) and offshore eastern Sardinia (Gamberi and Marani, 2007).

With these premises, it is not surprising that in Italy marine geohazards are abundant, different and distributed in different contexts.

Seismo-induced tsunamis are certainly the most dangerous processes, with little and doubtful evidence of tsunamis due to far-field events but with many tragic evidences of tsunamis due to events in the near-field, at distances less than a hundred km from the epicenter. Just to refer to

the main near-field tsunamigenic events, for which there is good evidence in the historic record, one remembers the tragic events of Gargano in 1627 (Tinti and Piantanesi 1996), eastern Sicily in 1693 (Argnani *et al*. 2012), Calabria in 1783-84 (Zaniboni *et al.* 2016), and Messina in 1908 (Barreca *et al.* 2021) (Fig.1).

Figure 1. Destroyed waterfront after the 1908 Messina-Reggio Calabria earthquake (M>7) and tsunami. It was the deadliest event in Italy of the 20th century. Tsunami waves reached up to 12m, affecting almost the whole eastern Sicily coast (from Messina to Siracusa, over 100 km of distance) as well as localities in the southern Tyrrhenian Sea.

<u>Tsunamis due to coastal or submarine landslides,</u> despite having an energy content orders of magnitude lower than seismo-induced tsunamis, are able to locally aggravate, even significantly, seismo-induced tsunamis (Tinti *et al*. 2005; Billi *et al*. 2008, Argnani *et al*. 2009, Zaniboni *et al.* 2021; see also Urgeles *et al*. 2024 in this volume). Tsunamis caused by submarine landslide "only" may however compete with seismo-induced tsunamis in terms of run up height in the nearfield (Tinti *et al.* 2008). The most recent cases are those of Scilla (1783), Gioia Tauro (1977), Stromboli (2002), that were caused by earthquakes, coastal engineering works and volcanic eruptions, respectively (Fig. 2).

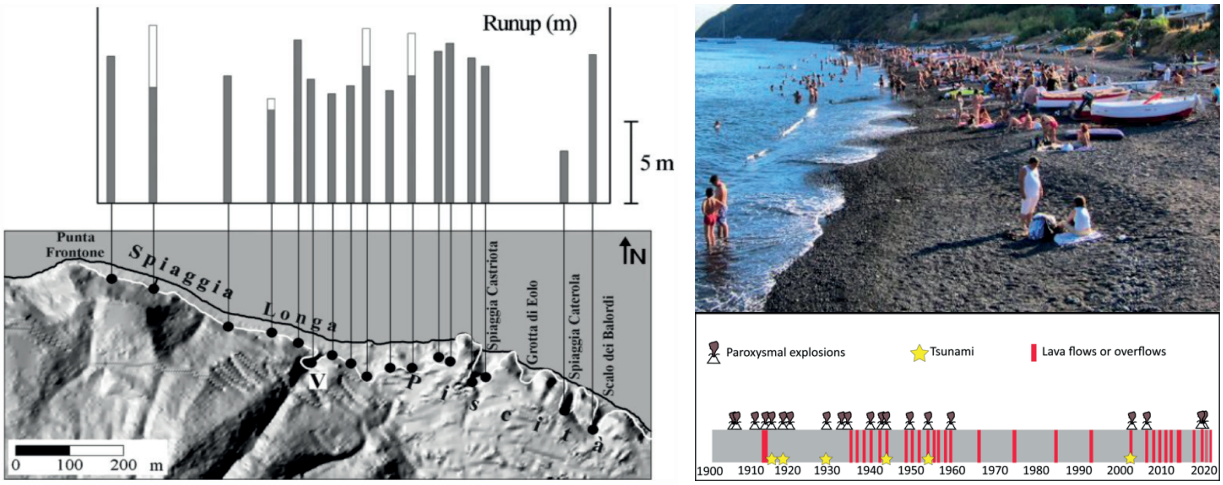

Figure 2. Left, run up of the December 2002 tsunami along the northern coast of the Stromboli Island (southern Tyrrhenian Sea, modified from Tinti *et al*. 2006). The tsunami did not cause any victim but given the tourist exploitation of the beaches (top right), if the same event had happened in the summer,

the consequences would have been much worse. Bottom right, records of tsunamis and eruptions that have occurred on the island in the last 120 years ([courtesy Di Traglia, Florence University].

Submarine eruptions are particularly abundant in the Sicily Channel where the last historical eruption of the Pantelleria volcano in 1891 occurred underwater (Conte *et al.* 2014) (Fig. 3), a few decades after the eruption of Ferdinandea/Giulia/Graham Island (Spatola *et al*. 2018), as it was named respectively by the Italians, French and English, before sea storms resolved the semantic - geopolitical issue by erasing it.

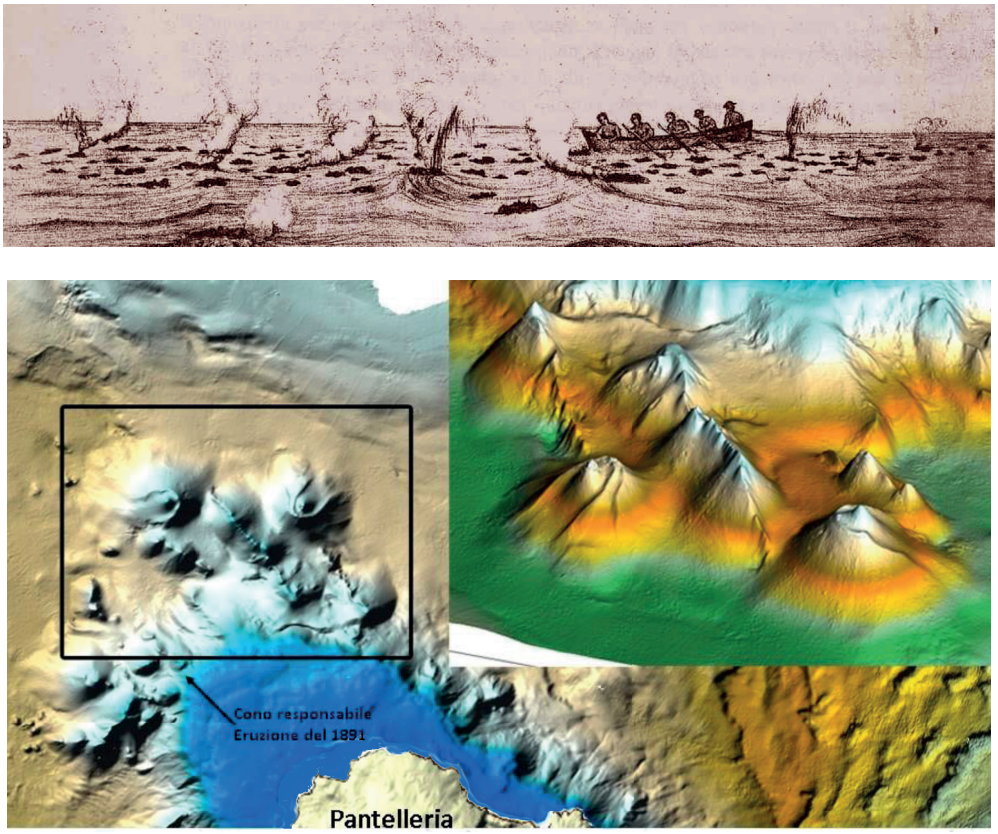

Figure 3. Top: Drawing of floating lava balloons (hollow basalt waste) collection during the eruption of Pantelleria in 1891 (after Riccò, 1892). Below, fields of volcanic cones in the northern sector of Pantelleria in plan and 3D view (inset top right). The arrows indicate the cone responsible for the eruption, which lasted about a week and was preceded by local seismicity and rise of the island's coast >50cm (Riccò 1892). It is important to note that the cone of the 1891 eruption is among the smallest in the area, indicating that the island is potentially exposed to eruptions of much greater intensity and/or duration.

Burst of fluids from the seafloor is a widespread phenomenon, witnessed by pockmarks and mud volcanoes throughout the Italian seas. They rarely occur in shallow water and are therefore only dangerous for infrastructures lying on the seabed such as cables and pipelines. However, in some cases the occurrence of gas eruptions in shallow water, for example at the mouth of the Tiber in 2013 (Ciotoli *et al*. 2016) and in the Tuscan archipelago in 2017 (Casalbore *et al.* 2020; Spatola *et al*. 2023b), can generate alarm in the population and represent a risk for navigation (Fig. 4).

Figure 4. Fluid burst (mainly CO_2) in the shallow waters of Fiumicino, at the mouth of the Tiber River in 2013. The phenomenon lasted a few days, causing alarm for the authorities and the population. A larger event occurred in 2017 at the Scoglio d'Affrica, in the Tuscan archipelago. There a column of water, mud and gas (in that case mainly methane) coming from a mud volcano with a summit at -7 m, raised a column of water of about 10 m near a fishing boat, threatening its safety.

Deep water submarine landslides generally have a low tsunamigenic potential (Harbitz *et al*. 2014), unless we hypothesize absolutely exceptional although infrequent and often highly debated events (Gallotti *et al.* 2021; Billi *et al.* 2008). Although they do not often cause tsunamis, they represent a significant hazard for infrastructures (essentially communications, but also energy production, both fossil and renewable). Submarine landslides can be very common spatially (a frequency of one landslide every 8 km^2 is reported for the southern part of Tyrrhenian Calabria, Casas *et al*. 2016) and this spatial frequency certainly corresponds to a high, albeit unknown, temporal frequency, given the high rates of sedimentation in the area (Fig. 5).

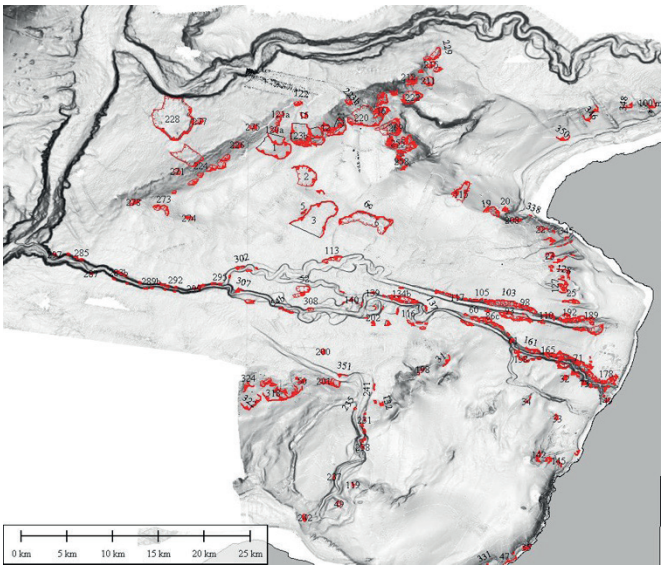

Figure 5. Submarine landslide scars in red on the Gioia Basin (southern Calabria slope of the Tyrrhenian Sea). Over 400 submarine landslides have been defined based on full-coverage seafloor mapping, with a density of 1 scar/8 km^2. [After Casas *et al*. 2016]

Migration of bedforms under the effect of bottom currents can represent a hazard for infrastructures located on the seabed (Bruschi *et al*. 2014). The problem is particularly pronounced in strait areas where the narrow gap between the subaerial land masses forces in a tight space the presence of numerous infrastructures on the seafloor (cables and pipelines), while the gap between the sea basins induces the currents to significantly increase speed and friction with the seabed (Rossi *et al*. 2023). Moreover, the mobility of the seabed may create potentially dangerous free spans (Fig. 6) in areas where maritime traffic is usually intense

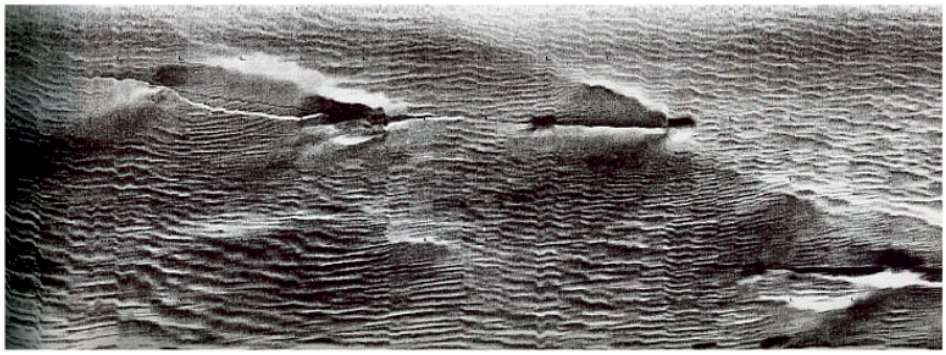

Figure 6. Side scan sonar image of sand waves (i.e. migrating dunes in the seafloor) interacting with natural gas pipeline in the Messina Strait. Pipeline generates high-backscatter (dark) straight stripe while its shadow generates null backscatter (white). When high and low-backscatter stripes diverge (as in the upper left part of the image), the pipeline is suspended between dune crests. Such free span caused by migrating bedforms represent a 'Natech' geohazard as pipeline damage and gas release in the water column may suddenly reduce buoyancy for overlying vessels.

Seacliff collapses are extremely frequent on volcanic and limestone coasts and in tectonically active areas (Fig. 7). They may only partially be considered marine geohazards because the phenomenon is essentially subaerial; however, the marine environment plays an important role in removing the debris produced by collapses and in exerting a weakening action on the foot of the cliff through physical, chemical and biological processes.

Figure 7. Collapse of a sea cliff near Otranto (southern Adriatic Sea). Each year in Italy several casualties are caused by these events, due to the fact that many pocket beaches and littoral shores occur at the foot of scenic sea cliffs that are heavily touristically exploited.

Multi-hazard and cascading effect As with many natural hazards, marine and coastal hazards may combine with each other (Fig. 8), resulting in damage amplification, and/or form cascading hazard chains, also including 'Natech' (Natural Hazards Triggering Technological Accidents, Steinberg *et al.* 2008). When large earthquakes occur, the tsunami can significantly increase the damage. Moreover, the earthquake can in turn generate submarine landslides, which can generate tsunami waves that may become the first cause of damage (Nakata *et al*. 2020; Kopp *et al*. 2021; Tappin *et al*. 2021). This hypothesis has been advanced for a number of coastal catastrophes such as Messina (1908), Puerto Rico (1928), Grand Banks (1929), Canada (1929), Papua New Guinea (1998), Japan (2011) and Indonesia (2018).

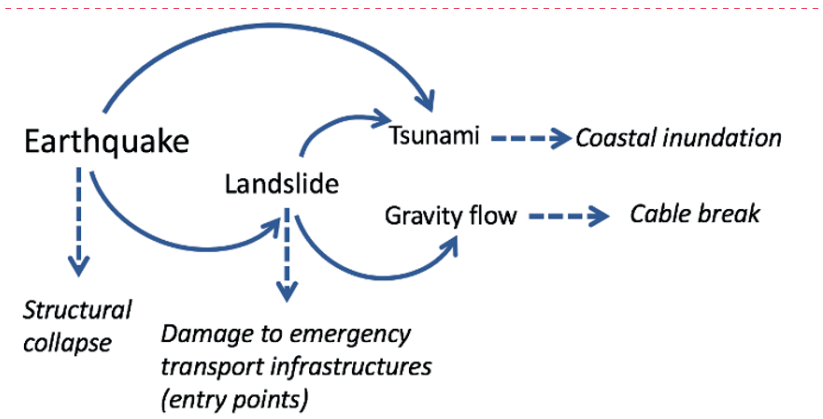

Figure 8. Potential chain of hazards (roman) and their consequences (italic) that may superimpose, causing the amplification of the primary event [from Kopp *et al*. 2021].

A good example of this type of hazard is the port of Gioia Tauro in southern Calabria, one of the most seismically active areas in the Mediterranean Sea. The port is the most important Italian infrastructure and among the largest transshipment ports in the Mediterranean region, with an intense naval traffic of > 3.3 million TEU in 2022. During its construction in 1977, the port experienced a partial collapse and very serious damage from waves up to 5 m high, due to an underwater landslide that developed at the head of the Gioia canyon, immediately in front of the port.

After the event, the port was redesigned and finished, and today the canyon head is located less than 100 m from the shoreline (Fig. 9 left). Its retrogressive erosion activity is certainly not over (Fig. 9 right). The port is one of the main entry points for the arrival of aids and relief supplies by sea in the event of a high-magnitude earthquake which could trigger the collapse of the road infrastructure in the region. It is clear that the stability of the port structure is strongly undermined by the canyon head retrogression.

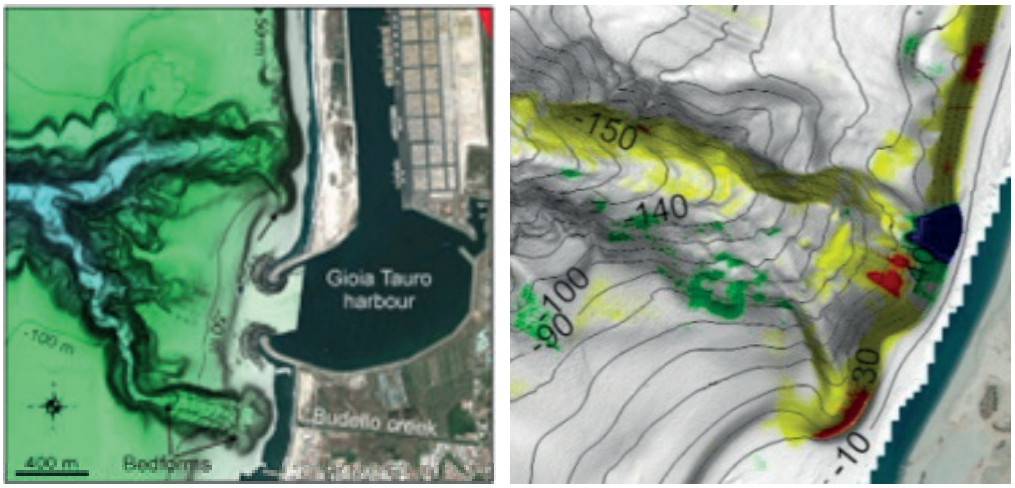

Figure 9. Entrance to the Gioia Tauro port in southern Tyrrhenian Calabria. The left image shows how the port is extremely close to the two heads of the Gioia canyon (from Casalbore *et al*. 2014). The northern head was affected by a tsunamigenic landslide in 1977 during the construction of the port. On the right, multibeam monitoring in this area illustrates the erosive activity (yellow color) and re-deposition (red color) within the head [From Kopp *et al*. 2021].

Small vs. large events

As already mentioned, the Mediterranean does not host the large seismic events typical of the Pacific Ring of Fire, where earthquakes up to M9 can occur and generate tsunami waves able of traveling for thousands of km. In the Mediterranean it is possible that M > 8 was reached (Kelly, 2004), but only once, for the tsunamigenic earthquake of Crete in 365 B.C. From a volcanic point of view, the large explosive eruptions typical of subduction zones occur rarely in the Mediterranean area, although with return times of thousands of years (Santorini eruption, Neapolitan Yellow tuff, Campanian ignimbrites) (Friedrich *et al*. 2006; Scarpati *et al*. 1993; Fitzsimmons *et al.*, 2013 respectively). Huge landslides generated by sector collapse and debris avalanches such as those of Ischia (Chiocci and De Alteris, 2006), Stromboli (Romagnoli *et al.* 2009) or Vesuvius (Milia *et al.* 2003), have comparable return times.

These events may obviously have a devastating impact both directly and indirectly due to the tsunamis they can produce. Tinti *et al.* (2011) estimated how a tsunami produced by the sector collapse and debris avalanche of Ischia could have generated waves > 10 m on the Tyrrhenian coast, both 150 km to the north and to the south of the island.

However, in estimating an hazard, what matters is not only the magnitude of the event, but also the temporal frequency, i.e. the probability that this event will occur in a given period of time. And then the hazard can be very high, even on a coast where mega-events are rare but where landslides or earthquakes of medium intensity - but still tsunamigenic - occur with sub-centenary frequencies (Fig. 10).

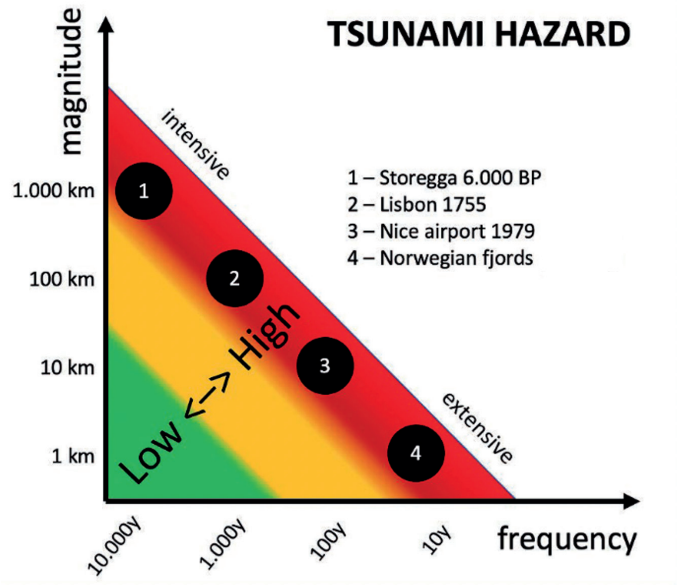

Figure 10. Relation between hazard (colour tones) and magnitude/time frequency of tsunami events that occurred in Europe (modified from Kopp *et al*. 2021)

Moving from hazard to risk, it is known that the latter is a factorial product with $R = H \times E \times V$ where E and V stand for exposure and vulnerability respectively. From this perspective, the Mediterranean presents a quite critical situation. As regards exposure, the Mediterranean coastal strip is a most densely inhabited area. The severe anthropization of the coasts is influenced by the proximity, in certain areas, of mountain chains which force the settlements to be close to the shoreline and, by the presence of port infrastructures and industries that require water supply. Vulnerability is also very high, essentially because in Mediterranean countries marine-coastal risks are little known, little discussed, and thus practically absent from the regulations. Therefore, no attention is paid to monitoring activities, to the design of critical infrastructures, or to the modeling of potentially very dangerous events.

Seafloor mapping for geohazard assessment

Knowledge of the processes occurring at the seabed is in general extremely poor, due to the difficulty of accessing the object of the study, to the high cost of marine geology research and the consequent lack of monitoring systems to know pre- and syn-event condition. Moreover, in submarine mass wasting the landslide mass usually transforms into gravitational flow and leaves only faint traces on the seabed.

But as in all hazards, the first step is fundamental to understand the occurrence of past events, to define the predisposition of a given part of the seafloor to certain processes. Looking into past events we may define the susceptibility to geohazard of a coastal stretch and provide information on the boundary conditions and on factors that control the development of geohazard-bearing processes. From this point of view, an important step (which has been taken in Italy) is the mapping of the seabed for the identification and characterization of geohazard features.

In the years 2007-2013, the MaGIC project (Marine Geohazards along the Italian Coasts) was developed, funded by the Civil Protection Department with €5.25 M, which involved the entire

Italian scientific community working in the field of marine geology (three institutes of the National Research Council, seven universities and the OGS institute) collaborating for the detection, interpretation and cartographic representation according to common standards of the geohazard features of the Italian seas (landslides, active faults, volcanic structures, canyons, areas with gas leaks, areas with migrating dunes, etc.) (see Fig. 11).

In addition to the important implications for Civil Protection, the resulting work constitutes a basic cartography for any management operation of the coasts and submerged territory, also in terms of blue energy, both for current technologies (e.g. wind farms) and for those that will increasingly develop in the near future (energy from waves and currents, food resources, mineral resources). It is a large-scale project that has aroused strong interest in the international field.

In addition to direct use for civil protection purposes, the project had the ambition of raising awareness among the public authorities responsible for managing the coastal environment of the geohazards present below sea level. These hazards are poorly perceived by technicians and not at all regulated by operational procedures. It was therefore believed that the dissemination of this information could be the best tool for transferring the knowledge acquired by the scientific community to local administrators, and increase the sensitivity towards these hazards. In fact, in a country like Italy, with such a large extension and intensive use of the coasts, marine geohazards represent a significant threat to populations and infrastructures. For this reason, an Atlas with all the project results was printed in over 2,000 copies and distributed to Local Authorities (Regions, Basin Authorities, Provinces and Coastal Municipalities), Port Authorities and Marine Protected Areas (Fig. 11).

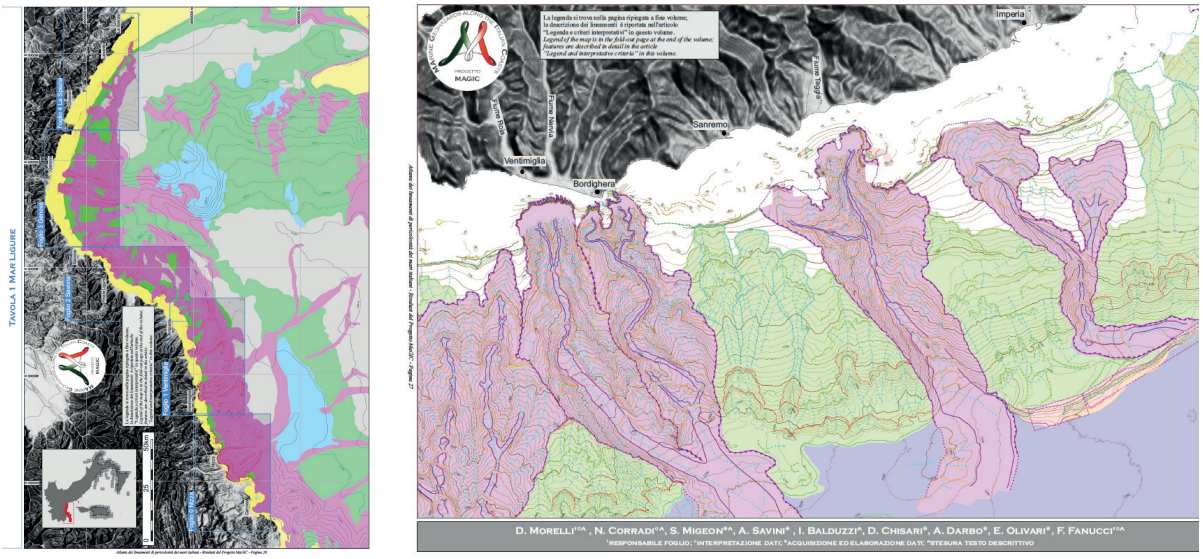

Figure 11. Atlas of the Italian MaGIC Project, an initiative to detect, interpret and map with the same standards the geohazard features of the Italian seas. On the left, the first-level interpretative map of the Ligurian Sea (1:250.000). On the right, the Ventimiglia sheet 1 (part of the Ligurian Sea) in which the hazard features are mapped in great detail (1:50.000).

It is worth notice how essential is a complete full-coverage and high-resolution mapping of all the seafloor and a morpho-bathymetric interpretation and representation based on common standards. In fact, the information derived from scientific data is often spatially incomplete because it is driven by scientific curiosity and biased by the large dimension of the studied features. As an example, we mention the compilation based on literature data of submarine landslides in the Mediterranean (Urgeles and Camerlenghi, 2013) in which the density of landslides is three orders of magnitude lower than the density obtained from an ad-hoc mapping based on full-coverage high-resolution morpho-bathymetric dataset (Fig. 12). The chapter by Urgeles *et al*. (2024, in this volume) further reports major biases towards younger submarine landslides in global catalogues.

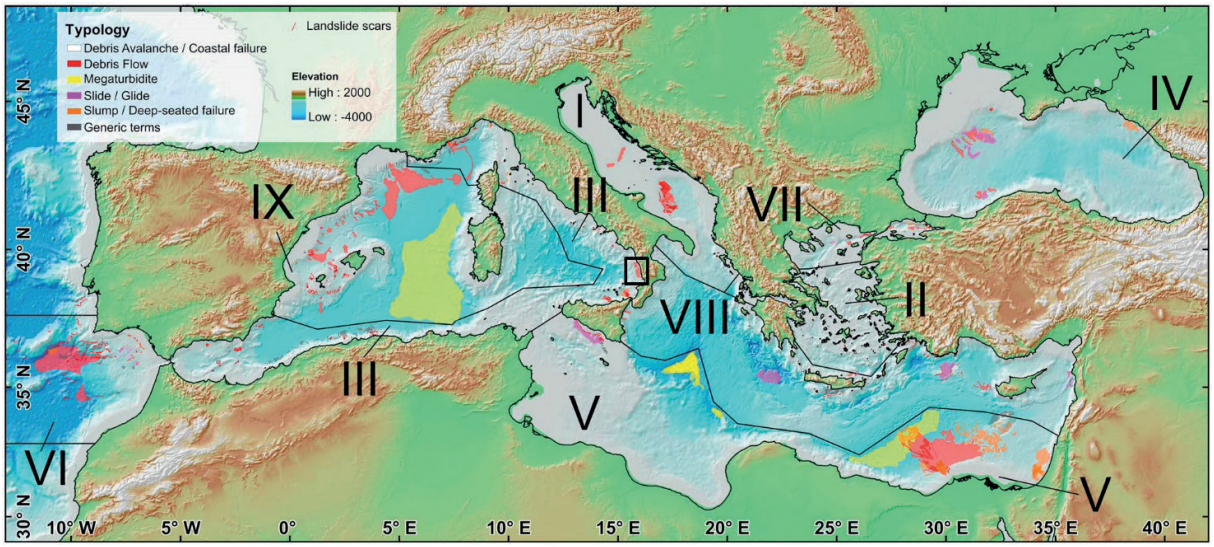

Figure 12. Census of over 700 underwater landslides in the Mediterranean from data present in the scientific literature (from Urgeles and Camerlenghi, 2013). This image, and the density of a landslide every 4.000 km^2, must be compared with the density of a landslide every 8 km^2, detected by Casas *et al*. 2016 in the small area indicated by the black box in the southeastern Tyrrhenian Sea, and reported in Figure 5.

Conclusion

Knowledge and perception of marine geohazards is an unavoidable reality to ensure safe and sustainable development of the blue economy. Coastal settlements, port and industrial infrastructures, roads and railways, can be at risk by a large number of geological events such as earthquakes, volcanic eruptions, coastal and submarine landslides, tsunamis (as secondary effects but often primary in terms of damage), fluid bursts from the seabed and bedform migration. In addition to direct damage to populations and coastal infrastructures, all these phenomena can damage or destroy submarine cables where 99% of telephone communications and internet traffic currently pass. In 2008, a few hours interruption of the FLAG cable off the coast of Alexandria in Egypt caused a loss of tens of millions of euros, cutting off the internet connection to 75 million people in the Middle East region. In 2003 an earthquake in Algeria caused a large number of underwater landslides along about a hundred km of the Mediterranean margin which damaged four submarine cables in some twenty different points (Cattaneo *et al.* 2012). Cables, pipelines and other infrastructures (for example those linked to renewable energy from waves,

currents and tides) will increasingly be installed on the seafloor and for this reason knowledge of geo-risks is fundamental for the development of economies linked to the sea.

Italy (and more broadly the Mediterranean region), as far as marine geohazards are concerned, has its own specificities:

1) the lack of large magnitude events (such as the ones occurring in subduction zones) is counterbalanced by events of medium magnitude but of great temporal frequency, which drive the hazard to be very high, especially in tectonically and volcanologically active areas;

2) the exposure of populations and of industrial, energy, transport and data transmission infrastructures is very high, especially in areas where the presence of coastal chains forces the infrastructures to be on the coast and especially in the summer season when many of the coasts are crowded by tourists;

3) vulnerability is high, due both to the lack of ad hoc regulations that favor risk mitigation and the lack of knowledge of marine geohazards. With reference to this last point, the implementation of the MaGIC project represented a first cognitive step needed in all countries whose continental margins are geologically active.

In this context, we can only return to Francis Bacon and conclude with another of his lines "*Ipsa scientia potestas est*" (knowledge itself is power).

To be cited as:

F.L. Chiocci, D. Casalbore, F. Falese, D. Spatola, E. Scacchia, M. Bianchini. 2024. Marine geohazards in Italy, their specificity and mitigation perspective. p 73- 88. In CIESM Monograph 52 [F. Briand, Ed.] Marine hazards, coastal vulnerability, risk (mis) perceptions – a Mediterranean perspective. CIESM Publisher, Paris, Monaco, 182 p.

References

Argnani A., Armigliato A., Pagnoni G., Zaniboni F., Tinti S. and C. Bonazzi. 2012. Active tectonics along the submarine slope of south-eastern Sicily and the source of the 11 January 1693 earthquake and tsunami. *Natural Hazards and Earth System Sciences* 12(5): 1311-1319.

Argnani A., Chiocci F.L., Tinti S., Bosman A., Lodi M.V., Pagnoni G. and F. Zaniboni. 2009. Comment on "On the cause of the 1908 Messina tsunami, southern Italy" by A. Billi *et al*. *Geophys. Res. Lett* 36, L13307.

Bacon F., Sir. 1620 Novum Organum. Collier.

Barreca G., Gross F., Scarfì L., Aloisi M., Monaco C. and S. Krastel. 2021. The Strait of Messina: Seismotectonics and the source of the 1908 earthquake. *Earth-Science Reviews* 218: 103685.

Billi A., Funiciello R., Minelli L., Faccenna C., Neri G., Orecchio B. and D. Presti. 2008. On the cause of the 1908 Messina tsunami, southern Italy. *Geophysical Research Letters* 35(6).

Bruschi R., Bughi S., Drago M. and F. Gianfelici. 2014. In-place stability and integrity of offshore pipelines crossing or resting on active bedforms or loose or soft soils. *Journal of Pipeline Engineering* 13(3).

Casalbore D., Bosman A. and F.L. Chiocci. 2012. Study of recent small-scale landslides in geologically active marine areas through repeated multibeam surveys: examples from the southern Italy. pp. 573-582 In *Submarine Mass Movements and their Consequences*: 5th International Symposium. Springer Netherlands.

Casalbore, D., Bosman A., Ridente, D. and F.L. Chiocci. 2014. Coastal and submarine landslides in the tectonically-active Tyrrhenian Calabrian Margin (southern Italy): examples and geohazard implications. pp. 261-269 In Submarine mass movements and their consequences: 6th international symposium. Springer International Publishing.

Casalbore D., Ingrassia M., Pierdomenico M., Beaubien S. E., Martorelli E., Bigi, S., ... and F.L. Chiocci. 2020. Morpho-acoustic characterization of a shallow-water mud volcano offshore Scoglio d'Affrica (Northern Tyrrhenian Sea) responsible for a violent gas outburst in 2017. *Marine Geology* 428: 106277.

Casas D., Chiocci F., Casalbore D., Ercilla G.and J.O. De Urbina. 2016. Magnitude-frequency distribution of submarine landslides in the Gioia Basin (southern Tyrrhenian Sea). *Geo-Marine Letters* 36: 405-414.

Cattaneo A., Babonneau N., Ratzov G., Dan-Unterseh G., Yelles K., Bracène R., ... & J. Déverchère. 2012. Searching for the seafloor signature of the 21 May 2003 Boumerdès earthquake offshore central Algeria. *Natural Hazards and Earth System Sciences* 12(7): 2159-2172.

Cavazza W., Roure F. and P.A. Ziegler. 2004. The Mediterranean area and the surrounding regions: active processes, remnants of former Tethyan oceans and related thrust belts. The TRANSMED Atlas. The Mediterranean Region from Crust to Mantle: Geological and Geophysical Framework of the Mediterranean and the Surrounding Areas, 1-29.

Ceramicola S., Praeg D., Coste M., Forlin E., Cova A., Colizza E. and S. Critelli. 2014. Submarine mass-movements along the slopes of the active Ionian continental margins and their consequences

for marine geohazards (Mediterranean Sea). pp. 295-306 In Submarine mass movements and their consequences: 6th international symposium. *Springer International Publishing.*

Chiocci F.L. and G. De Alteriis. 2006. The Ischia debris avalanche: first clear submarine evidence in the Mediterranean of a volcanic island prehistorical collapse. *Terra Nova* 18(3): 202-209.

Chiocci F.L. and D. Casalbore. 2017. Unexpected fast rate of morphological evolution of geologically-active continental margins during Quaternary: Examples from selected areas in the Italian seas. *Marine and Petroleum Geology* 82: 154-162.

Ciotoli G., Etiope G., Marra F., Florindo F., Giraudi C. and L. Ruggiero. 2016. Tiber delta CO2-CH4 degassing: a possible hybrid, tectonically active sediment hosted geothermal system near Rome. *Journal of Geophysical Research: Solid Earth* 121(1): 48-69.

Conte A.M., Martorelli E., Calarco M., Sposato A., Perinelli C., Coltelli M. and F.L. Chiocci. 2014. The 1891 submarine eruption offshore Pantelleria Island (Sicily Channel, Italy): Identification of the vent and characterization of products and eruptive style. *Geochemistry, Geophysics, Geosystems* 15(6): 2555-2574.

Fitzsimmons K.E., Hambach U., Veres D. and R. Iovita. 2013. The Campanian Ignimbrite eruption: new data on volcanic ash dispersal and its potential impact on human evolution. *PLoS One* 8(6), e65839.

Friedrich W.L., Kromer B., Friedrich M., Heinemeier J., Pfeiffer T. and S. Talamo. 2006. Santorini eruption radiocarbon dated to 1627-1600 BC. *Science* 312(5773): 548-548.

Gallotti G., Zaniboni F., Pagnoni G., Romagnoli C., Gamberi F. and S. Tinti. 2021. Tsunamis from prospected mass failure on the Marsili submarine volcano flanks and hints for tsunami hazard evaluation. *Bull Volcanol*. 83, 2.

Gamberi F. and M. Marani. 2007. Downstream evolution of the Stromboli slope valley (southeastern Tyrrhenian Sea). *Marine Geology* 243(1-4): 180-199.

Gamberi, F. and M. Marani. 2011. Submarine volcano geohazards in the Tyrrhenian Sea. pp. 89-99. In [F. Briand, ed.] *Marine geo-hazards in the Mediterranean.* CIESM Workshop Monographs n°42, CIESM Publisher Paris, Monaco.

Harbitz C.B., Løvholt F. and H. Bungum. 2014. Submarine landslide tsunamis: how extreme and how likely? *Natural Hazards* 72: 1341-1374.

Italiano F., De Santis A., Favali P., Rainone M.L., Rusi S. and P. Signanini. 2014. The Marsili volcanic seamount (southern Tyrrhenian Sea): a potential offshore geothermal resource. *Energies* 7(7): 4068-4086.

Kelly G. 2004. Ammianus and the great tsunami. The Journal of Roman Studies, 94: 141-167.

Kopp H., Chiocci F.L., Berndt C., Çagatay M.N., Ferreira T., Fortes C.J., Gràcia E., González Vega A., Kopf A.J., Sørensen M.B., Sultan N.and I.A. Yeo 2021. Marine geohazards: Safeguarding society and the Blue Economy from a hidden threat. [Muñiz Piniella, A. *et al*. Eds.]. Position Paper 26 of the European Marine Board, Ostend, Belgium. 120 p.

Micallef A., Camerlenghi A., Georgiopoulou A., Garcia-Castellanos D., Gutscher M.-A., Lo Iacono C., Huvenne V.A., Mountjoy J.J., Paull C.K., Le Bas T., Spatola D., Facchin L. and D. Accettella. 2019. Geomorphic evolution of the Malta escarpment and implications for the

Messinian evaporative drawdown in the eastern Mediterranean Sea. *Geomorphology* 327: 264–283. https://doi.org/10.1016/j.geomorph.2018.11. 012.

Milia A., Torrente M.M. and A. Zuppetta. 2003. Offshore debris avalanches at Somma–Vesuvius volcano (Italy): implications for hazard evaluation. *Journal of the Geological Society*, 160(2): 309-317.

Nakata K., Katsumata A. and A. Muhari. 2020. Submarine landslide source models consistent with multiple tsunami records of the 2018 Palu tsunami, Sulawesi, Indonesia. *Earth, Planets and Space* 72(1): 1-16.

OECD. 2016. The Ocean Economy in 2030. OECD Publishing.

Riccò A. 1892. Terremoti sollevamento ed eruzione sottomarina a Pantelleria nella seconda metà dell'Ottobre 1891. *Bollettino della Società Geografica Italiana* 130-156.

Romagnoli C., Kokelaar P., Casalbore D. and F.L. Chiocci. 2009. Lateral collapses and active sedimentary processes on the northwestern flank of Stromboli volcano, Italy. *Marine Geology* 265(3-4): 101-119.

Rossi V.M., Longhitano S.G., Olariu C. and F.L. Chiocci. 2023. Straits and Seaways: controls, processes and implications in modern and ancient systems. Geological Society, London, Special Publications, 523(1): 1-15.

Rovere M., Gamberi F., Mercorella A. and E. Leidi. 2014. Geomorphometry of a submarine mass-transport complex and relationships with active faults in a rapidly uplifting margin (Gioia Basin, NE Sicily margin). *Marine Geology* 356: 31-43.

Sammartini M., Camerlenghi A., Budillon F., Insinga D.D., Zgur F., Conforti A., ... and R. Tonielli. 2019. Open-slope, translational submarine landslide in a tectonically active volcanic continental margin (Licosa submarine landslide, southern Tyrrhenian Sea). *Geological Society, London, Special Publications* 477(1): 133-150.

Scarpati C., Cole P. and A. Perrotta. 1993. The Neapolitan Yellow Tuff—a large volume multiphase eruption from Campi Flegrei, southern Italy. *Bulletin of Volcanology* 55: 343-356.

Soukissian T.H., Denaxa D., Karathanasi F., Prospathopoulos A., Sarantakos K., Iona A., ... and S. Mavrakos. 2017. Marine renewable energy in the Mediterranean Sea: status and perspectives. *Energies* 10(10): 1512.

Soulet Q., Migeon S., Gorini C., Rubino J.L., Raisson F. and P. Bourges. 2016. Erosional versus aggradational canyons along a tectonically-active margin: The northeastern Ligurian margin (western Mediterranean Sea). *Marine Geology* 382: 17-36.

Spatola D., Micallef A., Sulli A., Basilone,L., Ferreri R., Basilone G., Bonanno A., Pulizzi M.and S. Mangano. 2018. The Graham Bank (Sicily Channel, central Mediterranean Sea): Seafloor signatures of volcanic and tectonic controls. *Geomorphology* 318: 375–389. https://doi.org/10.1016/j.geomorph.2018.07.006

Spatola D., Sulli A., Basilone L., Casalbore D., Napoli S., Basilone G.and F.L. Chiocci. 2023a. Morphology of the submerged Ferdinandea Island, the 'Neverland' of the Sicily Channel (central Mediterranean Sea). *Journal of Maps* 19(1): 2243305.

Spatola D., Casalbore D., Pierdomenico M., Conti A., Bigi S., Ingrassia M., Ivaldi R., Demarte M., Napoli S. and F.L. Chiocci. 2023b. Seafloor characterisation of the offshore sector around Scoglio d'Affrica islet (Tuscan Archipelago, northern Tyrrhenian sea). *Journal of Maps* 19(1): 2120836.

Steinberg L.J., Sengul H. and A.M. Cruz. 2008. Natech risk and management: an assessment of the state of the art. *Natural Hazards* 46: 143-152.

Syvitski J.P.,and A.J. Kettner. 2007. On the flux of water and sediment into the Northern Adriatic Sea. Continental Shelf Research, 27(3-4): 296-308.

Tappin D.R. 2021. Submarine landslides and their tsunami hazard. Annual Review of Earth and Planetary Sciences 49: 551-578.

Tinti S. and A Piatanesi. 1996. Numerical simulations of the tsunami induced by the 1627 earthquake affecting Gargano, Southern Italy. *Journal of Geodynamics* 21(2): 141-160.

Tinti S., Armigliato A., Tonini R., Maramai A. and L. Graziani. 2005. Assessing the hazard related to tsunamis of tectonic origin: a hybrid statistical-deterministic method applied to southern Italy coasts. *ISET Journal of earthquake technology* 42(4): 189-201.

Tinti, S., Pagnoni, G. and F. Zaniboni. The landslides and tsunamis of the 30th of December 2002 in Stromboli analysed through numerical simulations. Bull Volcanol 68, 462–479 (2006). https://doi.org/10.1007/s00445-005-0022-9 »

Tinti S., Zaniboni F., Pagnoni G. and A. Manucci. 2008. Stromboli Island (Italy): scenarios of tsunamis generated by submarine landslides. *Pure and applied geophysics* 165: 2143-2167.

Tinti S., Chiocci F.L., Zaniboni F., Pagnoni G. and G. De Alteriis. 2011. Numerical simulation of the tsunami generated by a past catastrophic landslide on the volcanic island of Ischia, Italy. *Marine Geophysical Research* 32: 287-297.

Urgeles R. and A. Camerlenghi. 2013. Submarine landslides of the Mediterranean Sea: Trigger mechanisms, dynamics, and frequency-magnitude distribution. *J Geophysics Research Earth Surface*. https://doi.org/10.1002/2013JF002720.

Urgeles R., Camerlenghi A., Rüther D.C., Fantoni L., Brückner N.W. and Y. de Pro Díaz. 2021. The Euro-Mediterranean Submarine landSlide database (EMSS21).

Urgeles R., Beyer S., Cattaneo A., de Gail M., Gamboa D., León R., Løvholt F., Vanneste M. and C. Vila. 2024. Geohazard trends from submarine landslides and related tsunamis, a geological perspective and implications for present climate change. In: Briand, F. (Ed.), Marine hazards, coastal vulnerability, risk (mis)perceptions – a Mediterranean perspective, CIESM Workshop Monographs. Monaco.

Zaniboni F., Armigliato A. and S. Tinti. 2016. A numerical investigation of the 1783 landslide-induced catastrophic tsunami in Scilla, Italy. *Natural Hazards* 84: 455-470.

Zaniboni F., Pagnoni G., Paparo M. A., Gauchery T., Rovere M., Argnani A., ... and S. Tinti. 2021. Tsunamis from submarine collapses along the eastern slope of the Gela Basin (Strait of Sicily). *Frontiers in Earth Science* 8: 602171.

From Sumatra 2004 to Tonga 2022 - Progress and Challenges of Tsunami Early Warning Systems

Maria Ana Baptista

Instituto Dom Luiz Faculdade de Ciências da Universidade de Lisboa
Instituto Superior de Engenharia de Lisboa, Portugal

Abstract
Tsunamis are among the most devastating natural disasters that can strike coastal regions worldwide. These events, most often triggered by undersea earthquakes, have the potential to cause widespread destruction and loss of life. Some countries have developed and implemented tsunami warning systems to mitigate the catastrophic impacts of tsunamis. These systems have come a long way in development and implementation but face significant challenges. Present operational Tsunami Early Warning Systems (TEWS) were conceived to deal with earthquake-induced tsunamis and still face challenges in monitoring and detection. Moreover, none of those systems can effectively deal with non-seismic tsunami events.
This paper presents a short overview of the evolution and challenges of tsunami warning systems, the advancements made since then and the challenges that still need to be addressed.

Keywords: tsunamis; early warning systems

1. Introduction

Tsunamis, often triggered by undersea earthquakes, volcanic eruptions, or landslides, have the potential to inflict widespread destruction and loss of life. It was only in the mid-20th century that efforts to establish formal warning systems began. Japan installed its tsunami warning system in 1941 (Imamura *et al.* 2019). In 1948, the United States established the Pacific Tsunami Warning Center (PTWC) in Ewa Beach, Hawaii. However, it was not until after the 1960 tsunami triggered by a 9.5 earthquake (Cisternas *et al*. 2005) that its mission included the monitoring and warning for tsunamis across the Pacific Ocean. The 1960 Chilean Tsunami was a catastrophic event that reshaped the approach to tsunami preparedness and response. This even triggered the establishment of the Pacific Tsunami Warning Center at international level, under the umbrella of UNESCO, advancements in seismology and oceanography, and increased public awareness on tsunamis. This Center aimed to detect undersea earthquakes, a primary precursor to tsunamis based on the fact that seismic waves propagate much faster across the globe than tsunami waves propagate in the ocean.
By the end of 2004, the Boxing day tsunami shocked the world and surprised the scientific community; the event caused casualties and widespread devastation along the coasts of the Indian Ocean. Since then, the earthquake-induced tsunami of 11 March 2011 in Japan and the tsunamis that followed the eruptions of the Anak Krakatau and the Hunga Tonga volcanoes in 2018 and 2022 served as poignant reminders of the immense destructive power of these natural phenomena. However, they have also spurred innovations and reforms in tsunami warning systems on a global scale.

Figure 1. Village near the coast of Sumatra after tsunami impact (Photo credit: Philip A. McDaniel, U.S. Navy); NGDC/WDS

2. Events

2.1 The 2004 Indian Ocean Tsunami

One of the most significant turning points in the history of tsunami warning systems was the Indian Ocean tsunami of December 26, 2004. The magnitude 9.1 undersea earthquake off the west coast of northern Sumatra impacted Bangladesh, India, Malaysia, Myanmar, India, Thailand, Sri Lanka and the Maldives (Lay *et al*. 2005). It triggered a tsunami that resulted in widespread devastation and the loss of hundreds of thousands of lives (Fig. 1). The event caught the scientific community by surprise, as such a mega-event was unexpected in that area.
The earthquake began at 7:59 a.m. local time. It soon was recorded at the network of seismic stations of the Pacific Tsunami Warning Center (PTWC) that issued an information bulletin for the countries bordering the Pacific Ocean. The initial information received by PTWC suggested that the earthquake had a moment magnitude of 8.0 with no tsunami threat to the coasts of the Pacific Coast. However, one hour later, the magnitude of the earthquake was revised to 8.5, and PTWC upgraded the level of alert by issuing a warning stating that no threat was expected along the Pacific Ocean but alerting for the possibility of a tsunami near the epicentre (Kelman 2006). The final revised magnitude of the earthquake was 9.1 (Satake 2014).
Even though the PTWC detected and alerted the countries along the Pacific Ocean, there was no mandate to warn the nations in the Indian Ocean. At the time, the absence of a tsunami warning system in the Indian Ocean and the almost total lack of awareness and preparedness of the populations at risk resulted in such a disaster (Okal 2015). The tsunami claimed nearly 230,000 lives across 14 countries.

In summary, the 26 December 2004, earthquake was massive, with a magnitude of 9.1; the rupture length was more than 1000 km, generating a transoceanic tsunami. There was no

tsunami warning system in the region, taking coastal residents and tourists by surprise. The disaster emphasized the need for international cooperation in monitoring and warning efforts. Prior to the 2004 tsunami, public awareness and education regarding tsunamis were generally low in the Indian Ocean region. Many coastal communities were unfamiliar with the signs and dangers associated with tsunamis, resulting in delayed responses and increased casualties. After the 2004 Indian Ocean tsunami, the Intergovernmental Oceanographic Commission of UNESCO recognized the need for a Global Tsunami Warning System and divided the global ocean into four basins: the Indian Ocean, the Pacific, the Caribbean and the Northeastern Atlantic, Mediterranean and Adjacent seas (see Fig. 2).

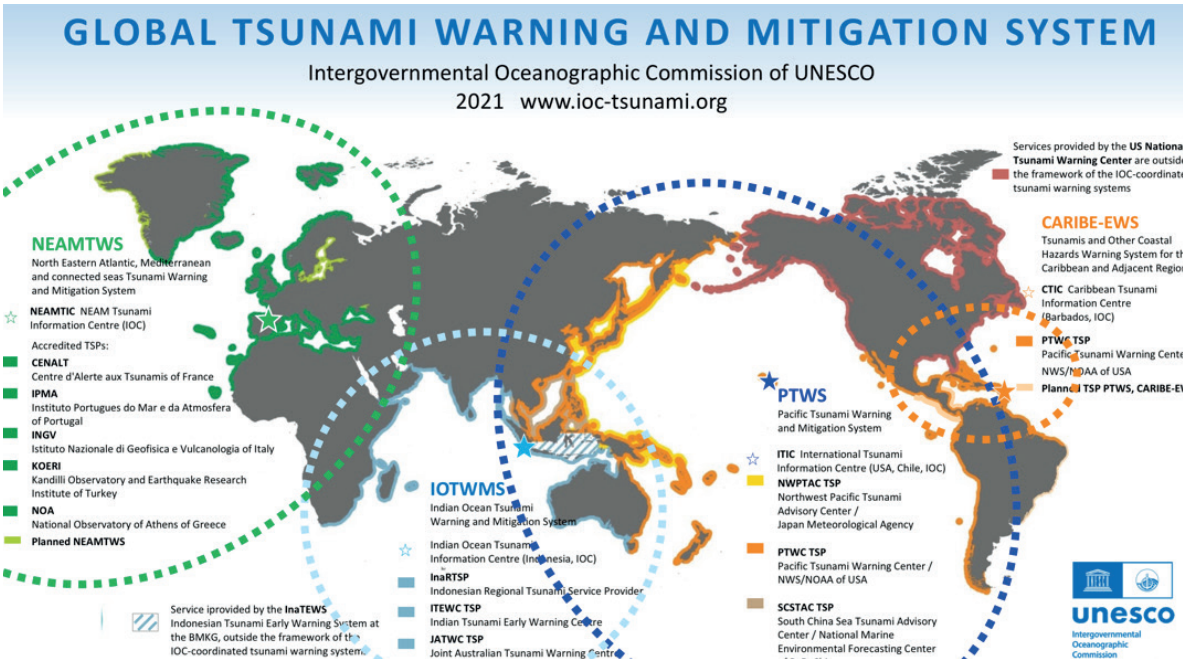

Figure 2. Global Tsunami Warning and Mitigation System (Courtesy of IOC/ UNESCO)

2.2. The 11 March 2011 Tohoku tsunami

On 11 March 2011, a massive magnitude-9.0 earthquake struck off the coast of Japan, generating a powerful tsunami that devastated the northeastern region of Tōhoku. The event caused 18500 dead and missing persons (see Fig 3).

Japan has an extensive network of seismometers, tide gauges, and ocean buoys to detect and measure tsunamis accurately. The network of seismometers enabled the JMA to issue prompt warnings and provide precise information about the tsunami's arrival time. The tsunami was first detected six minutes after the earthquake in a cable bottom pressure gauge. The Japan Meteorological Agency, responsible for tsunami warnings in Japan, issued the first message three minutes after the earthquake with an estimated tsunami height of six meters based on the first estimate of the earthquake magnitude of 7.9 (Satake 2014).

This alert was upgraded 28 minutes after the earthquake with a new estimation of tsunami heights. The tsunami waves reached heights of up to 40 meters in some areas, causing widespread destruction and the tragic loss of thousands of lives. This event also resulted in the Fukushima nuclear disaster.

Figure 3. Building toppled down by the 11 March 2011 tsunami (photo by M.A. Baptista, Feb. 2012)

In summary, the first warning issued by JMA, together with the strong shaking felt by a well-prepared population, saved many lives. The upgrade of the tsunami warning, 30 minutes after the earthquake, before the tsunami's arrival on the coast, proved ineffective because of the failure of communications. The Japanese Meteorological Agency, JMA (2013) concluded that the first estimation of the magnitude of 7.9 used to forecast the initial tsunami wave heights resulted in an underestimation of the tsunami. One of the immediate consequences was that some people thought the sea walls would protect them.
However, unlike the 2004 event, this tsunami caused only one casualty outside Japan, demonstrating the efficacy of the tsunami warning for the Pacific Ocean. Japan's warning system provided crucial alerts, leading to the successful evacuation of thousands and minimizing casualties compared to the scale of the disaster.

2.3 The 28 December 2018 Anak Krakatau tsunami

Tsunamis generated by volcanic activity are much less frequent than those generated by submarine earthquakes. The phenomena that cause this type of tsunamis are volcanic earthquakes, gravitational and caldera collapses, pyroclastic flows, underwater explosions and volcanic blasts (Latter 1981). In general, tsunami-induced by volcanic eruptions typically, trigger localized tsunamis that dissipate energy very efficiently with distance.

On 22 December, 2018, a violent eruption occurred, which led to a partial collapse of the volcano's flank. This collapse resulted in a massive underwater landslide, displacing a significant volume of seawater (Ye *et al*. 2020). The displacement of seawater generated a series of powerful tsunami waves that propagated outward from the volcano.

Unlike traditional earthquake-generated tsunamis, the Anak Krakatau tsunami was triggered by an underwater landslide caused by a volcanic eruption. This made it difficult to anticipate and issue timely warnings, as the event occurred rapidly and without the usual seismic precursors associated with earthquake-generated tsunamis.

Anak Krakatau's volcanic activity had been ongoing for some time prior to the eruption in December 2018. However, predicting the exact timing and scale of a volcanic eruption is extremely challenging. The eruption and the associated flank collapse were sudden events that caught monitoring agencies off guard.

Monitoring and early warning systems in the area were not equipped to handle a volcanic-induced tsunami of this nature. While Indonesia has a network of seismometers and tsunami buoys, that can handle earthquake-induced tsunamis, there are no monitoring systems in place to detect the underwater landslides associated with volcanic eruptions.

Moreover, volcanic tsunamis, like the one triggered by Anak Krakatau, are relatively rare and less well-understood compared to earthquake-generated tsunamis. The lack of historical data on similar events in the region further contributed to the difficulty in predicting and warning about the tsunami.

2.4. The 15 January 2022 Tonga tsunami

On 15 January 2022, a massive volcanic eruption of the Hunga Tonga-Hunga Ha′apai volcano occurred. This explosion, in the Kermadec-Tonga intraoceanic volcanic arc is one of the largest in the last 30 years, generated atmospheric waves (Duncombe 2022) and an exceptionally fast-travelling global tsunami with minimal dissipation in the far field.
(Omira *et al.* 2022) explained that the cause of the global observed tsunami was a moving atmospheric source mechanism that forced the ocean surface and accompanied both the formation and the propagation of tsunami waves.

The tsunami travel times at most stations were much shorter than theoretically expected for a "classical" tsunami wave propagating away from Tonga but coincident with the passing of a fast-moving atmospheric pressure wave generated in the volcanic explosion (Omira *et al.* 2022; Tarumi and Yoshizawa 2023). Considering the time of the eruption, the average speed of a tsunami in deep ocean and distance between the volcano and Japan, the first tsunami waves were expected by 10:30 local. However, the first waves to arrive were not from a classic tsunami and reached Japan two hours earlier

The tsunamis generated by the 15 January eruption provided plenty of surprises. One of them occurred in Japan. Based on the time of the eruption, its distance from Japan, and the average speed of tsunami waves in the Pacific Ocean—between 450 and 500 miles per hour, comparable to the speed of a commercial airliner—the first tsunami waves should have reached Japan's Osagawara islands around 10:30 p.m. local time.

The tsunami travel times at most stations were much shorter than theoretically expected for a "classical" tsunami wave propagating away from Tonga but coincident with the passing of a fast-moving atmospheric pressure wave generated in the volcanic explosion (Omira *et al.*

2022). In Japan JMA were expecting the arrival of classic tsunami—triggered by displacement of the massive volume of seawater at the tsunami's source. However, the first waves to arrive were not from a classic tsunami (USGS 2022; Imamura *et al*. 2022).

3. Progress since 2004

Following the Sumatra 2004 disaster, the Intergovernmental Oceanographic Commission of IOC UNESCO recognized the need to establish TEWS all over the globe.
Since then, substantial progress has been made in improving tsunami-warning systems worldwide. Investments in detection and monitoring technologies, enhanced communication infrastructure, and international collaboration have significantly enhanced the ability to detect and respond to tsunami threats of earthquake origin.

Presently, there are four regional systems (see Fig.2): the NEAMTWS – North East Atlantic, Mediterranean and Adjacent Seas Tsunami Warning System, the IOTWS – Indian Ocean Tsunami Warning System, the PTWS – Pacific Tsunami Warning System and the Caribe Early Warning System. Tsunami Service Providers operating under the framework of UNESCO officially provide this information to the designated Tsunami Warning Focal Points / National Tsunami Warning Centres (TWFP/NTWC) of Member States.

These systems rely on seismic networks, tide gauge networks, and in data-sharing mechanisms. In the Pacific and Indian Oceans, bottom pressure recorders (tsunameters) complement the seismic and tide gauge networks, providing tsunami information much before the tsunami reaches the shore. This is not the case for the NEAMTWS operating in the Mediterranean and North-Eastern Atlantic (Amato 2020). This area was home to catastrophic events in the past. The Mediterranean hosted one of the deadliest tsunamis generated by the AD 365 Crete earthquake; Another major tsunami occurred in 1908 in Messina. Recently the area was home to the 2002 tsunami in Stromboli (Italy), the 2003 tsunami caused by an earthquake offshore Boumerdés (Algeria), and the 2017 Kos-Bodrum or the 2020 Samos-Izmir events of tectonic origin (Fig. 4)

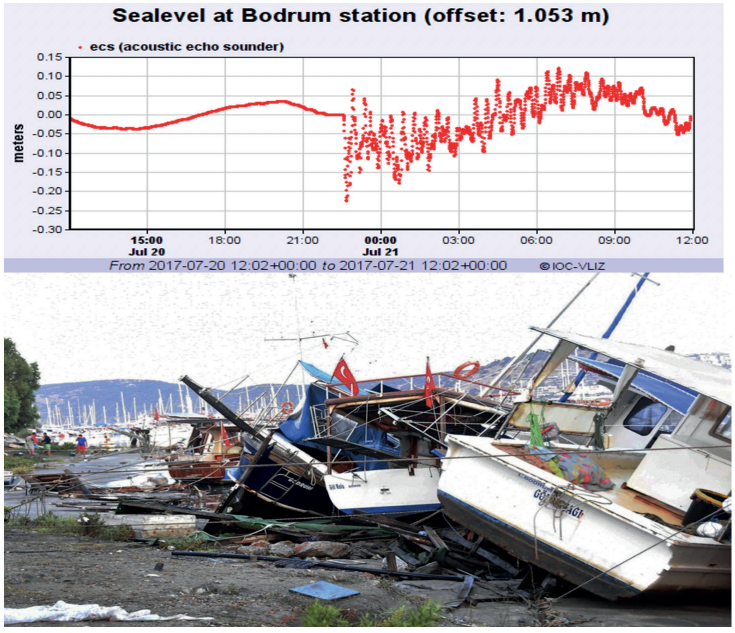

Figure 4. Kos-Bodrum earthquake 2020;

Upper panel : tide-record at Bodrun sealevel station (http://www.ioc-sealevelmonitoring.org/);

Lower panel : Damage caused by the tsunami in Bodrum (courtesy of Prof. Y. Alciner)

The North-Eastern Atlantic was home to two (confirmed) ocean-wide tsunamis in 1755 and 1761. In the 20th century, three earthquakes of magnitude greater than 7 (see Fig. 5) occurred between Iberia and the Azores in 1941, 1969 and 1975 (Baptista and Miranda 2009).

Here the tsunami warning centers operating in the area rely on seismic and tide gauge networks only. However, in the Atlantic, the area of generation of the 1st November 1755 Lisbon tsunami and home of several other tsunamis will benefit from the installation of new submarine communication cables (Fig. 5) that will be equipped with seafloor sensors able to contribute to shorten the latency between the earthquake detection and the tsunami warning.

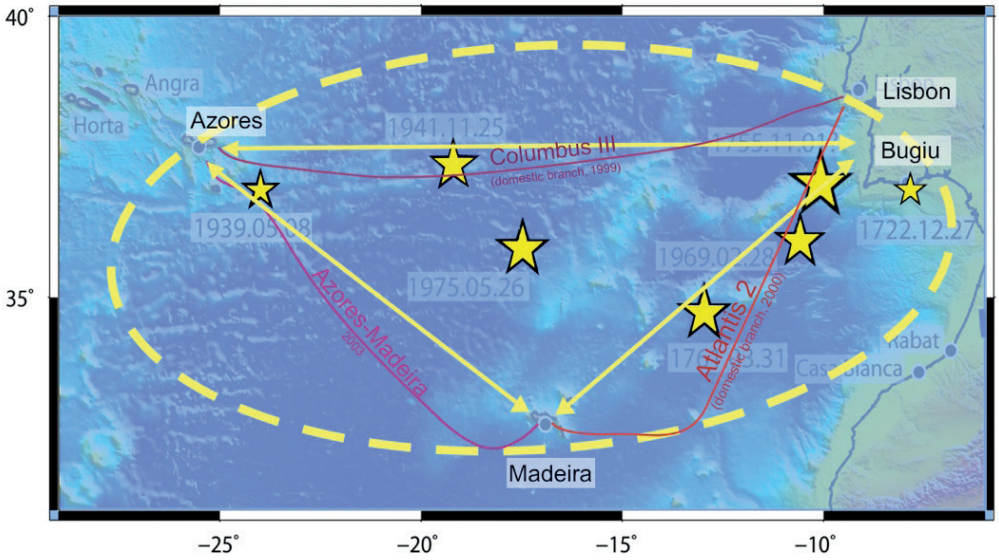

Figure 5. Tsunamis in the North-Eastern Atlantic (adapted from Baptista 2020). Yellow stars represent the epicenters of the tsunamigenic earthquakes; red lines represent present submarine communication cables

4. Challenges

Current tsunami warning systems operate in the need for fast analysis of seismic data. However, the recent developments in seismic data analysis permit the rapid assessment of earthquake source parameters and assess the size of with acceptable accuracy and estimate the potential tsunami size, in order to issue tsunami warnings in less than half an hour for global earthquakes (Satake 2014). However, the assessment of earthquake source characteristics for near-source events, to enable timely and appropriate community responses, will limit unnecessary disruption and enhance public trust (Amato 2020).

Tsunami warning systems are primarily designed to detect seismic activity and its associated tsunamis. Non-seismic tsunamis are relatively rare and less well-documented compared to earthquake-induced tsunamis. This lack of data and scientific understanding further complicates the development of warning systems for these events. Moreover, tsunamis triggered by non-seismic events can be highly variable in size, direction, and timing. This makes it challenging to develop a one-size-fits-all warning system for such events.

Volcanic tsunamis, for example, are often triggered by underwater landslides or the sudden collapse of a volcanic island, events that may not generate the seismic signals typical of earthquake-induced tsunamis.

Operational tsunami early warning systems around the globe were not fully prepared to respond to an atypical tsunami like the Tonga event (Gusman *et al.* 2022). The full hazard extent of atmospheric-driven tsunamis triggered by volcanic activity is still unknown and, therefore, rarely considered in the design of tsunami early-warning systems (Omira *et al*. 2022).

5. Final Considerations

Tsunami warning systems primarily focus on tsunamis of seismic origin, as they are the most common and predictable type. These systems rely on seismometers to detect undersea earthquakes and the potential for a resulting tsunami. When an earthquake is detected, various warning centers use the seismic data to assess the tsunami threat and issue alerts to coastal areas at risk.

However, tsunami warning systems are less effective in dealing with tsunamis of non-seismic origin, such as those caused by volcanic eruptions and landslides. Non-seismic tsunamis often occur with little to no warning or precursor signals. Earthquakes provide some lead time for warning systems to assess the potential of a tsunami being generated. Tsunamis triggered by non-seismic events can be highly variable in size, direction, and timing.

While warning systems can be adapted to incorporate some elements of non-seismic tsunami monitoring, such as the monitoring of volcanic activity and the potential for flank collapses, these efforts are generally in their early stages and may be more region-specific. In the case of volcanic tsunamis, for example, monitoring agencies may install specialized equipment near active volcanoes to detect signs of potential tsunamis caused by eruptions or landslides.

In summary, tsunami warning systems are better equipped to deal with tsunamis of seismic origin, and they are less effective in handling non-seismic tsunamis due to the unique challenges and complexities associated with these events. Monitoring and warning efforts for non-seismic tsunamis are works in progress, and there is ongoing research and development in this area to improve preparedness and reduce the risks associated with such events. Operational tsunami warning systems evolved since the Indian Ocean tsunami in 2004. Despite the improvements in detection monitoring and communication systems, Tsunami Early Warning Systems are successful only if countries effectively disseminate alerts to their citizens and if these citizens know what to do.

To be cited as:

M.A. Baptista. 2024. From Sumatra 2004 to Tonga 2022 - Progress and Challenges of Tsunami Early Warning Systems. p 89- 98. In CIESM Monograph 52 [F. Briand, Ed.] Marine hazards, coastal vulnerability, risk (mis)perceptions – a Mediterranean perspective. CIESM Publisher, Paris, Monaco, 182 p.

References

Amato A. 2020. Some reflections on tsunami early warning systems and their impact, with a look at the NEAMTWS. *Bollettino di Geofisica Teorica ed Applicata.*

Baptista M. A and J.M Miranda. 2009. Revision of the Portuguese catalog of tsunamis. *Natural hazards and earth system sciences* 9(1): 25-42.

Baptista M. A. 2020. Tsunamis along the Azores Gibraltar plate boundary. *Pure and Applied Geophysics* 177(4): 1713-1724.

Cisternas M., Atwater B., Torrejón F. *et al*., Predecessors of the giant 1960 Chile earthquake. *Nature* 437: 404–407 (2005). https://doi.org/10.1038/nature03943

Duncombe J. 2022. The surprising reach of Tonga's giant atmospheric waves. *Eos* 103: (10.1029).

Gusman A. R., Roger J., Noble C., Wang X., Power W and D. Burbidge. 2022. The 2022 Hunga Tonga-Hunga Ha'apai Volcano Air-Wave Generated Tsunami. *Pure and Applied Geophysics* 179(10): 3511-3525.

Imamura F., Boret S. P., Suppasri A., and A. Muhari. 2019. Recent occurrences of serious tsunami damage and the future challenges of tsunami disaster risk reduction. *Progress in Disaster Science 1*, 100009.

Imamura F., Suppasri A., Arikawa T. *et al*. 2022. Preliminary Observations and Impact in Japan of the Tsunami Caused by the Tonga Volcanic Eruption on January 15, 2022. *Pure Appl. Geophys.* 179, 1549–1560 (2022). https://doi.org/10.1007/s00024-022-03058-0

Japan Meteorological Agency (JMA). 2013, Lessons Learned from the Tsunami Disaster Caused by the 2011 Great East Japan Earthquake and Improvements in JMA's Tsunami Warning System. See http://www.data.jma.go.jp/svd/eqev/data/en/tsunami/LessonsLearned_Improvements_brochure.pdf. Google Scholar

Kanamori H. 1977. The energy release in great earthquakes. *Journal of geophysical research*, *82*(20): 2981-2987.

Kelman I. 2006. "Warning for the 26 December 2004 tsunamis", Disaster Prevention and Management, Vol. 15 No. 1, pp. 178-189. https://doi.org/10.1108/09653560610654329

Latter J. N. 1981. Tsunamis of volcanic origin: summary of causes with particular references to Krakatoa, 1883. *Bull. Volcanol.* 443: 467–490 (1981)

Lay T., Kanamori H., Ammon C. J., Nettles M., Ward S. N., Aster R. C., Beck S. L., Bilek S. L., Brudzinski M. R., Butler R., DeShon H. R., Ekström G., Satake Kand S. Sipkin. 2005. The Great Sumatra-Andaman Earthquake of 26 December 2004. *Science*, 308(5725): 1127–1133. http://www.jstor.org/stable/3842093

National Geophysical Data Center / World Data Service (NGDC/WDS). 2012: NCEI/WDS Natural Hazards Image Database. First. https://doi.org/10.7289/V5154F01. Accessed [2023.11.14].

Okal E. A. 2015. The quest for wisdom: lessons from 17 tsunamis, 2004–2014. *Phil. Trans. R. Soc. A.* 373: 20140370

Omira R., Ramalho R. S., Kim J., González P. J., Kadri U., Miranda J. M., ... and M.A Baptista. 2022. Global Tonga tsunami explained by a fast-moving atmospheric source. *Nature*, 609(7928): 734-740.

Satake K. 2014. Advances in earthquake and tsunami sciences and disaster risk reduction since the 2004 Indian ocean tsunami. *Geoscience Letters*, *1*(1), 1-13.

Stein S. and E.A Okal. 2011. The size of the 2011 Tohoku earthquake need not have been a surprise. *Eos, Transactions American Geophysical Union*, *92*(27), 227-228.

Tarumi K and K. Yoshizawa. 2023. Eruption sequence of the 2022 Hunga Tonga-Hunga Ha'apai explosion from back-projection of teleseismic P waves. *Earth and Planetary Science Letters*, 602, 117966.

USGS. 2022. https://www.usgs.gov/centers/pcmsc/news/depth-surprising-tsunamis-caused-explosive-eruption-tonga (accessed 11.08.2023)

Ye L., Kanamori H., Rivera L., Lay T., Zhou Y., Sianipar D and K. Satake 2020. The 22 December 2018 tsunami from flank collapse of Anak Krakatau volcano during eruption. *Science advances*, 6(3), eaaz1377.

Nile surf zone - past and future according to climate change

Rania E. Mohamed

Hydraulics and Irrigation Engineering Department, Alexandria University, Egypt
rania_mohamed@alexu.edu.eg

Abstract

The Egyptian Mediterranean coastline is a most complex ecosystem where ecology, geomorphology and intense human activities all interact. In Egypt, Mediterranean beaches not only experience diverse natural processes (waves, winds, sea level changes, currents, near-shore sediment transport, etc.), but they are also severely threatened by climate change, particularly in the low-lying delta. Concerns include sea level rise (SLR), more intense extreme weather events, pollution, disruption of ecosystem balance, saltwater intrusion, soil salinization, and issues with outlet siltation. SLR causes serious environmental and coastal risks such as land subsidence, flooding, and coastline erosion. To manage and mitigate the region's challenges which affect both coastal populations and ecosystems, it is essential to understand these effects. This article covers the history of the Nile surf zone, the effects of climate change on the area, different strategies for adaptation and mitigation of sea level rise, and the future conditions necessary to keep the Nile surf zone safe from anticipated climate change.

Keywords: Egyptian Mediterranean coastline, climate change, Nile Delta, coastal erosion, sea level rise.

Introduction

The coastal zones of Egypt extend for over 3,000 km in length along the Mediterranean and Red Seas. The Egyptian Mediterranean coastline extends for about 1,050 km, covering the northern territory of Egypt as shown in Figure 1. This coastline is divided into several sectors, ranging from the northwestern coast, Nile Delta coast, northeastern coast, to the Red Sea and Gulfs coastal sectors.

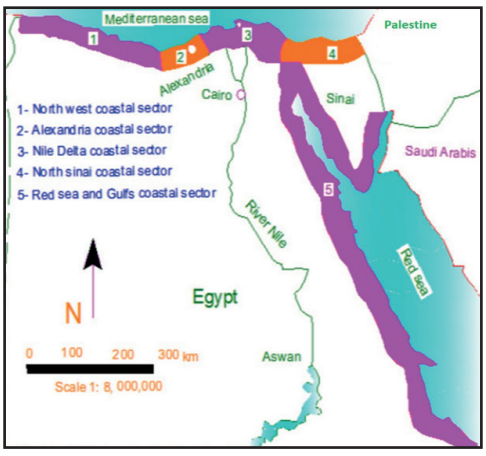

Figure 1. The Egyptian coastal zone areas.

The Egyptian Mediterranean coastline is a complex ecosystem, home to several coastal cities, including Port Said, Damietta, and Alexandria. In addition, it has two promontories (Rosetta and Damietta), and three lagoons (from west to east, Idku, Burullus, and Manzala) connected with the Mediterranean Sea. These lakes represent 25% of the total wetland area of Egypt. There are five fishing harbors (Abo Qir, El Maadiya, El Burullus, Ezbt El Borg and Port Said). Dunes exist near Idku, El Burullus, Baltium, and Gamasa.

Climate change is posing significant threats to the Egyptian Mediterranean coast, particularly in the low-lying delta, causing sea level rise, intensifying extreme weather events, saltwater intrusion, soil salinization, and siltation problems, althogether disrupting ecosystem balance. Sea level rise (SLR) generates significant hazards to the environment and coastal areas worldwide by way of land subsidence, coastline erosion, and flooding as covered in all chapters of this volume. Therefore, understanding these impacts is crucial for coastal communities and ecosystems, so as to develop optimal adaptation strategies.

This article provides an historical overview of the Nile surf zone, reviews the impacts of climate change on the region, proposing various adaptation and mitigation approaches to deal with SLR so as to better protect the Nile surf zone from climate change in the future.

Historical overview of the Nile surf zone

An historical map of Egypt's Mediterranean coastline is shown in Figure 2, with three distinct sectors:

A. The northwestern coast extends from Alexandria to the western Egyptian-Libyan border. It is characterized by sand with rocky sandstone, clear blue water, and mild weather - all features that make this area particularly attractive for tourism and development, although steep slopes of the surf zone and rip current generation may cause trouble for swimming (Fanos *et al.* 1995).

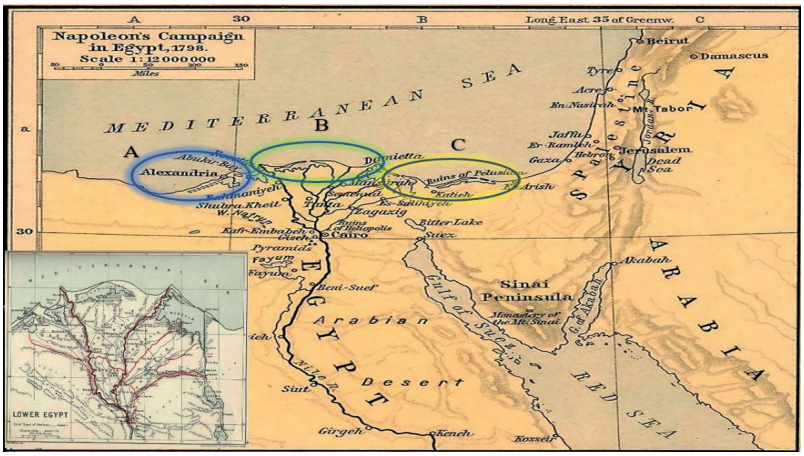

Figure 2. Historical map of the Egyptian Mediterranean coastlines.

B. The Nile Delta extends about 240 km from the east of Alexandria to the west of Port Said. It is very densely populated, full of agriculture, industry, and fishing activities, and is of

great importance to the Egyptian economy. It is a historically important and beautiful area for tourism and investment. The Nile Delta is one of the oldest deltaic systems in the world and forms a highly dynamic natural environment. The Nile River is the main source of water and sediments that built the Delta in the past and comprises two main branches (Rosetta and Damietta). The Nile Delta was formed by combining the action of coastal processes such as tides, waves, and currents with the continual transport of sediment from the Nile River into the sea. The sediment and flow quantities discharging into the sea became nil after the construction of the High Aswan Dam in 1964. Trapping the sediments caused severe erosion of the Delta coast and more sedimentation problems for the estuaries. Many researchers (for ex. Sharaan and Udo, 2020) consider that the Nile Delta is the most vulnerable coastal area in the Mediterranean Sea as environmental issues include erosion due to wave impacts, local erosion due to coastal protection structures, siltation problems from waves and sea currents, and heavy pollution in the Nile Surf Zone and surrounding lagoons.

C. The northeastern coast starts from Port Said to the eastern border and consists of two sections. The western section presents great similarity to the Nile Delta coastline; it can be considered as part of the Nile Delta proper as it consists of sandy silty soil as an old Nile branch was passing by this area. The eastern section is a sandy dune coast. Many tourist villages have been constructed along the shoreline in this part.

Climate change impacts on the Nile surf zone

The Nile Delta coast is a highly risky area as it is affected by natural climatic factors and man-made activities that significantly change the shoreline dynamics. It also suffers from coastal erosion, sea level rise, and land subsidence. In addition, coastal flooding presents a difficult challenge as it can destroy coastal cities, historical sites, critical infrastructure and dune systems. In the last few years, the shores of Alexandria faced significant flooding problems: in the winters 2003- 2006 and 2010 they were struck by a series of surge storms, water and sand overtopped the seawall and destroyed many parts of it. Figure 3 illustrates this serious problem.

In coming years, such storms are expected to increase due to sea level rise (Mohamed 2012). Many studies were conducted to predict and evaluate the impact of flooding along the Nile Delta coasts. According to recent projections, a one-meter sea level rise will result in the inundation and loss of 20–30% of the Nile Delta region.

Figure 3. Flooding at the Alexandrian coastline.

Coastal wetlands act as natural buffers against erosion, but their degradation due to human activities exacerbates the problem. In addition, the growing instability of coastal dunes (Figure 4) that are essential for preserving the coastline system is responsible for aggravating the erosion problems on the Nile Delta coasts. Habitats recognized as coastal dunes decreased by around 45% in the Nile Delta between 1990 and 2014 (Mohamed and Abd-El-Mooty, 2023a).

Figure 4. Natural dunes along the Nile Delta, Egypt.

Land subsidence refers to the lowering or emergence of the ground surface around a geodetic datum, influenced by isostasy, tectonism, compaction and anthropogenic influences. Stanley (1997) showed that the northeastern side of the delta has higher values (lowering to 5 mm/year). Becker and Sultan (2009) used radar interferometry to reconstruct modern subsidence rates of as much as 8 mm/yr around the Damietta mouth. They also found that the Al Manzala Lagoon area suffered moderate subsidence rates (4-6 mm/yr.) in the northern part of the delta. They concluded that the Delta's subsidence is influenced by recent sediment deformation, with extreme threats at the Damietta and Rosetta branches, where active deposition is occurring. As shown in Figure 5 the lowest subsidence rates are in the areas situated inland that are more than 2 m above sea level (Marriner *et al.* 2012).

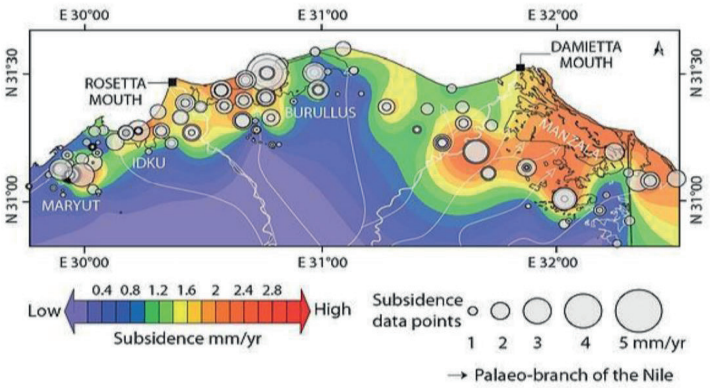

Figure 5. Subsidence in the Nile Delta (after Marriner *et al.* 2012)

Urgent action is clearly needed to mitigate these impacts, adapt to the changing climate, and protect the invaluable resources of the Nile Surf Zone for current and future generations. The challenges are immense but with global cooperation and innovative solutions we can work towards a more resilient and sustainable future for this critical region.

Egyptian projects to adapt the Nile Delta coastline to sea level rise

The Egyptian government is working to secure the Nile Delta coasts from climatic threats, with a national plan for coastal adaptation to SLR. The government has implemented several protection structures, such as seawalls, revetments, and beach nourishment. Others are under construction and consideration (rehabilitation of dunes, experimental dunes, enforcing coastal roads, combined technologies) to address the natural process of SLR. The most popular seawall in Egypt is the Mohamed Ali seawall (see Fig. 6), located at the coast of Abo Qir Bay mainly for protecting the low backward land (1.5–2.5 m below SLR) (Iskander 2010). Also, revetment protection technology was implemented at different beaches along the Nile Delta, such as the Rosetta promontory, east of Burg El-Burullus. Some projects have been reinforced with additional armor units, and protected beaches with seawalls are nourished by sand or sandbags for increased stability and durability.

Figure 6. Examples of the implemented hard structures as a protection adaptation option to SLR (Iskander 2010).

The Egyptian General Authority for Shores Protection (SPA) and the Egyptian Environmental Affairs Agency (EEAA) are working together to achieve a sustainable coastal environment. They have implemented numerous projects, costing around 63 million USD. The current project, an artificial dune implemented along 30 km of the low-lying coastal area between El-Burullus and Rosetta promontory, is costing around 9 million USD. Recent progress in adaptive Nile Delta coast projects, particularly artificial dunes, shows promising results, keeping in mind that public awareness and community participation are crucial for success, and that integrating management concepts can further support local authorities' efforts (Sharaan *et al.* 2022).

Case studies and best practices

Examining successful adaptation and mitigation projects in different coastal regions provides valuable lessons. Collaboration among stakeholders, early warning systems, and community engagement are all essential components of effective climate resilience strategies. The next

section will examine three regions along the Egyptian Mediterranean coast (Alexandria, Rosetta, and Damietta promontories).

Alexandria

The Alexandria coast lies on the northern coast of Egypt, bordering the Mediterranean Sea. It is also located in the western part of the Nile Delta. Alexandria Beach is characterized by its narrowness, flatness, and parallel limestone ridges. It is popular for its stunning coastlines, fascinating views, and energetic environment as shown in Figure 7. It has been a significant port city since ancient times, and the region's development both historically and culturally is greatly affected by its coastal location. Due to both natural and human activities, its beaches are vulnerable to a variety of environmental issues, such as water pollution, beach erosion, loss of biodiversity and climate change impacts (Mohamed and Abd-El-Mooty 2023a).

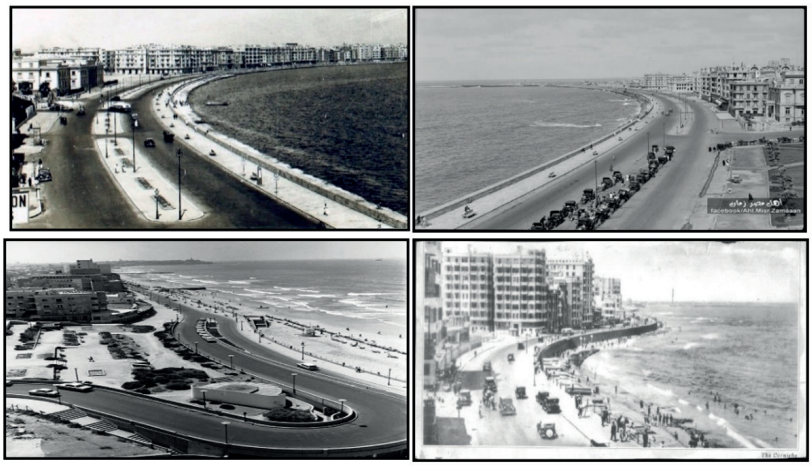

Figure 7. Old beaches of Alexandria

Climate change impacts along the Alexandria coastline

Alexandria shores have faced several problems over the last decades, ranging from extreme rates of erosion, flooding and run-up, ecosystem pollution, and degradation. Two major challenges for the Alexandria coastline are flooding and erosion. Because of natural forces including storms, wave action, and rising sea levels, the beaches experience severe erosion. Erosion is exacerbated by human activities such as building near the coast and blocking the flow of natural sand. This has led to the loss of beaches, damage to infrastructure, and increased vulnerability to flooding (see Fig. 8), that are magnified by the rapid growth of urban areas. To address these issues, the Egyptian government and the concerned local authorities have started several projects, such as building seawalls and breakwaters and conserving beaches. Long-term strategies include coastal zone management plans, environmentally friendly methods of urban growth, and awareness about the importance of preserving the natural resources along the shore.

Figure 8. Waves' impacts along the Alexandria coastline.

Recent coastal protection structures along the Alexandria coastline

The eastern shore of Alexandria has small beaches and rocky headlands that stretch from El Silcila to Abu Quir. Based on morphology and coastal protection, the area is divided into three zones: Zone I has narrow sand beaches, Zone II is protected, and Zone III has either narrow or no beaches as shown in Figure 9.

Figure 9. Alexandria coastal zones.

Submerged breakwaters and sand nourishment are key components of coastal projects aimed at addressing current problems in the Al-Montazah, Al-Mandara and Al-Asafra areas. These projects aim to mitigate erosion, narrow sandy beaches and sand nourishment, ensuring the safety and accessibility of these areas for visitors. The coastal projects that were executed in Zone I are illustrated in Figure 10. Submerged breakwaters and sand nourishment work protect the Corniche wall to mitigate extreme erosion in Zone II beaches.

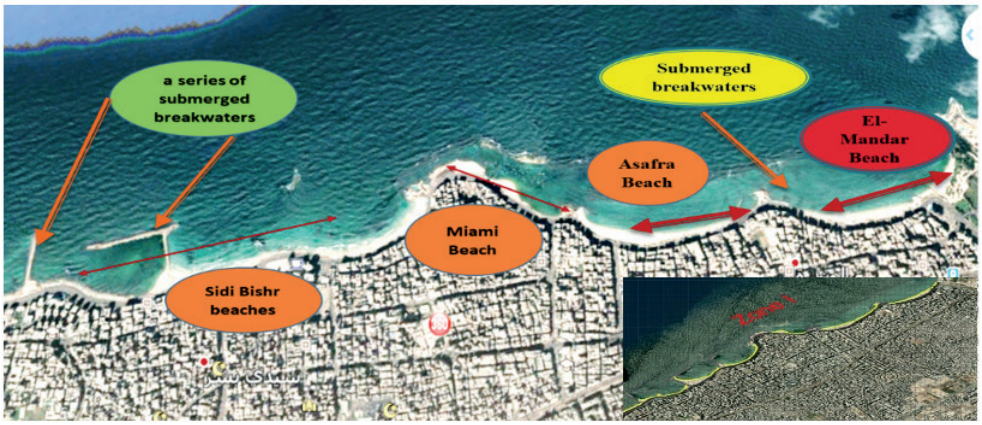

Figure 10. The protection works that were executed in Zone I.

San Stefano Beach and the club area from Saba Pasha to Sidi Gaber are fully protected as shown in Figure 11.

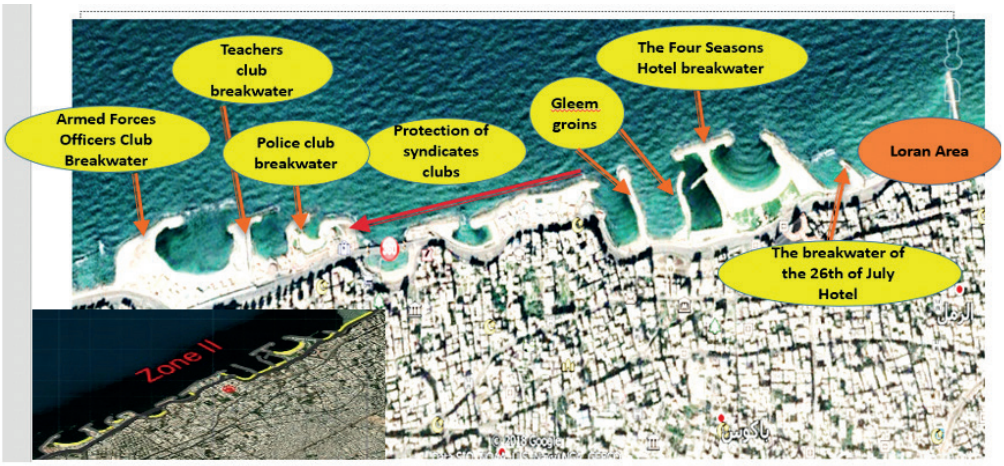

Figure 11. The protection works that were executed in Zone II.

In the Sidi Gaber region, three submerged breakwaters will be constructed up to El Silcila, covering an area of 4 km as shown in Figure 12. To prevent winter waves, existing protection blocks will be removed, and new beaches will be created using sand nourishment (Mohamed and Abd-El-Mooty 2023b).

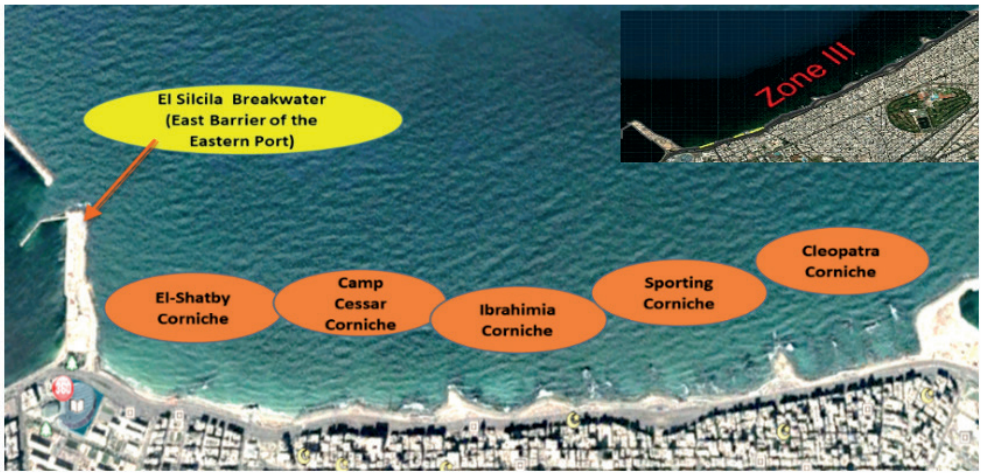

Figure 12. The executed coastal protection works in Zone III.

Qaitbay Castle faces erosion and high waves, causing gaps and potential collapses. To preserve submerged ruins and attract tourism, a coastal structure project was executed, including a 550m breakwater, a 100m marina, and a 132m walkway. Sand nourishment is used to create beaches, ensuring the castle's protection and development (see Fig. 13).

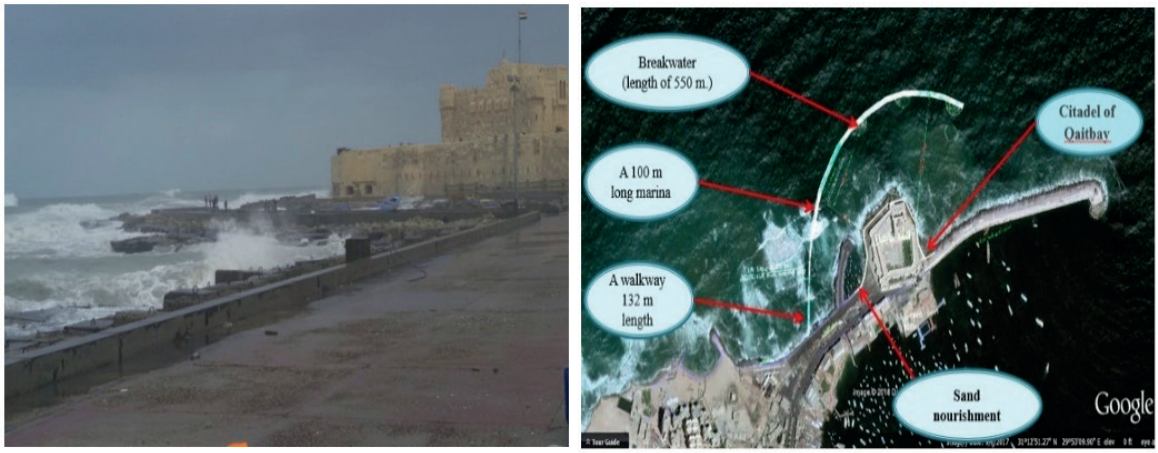

Figure 13. Qaitbay Citadel - the project area before and after starting implementation.

Rosetta promontory

The Rosetta promontory, which extended 14 km seaward, experienced significant changes in shoreline position in the last 500 years. Between 1500 and 1900, sediment supply exceeded natural losses driven by wave and current action, but climate change, dams and barrages construction, irrigation needs, and man-made activities have reduced water flow and sediments carried by the Rosetta branch. Between 1900-1964, the western and eastern sides lost 879-1282 meters, with an average erosion rate of 13.7-20 m/yr. Between 1964 and 2006, the Nile water storage increased the erosion rate to 95.3-124.8 m/yr. (Fanos 1995). Figure 14 shows the shoreline advance and retreat during the period extending from 1500 to 2005.

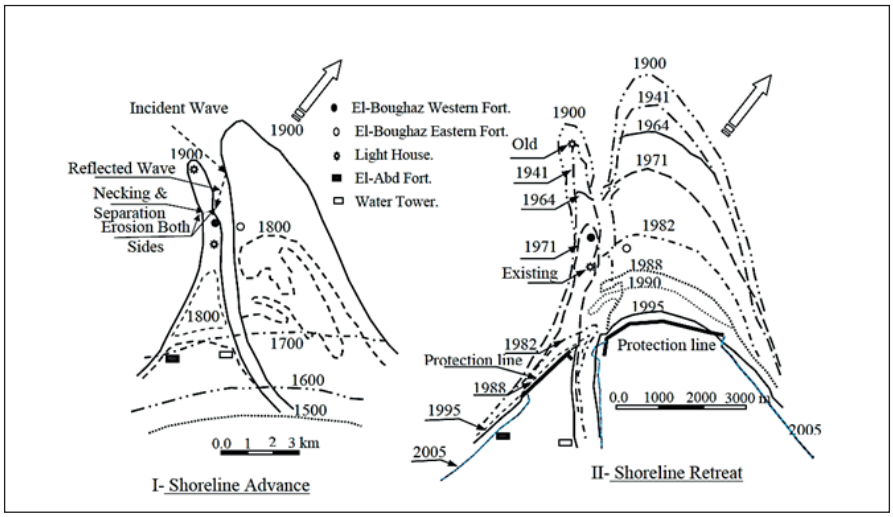

Figure 14. Rosetta Promontory - shoreline advance and retreat (1500-2005).

Coastal protection works

Several structures have been constructed to cope with the erosion and sedimentation issues at the Rosetta Promontory. To reduce erosion at the outer tip of the Rosetta promontory, two Dolos revetments of 1.5 and 3.5 km were constructed between 1989 and 1991 on the land (see Fig 15 A). The lengthening of the promontory has been successfully stopped and reduced by these revetments. However, sediment flow in front of revetments, waves, and currents caused the land to disappear. Erosion on the eastern and southern faces of the promontory reached 80 m/year due to coastal forces. In 1998, five 500-meter rubble mound groins were built to protect 5 km of beachfront. In 2000, 40 rubber-tube submerged groins were built to protect 2 km along the western revetment but failed.

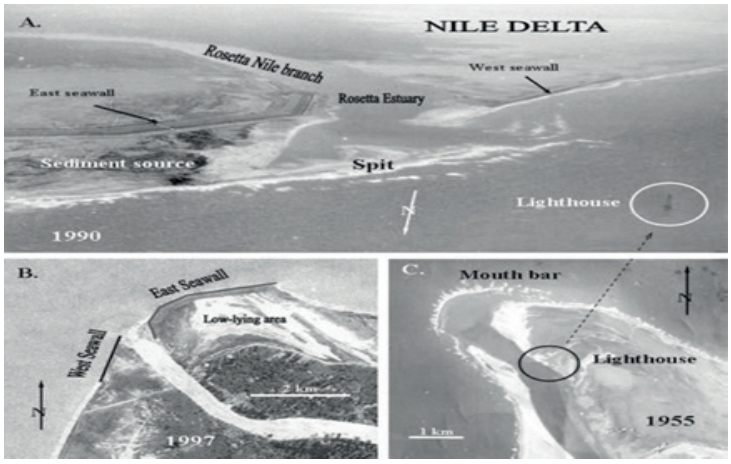

Figure 15. Aerial photographs of the Rosetta Nile branch (from Fanos 1995)

Because erosion continued in this area and extended towards its down-drift side, a basalt wall was executed to protect the area. In 2005, a new construction project featured nine rubble mound groins, spanning 250-450 meters and 5 km from the southern end of the western revetment. All

recent structures are shown in Figure 16). Over the past few years, local shoreline changes have occurred, particularly near protective engineering features like seawalls and breakwaters. This accretion is caused by eroded sediments transported by long-shore currents and offshore movement, with a maximum net erosion of 6.1 x 10^6 cubic meters from 1919/1922 to 1986 (Fanos *et al.* 2007).

Figure 16. The current protective structures along the Rosetta Promontory.

Damietta promontory

The Damietta Promontory, located northeast of the Nile Delta, depends on fishing and tourism to sustain its economy. Before the High Dam was built, it was subject to yearly discharges of over 150 million m^3 of sediment and seasonal flooding. The promontory expanded seaward between 1800 and 1900, but as illustrated below in Figure 17, a reversed condition of erosion started about 1900 because of the Nile River's reduced capacity to carry sediment to the Damietta Branch. The subsequent coastline shift at Damietta Promontory was caused by both sea level rise of 5-7.9 mm/yr. and land subsidence of up to 5 mm/yr. (El-Gamal *et al*. 2020).

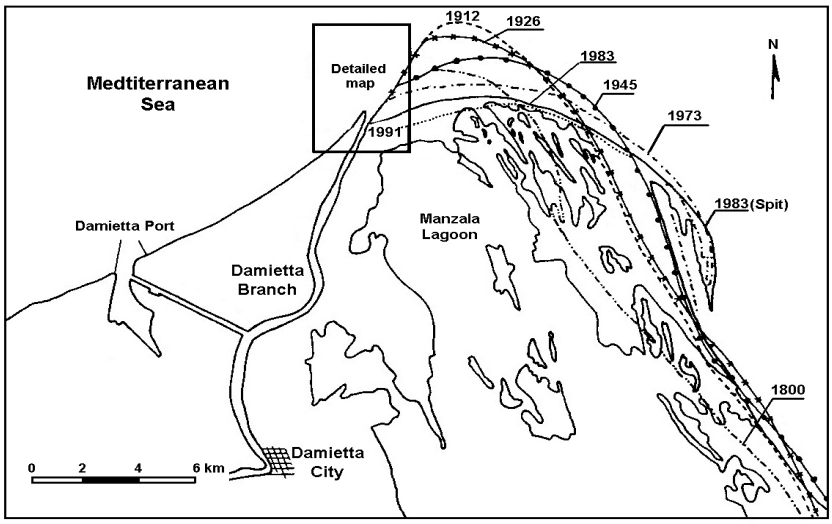

Figure 17. Morphological changes of the Damietta mouth from 1800 to 1991 (from Fanos 1995).

Erosion in the Damietta promontory started around 1900, averaging 40.7 m/yr, and increased to over 100 m/yr after the High Dam's construction. The western and eastern sides experienced a 4.5 km long spit, which was observed in 1983 aerial photos (see Fig. 18).
Coastline changes of the Damietta promontory are comparable to those of the Rosetta area: it experienced erosion starting around 1900, losing 3.7 km between 1900-1991. The rate increased to over 100 m/yr after the High Dam construction, with some protected walls and groins. W/E currents accreted a 4.5 km long spit near the eastern side of the Damietta promontory, that appeared in the 1983 aerial photos recorded by Fanos (1995).

The overall pattern of erosion and accretion is similar in both promontories, with the maximum erosion occurring at the promontory tip, and accretion taking place along its flank, particularly to the east. Ras El Bar's western flank experienced less change due to 1941 protection. The lighthouses have disappeared due to erosion, and were replaced by a new one situated 220 m landward.

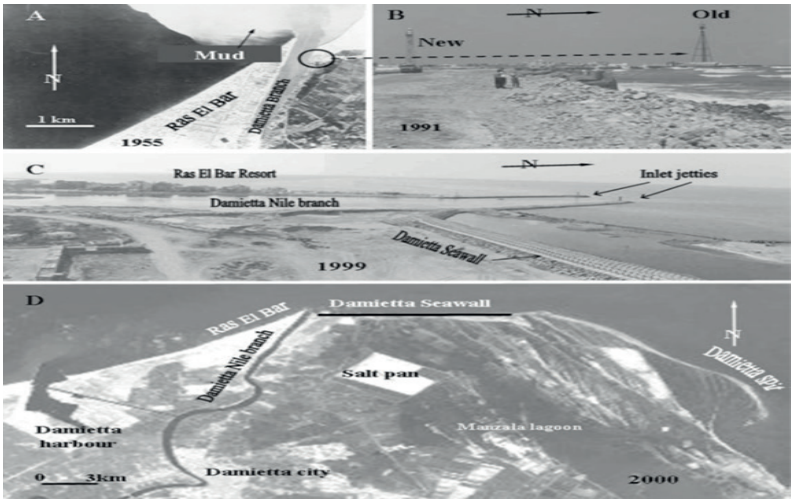

Figure 18. The aerial photograph of the Damietta promontory (Fanos 1995)

Since 1941 several structures have been built along the Damietta promontory to mitigate erosion as shown in Figure 19. A 240 m jetty was built in 1941 to reduce sediment deposition; another 290 m jetty was built in 1976 to minimize shoaling. In 1963, a concrete revetment was built to stop coastal erosion, which was later modified into a rubble revetment. In 1971, three concrete groins were constructed. Between 1991 and 2002, eight breakwaters were established to combat shore erosion. In 2000, a 6-km long seawall-oriented E-W was built onshore.

Figure 19. Recent protective structures along the Damietta Promontory.

Future scenarios for the Nile surf zone

Climate change is expected to significantly impact the Nile Surf Zone in the coming decades, causing rising sea levels, increased temperatures, and changing storm patterns. These changes could lead to coastal erosion and flooding, intensified heat waves, prolonged droughts, and altered precipitation patterns, which could impact agriculture and water availability.

Additionally, climate change is likely to alter the frequency and intensity of storms, resulting in destructive storm surges and flooding. These impacts present significant challenges for both ecosystems and human communities. In addition, ecological changes in the Nile surf zone are linked to climate change and pose significant challenges, including loss of biodiversity, saltwater intrusion, erosion, and coastal degradation. Scientific research plays a pivotal role in understanding and mitigating these impacts. It aids in climate modeling, adaptation strategies, policy formulation, and international collaboration. It also provides data for climate projections, aids in designing resilient infrastructure, and promotes sustainable practices that can withstand the changing climate. It also aids in advocating policies prioritizing climate resilience and mitigation. The global nature of climate change necessitates cooperation among nations and organizations.

Conclusion

The Nile surf zone, particularly the Nile Delta coast in Egypt, is facing severe impacts from climate change and sea level rise, including shoreline erosion, flooding, and deterioration of tourism facilities, industrial activities, and agricultural activities. To protect the Nile Delta coastline, Egyptian efforts towards an adaptive coast are being highlighted. The most appropriate

adaptation approach is based on coastal site-dependent assessments, with protection being the most effective. Egypt has implemented various protection structures, including seawalls, revetments, beach nourishment, and restoration of dune systems. The transition to environmentally friendly adaptation protection technologies is also being adopted globally. Mutual participation between coastal managers, researchers, policy, and decision-makers could provide an integrated framework for promoting coastal sustainability and dealing with future challenges.

To be cited as:

R.E. Mohamed. 2024. Nile surf zone - past and future according to climate change. p 99- 114. In CIESM Monograph 52 [F. Briand, Ed.] Marine hazards, coastal vulnerability, risk (mis)perceptions – a Mediterranean perspective. CIESM Publisher, Paris, Monaco, 182 p.

References

Becker R. and M. Sultan. 2009. Land subsidence in the Nile Delta: inferences from radar interferometry. *The Holocene* 19 (6): 949-954.

CoRI/UNESCO/UNDP. 1978. Coastal Protection Studies, Final Technical Report, Volume 1 and 2, 1978, Academy of Scientific Research and Technology.

El-Gamal A., Balbaa S., Rashed M. and A. Mansour. 2020. Three decades monitoring of shoreline change pattern of Damietta Promontory, Nile Delta, Egypt. *Aquatic Science and Technology* 8 (2): 1-14.

Fanos A., Sayed W.R., Ali M.A. and M. Iskander. 2007. Evolution of Rosetta promontory on Nile delta coast during the period from 1500 to 2005, Egypt. Proceedings of the 8th International Conference on the Mediterranean Coastal Environment, MEDCOAST 2007. 2. 1003-1016.

Fanos A., Khafagy A. and R. Dean. 1995. Protective works on the Nile delta coast. *Journal of Coastal Research* 11: 516-528.

Fanos A. 1995. The impact of human activities on the erosion and accretion of the Nile Delta coast, *J. Coast. Res.* 11(3): 821-833.

Iskander M.M. 2010. Environmental friendly methods for Egyptian coastal protection. In: First International Conference on Coastal Zone Management of River Deltas and Low Land Coastlines. Alexandria, Egypt.

Marriner N., Flaux C., Morhange C., and D. Kaniewski. 2012. Nile Delta's sinking past: Quantifiable links with Holocene compaction and climate-driven changes in sediment supply? *Geology* 40 (12): 1083-1086.

Mohamed R. 2012. Using Submerged Artificial Reefs Technique to Protect Alexandria City Coastline, Master thesis, Alexandria University.

Mohamed R. and M. Abd-El-Mooty. 2023. Coastal Environmental Issues of Climate Change Along the Nile Delta Coastline. Twenty-Third International Water Technology Conference, IWTC23, Port Said, 09-11 March 2023.

Mohamed R. and M. Abd-El-Mooty. 2023. Sustainable environmental Coastal development of the surf zone of Alexandria. Proceedings of the 4th International Conference of Chemical, Energy, and Environmental Engineering (ICCEE, 2023), Egypt Japan University of Science and Technology, Alexandria, Egypt.

Sharaan M., Iskander M. and K. Udo. 2022. Coastal adaptation to Sea Level Rise: An overview of Egypt's efforts. *Ocean & Coastal Management* 218: 106024.

Sharaan, M. and K. Udo. 2020. Projections of proper beach nourishment volume as an adaptation to beach recession based on SLR along the Nile delta coastline of Egypt. *J. Coast Res.* 95: 637–642.

Stanley D.J., 1997. Mediterranean deltas: subsidence as a major control of relative sea-level rise. pp. 35-62 in Transformations and evolution of the Mediterranean coastline. ClESM Science Series 3, 244 p. [F. Briand, ed.] *Bull. lnstit. Oceanogr. Monaco,* n° special 3.

Exposure to coastal erosion and flooding in the northeastern Aegean islands, Greece

D. Chatzistratis, IM Monioudi*, A.F. Velegrakis, Th. Chalazas, E. Tragou

Department of Marine Sciences, University of the Aegean, Greece

imonioudi@marine.aegean.gr *(corresponding author*)*

Abstract

This paper presents an assessment of the exposure to erosion and flooding of the island beaches of the NE Aegean Sea under the rising relative mean sea level and extreme sea levels (ESLs) due to climate variability and change. An analytical and a dynamic model ensemble are used to predict long-term and episodic beach erosion. For the flood risk assessment two approaches were employed. First, a GIS-based method applied on a 25 m resolution DEM offered a rapid flood risk assessment for all NE Aegean island beaches, whereas the 2-D hydrodynamic model LISFLOOD-FP was used in selected beaches using a fine (2x2 m) resolution grid for detailed projections of the flood extent and depth. The findings show an increased risk of beach erosion and coastal flooding under long-term mean sea level rise and episodic ESL respectively for most island beaches studied. Based on the median estimates of ensemble predictions, it is found that by 2100 and under the RCP8.5 scenario about 30 % of all 658 beaches will disappear completely. Already in 2050, under the moderate RCP4.5 scenario, 40 % of all beaches are threatened with total retreat under the impact of the 1-100 year ESLs. Regarding the flood risk, the supervisory assessment revealed extensive parts of coastline of each island to be exposed to ESL-induced flooding mainly due their low relief. The LISFLOOD simulations for two low-lying touristic sandy beaches in Limnos and Samos under the 1-100 year extreme event showed extended inundation reaching up to 340 m and 107 m, respectively in 2050. Predictions are more severe for 2100, when substantial increases in the flooded areas are expected including for the backshore dune system in Keros beach (Limnos) and protected wetlands in the Potokaki beach (Samos) where negative impacts are also expected for the nearby port infrastructure. Comparison of the two flood assessment methods highlights the increased accuracy of hydrodynamic modelling at local scales.

Keywords: beach erosion, Aegean Sea, coastal flooding, sea level rise, LISFLOOD

1. Introduction

Beaches are dynamic coastal environments of high environmental importance that can also act as buffers against the flooding of backshore habitats and assets/infrastructure. At the same time, many beaches worldwide are already under erosion (Mentaschi *et al*. 2018), whether of long-term or episodic nature.

The former refers to the landward retreat of the shoreline due to mean sea level rise and/or reduced terrestrial sediment supply to the coast. In the case of beaches backed by cliffs or human infrastructure such shoreline retreats can lead to permanent beach drowning/loss. In coastal areas,

long-term sea level changes are also controlled by the vertical land motions, land subsistence due to negative sediment budgets and aquifer overextraction, and extreme loading due to extensive, high-rise construction (e.g., Cao *et al*. 2021). The latter refers to the temporary beach retreat under the combined action of extreme storm waves and surges. In addition to temporary beach morphological changes such events can result in flood inundation of inland areas.

Coastal extreme sea levels (ESLs) depend on sea level rise, tides, extreme storm surges and wave set-ups. They are also controlled by seasonal climatic periodicities; offshore mesoscale eddies and changes in river flows. These hazards can negatively affect coastal populations, assets/infrastructures and activities as well as coastal habitats and biological resources and are projected to worsen considerably under climate variability and change –both in magnitude and frequency (Vousdoukas *et al.* 2018; IPCC 2019, 2023).

In the Eastern Mediterranean many coastal areas are also major tourism destinations, an economic sector accounting for a large fraction of the GDP in many coastal and island States (UNWTO 2019). The increasing erosion and/or more frequent flooding of beaches and their backshore assets will damage and reduce beach carrying capacity with adverse effects for coastal tourism and other economic activities (Garola *et al.* 2022). Coastal infrastructure, such as seaports and their inland transport connections will be also affected (see UNECE 2020). Coastal habitats, fisheries, aquaculture, as well as coastal agriculture will be also impacted to varying degrees, due to permanent and/or temporary coastal erosion and flooding, aquifer salinisation, seawater acidification, precipitation changes, droughts and wildfires. Therefore, assessments of exposure to the projected erosion and flooding at regional/island scale are needed in order to determine effective protection strategies. The present contribution focuses on climatic hazards and their potential impacts on the Greek islands of the northeastern Aegean Sea and particularly on the effects of sea level rise on coastal areas.

2. The study area

The study area comprises the seven islands that form part of the North Aegean Administrative Region: Lesvos, Chios, Limnos, Samos, Ikaria, Agios Eustratios and Psara (Fig. 1). The area is characterized by a high relief due to complex regional tectonics and comprises different geomorphological units (Poulos 2009) including the extensive N. Aegean Shelf, and the tectonic N. Aegean Trough. It is part of the Aegean Archipelago whose complex physiography results in relatively mild wind and wave climate due to the limited fetches (Monioudi *et al*. 2017) with prevailing wind and waves from the North direction (Androulidakis *et al.* 2015). The area is characterized by a microtidal regime, with tidal ranges rarely exceeding 0.2 m (Tsimplis *et al*. 1995; Marcos *et al.* 2009). Low salinity water inputs received from the Black Sea through the Dardanelles Straits are the main control factors of the complex circulation and hydrographic patterns of the region (Androulidakis and Kourafalou 2011).

The Eastern Mediterranean sea level depends on a number of processes, including sea-level changes propagating from the ocean (e.g. Calafat *et al*. 2012) and atmospheric forcing (e.g., Tsimplis and Shaw 2010). The average rate of mean sea level rise (MSLR) in the Mediterranean was calculated at around 1.7 mm yr^{-1} for the past century (Wöppelman and Marcos 2012). For the Greek Seas, during the period 1993-2021 alone, the average rate of MSLR was estimated at 3.6 mm yr^{-1}, with higher seasonal peaks in autumn and winter linked with low-pressure systems. The morphological complexity of the archipelago decreases the wind impact on storm surge formation compared to the pressure (see Androulidakis *et al.* 2023).

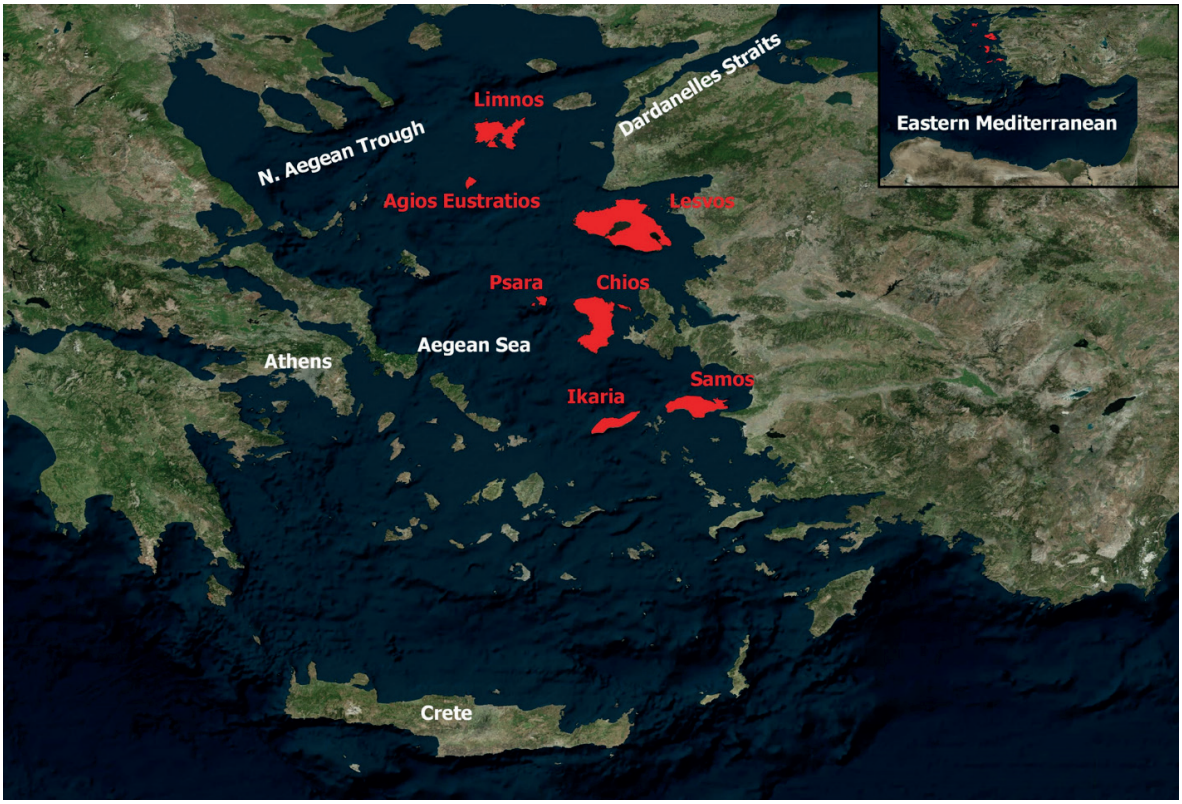

Figure 1. The Aegean archipelago and the NE Aegean islands (shown in red).

In the NE Aegean, the relative sea level rise (RSLR) in coastal waters has been projected as 0.1 and 0.2 m by 2050 under the IPCC RCP4.5 (intermediate) and RCP8.5 (high end) climatic scenarios, respectively. RSLR is projected to accelerate in the later part of the century: by 2100, the RSLR is projected as 0.5 m and 0.8 m under the RCP4.5 and RCP8.5 scenarios, respectively (Jevrejeva *et al*. 2016, Vousdoukas *et al.* 2018) with no spatial differentiations over the Aegean Sea.

Projections of the 1-100 year event ($ESLs_{100}$) for 2050 and 2100 along the Greek coastline (spatial resolution of about 25 km) are found in the global database of Vousdoukas *et al*. (2018). The baseline ESL_{100} (mean of the period 1980 - 2014) varies along the NE Aegean coastline, with the highest values in the Aegean Sea found in the north (Limnos island, up to 1.17 m above MSL). By 2050, $ESLs_{100}$ will increase by 0.12 - 0.25 m under the scenarios studied, with pronounced increases projected for some NE Aegean island coasts. By 2100, ESL_{100} increases might be substantial, reaching up to 0.75 m above the baseline values under the RCP8.5 scenario.

Further, it is noted that highly energetic events (Tropical Like Cyclones - TLCs or Medicanes) are also observed in the Mediterranean (Miglietta and Rotunno, 2019), which can induce catastrophic winds and severe coastal (and inland) flooding (Romera *et al*. 2017; Smart 2020). Projections suggest that these extreme events may become less frequent in the future, while the intensity of the most energetic events may increase.

3. Methodology

Beach exposure to erosion and flooding induced by climate variability was assessed at island scale. First, regarding the erosion risk, projections of waves, storm surge levels and RSLR along the 21st century were assigned for each beach based on the relevant projections of Vousdoukas *et al*. (2018). Second, the long-term and episodic beach erosion for the 658 identified/recorded

beaches of the NE Aegean islands were estimated using morphodynamic model ensembles, and compared with present beach maximum widths (BMWs) to assess the impacts. Third, indicative volumes of material for beach nourishment were approximated for each beach. Concerning the coastal flood risk, a GIS-based method was used as a supervisory tool for risk assessment at island scale, whereas a dynamic model (LISFLOOD-FP) was applied in two beaches in order to test its capabilities to resolve the flood risk in fine detail.

3.1 Hydrodynamic forcing

The coastal morphodynamic models that were used for the prediction of beach erosion (see section 3.2) were forced by the projections of the RSLR and Extreme Sea Levels (ESLs) under the RCP4.5 and RCP8.5 which were extracted from the dataset (https://data.jrc.ec.europa.eu/dataset/jrc-liscoast-10012) of Vousdoukas *et al*. (2018). The ESL is driven by extreme weather events and combines the MSL, the astronomical tide (small in the N. Aegean Sea) and the episodic coastal water levels n_{ce} that is the combined result of the storm surge and wave set up, with the latter being generically approximated as 0.2 of the significant wave height H_s. The ESLs used in this study correspond to storm events with a return period T_r of 100 years, for two reference years (2050 and 2100).

3.2 Erosion model ensembles

The projections of the coastal response to sea level rise forcing are based on the results of two ensembles of cross shore (1-D) morphodynamic models:

a) an ‘analytical’ model ensemble comprising the models of Bruun (1988), Dean (1991) and Edelman (1972); and

b) a dynamic ensemble comprising the numerical models Leont’yev (1996), SBEACH (Larson and Kraus, 1989), Xbeach (Roelvink *et al*. 2009) and a model whose hydrodynamic component is based on the Boussinesq approximation (see Karambas and Koutitas 2002).

The analytical ensemble is set to estimate the long-term beach erosion due to RSLR while the dynamic ensemble is used for the prediction of episodic coastal retreat under ESLs. The approach allows for balanced projections of potential coastal retreat (ranges of minimum and maximum), which can be then compared to the recorded maximum ‘dry’ beach widths. Further details about the model characteristics and validation will be found in Monioudi *et al*. (2017).

The models were run in a stationary mode, using plausible ranges of beach sediment sizes and bed slopes; the regional scale of the application does not allow for more detailed inputs. The sediment texture was characterized through visual inspection of high-resolution Google Earth satellite images (and relevant photo-images), being classified into 3 classes: stones/gravel, mixed (gravel and sand) and sandy beaches. Since the beach bed slope is likely to be controlled by the beach sediment texture (Reis and Gama 2010), the bed slope range used in the models for each beach was estimated using the values of Table 1. The closure depth - a required parameter for the analytical models - was extracted from the global dataset of Athanasiou (2019).

Table 1. Sediment bed slope and sediment texture (Bujan *et al*. 2019). D_{50}, median grain-size.

Sediment Texture	D_{50} min (mm)	D_{50} max (mm)	Bed Slope (min)	Bed Slope (max)
Sand	0.2	0.5	0.034	0.05
Mixed	0.8	1	0.067	0.1
Cobbles/Pebbles	2	5	0.1	0.1

Finally, the median values of ensemble predictions of beach erosion/retreat were calculated for each beach and compared with the recorded 'dry' maximum beach widths to get an indication of the beach erosion impact, including beach carrying capacity and backshore infrastructure/assets.

The maximum 'dry' beach widths were recorded through beach polygons digitized on the available high resolution Google Earth images and are contained in the (AEGIS+) beach repository for the NE Aegean islands along with socio-economic and environmental beach variables (sdi-portal.aegean.gr/portal/apps/webappviewer/index.html?id=b71071d0730740a499a1ca41385b3802). On the basis of a multicriteria analysis (for more information about the methodology, see Andreadis *et al*. 2021) involving a subset of these variables, the beaches of all islands were graded according to a Beach Vulnerability Index (BVI) based on their erosion risk and their socio-economic significance.

In addition, the required volumes of marine aggregates (Velegrakis *et al.* 2010) for implementation of beach replenishment schemes were estimated for every beach following the approach of Equilibrium Beach Profile proposed by Dean (2002). The granulometry of the filling sediments was chosen to be the same with the native material while the beach berm height was associated with the sum of RSLR and the wave runup (approximated by the parametric relationship of Stockdon *et al.* (2006). Nourishment volumes were estimated on the basis of beach protection under extreme storm events. Therefore, the beach erosion projections of the dynamic ensemble for 2050 were considered to be remedied through beach replenishment and the desired offshore extensions of the eroded beaches.

3.3 Flood risk modeling

The flood risk was assessed using two different approaches: a static method based on GIS and a dynamic method based on hydrodynamic modeling. Under the static method the areas prone to flooding are identified as those with elevation lower than the projected ESL. This method, known as 'bathtub approach', has been widely used in previous studies on flood risk assessment (Kont *et al*, 2008; Seenath *et al,* 2016). In the present study it has been applied for a supervisory assessment of flood risk on all the beaches of NE Aegean islands using a 25 m resolution Digital Elevation Model (DEM) (https://ec.europa.eu/eurostat/web/gisco/geodata/reference-data/elevation/eu-dem).

In addition, a dynamic approach was also used to assess the flood risk in selected NE Aegean beaches, using the 2-D model LISFLOOD-FP (Bates and de Roo, 2000). The model uses a structured grid and a raster coastal DEM. Hydraulic continuity principles are applied to calculate water depth in each cell of the raster grid and water is routed across the terrain based on the difference in hydraulic head between adjacent cells. Flow rates are computed based on terrain slopes and the Manning friction coefficient. While the model was initially designed to simulate river floods, it is increasingly used in coastal flood applications as well (e.g., Le Gal *et al.* 2022).

The LISFLOOD-FP model was used for selected beaches. For the selection both the BVI ranking and suitability for the LISFLOOD-FP application were considered, so that sites that form wide areas with low bed slopes resembling floodplains were prefered. Representative examples cases are shown here, for Keros beach in Limnos and Potokaki beach in Samos. In addition to the selection criteria discussed above, both beaches, listed among NATURA 2000 sites, are of high environmental value.

The model was applied to the 1-100 year extreme event under the RCP8.5 for the two reference years 2050 and 2100. The hydrodynamic forcing involved the ESLs estimated for these beaches

and set along the shoreline boundary; the storm duration of the simulation was set to 10 hours, following the analysis of Mediterranean storm events (Martzikos *et al*. 2021). A high resolution (2x2 m) DEM available from the Greek Cadastre was applied for the subaerial topography, while the Manning friction coefficient was estimated through the Land Use/Land Cover types according to Papaioannou *et al*. (2018).

4. Results

4.1. Beach erosion predictions

4.1.1 Long term erosion

Regarding the long-term beach erosion due to RSLR, the predictions of the analytical ensemble for 2050 under the RCP4.5 scenario range between 1.9 and 4.7 m. For 2100, under the RCP8.5, beach erosion ranges between 7.7 and 23 m. The projections indicate that by 2100 68.7 % of all NE Aegean island beaches will retreat/ be eroded by at least 50 % of their currently recorded maximum 'dry' beach width (BMW), whereas 29 % will retreat by a distance equal to their BMW (Fig. 2). The most severe results concern the four larger islands (Lesvos, Chios, Lemnos and Samos) where 76.5 % and 35.6 % of the beaches will retreat by 50 % and 100 % of their current BMW respectively. Given that the majority of island beaches in NE Aegean are pocket beaches backed with cliffs and/or coastal assets that do not allow landward beach migration, these beaches are threatened with permanent drowning/extinction. Clearly, the long-term beach erosion will substantially reduce the beach carrying capacity and aesthetics, with negative economic consequences on the local tourist industry.

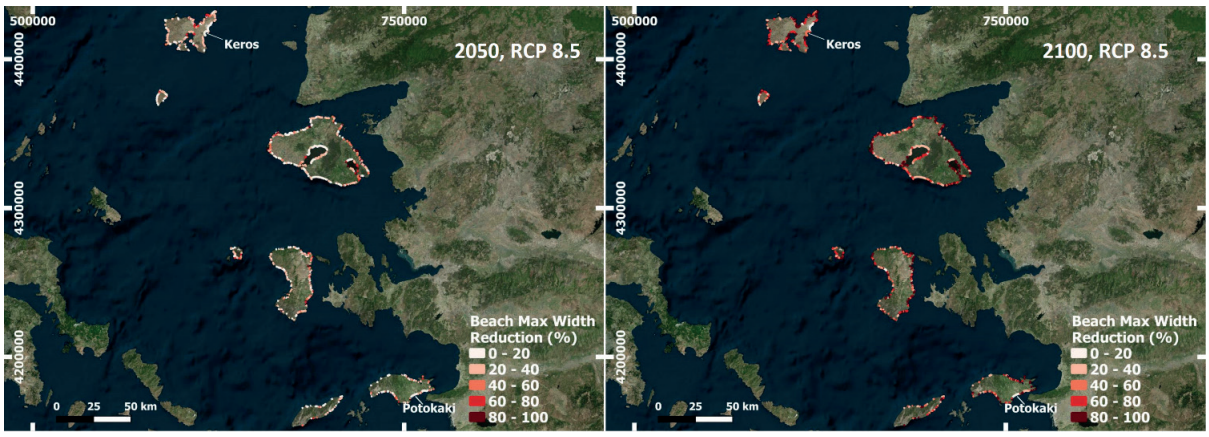

Figure 2. Median predictions of long-term erosion, expressed as percentage of the recorded beach maximum width, for the beaches of NE Aegean islands for 2050 and 2100 under RCP8.5 scenario. Red colours indicate higher reduction of beach width compared to the recorded values.

4.1.2 Episodic erosion

Regarding the episodic beach retreat, in 2050 under the intermediate scenario (RCP4.5) the median coastal erosion is estimated as high as 17.7 m (range of 9 – 29 m) while under the RCP8.5 it increases to 25 m (range of 13.5 – 41.5 m). When comparing the predictions to the recorded dry maximum beach widths it appears that in 2050, under the RCP4.5, 78.4 % of all beaches will at least temporarily retreat by 50 % of their maximum 'dry' width; 40.8 % of them are projected to temporarily retreat/be eroded by a distance equal to their BMW. Erosion

predictions are even worse for the remaining cases examined, as 58.7 % of all beaches would face temporary extinction under extreme events in 2100 (RCP8.5) (Fig. 3). One notes again that beach erosion will be particularly pronounced in the four larger islands (Lesvos, Chios, Limnos, Samos), where 73.5 % of the beaches are projected to be totally eroded (at least temporarily) under the tested extreme events in 2100 (RCP8.5). The impact of erosion may be devastating for the (current) backshore assets if no protection measures are taken. Focusing on those beaches (134 out of 658) where 25 % of the length at least is backed by assets, it is projected that under an extreme event, based on the moderate RCP4.5 scenario, 48.5 % of them will be fully eroded (at least temporarily) in 2050, threatening with damages or total losses the backshore assets. Predictions are worse for the other scenarios examined, as up to 72 % of the beaches may face temporary extinction under an extreme event for the RCP8.5 scenario in 2100.

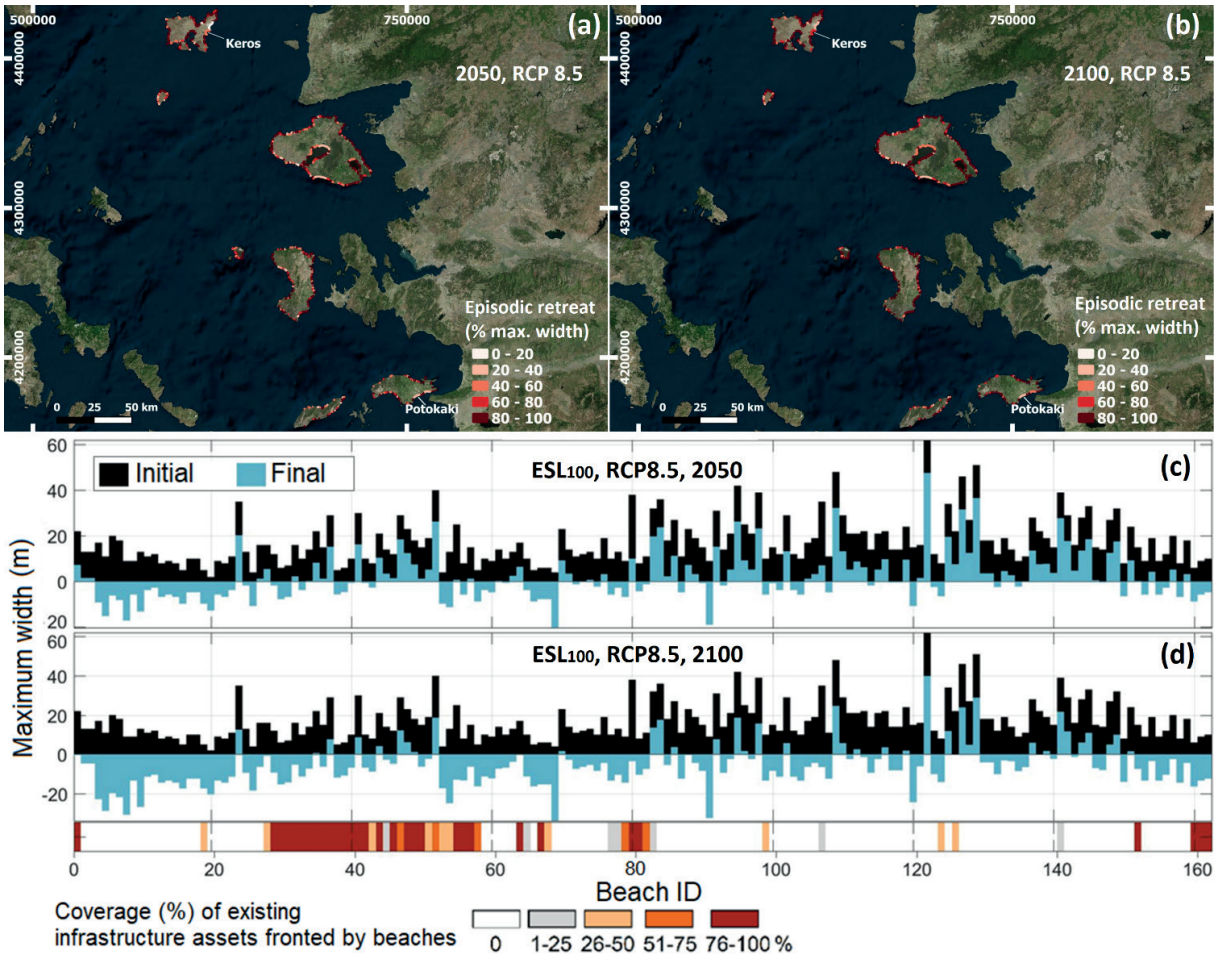

Figure 3. Median predictions of episodic erosion, expressed as percentage of the recorded beach maximum width (BMW), for the beaches of NE Aegean islands in (a) 2050 and (b) 2100 under the RCP8.5 scenario. Red colours indicate higher reduction of beach width compared to the recorded values. In the lower panels (c) and (d), the (median) projected episodic retreats are shown together with the recorded coverage of the frontline backshore assets (as a percentage of beach length); the current (initial) BMWs (black bars) are compared to those resulting from the beach retreat projections (blue bars); negative values indicate beach retreat more than the current BMW.

An estimation of the required material volumes for beach replenishment yields varying results ranging up to 2,259,640 m^3, with maximum values corresponding to beaches longer than 7 km

(e.g., Kalloni beach, Lesvos). As an indication, for two long touristic beaches, Keros and Potokaki (Figs 2, 3), the required volumes have been estimated between 1,445,890 – 1,537,110 m^3 and 504,750 - 619,320 m^3.

4.2. Flood risk assessment

The outputs of the bathtub method show that most beaches of Limnos and Lesvos will be inundated under an extreme event, especially on the SW and NW sectors respectively. In Chios, flooding is projected mainly for the SW coast, while it is predicted for nearly all beaches along the northern coast in Samos. Overall, the severity of flooding increases through the different scenarios, with the maximum flood depth projected at 1.28 m under RCP4.5 for 2050 and at 1.89 m under RCP8.5 for 2100 (Fig. 4).

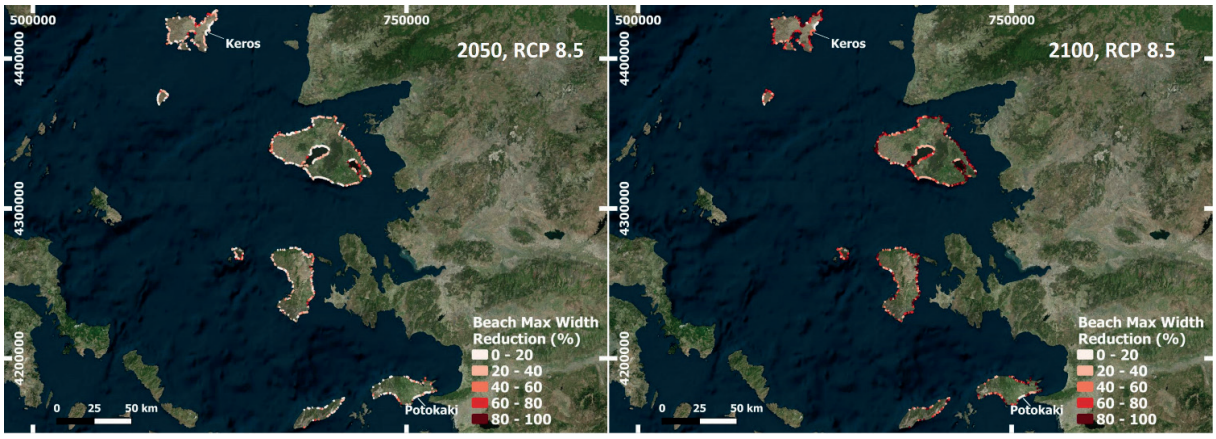

Figure 4. Predictions of flood risk for the beaches of NE Aegean islands for 2050 and 2100 under RCP8.5 scenario. The different colours stand for the estimated flood depth, with red colours indicating higher flood depths.

The following section will provide examples of the application of the dynamic method in selected beaches. Keros beach is a 5 km long, relatively narrow beach on the eastern coast of Limnos (Fig. 3). It is one of the NATURA 2000 sites. An extensive dune system with low vegetation forms its inland boundary which extends further inland along the central and northern part of its backshore. Further inland the protected Asprolimni and Chortarolimni bird habitats are also found. Projections (see Fig. 5) show that a large part of the area will be flooded with a maximum flood extent of 340 m for both reference years, with a 100 % flooding of the beach. By 2050 already, the coastal flood may inundate a substantial part of the backshore, especially in its northern and southern sections.

In 2100, the inundation extent appears much higher as most sand dunes will be overwashed and the flood will propagate further inland (as far as 70 m) in the central section of the beach, inundating up to 50 % of the backshore dune system. Furthermore, in the southern section between the beach and Chortarolimni, more than 1700 acres of land are projected to be flooded. Taking into account that LISFLOOD does not incorporate morphodynamic processes such as dune breaching, these projections may be conservative.

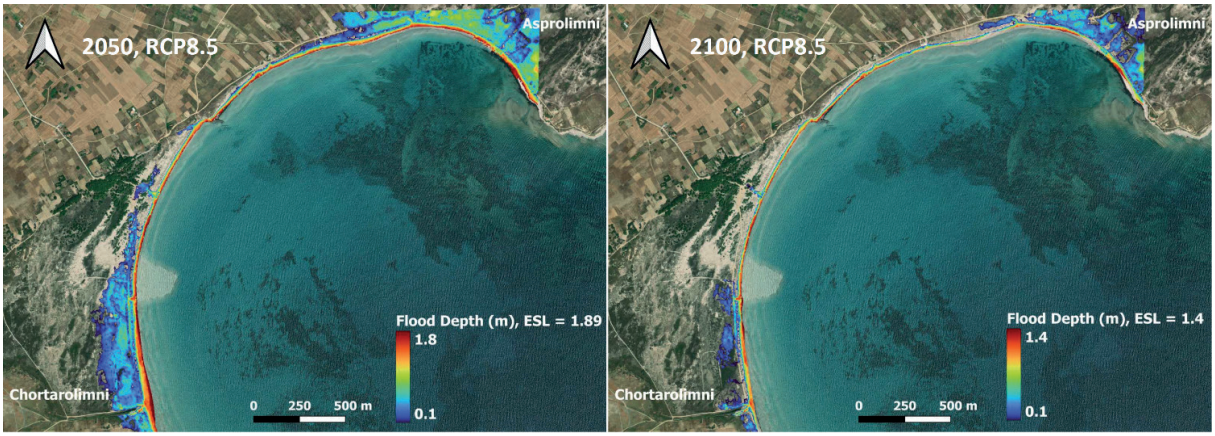

Figure 5. Flood extent on Keros beach for 2050 and 2100. The different colours stand for the estimated flood depth. On the SW edge of the site is the Chortarolimni habitat and on the BE edge the Asprolimni habitat.

Potokaki beach (Samos) is a 4.6 km long and narrow (20 m) low lying beach (Fig.3). At its backshore, the eastern end of the Samos airport runway is located, whereas there is also significant coastal development settlement and a wetland protected habitat. The city of Pythagorio and its port are located to the northeast of the beach. The LISFLOOD simulations project flooding for large areas (Fig. 6), with a maximum flood extent of 107 m in 2050 and 220 m in 2100; corresponding flood coverage of the beach are 87 % and 100 % respectively. By 2050 already flood is shown to inundate large parts of the backshore coastal development as well as the coastal road and parts of the wetland protected habitat. In addition, the main dock at the port of Pythagorio will be fully inundated, as well as the other port infrastructure.

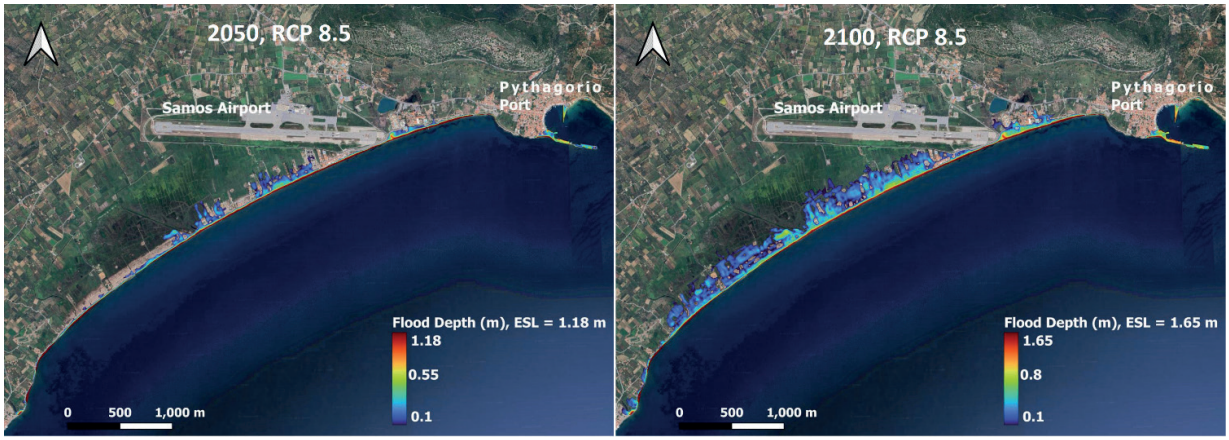

Figure 6. Flood extent on Potokaki for 2050 and 2100. The different colours stand for the estimated flood depth. On the east side the city and port of Pythagorio are shown.

Predictions are worse for 2100 when more than 50 % of the backshore assets/infrastructure are projected to be inundated, with flood depths reaching up to 0.5 m. Flood extent in some locations reaches the road between the airport runway and the beach, whereas 28 acres of the wetland are also flooded. In the port dock severe flooding is projected, with flood depth up to 0.8 m.

5. Discussion and conclusions

Our findings show an increased risk of beach erosion and flooding for most island beaches in the NE Aegean Sea. Compared to the current maximum beach dry width, it appears that 29 % of the beaches will permanently retreat by a distance equal to their current maximum width by 2100 due to the slow-onset RSLR. Moreover, severe erosion is predicted under an -100 year extreme event. Between 40.8 % (RCP4.5, 2050) and 58.7 % (RCP8.5, 2100) of all beaches are projected to be entirely eroded, at least temporarily. These estimates fall within the ranges found in a previous beach erosion study in the Aegean Archipelago (Monioudi *et al*, 2017), in which the hydrodynamic forcing included slightly different RSLR values (Hinkel *et al*, 2014) and the ESLs were based on storm level predictions without considering changes in the return period (Tsimplis and Shaw, 2010). Based on the minimum and maximum estimates of model ensembles instead of the median value, it is found that by 2100 between 12.4 - 68 % and 39.1 - 91 % of all beaches will face total permanent and temporary erosion, respectively. In an erosion assessment of the Cyprus beaches (Monioudi *et al*, 2023) which are also characterized by narrow widths and limited terrestrial sediment supply similar to the NE Aegean islands, the median estimates of the model ensemble project similar rates of erosion, indicating increasing pressure on the Mediterranean islands.

Our findings further suggest that by the end of the century the exposure to episodic erosion will increase mostly due to RSLR, as storm surges and waves in the Aegean Sea are not projected to change substantially over time (Androulidakis *et al*. 2015). Therefore, our results correlate well with those of the global analysis on future erosion of sandy beaches (Vousdoukas *et al*. 2020), which showed an increasing erosive trend driven mainly by RSLR, which may result in the extinction of about half of world's beaches. The relative importance of storm driven erosion due to the 1-100 year event was found to decrease with time; however, the authors underlined the increased vulnerability of backshores to coastal flooding under storm events, due to the predicted long-term erosion.

Regarding the calculation of flood risk two distinct approaches were used. First, a supervisory flood index was estimated for all beaches with the bathtub approach applied on a 25 m resolution DEM, which was considered sufficient for island scale applications. Exposure to flood risk was studied in more detail in selected beaches, using the LISFLOOD hydrodynamic model on a fine (2x2 m) grid with increased elevation accuracy compared to the 25 m DEM. Results of the two methods were compared for the Potokaki beach in order to highlight the advantages of the numerical simulation over the GIS based method (Fig. 7). Although outlier points that were not hydraulically connected with the rest of the predictions were manually removed, inundation is still highly overpredicted by the bathtub approach with maximum values extending more than 500 m inland compared to LISFLOOD maximum extent. The predicted flooded area in the wetland is estimated ten times higher than with the numerical model (374 vs 38 acres). The main reason behind these discrepancies is that bed friction effects on the water flow dynamics are simply ignored by the GIS method (Seenath *et al*, 2016). In addition, overestimation is introduced by the elevation inaccuracies on the 25 m DEM; in the wetland elevations are found to be systematically 1 m lower compared to the Greek Cadastre fine DEM. These differences seem to substantially mislead the GIS analysis when comparing with an ESL of 1.18 m. Overall, together with Seenath *et al*. (2016) we find the bathtub approach appropriate for rapid flood risk assessment on large scales, where numerical modeling on fine grids is not applicable due to the computational cost. In addition, LISFLOOD-FP provides outputs of flood evolution at defined timesteps, which can be crucial on the coastal management and preparedness to flood risk.

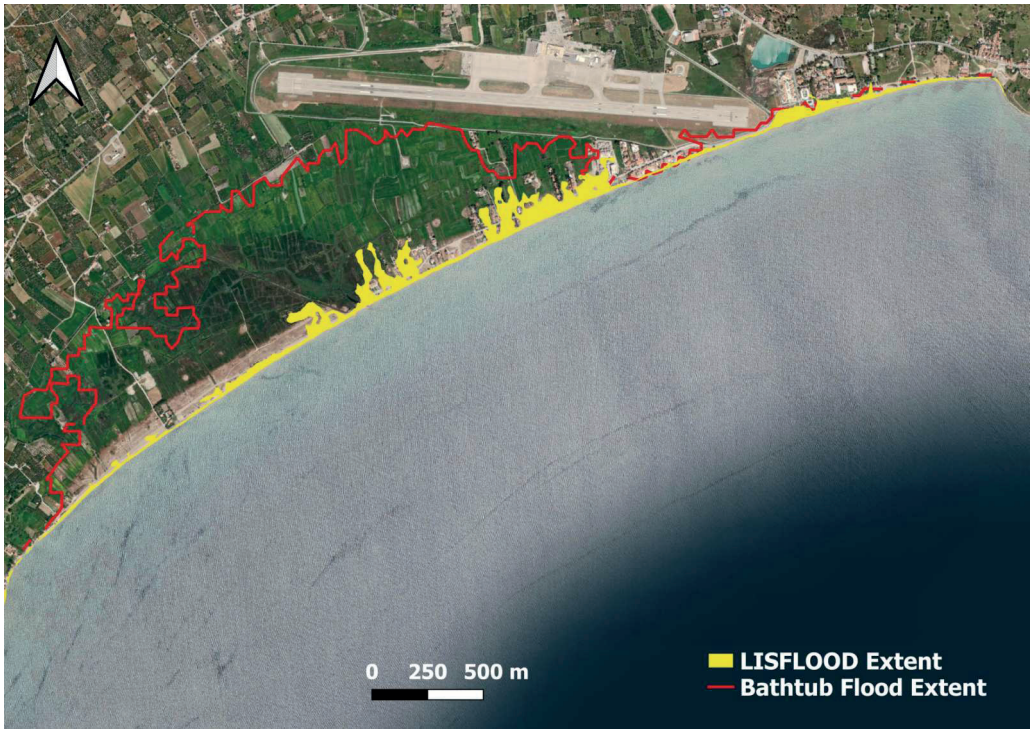

Figure 7. Comparison of flood inundation extent as predicted by the bathtub method (red line) and the LISFLOOD simulation (yellow) for the Potokaki beach (RCP8.5, 2050).

Collated information on the beach natural and socioeconomic characteristics (not shown in detail in the present article) can be highly beneficial when assessing the exposure to erosion and flood risk on island/archipelago scale. Recording of the recent beach maximum widths is crucial in order to identify those most exposed to erosion. Furthermore, recording of backshore assets allows identifying sites where erosion/flooding will potentially have the greater negative consequences on human assets and activities.

The severe predictions for the majority of NE Aegean island beaches imply that immediate action should be taken for the design of coastal protection and mitigation. Art. 8.2 of ICZM Protocol to the Barcelona Convention (ICZM 2008), which refers to the allocation of 'set-back' zones where further development and construction shall not be allowed, could be beneficial for the beaches in the region, where asset density is relatively low. Greece, however, has not yet ratified the ICZM Protocol and it currently defines set-back zones with a maximum width of 50 m. To gauge the perceptions and policy prioritization by local decision makers, a structured process is required through which priorities could be identified in terms of wider policy objectives (e.g. Kontopyrakis *et al.* 2024). This prioritization can affect the distribution of the available human and financial resources for efficient management responses. Local decision makers in coastal planning, and a crucial control of the coastal climatic exposure. Clearly Existing ICZM policies and legislation should properly take into consideration the local perceptions and environmental and socio-economic particularities.

In addition, hard engineering solutions such as offshore breakwaters, appear inadequate to protect beaches against RSLR (Dean and Houston 2016) and are more expensive (Narayan *et al.* 2016) than nourishment projects which through beach widening simultaneously protect backshore assets, increase beach carrying capacity for leisure activities and do not disturb beach

aesthetics (Cantasano *et al*. 2023).

Finally, it must be noted that EU Member States must comply with the Flood Directive – FD (2007/60/EC) which establishes a framework for flood risk management, including in coastal zones, and requires coastal flood risk assessments, mapping of flood extent, of assets and humans at risk, plus adequate and coordinated measures to manage the risk. The results of this study provide a first approximation of the required information, as well as indications on the needed approach for the accurate mapping of flood extent and quantification of its potential impacts.

Acknowledgements

This work was supported by the project 'Coastal Environment Observatory and Risk Management in Island Regions AEGIS+' (MIS 5047038), implemented within the Operational Programme 'Competitiveness, Entrepreneurship and Innovation' (NSRF 2014-2020), co-financed by the Hellenic Government (Ministry of Development and Investments) and the European Union (European Regional Development Fund).

To be cited as:

I.M Monioudi, D. Chatzistratis, A.F. Velegrakis, Th. Chalazas, E. Tragou. 2024. Exposure to coastal erosion and flooding in the northeastern Aegean islands, Greece. p 115- 130. In CIESM Monograph 52 [F. Briand, Ed.] Marine hazards, coastal vulnerability, risk (mis)perceptions – a Mediterranean perspective. CIESM Publisher, Paris, Monaco, 182 p.

References

Andreadis O., Chatzipavlis A., Hasiotis T., Monioudi I., Manoutsoglou E.and A. Velegrakis. 2021. Assessment of and Adaptation to Beach Erosion in Islands: An Integrated Approach, *J. Mar. Sci. Eng.* 9(8): 859. https://doi.org/10.3390/jmse9080859

Androulidakis Y.S and V.H. Kourafalou. 2011. Evolution of a buoyant outflow in the presence of complex topography: The Dardanelles plume (North Aegean Sea). *Journal of Geophysical Research*, vol 116 doi.org/10.1029/2010JC006316

Androulidakis Y.S., Kombiadou K.D., Makris C.V., Baltikas V.N. and Y.N. Krestenitis. 2015. Storm surges in the Mediterranean Sea: Variability and trends under future climatic conditions, *Dynam. Atm. Oceans* 71: 56–82.

Androulidakis Y.S., Makris C., Mallios Z. and Y. Krestenitis. 2023. Sea level variability and coastal inundation over the northeastern Mediterranean Sea. Coastal Engineering Journal. doi.org/10.1080/21664250.2023.2246286

Athanasiou P. 2019. Global distribution of nearshore slopes. Version 1, dataset. Internet:4TU. Centre for Research Data. doi: 10.4121/uuid:a8297dcd-c34e-4e6d-bf66-

Bates, P.D. and A.P.J. De Roo. 2000. A simple raster-based model for flood inundation simulation. *J. Hydrology* 236: 54-77 doi.org/10.1016/S0022-1694(00)00278-X

Bruun P. 1988. The Bruun Rule of erosion by sea level rise: A discussion on large-scale two- and three-dimensional usages, *Coastal Research* 4(4):622-648.

Calafat F.M., Chambers D.P. and Tsimplis M.N. 2012. Mechanisms of decadal sea level variability in the eastern North Atlantic and the Mediterranean Sea. *Journal of Geophysical Research*, vol 117 (C09) doi.org/10.1029/2012JC008285

Cantasano N., Boccalaro F., and F. Ietto. 2023. Assessing detached breakwaters and beach nourishment environmental impacts in Italy: a review. Environ. Monit. Assess. 195:127 doi.org/10.1007/s10661-022-10666-9

Cao A., Esteban M., Paolo V. *et al*. 2021. Future of Asian Deltaic Megacities under sea level rise and land subsidence: current adaptation pathways for Tokyo, Jakarta, Manila, and Ho Chi Minh City. Current Opinion in Environmental Sustainability 50: 87-97. https://doi.org/10.1016/j.cosust.2021.02.010

Dean R. G. 1991. Equilibrium beach profiles: characteristics and applications. *J. Coastal Research* 7(1): 53-84.

Dean R. G. 2002. Beach Nourishment: Theory and practice. In Advanced Series on Ocean Engineering World Scientific Publishing Company: Singapore

Dean R.G.and J.R. Houston. 2016. Determining shoreline response to sea level rise. Coastal Engineering 114: 1-8. doi: 10.1016/j.coastaleng.2016.03.009

Edelman T. 1972. Dune erosion during storm conditions, in: Proceedings of the 13th International Conference on Coastal Engineering ASCE, pp. 1305-1312.

Garola A., Lopez-Doriga U. and J.A. Jimenez. 2022. The economic impact of sea level rise-induced decrease in the carrying capacity of Catalan beaches (NW Mediterranean, Spain). Ocean Coastal Management 218: 106034 doi.org/10.1016/j.ocecoaman.2022.106034

Hinkel, J., Lincke, D., Vafeidis, A. T., Perrette, M., Nicholls, R. G., Tol, R. S., Marzeion, B., Fettweis, X., Ionescu, C., and A. Levermann 2014. Coastal flood damages and adaptation costs under 21st century sea-level rise, Proceedings National Academy of Science USA, 111: 3292–3297.

ICZM. 2008. Protocol to the Barcelona Convention on Integrated Coastal Zone Management (ICZM) in the Mediterranean. Available at: https://www.unep.org/unepmap/who-we-are/contracting-parties/iczm-protocol [Accessed October 15, 2023].

IPCC. 2019. Special Report on the Ocean and Cryosphere in a Changing Climate. [H.-O. Pörtner, D.C. Roberts, V. Masson-Delmotte Eds.] https://www.ipcc.ch/srocc/

IPCC. 2023. AR6 Synthesis Report: Climate Change 2023. https://www.ipcc.ch/report/sixth-assessment-report-cycle/

Jevrejeva S., Jackson L.P., Riva R.E.M., Grinsted, A. and J.C. Moore. 2016. Coastal sea level rise with warming above 2 °C. *Proceedings of the National Academy of Sciences* 113: 13342–13347. doi: 10.1073/pnas.1605312113.

Karambas T. V., and Koutitas C., 2002. Surf and swash zone morphology evolution induced by nonlinear waves. *Waterway, Port, Coastal and Ocean Engineering,* 128 (3):102-113. doi. org/10.1061/(ASCE)0733-950X(2002)128:3(102)

Kont A., Jaagus J., Aunap R., Ratas U.and R. Rivis. 2008. Implications of sea-level rise for Estonia. *J. Coast. Res.* 24 (2): 423 – 431.

Kontopyrakis K.E., Velegrakis, A.F., Monioudi I.N. and A. Ćulibrk, 2024. Prioritizing environmental policies in Greek coastal municipalities. *Anthropocene Coasts* 7, 1. https://doi.org/10.1007/s44218-023-00035-5

Larson M. and N. C. Kraus. 1989. SBEACH: numerical model for simulating storm-induced beach change; report 1: empirical foundation and model development, Technical Report - US Army Coastal Engineering Research Center 89-9.

Le Gal M., Fernández-Montblanc T., Montes J., Souto Ceccon P. , Duo E., Gastal V., Delbour S. and P. Ciavola 2022. A flood map catalogue for integration into a European flood awareness system (ECFAS). EGU22, 24th EGU General Assembly, 23-27 May, 2022. Vienna. doi:10.5194/egusphere-egu22-9832

Leont'yev I.O. 1996. Numerical modelling of beach erosion during storm event. *Coastal Engineering* 29(1-2):187-200. https://doi.org/10.1016/S0378-3839(96)00029-4

Marcos M., Tsimplis M.N. andA.G.P. Shaw, 2009. Sea level extremes in southern Europe. *Journal of Geophysical Research*, 114 (C010007). doi.org/10.1029/2008JC004912

Martzikos N., Prinos P., Memos C. and V. Tsoukala, 2021. Statistical analysis of Mediterranean coastal storms. *Oceanologia,* 63(1): 133-148. doi.org/10.1016/j.oceano.2020.11.001

Mentaschi L., Vousdoukas M.I., Pekel J.F., Voukouvalas E.and L. Feyen. 2018. Global long-term observations of coastal erosion and accretion. *Sci. Rep*. 8 12876 DOI:10.1038/s41598-018-30904-w

Miglietta M.M., Rotunno R. 2019. Development mechanisms for Mediterranean tropical like cyclones (medicanes). *Quarterly Journal of the Royal Meteorological Society*, 145 (721B), 1444-1460

Monioudi I., Velegrakis A.F., Chatzipavlis A. *et al*. 2017. Assessment of island beach erosion due to sea level rise: The case of the Aegean Archipelago (Eastern Mediterranean. *Natural Hazards and Earth System Science,* 17: 449–466.

Monioudi I., Velegrakis A., Chatzistratis D. *et al*. 2023. Climate Change – induced hazards on touristic island beaches: Cyprus, Eastern Mediterranean. *Front. Mar. Sci.,* 10: 1188896. doi:10.3389/fmars.2023.1188896

Narayan S., Beck M.W., Reguero B.G., Losada I.J., van Wesenbeeck B., Pontee N., Sanchirico J.N. Ingram J.C., Lange J.-M., Burks-Copes K.A.. 2016. The Effectiveness, Costs and Coastal Protection Benefits of Natural and Nature-Based Defences. *PLoS ONE,* 11(5): e0154735. doi.org/10.1371/journal.pone.0154735

Papaioannou G., Efstratiadis A., Vasiliades L., Loukas A., Papalexiou S., Koukouvinos A., Tsoukalas I. and P. Kossieris. 2018. An operational method for flood directive implementation in ungauged urban areas. *Hydrology*, 5: 24. doi.org/10.3390/hydrology5020024

Poulos S.E. 2009. Origin and distribution of the terrigenous component of the unconsolidated surface sediment of the Aegean floor: A synthesis. *Cont. Shelf Res.*, 29: 2045–2060.

Reis, A.H. and C. Gama. 2010. Sand size versus beachface slope — An explanation based on the Constructal Law. *Geomorphology,* 114: 276–283. doi: 10.1016/j.geomorph.2009.07.008

Roelvink, D., Reniers, A., van Dongeren, A., van Thiel de Vries, J., McCall R. and J. Lescinski. 2009. Modelling storm impacts on beaches, dunes and barrier islands. *Coastal Engineering,* 56:1133-1152. https://doi.org/10.1016/j.coastaleng.2009.08.006

Seenath A., Wilson, M., and K. Miller. 2016. Hydrodynamic versus GIS modelling for coastal flood vulnerability asessment: Which is better for guiding coastal management? *Ocean & Coastal Management,* 120: 99-109. doi.org/10.1016/j.ocecoaman.2015.11.019

Smart D. 2020. Medicane 'Ianos' over the central Mediterranean 14–20 September 2020. *Weather* 75 (11): 352-353. https://doi.org/10.1002/wea.3871

Stockdon H. F., Holman R., Howd P.A.and J.R. Sallenger . 2006. Empirical parameterization of setup, swash and runup. *Coastal Engineering*, 53: 573-588. doi.org/10.1016/j.coastaleng.2005.12.005

Tsimplis M.N., Proctor R., Flather R.A. 1995. A two-dimensional tidal model for the Mediterranean Sea. *Journal of Geophysical Research: Oceans*, 100 (C8): 16223-16239.

Tsimplis M.N.and A.G. Shaw. 2010. Seasonal sea-level extremes in the Mediterranean Sea and at the Atlantic European coasts. *Natural Hazards Earth System Science*, 10: 1457–1475.

UNECE. 2020. Climate Change Impacts and Adaptation for Transport Networks and Nodes. United Nations Economic Commission for Europe (UNECE), Expert Group Report ECE/TRANS/283. 216 pp. https://unece.org/fileadmin/DAM/trans/doc/2020/wp5/ECE-TRANS-283e.pdf

UNWTO. 2019. International tourism highlights. World Tourism Organisation.

Velegrakis A.F., Ballay A., Poulos S., Radzevicius R., Bellec V. and F. Manso. 2010. European marine aggregates resources: origins, usage, prospecting and dredging techniques. *J. Coast. Res.,* 51: 1–14. doi: 10.2112/si51-002.1

Vousdoukas M.I., Mentaschi L., Voukouvalas E. *et al*., 2018. Global probabilistic projections of extreme sea levels show intensification of coastal flood hazard. *Nat. Comm.* 9, 2360 DOI: 10.1038/s41467-018-04692-w

Vousdoukas M.I., Ranasinghe R., Mentaschi L. *et al*. 2020. Sandy coastlines under threat of erosion. *Nature Climate Change* 10: 260–263. https://doi.org/10.1038/s41558-020-0697-0

Wöppelman, G. and M. Marcos. 2012. Coastal sea level rise in southern Europe and the nonclimate contribution of vertical land motion. *Journal of Geophysical Research*, 117, (C01007) doi.org/10.1029/2011JC007469

A practical approach for the "maximum" Tsunami runup in variable cross-section bays and its implementation in machine learning-based Tsunami warning systems

M. Sinan Özeren
Istanbul Technical University ozerens@itu.edu.tr

The comprehension of the physics governing the runup of tsunami or storm surge wavetrains within bays of varying cross-sectional configurations remains a formidable challenge. Numerous coastal communities are situated along bays and gulfs characterized by diverse shapes and aspect ratios, bringing in the urgent need for a swift yet rigorously physics-based evaluation of tsunami runup to assess associated risks effectively. The integration of this knowledge into warning algorithms assumes a pivotal role in enhancing warning systems. The intricacy of this problem primarily arises from the imperative consideration of both energy-transmitting and decaying modes, along with the complex scattering phenomena occurring outside the confines of the bay, all of which are essential for an accurate representation of maximum runup. However, one can navigate these complexities adeptly by strategically employing a straightforward Dirichlet boundary condition at the entrance of the bay. Although the method proposed in this study may introduce discrepancies in the long-term behavior of the tsunami wave field, its promise lies in its ability to yield reliable results concerning maximum runup within bays, with significant errors emerging only after the peak runup has occurred. Remarkably, this method proves applicable to narrow bays of arbitrary cross-sectional shapes, provided that the depth variations do not occur abruptly. The method can be incorporated in a machine learning-based warning scheme and reduce its computational load further by reducing the detection time for particular bay regions. Further work is needed to design an optimal way of existing ML-based detection schemes to make use of the maximum runup approach adopted here.

Introduction

The examination of how tsunami wavetrains behave within bays stands as a crucial topic in hazard assessment. The 2011 Tohoku Tsunami, in the northeastern tip of Japan, provided invaluable insights into both the offshore propagation characteristics of the tsunami wavefield and its impact on bays of varying configurations in the Sanriku region and the broader northern Tohoku coastal area. Notable contributions in this regard have been made by researchers such as Mori *et al.* (2011), Shimozono *et al.* (2012, 2014), and Wei *et al.* (2013). Particularly, in the Yamada Bay area, the runup reached extraordinary heights, with the highest measurement at approximately 40 meters and an inundation distance of 500 meters, as documented by Okayasu *et al.* (2012). Additionally, along the coastal regions bordering the Ria, situated roughly 50 to 200 kilometers north of Sendai, the presence of narrow bays directed the tsunami waves, leading to the most significant inundation levels and wave run-up. To comprehend the complex interactions between tsunamis and bays, a spectrum of approaches has been employed, including fully numerical, analytical, and semiclassical methods, such as the WKB technique, as demonstrated in studies by Bautista *et al.* (2011), Zahibo *et al.* (2006), and Didenkulova and Pelinovsky (2011). Furthermore, resonance phenomena within the context of runup have been explored, as evidenced by the work of Stefanakis *et al.* (2015) and Ezersky *et al.* (2013).

Due to complex bathimetries, the runup and inundation heights of the tsunamis exhibit remarkable variations along the bayshores and the need for numerical simulations is obvious (Cui *et al*. 2010, 2012). However a quick methodology to work out roughly the maximum runup given the incident wavetrain would also be highly useful. While formulating such a maximum runup algorithm, one obvious difficulty is that it is not clear how to impose the offshore boundary condition as the field evolves and scattering and reflection occur (Løvholt *et al* 2015, Pedersen 2016, Shimozono 2016). A practical question that arises is: can the offshore boundary condition be simplified and still give satisfactory results as far as the maximum runup is concerned? Here we show that the answer to this question is affirmative: a single Dirichlet condition applied at a specific offshore point suffices for analyzing the run-up properties of tsunami-like incident waves in most bay configurations. Here I will give mainly the physical insight, rather than the full mathematical detail which is rather involved.

A simple case: infinitely wide shelf

Most of the theory mentioned here can be found in detail in Postacioglu and Ozeren (2021). Here I will outline the results that are relevant for Tsunami warning systems. The starting point for the analysis is to recognize that for an infinitely wide, flat shelf connected to an infinite ocean with flat bathymetry, in the context of linear shallow water theory, the ratio between the transmitted energy and the incident wave's total energy is independent of the wavelength with the transmission coefficient being equal to

$$2\frac{\sqrt{H_0}}{\sqrt{H_0}+\sqrt{H_1}}$$

where H_0 and H_1 are the depths of the deep ocean and of the shelf respectively. In the limit of an infinitely deep ocean, the wave field over the shelf is basically this transmission coefficient times twice the incident wave amplitude at the shelf edge. In other words, a simple Dirichlet condition at the shelf edge gives a perfect solution in case of an ocean with infinite depth. When the depth discontinuity is large but not infinite, the above-mentioned Dirichlet condition will remain valid only for a finite amount of time. Although we will be looking at confined bays, this simple principle is key in understanding the principle behind the practicality of the method. Figure 1 shows the evolution of the wave in the geometry mentioned above for $H_0/H_1 = 200$ (with x_0 being the position of the shelf discontinuity).

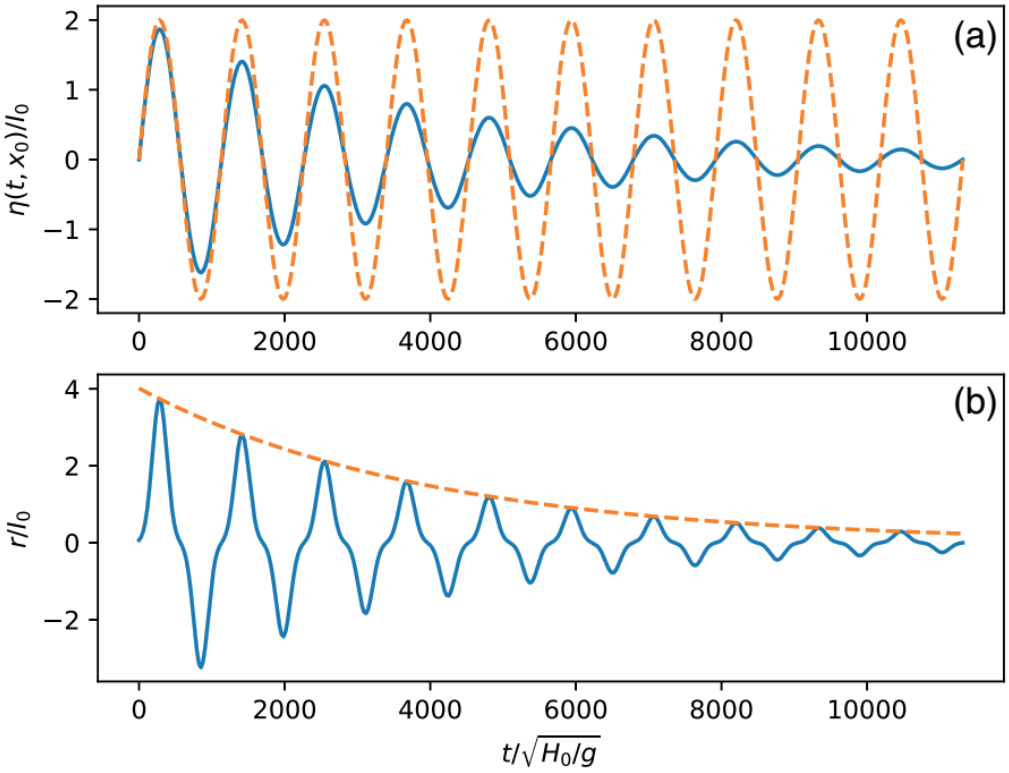

Figure 1. Incident wave approaching a shallow shelf of infinite width.

Panel A: the continuous curve is the normalised free surface disturbance at $x = x_0$ (the toe of the slope) for an incident wave given by $I_0\theta\left(\sqrt{gH_0}t + (x - x_0)\right)\sin\left(\omega\left(t + \frac{x-x_0}{\sqrt{gH_0}}\right)\right)$ with θ being the step function. The frequency ,ω, of the incident wave is $\sqrt{gH_1}\pi/(2x_0)$ and $x_0/H_0 = 20$. The broken curve is twice the amplitude of the incident wave at the toe.

Panel B: the continuous curve is the time evolution of the normalized runup for an incident wave of Gaussian shape given *by*I_0 exp $\left(-4\frac{gH_1}{x_0^2}\left(t + \frac{x-x_0}{\sqrt{gH_0}}\right)^2\right)$ for the same bathymety as Panel A. The dashed curve is the decay envelope given by $(r_{\max}/I_0)\exp\left(-|\mathrm{I}\omega_k|(t - t_{\max})\right)$ where ω_k is a natural frequency of the radiating mode given by $\omega_n = \frac{\sqrt{gH_1}}{x_0}\left(\frac{\pi}{2} + n\pi + i\tanh^{-1}\left(\sqrt{H_1/H_0}\right)\right)$, n = 0,1,2... Note that the imaginary part of the frequencies of all modes are equal. For both panels the width is infinite.

Rectangular Channel with flat bottom

Here I will show the comparison between the "exact" result for a rectangular channel of uniform depth (where some virtual sources have been utilized at the channel entry) and the solution where the simplified Dirichlet condition is used for the maximum runup. Figure 2 shows this comparison for the runup generated by a Gaussian incident wave. The same figure also shows the perturbative corrections to the solution obtained by virtual sources. The solution with the virtual sources is formulated using Hankel functions, coefficients of which are calculated as a solution to an integral equation satisfying the free surface and flux continuities at the channel entrance.

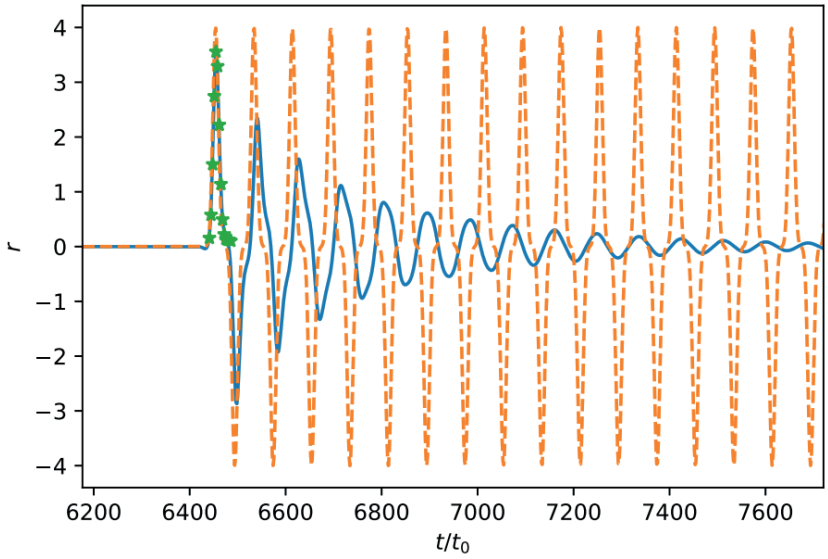

Figure 2. Run-up generated by a Gaussian incident wave given by exp $\{-[(x + \sqrt{gH}0)(t - T/2)/(0.4x_0)]^2\}$ entering a rectangular bay of aspect ratio $x0/(2Y_0) = 10$. The continuous curve is the "exact" solution of integral equation, dashed curve is $r(0)(t)$ (undisturbed solution of Dirichlet problem), and the stars are $r(0)(t) + r(1)(t)$. The timescale t_0 is $Y0/\sqrt{gH}$, and T is the duration of sampling. Maximum run-up associated with $r(0)$ and $r(0) + r(1)$ is 4.0 and 3.6, respectively. The "exact" maximum is 3.52.

This solution can be further generalized for more intricate geometries (Postacioglu and Ozeren 2021). In the following section I will discuss the ways in which this approach can be used in Tsunami warning systems.

Implementation in machine learning-based Tsunami Warning Systems

Bays represent an ubiquitous and integral facet of coastal landscapes worldwide, serving as prominent geographical features that demand unwavering attention in any comprehensive coastal hazard study. Thus, any endeavor aimed at assessing and mitigating the risks associated with coastal hazards must inherently consider the unique vulnerabilities and challenges posed by these intricate coastal features. To emphasize the diversity of beach geometries in the Tsunami context, Figure 3 illustrates the Sanriku coast with its several variable aspect-ratio bays that were significantly affected by the 2011 Tohoku Tsunami together with various historical event sources. In conventional Tsunami warning systems the bay runup is calculated using numerical methods based on discretizations of finite differences, finite elements or finite volumes type. These are computationally very costly and even more so in case of the presence of bays. Furthermore, numerical schemes that aim to resolve the wave field and runup in bays may not be very reliable despite the sophistication of the numerical methods. This is due to the fact that the waves in a slender domain such as a bay can preserve its nonlinear nature more effectively unlike the open ocean where the geometric spreading diminishes such effects.

The other alternative is to use one of several analytical or semi-analytical approaches to have a rough estimate of runup based on the incident wave field. However there are very few such approaches and the ones developed for U or V-shaped basins have mathematical complications that render the generalization difficult and impractical for more general shapes. In the extreme case of very short wavelengths, the solution explained in the previous section can be regarded as a combination of incoming and reflecting waves, both of which adhere to Green's law in

the distant region (close to the opening). Consequently, near the opening, these waves exhibit forward propagation. As a result, a straightforward connection exists between the disturbance on the free surface and the fluid velocity, u, making it suitable for the perturbative methods. This makes it very attractive for the method to be exploited in any warning system that uses buoy and current-meter measurements.

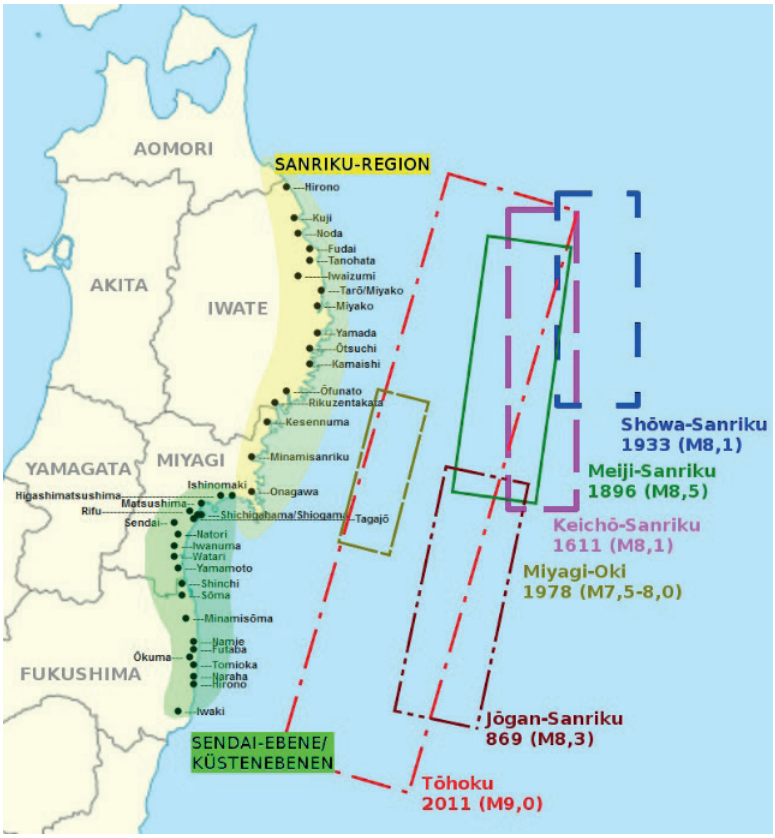

Figure 3. Sanriku coast, northeastern Japan, with several past Tsunami sources offshore. (after Wikipedia)

The practical challenge is how to optimize a warning system that uses several buoy measurements based on machine-learning to employ the method mentioned in this paper. In instances of near-field occurrences, such as Tohoku, it becomes crucial to have detailed spatial data regarding the maximum heights or depths of tsunami waves. This information is vital for guiding prompt evacuation procedures immediately after detecting earthquakes capable of generating tsunamis. The swift availability of an inundation map could significantly augment existing resources for mapping out evacuation routes and identifying safe zones in tsunami-prone areas. This enhanced map would provide authorities, including law enforcement, firefighters, and operations managers, with more precise guidance for executing efficient tsunami evacuation protocols. Since the machine-learning based systems utilize correlations, trained from previous numerical simulations (see for instance Mulia *et al*. 2022; Makinoshima *et al*. 2021), they can exploit the analytical technique described here alongside a library of previous numerical simulations to produce a more precise warning streamlined for individıual bays.

I propose to detect the excitation of the energy-transmitting mode towards the tips of the bays and come up with correlative patterns to this end for each bay, using a number of buoys for which the distance from the shore has to be fine-tuned according to the modal characteristics. Such a correlation-based approach would be computationally far less expensive since the

analytic calculations provide travel time for the incident waves in bays of which the geometry can be roughly approximated to fit the formulation presented here. Schematically, this can be explained by way of Figure 4.

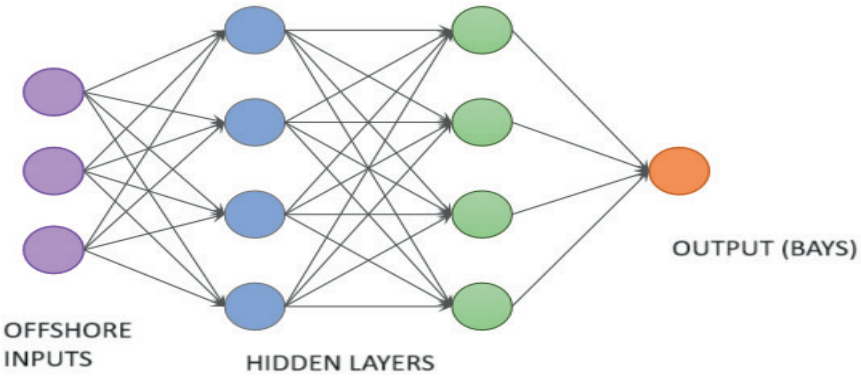

Figure 4. A simplified depiction of a convolution-based deep learning algorithm for Tsunami warning where the training aims streamlined output for bays.

This is very similar to many other convolution-based deep-learning schemes to detect Tsunamis in works such as Nuñez *et al*. (2022) which exploits one-dimensional convolutional neural networks.

Conclusion

In this study we show that a simplified offshore boundary condition can be used to estimate the maximum runup of Tsunami waves within bays, provided that the depth variation is not very rapid. Comparisons with integral-equation based results (both perturbed and unperturbed) show that as far as the maximum runup is concerned the solutions with the simple Dirichlet-type boundary condition are satisfactory for risk-assessment purposes. We propose to use this result for Tsunami warning using an implementation within a deep-learning based system. Deep-learning and machine-learning based techniques for Tsunami early warning have already proved to have much greater success (both in terms of effectiveness and computational time) compared to the methods based solely on numerical simulations. Fine-tuning the training sets using the analytical method explained in this paper would be beneficial for warning, especially for bays.

To be cited as:

M.S. Özeren. 2024. A practical approach for the "maximum" Tsunami runup in variable cross-section bays and its implementation in machine learning-based Tsunami warning systems. p 131- 138. In CIESM Monograph 52 [F. Briand, Ed.] Marine hazards, coastal vulnerability, risk (mis)perceptions – a Mediterranean perspective. CIESM Publisher, Paris, Monaco, 182 p.

References

Bautista E.G., Méndez F., Bautista O. and A. Mora. 2011. Propagation of shallow water waves in an open parabolic channel using the WKB perturbation technique. *Appl. Ocean Res*. 33: 186–192.

Cui H., Pietrzak J.D. and G.S Stelling. 2010. A finite volume analogue of the P1NC-P1 finite element: With accurate flooding and drying. *Ocean Modelling 35*(1–2): 16–30.

Cui H., Pietrzak J.D. and G.S Stelling. 2012. Improved efficiency of a non-hydrostatic, unstructured grid, finite volume model. *Ocean Modelling* 54–55: 55–67.

Didenkulova I. and E. Pelinovsky. 2011. Runup of tsunami waves in U-shaped bays. *Pure Appl. Geophys*. 168: 1239.

Ezersky A., Tiguercha D. and E. Pelinovsky. 2013. Resonance phenomena at the long wave run-up on the coast. *Natural Hazards Earth Syst. Sci*. 13: 2745.

Løvholt F., Glimsdal S., Lynett P. and G. Pedersen. 2015. Simulating tsunami propagation in fjords with longwave models. *Natural Hazards Earth Syst. Sci*. 15: 657.

Makinoshima F., Oishi Y., Yamazaki T. *et al.* 2021. Early forecasting of tsunami inundation from tsunami and geodetic observation data with convolutional neural networks. *Nat. Comm.* 12: 2253 https://doi.org/10.1038/s41467-021-22348-0

Mori Nobuhito, *et al.* 2011. Survey of 2011 Tohoku earthquake tsunami inundation and run-up. *Geophysical research letters,* 38.

Mulia I.E., Ueda N., Miyoshi T. *et al.* 2022. Machine learning-based tsunami inundation prediction derived from offshore observations. *Nat. Comm.* 13, 5489. https://doi.org/10.1038/s41467-022-33253-5

Núñez J., Catalán P.A., Valle C. *et al.* 2022. Discriminating the occurrence of inundation in tsunami early warning with one-dimensional convolutional neural networks. *Sci. Rep.* 12, 10321 https://doi.org/10.1038/s41598-022-13788-9

Okayasu A., Shimozono T., Sato S., Tajima Y., Liu H., Takagawa T. and H.M. Fritz. 2012. 2011 Tōhoku Tsunami runup and devastating damages around Yamada Bay, IWATE: Surveys and numerical simulation. *Coastal Engineering Proceedings* 33: 4-4.

Pedersen G. 2016. Fully nonlinear Boussinesq equations for long wave propagation and run-up in sloping channels with parabolic cross sections. *Nat. Hazards* 84: 599.

Postacioglu N. and M.S. Özeren. 2021. Maximum run-up produced by tsunami wave trains entering bays of variable cross section. *N. Phys. Rev. Fluids* 6: 034803.

Shimozono T., Sato S., Okayasu Y., Tajima Y., Fritz H.M., Liu H. and Takagawa, T. 2012. Propagation and inundation characteristics of the 2011 Tohoku tsunami on the central Sanriku Coast. *Coastal Eng. J.* 54(1): 1250004.

Shimozono T., H Cui, J. D. Pietrzak, H. M. Fritz, A. Okayasu and A. J. Hooper. 2014. Short wave amplification and extreme runup by the 2011 Tohoku tsunami. *Pure Appl. Geophys*. 171: 3217.

Shimozono T. 2016. Long wave propagation and run-up in converging bays. *J. Fluid Mech*. 798: 457.

Stefanakis T. S. , S. Xu D. Dutykh and F. Dias. 2015. Run-up amplification of transient long waves. *Q. Appl. Math*. 73, 177.

Wei Y., Chamberlin C., Titov V.V., Tang L., and E.N. Bernard. 2013. *Modeling of the 2011* Japan tsunami: lessons for near-field forecast. *Pure Appl. Geophys*. 170: 1309-1331.

Zahibo N., E. N. Pelinovsky, V Golinko and N Osipenko. 2006. Tsunami wave runup on coasts of narrow bays. *Int. J. Fluid Mech. Res*. 33 (1): 106-118.

Moroccan coastal hazards

Nadia Mhammdi

Institut Scientifique, Geophysics and Natural Hazards Laboratory, Mohammed V University, Rabat, Morocco
nadia.mahmmdi@is.um5.ac.ma

Marine geohazards are events caused by geological processes that dramatically change environmental conditions and present severe threats to coastal populations, offshore and onshore properties and offshore built infrastructures. Earthquakes, submarine landslides, volcanic eruptions, and tsunamis are typical examples of such natural events and their consequences. They also include rapid changes on the seafloor such as migrating bedforms, seabed liquefaction and gas migration that can lead to local overpressure in sediments and potential underwater landslides. While the pre-conditions usually form over geological times, the onset of the hazard can be very sudden and infrequent, and hence difficult to predict. To date, most of the geohazard features that occur on the seafloor are unknown, ill-characterized, and difficult to monitor (with present-day technology).
Offshore, geological processes and human activities, for instance in connection with offshore petroleum exploration and production, can contribute to cause man-made geohazards. Earthquakes are often considered the most important geohazards but much of the damage may be caused by the submarine slides and large mass flows triggered by them.

Moroccan coastal risks

Because of its geographical situation in the northwestern corner of Africa within moderate latitudes and along the northern border of the African plate (see Fig. 1), Morocco is exposed to several types of hazards of meteorological and seismo-tectonic origins:

- global climate change and associated sea-level rise (Satta *et al*. 2016, Snoussi *et al*. 2009);

- earthquakes of moderate to large magnitude and intensity (Cherkaoui 1988; El Mrabet 2005; Cherkaoui and El Hassani 2012)

- major tsunamis, especially the Lisbon tsunami on 1st November 1755, which remains the most devastating to date observed in Morocco where it caused large destructions and thousands of victims (El Mrabet 2005; Mhammdi *et al.* 2008; Blanc 2009; Kaabouben *et al*. 2009; Medina *et al*. 2011; Mhammdi *et al*. 2015)

- landslides (Mastere 2011)

- inundations (Saidi *et al.* 2010)

- marine storms (Simonet and Tanguy 1956; El Messaoudi *et al*. 2016, Belkhyat *et al.* 2017, 2019, Mhammdi *et al*. 2020). The Moroccan coast is frequently and severely hit by the marine winter storms associated with swells engendered by the North Atlantic depressions, and by sporadic cyclones such as Vince (8–11 October 2005), Delta (22–30 November 2005) and Leslie (11–14 October 2018), leading to severe damage of infrastructures, beach and cliff erosion and sediment redistribution.

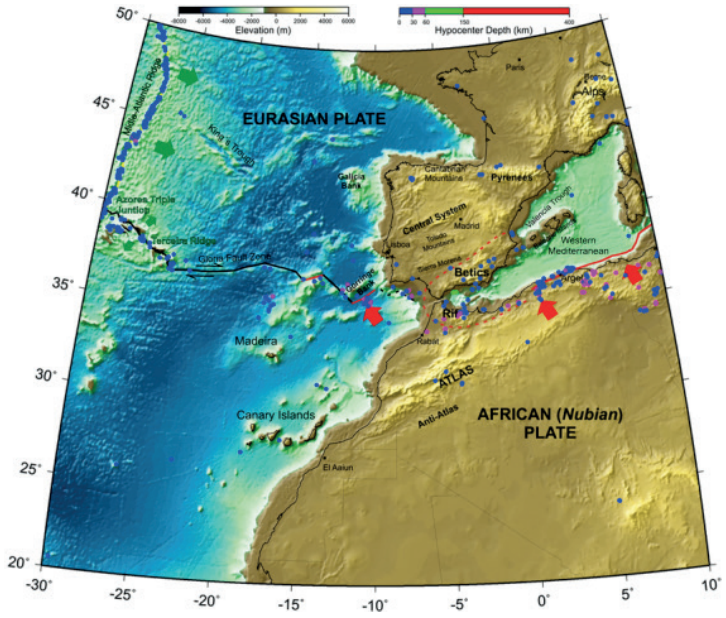

Figure 1. Simplified tectonic map of the western Africa–Eurasia plate boundary superimposed on the topography extracted from GTOPO30 and GEBCO 2003 databases. Broken lines indicate, approximately, tectonic boundaries, microplates and block limits (modified by Muñoz-Martín *et al*. 2010 from De Vicente and Vegas 2009). Red arrows indicate the present-day collisional push between Africa and Eurasia, and green arrows the Mid-Atlantic Ridge push. Colour dots show epicenters and focal depths from the EHB Bulletin (International Seismological Center 2009).

For instance, on 7 January 2014, one of the strongest marine storms crossing the North Atlantic, named Hercules (or Christina), hit the Atlantic coastal areas of southwestern Europe and those of Morocco, leading to intense flooding and huge damage of infrastructures- mainly roads and touristic facilities. The effects of this storm were described in detail for France (Castelle *et al*. 2015), Portugal (Santos *et al.* 2014; Diogo *et al.* 2014) and Spain (Ponce De León and Soares 2015) but a few details were exposed for Morocco El Messaoudi *et al*. 2016.

Global climate change and associated sea-level rise

The world is experiencing many climate, environmental and social challenges, and coastal communities are engaged in vast efforts to tackle the impacts of such changes.

The coastal zone of Morocco extends for nearly 3500 km, along the Mediterranean Sea and the Atlantic Ocean. Geomorphologically, this zone consists of low-lying coastal plains, sandy beaches, rocky shores, estuaries, lagoons, salt marshes and narrow to wide continental shelf. These natural features provide a priceless natural resource from an ecological, social and economic perspective. Indeed, the Moroccan coast forms one of the main socioeconomic areas of the country, with more than 60% of the population inhabiting coastal cities, and incorporating 80% of the industry. Furthermore, beaches and coastal resorts constitute a large percentage of the gross domestic product (GDP). In spite of their high ecological and economic value, Moroccan coastal systems have received relatively little attention, especially with regard to environmental

conditions and risks. Yet, many of them continue to suffer impacts originating from both sea and land-based activities (urbanization, agriculture, fisheries, tourism, ports, industry, etc.) and are experiencing acute environmental problems. However, despite the growing awareness of climate change impacts, a systematic study of sea-level rise impacts on the whole coastline has not been undertaken to date, and only a few investigations have been conducted (Niazi 2007; Khouakhi 2008; Snoussi *et al*. 2008, 2009).

A World Bank study (2011) on "Climate Change Adaptation and Resilience to Natural Disasters in Coastal Cities of North Africa," concluded that with a temperature increase of 4°C, 2.1 million people in Morocco would be affected by flooding. There is a high vulnerability to sea level rise in coming decades that is related to the high concentration of populations and activities in coastal areas, and increased risks due to an increase in global sea levels, storms, and local coastal erosion. Morocco's coastal GDP has been listed among the Top 10 countries at risk from increasing storm surges (Dasgupta *et al*. 2009).

Tsunamis

Tsunamis can be caused by a number of events: underwater earthquakes, landslides, underwater volcanic eruptions, falling meteorites, etc., but the majority is of seismic origin. The tsunamigenic earthquakes that threaten the Moroccan coast occur mainly in the Alboran Sea, western Mediterranean, and above all in the Gulf of Cadiz on the Atlantic side (Fig. 2).

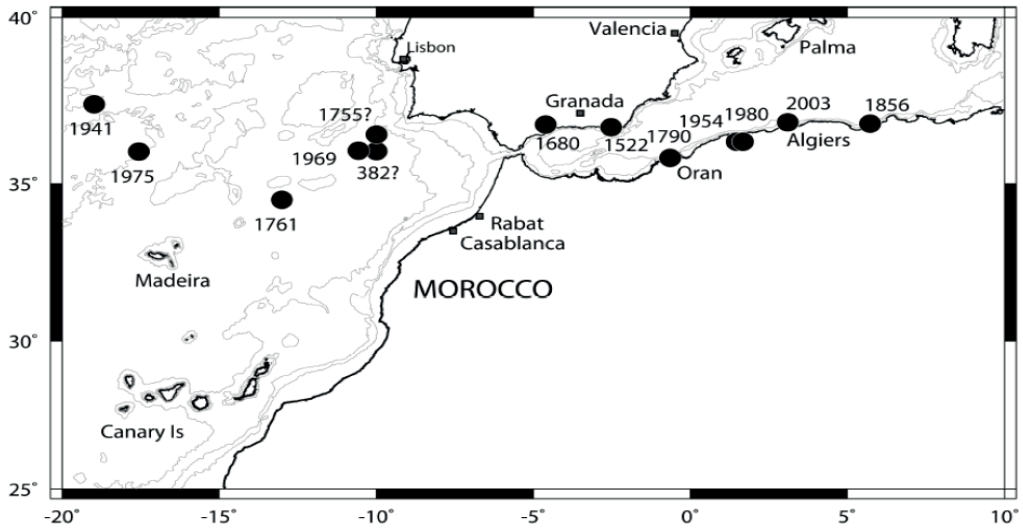

Figure 2. Map of tsunami events which affected the Moroccan coasts (Kaabouben *et al*. 2009)

Morocco is located in a collision zone - corresponding to the convergence of the African and Eurasian plates - which generates high levels of tsunamigenic seismic activity. On 1 November 1755, an earthquake measuring 9 on the Richter scale generated a very large tsunami around the Gulf of Cadiz, destroying Lisbon and causing considerable damage to a large number of coastal atlantic Moroccan cities from Tangier to Agadir. In particular, the cities and inland area of Tangier, Asilah, Larache, Salé, El Jadida Safi, Essaouira were impacted by waves higher than 15 m in some places. This is the only tsunami on this scale known in the North Atlantic (the others were smaller), and so it remains a benchmark event for establishing risk scenarios in this area. Tsunamis continue to have devastating effects on coastal populations and activities,

as demonstrated by the events of 26 December 2004 in the Indian Ocean (227898 deaths) and 11 March 2011 on the north-west coast of Japan (20,319 deaths). Although Morocco has not been spared from this hazard, as revealed by several historical and even geomorphological and sedimentological records, the risk of tsunamis remains underestimated, if not totally ignored, in the country.

The Gorringe bank is known to be the locus of strong earthquakes that caused serious damage in Portugal, Spain and Morocco, which was amplified in some cases by tsunami waves in coastal areas. While the whole Atlantic coast of Morocco between Tangier and Agadir is exposed to the effects of Atlantic tsunamigenic earthquakes, the Mediterranean coast of Morocco is not sheltered from tsunamis either. Historical seismicity reveals that following the 1522 earthquake the region of Al Hoceima was submerged by the sea (Cherkaoui and Asebriy 2003). Earthquakes' epicenters in the Mediterranean domain are distributed in a broad sector covering the Alboran sea, southern Spain and northern Morocco. The southernmost limit of this continuous seismicity area extends towards the east, to the north of Algeria and Tunisia till the Calabria arc in Sicily. Earthquake magnitudes are relatively small or moderate (see Table1).

The most recent tsunami event took place on 21 May 2003, as a consequence of an Mw=7 earthquake. The tsunami generated was detected in the western Mediterranean basin, with noted impacts on the Balearic Islands. Eyewitnesses reported wave heights of two meters and an average period of 10–12 min in Mallorca. The tide gauge localized in Palma de Mallorca showed a maximum height of about 60 cm, with peak to peak amplitude of 1.17 m. The earthquake was not felt in Morocco, although it was recorded by the broadband seismic network. We could not find any documents of sea agitation in Morocco newspapers.
Tinti *et al.* (2005) claimed for negligible tsunami effects at Costa Blanca in Spain, while the earthquake models of Alasset *et al*. (2006) illustrate that most of the energy radiates towards theBalearic Islands and the coast of Spain.

Table 1. List of possible tsunamis on Moroccan coasts. We indicate, for each case, the generation of a noticeable tsunami, the availability of historical documents and maregrams in Morocco and the likelihood classification attributed in GITEC catalogue; Lon –Longitude, Lat – Latitude, Reliability according to the Sieberg-Ambraseys scale.

Year	Month	Day	Hour	Min	Longitude	Latitudee	Souce Area	Mw	Reliability	Source
382	–	–	–	–	−10 00	36.00	South West Iberia	–	2	3,4
881	5	22		–			West Mediterranean	–	4	1
1522	9	22	10	–	−02.66	36.97	West Mediterranean	6.5	4	1
1680	10	9	7	–	−04.60	36.80	West Mediterranean	6.8	4	1
1733	–	–	–	–	–	–	West Mediterranean		0	19
1755	11	1	10	16	−10 00	36.50	South West Iberia	8.7	4	1,3,5,6,7,8
1761	3	31	12	15	−13.00	34.50	Gloria Fault	8.5	3	2,9
1790	10	9	1	15	−00.60	35.70	West Mediterranean	6.7	1	1
1856	8	21	21	30	+05.72	36.83	West Mediterranean	–	0	20
1941	25	11	18	04	−18.98	37.42	Gloria Fault	8.2	4	6,10
1969	2	28	2	40	−10.57	36.01	South West Iberia	7.9	4	11,12,13,14,15,16,17
1975	5	26	9	11	−17.56	35.98	Gloria Fault	7.9	4	11,18
1980	10	10	12		+01.68	36.28	West Mediterranean	5.8	0	20
2003	5	21	18	44	+03.08	36.80	West Mediterranean	7.0	0	21, 22, 23

Sources: (1) El Mrabet (1991, 2005); (2) Baptista *et al.* (2006); (3) Catalogo GITEC; (4) Sousa (1678); (5) Gazette de Cologne (1756); (6) Debrach (1946); (7) Moreira (1968); (8) Heinrich *et al*. (1994); (9) Gjevik *et al*. (1997); (10) Rabinovich *et al*. (1998); (11) Kaabouben *et al*. (2008); (12) Soloviev (1990); (13) USGS online database; (14) Tinti *et al.* 2005); (15) Alasset *et al*. 2006; (16) Tel *et al.* 2004 ; (17) Yelles-Chaouche (1991).

Hazard prevention or mitigation should begin with a study of their past occurrences and consequences. However, historical records are often very scarce to determine their return periods and evaluate their intensities. Accordingly, the scientific community increasingly uses sedimentary archives from coastal environments, since they offer a viable alternative to historical archives. Several studies using this approach have been recently conducted on the Moroccan coast. The search for sedimentary markers **(**Fig.3**)** of extreme events such as tsunamis provides additional information to archives on past events. During a tsunami, volumes of marine sediment are transported from the sea to the land and deposited in areas that may or may not be suitable for their preservation. The identification of these deposits is based on a multidisciplinary approach that makes it possible to describe the tsunamigenic character and also to distinguish tsunami deposits from storm deposits. At the same time, studying the impacts of storms has raised questions about the vulnerability of coastal areas. These results have thus enriched the data on extreme events on the Moroccan coast.

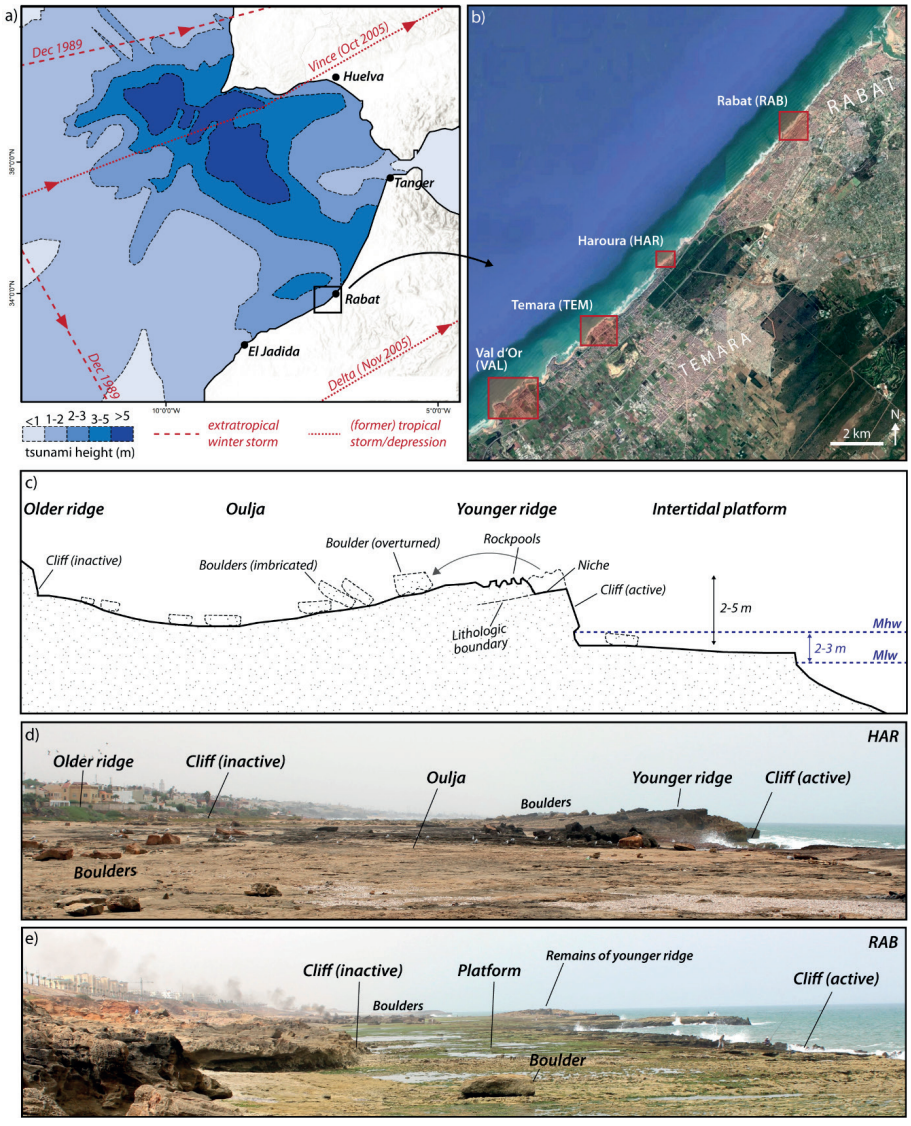

Figure 3. Flooding hazard and geomorphological setting of the Rabat coast.

a) Exposure of the Moroccan Atlantic coast to tsunamis and storms, including modelled wave heights for the 1755 Lisbon tsunami (Renou *et al*. 2011), tracks of former tropical storms crossing the area between 1851 and 2016 (NOAA 2019), and extratropical winter storms in the period 1989-2009 (Reading University 2019).

b) The Rabat coast with the four study sites (based on Google Earth images).

c) Schematic geomorphological cross section through the Rabat coast (modified from Mhammdi *et al.* 2008).

d) The coastal platform at Hahoura (HAR, view towards Southwest).

e) The coastal platform at Rabat (RAB, view towards Southwest).

While instrumental and historical records demonstrate a flooding hazard for the Moroccan coast due to both storms and tsunamis, all documented events - except the 1755 Lisbon Tsunami - were restricted to the last decades. This does not allow for robust estimates of long-term tsunami and storm occurrence or of all possible magnitudes of storm surges and tsunami inundation. Most published geological tsunami and storm evidence for the pre-instrumental era is restricted to Spain and Portugal (e.g. Dawson *et al.* 1995; Hindson and Andrade 1999; Lario 2011; Costa *et al.* 2011; Feist *et al*. 2019), but fields of wave-emplaced boulders offer records of past storms and/or tsunamis for Morocco (Mhammdi *et al*. 2008; Medina *et al.* 2011) that could inform about the regional long-term hazard if robust chronological data were available.

The most prominent boulder fields are reported from a 30 km long NE-SW oriented coastal section between Rabat and Skhirat (see Fig. 4), consisting of hundreds of boulders with estimated masses between a few and more than 100 t (Mhammdi *et al*. 2008; Medina *et al*. 2011). The geomorphology and geology of this area is characterised by a succession of coast-parallel, Pleistocene calcarenite ridges that are related to sea-level high stand sand rest on a Palaeozoic basement (Chakroun *et al.* 2017). A typical cross section is composed of (i) the intertidal platform with an active coastal cliff; (ii) the youngest lithified calcarenite ridge, formed during MIS 5; (iii) an inter-ridge depression, called Oulja, which may be flooded at high tide (the spring tide range is 2-3 m), and is covered by recent and/or Holocene beach deposits; and (iv) an older calcarenite ridge, probably formed during MIS 7, including an inactive cliff (Medina *et al*. 2011; Chakroun *et al.* 2017; Chahid *et al*. 2017). Towards Rabat, the younger calcarenite ridge is replaced by a simple sandstone platform.

As described by Mhammdi *et al.* (2008) and Medina *et al.* (2011), most of the sandstone boulders were sourced from the active cliff (Fig. 4c). Since detachment is guided by lithological boundaries between the calcarenite and interbedded clay units, most of the boulders have compact shapes; only occasionally were boulders derived from subtidal positions and lifted up to 5 m to the top of the first calcarenite ridge, as indicated by vermetids, or sourced from younger sandstones covering the Oulja. The boulders are deposited as single clasts, clusters, or imbricated stacks that rest on top or at the backward slope of the first calcarenite ridge in the Oulja, or rarely at the seaward slope of the older calcarenite ridge up to 300 m inland (Fig. 4c). The position and orientation of bio-erosive rock pools formed on the surface of the youngest ridge (i.e. the pre-transport surface of most boulders) offer insights into transport modes. While some boulders moved by sliding only, others were overturned during transport, as indicated by down-facing rock pools on the pre-transport surface). For some of the larger boulders, sliding movement by storm waves after their initial detachment from the cliff is documented on satellite images. Movement of smaller boulders with masses of up to ~1 m³ was frequently observed after recent winter storms such as Hercules/Christina in January 2014 (Mhammdi *et al*. 2020). At some places along the coast between Rabat and Casablanca even boulders exceeding 10 t have been pushed landward during recent winter storms.

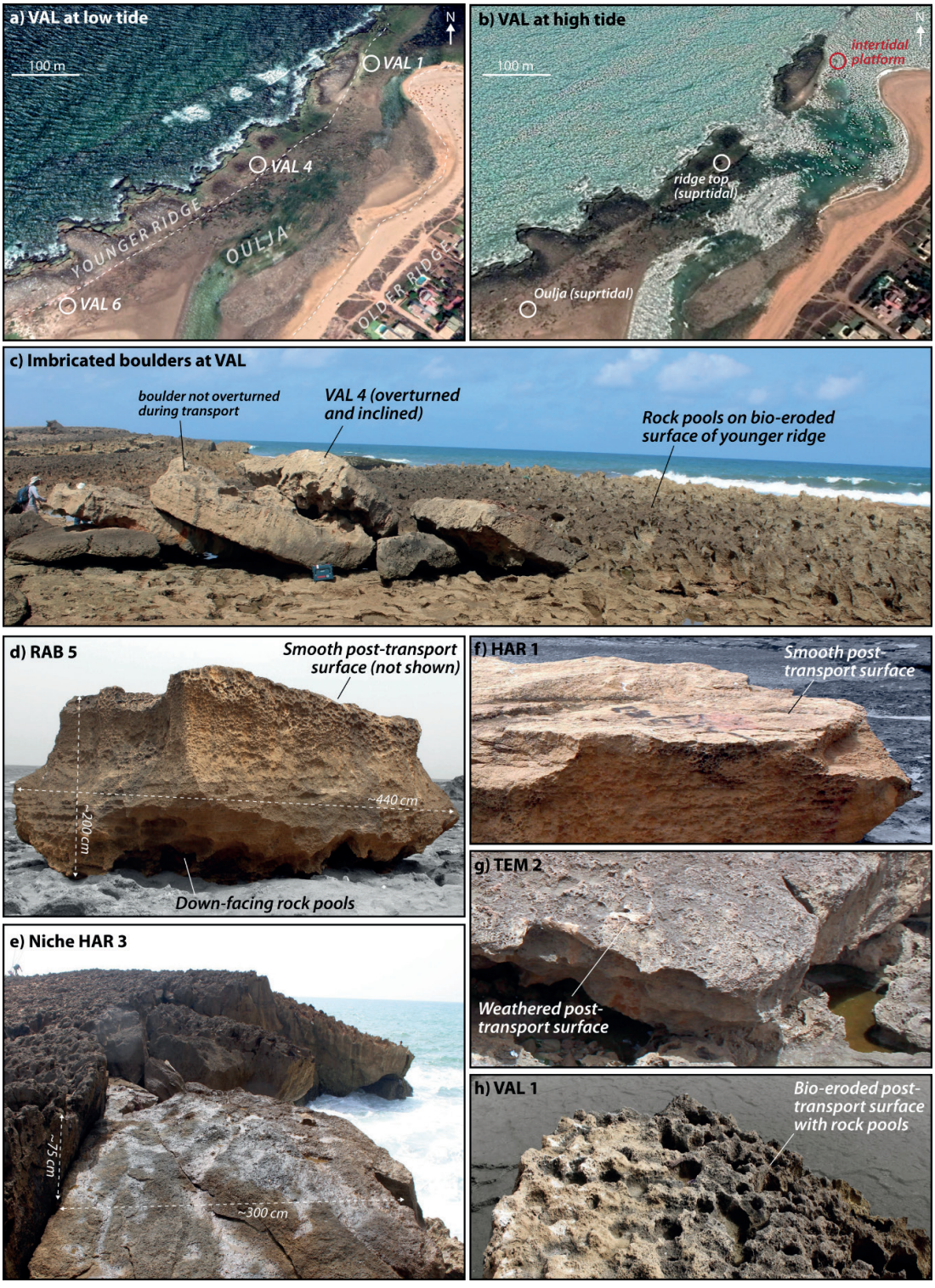

Figure 4. Coastal boulders at the Rabat coast.

a) Satellite images of Val d'Or taken at low tide
b) and high tide illustrate different boulder settings on top of the younger ridge, within the Oulja and on the intertidal platform (Google Earth images from July 2018 and February 2016).
c) Boulder VAL 4 as part of a stack of imbricated boulders in ridge top position.
d) Down-facing rock pools of the former cliff surface at the bottom surface of RAB 5.
e) Niche HAR 3 formed by detachment of the associated boulder.
f-h) Surface roughness of the sampled boulders varies from smooth (HAR 1), over slightly weathered (TEM 2), to rock-pool covered (VAL 1). (Brill *et al*. 2020)

Storms

Storms constitute a real, relatively frequent (see Table 2) threat to coastal cities along the Rabat-Casablanca segment. The analysis of recent storminess in Morocco reveals that storms are an underrated natural hazard, probably because of the lack of general studies since the 1960s. During the last decade, the Moroccan Atlantic coast was severely hit by various marine winter storms associated with swells engendered by the North Atlantic depressions and by sporadic cyclones. On 7 January 2014, storm Hercules/Christina led to intense flooding and huge damage of infrastructures and touristic facilities from Salé to Casablanca.)

Historical data on storms in Morocco show that the normal significant heights of swell are low, in the range 0.5–1.5 m, and that the 4.5 m value can be adopted as a threshold for storm waves, similarly to the norm adopted for the western segment of the Portuguese coast. We set 33 tons as a new regional upper limit of the weight of boulders that can be transported by current winter storms (hurricanes excluded), keeping in mind that the shape of the boulder is a fundamental parameter for the displacement. A major lesson from Hercules is that much effort has to be invested by scientists, district authorities and real estate managers for the management and prevention of this type of hazards, given the growing coastal population and economic activity.

Based on reports and newspaper articles dating back to the beginning of the 20th century, coastal geologists and engineers have investigated the sedimentary efects and damage caused by marine/ coastal storms. Their descriptions proved very useful for comparing wave parameters and setting a wave threshold for regional / local storms. Examples are found in the papers of Ribera *et al*. (2011) who used press articles on the storms of the Gulf of Cadiz from 1929 to 2005, in those of Máyer Suárez (1999), Yanes and Marzol (2009) for the Canary Islands between 1607 and 2009 and for Tenerife alone between 1985 and 2003.

Generally, data on the storms that affected the Moroccan coasts in the early 20th century remain scarce, as the French marine archives, summarized by Simonet and Tanguy (1956), have not yet been analyzed in detail. One of the earliest reports is that of Gallois (1920) who described the arrival of sudden strong swell waves to the Casablanca roadstead (before the construction of the harbor) on 6 January 1913 at 9 h. The waves destroyed 16 boats, damaged 13 others and delayed commercial traffic for several years.

Table 2. Compilation of the main storms that affected the Moroccan Atlantic coast since the early 20th Century

Compilation of the main marine storms that affected the Moroccan Atlantic coast since the early XXth Century.

Date DD/MM/YY	Name (if given)	H_{max} (m)	Period (s)	Trend (°)	Reference
23-25/03/2018	Hugo				AEMET[a]
14-15/03/2018	Giselle				AEMET
09/03–11/03/2018	Felix				AEMET
28/2–03/03/2018	Emma				AEMET
28/02–1/03/2017		> 7			Belkhayat et al. (2017); MTTP (2014)
05-07/01/2014	Hercules	13.62	21.60	320°	El Messaoudi et al. (2016)
21-22/08/2012	Gordon		14		AEMET[b]
February 27, 2010	Xynthia				El Messaoudi et al. (2016)
January 31, 2009					AEMET
January 04, 2008		15.85	18.80	320°	El Messaoudi et al. (2016)
22-28/11/2005	Delta				Beven et al. (2008)
					AEMET (Martin Leon et al.) [c]
08-11/10/2005	Vince				Beven et al. (2008)
					AEMET[d]
January 19, 2005		12	17	330°	El Messaoudi et al. (2016)
April 13, 2003		11.28	14	313.6°	El Messaoudi et al. (2016)
March 11, 2003		11.14	19.3	324.8°	El Messaoudi et al. (2016)
December 27, 2002		10.04	14.4	324.8°	El Messaoudi et al. (2016)
November 14, 2002		11.52	11.7	331.9	El Messaoudi et al. (2016)
February 16, 2002		11.25	15.6	347.3	El Messaoudi et al. (2016)
January 08, 1996		7.5	18.5	308°	El Messaoudi et al. (2016)
February 16, 1995		6.6	17	305°	El Messaoudi et al. (2016)
17-19/02/1986					Minoubi et al. (2013)
01-03/02/1986					Minoubi et al. (2013)
03-06/01/1986					Minoubi et al. (2013)
February 28, 1978		8	19	300	El Messaoudi et al. (2016)
??/12/1973		7		NW?	Minoubi et al. (2013)
February 21, 1966		10	15–20	283; WNW	Minoubi et al. (2013);
					El Messaoudi et al. (2016)
December 28, 1951		6.7	nd	nd	El Messaoudi et al. (2016)
02-03/02/1949					Minoubi et al. (2013)
December 19, 1945		> 7	18 (Casa)	W; NW	Simonet and Tanguy (1956)
December 16, 1942		> 7		NW	Simonet and Tanguy (1956)
February 16, 1941		> 7		NW	Simonet and Tanguy (1956)
November 18, 1940		> 7		NW	Simonet and Tanguy (1956)
December 11, 1938		> 7		NW	Simonet and Tanguy (1956)
25-27/01/1937		> 7	20 (Rabat)	W; NW	Simonet and Tanguy (1956)
February 28, 1935		> 7		W	Simonet and Tanguy (1956)
March 13, 1934		> 7	13 (Rabat)	W	Simonet and Tanguy (1956)
January 04, 1933		> 7		W; NW	Simonet and Tanguy (1956)
December 07, 1932		> 7		W	Simonet and Tanguy (1956)
March 27, 1932		> 7		W; NW	Simonet and Tanguy (1956)
November 11, 1931		> 7		NW	Simonet and Tanguy (1956)
March 19, 1931		> 7		SW	Simonet and Tanguy (1956)
January 14, 1931		> 7	17	NW	Simonet and Tanguy (1956)
January 04, 1931		> 7		NW; W; SW	Simonet and Tanguy (1956)
01-02/02/1930		> 7	18	NW; W	Simonet and Tanguy (1956)
January 17, 1930		> 7		SW	Simonet and Tanguy (1956)
January 13, 1930		> 7		NW	Simonet and Tanguy (1956)
December 05, 1929		> 7		W	Simonet and Tanguy (1956)
November 21, 1929		> 7	19		Simonet and Tanguy (1956)
February 19, 1929		> 7	17–20	W (Safi)	Simonet and Tanguy (1956)
October 25, 1928		> 7	20		Simonet and Tanguy (1956)
April 10, 1928		> 7			Simonet and Tanguy (1956)
February 26, 1928		> 7	17		Simonet and Tanguy (1956)
??/10/1913					Cherfaoui & Doghmi (2002)
January 06, 1913					Gallois (1920),
					Cherfaoui & Doghmi (2002), El Messaoudi et al. (2016)
??/12/1912					Cherfaoui & Doghmi (2002)
Winter 1910–1911					Cherfaoui & Doghmi (2002)
Winter 1909–1910					Cherfaoui & Doghmi (2002)
April 20, 1905		10.4			El Messaoudi et al. (2016)

[a] Author's monitoring through Agencia Estatal de Meteorologia, Spain (www.aemet.es).

Mediterranean storms

Storm deposits are generally considered to have smaller spatial dimensions when compared to tsunami deposits, as their deposition is typically restricted to a zone of a few hundred meters from the shore (Judd *et al*. 2017; May *et al*. 2012; Morton *et al*. 2007). However, exceptionally large storms such as tropical events are capable of moving sediments over long distances. The most powerful (tropical-like) Mediterranean storms are uncommon in the Mediterranean coast of Morocco (see Tous and Romero 2011) but their past existence cannot be excluded. Indeed, evidence for old inlets and large washovers attributed to extreme storms of the last century is to be seen in the Nador lagoon barrier island (Hamoumi 2012; Raji *et al*. 2013). Moreover, Raji *et al*. (2015) identified one of the sand layers sampled in the MC45 sediment core (situated at over

1.2 km from the lido) as the landward extent of a backbarrier washover created in the wake of an 1889 storm event which was caused by north-to-northeast winds resulted in a 150 m wide inlet to form.

Earthquakes

An earthquake manifests in the sudden movement of the Earth's surface, resulting from an abrupt release of energy by the rupture of faults in the crust and upper mantle of the Earth. This is among the most damaging of geohazards, frequently causing devastating loss of lives, assets and infrastructure, especially in densely populated areas. Since 1998, earthquakes have caused a higher number of deaths than all other geophysical (e.g. mass movement, volcanic activity) and hydro-meteorological hazards (e.g. floods, storms, extreme temperatures) combined.

The magnitude of an earthquake is the amount of energy released, and the Moment Magnitude (Mw) is expressed for larger events. The greatest submarine earthquakes (Mw>8) occur along destructive tectonic plate boundaries, referred to as subduction zones (e.g. Sallarès and Ranero 2019) where one tectonic plate is thrust underneath another.

Recent examples are the Sumatra-Andaman (Indonesia, 2004) and Tohoku-Oki (Japan, 2011) earthquakes (both Mw>9), which both ruptured undersea faults and triggered destructive tsunamis. Indirect earthquake effects also include submarine mass movements that may cause extensive cable breaks. In the Mediterranean, the largest and most destructive subduction zone earthquake with Mw>8 occurred in 365 AD offshore Crete Island (Shaw *et al.* 2008), leading to an instantaneous uplift of western Crete by more than 6 m and triggering a catastrophic tsunami that impacted nearly all coastal areas around the Eastern Mediterranean Sea.

In Morocco, the review of historical documents shows that much larger earthquakes occurred in the past, and that cities like Fez, Meknes, Melilla and those along the Atlantic coast between Tangier and Agadir have suffered many times from earthquakes' damages.
Compared to other Mediterranean countries (Algeria, Italy, Greece, Turkey, etc.), Morocco is affected by a moderate seismic activity largely related to the convergence between Africa and Eurasia. However, every year there are earthquakes felt by the population that in some cases cause important local damage, and the National Institute of Geophysics' seismic monitoring stations record hundreds of earthquakes of varying magnitudes each year. We have still present in memory the Agadir 1960 catastrophic earthquake with 12,000 deaths and that of Al Hoceima 2004 and its 629 victims. Most recently, in September 2023, a powerful earthquake of magnitude 6.8 struck Morocco at 18.5 km depth, causing nearly 3000 casualties and 5500 injuries, with hundreds of thousands displaced. This earthquake was the worst in North Africa in the last half-century. The epicenter was in the High Atlas Mountains, 71km (44 miles) south-west of Marrakech.

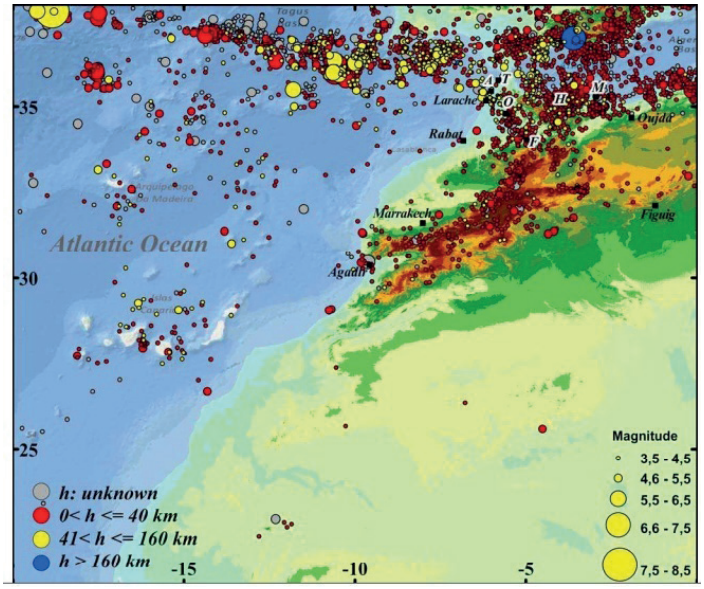

Figure 5. Seismicity of Morocco and surrounding area from 1901 to 2010 with M ≥ 3.5. Abbreviations: A= Asilah, F= Fez, H= Al Hoceima, M= Melilla, O= Ouezzane, T= Tangier. [after Cherkaoui and El Hassani 2012]

Conclusion

We have compiled all available information from bibliographic and historical records, including the most recent, on the historical coastal hazards that could have affected Atlantic and Mediterranean Moroccan coasts. While Morocco is subject to destructive earthquakes and tsunamis in the Atlantic sector, our state of knowledge in this area remains scarce and in need of much consolidation to allow proper risk assessment and guide future prevention programs.

To be cited as:

N. Mhammdi. 2024. Moroccan coastal hazards. p 139- 154. In CIESM Monograph 52 [F. Briand, Ed.] Marine hazards, coastal vulnerability, risk (mis)perceptions – a Mediterranean perspective. CIESM Publisher, Paris, Monaco, 182 p.

References

Alasset P.J., Hébert H., Maouche S., Calbini V. and M. Meghraoui. 2006. The tsunami induced by the 2003 Zemmouri earthquake (Mw=6.9, Algeria): modelling and results. *Geophys. J. Internatl 166*(1): 213-226.

Baptista M.A., Miranda J.M. and J.F. Luis. 2006. In search of the 31 March 1761 earthquake and tsunami source. *Bull. Seismol. Soc. America 96*(2): 713-721.

Baptista M.A., Miranda J.M., Batlo J. and H. Ferreira. 2012. Tsunami flooding along Tagus estuary, Portugal, the 1531 event. In *EGU General Assembly Conference Abstracts* (p. 4910).

Belkhayat Z., El Aoula R. and N. Mhammdi. 2017. Effects of the winter storms of 2017 on the Atlantic coast of Rabat: a preliminary evaluation. *Bull. Inst. Scient., Rabat 39*: 135-139.

Blanc P.L. 2009. Earthquakes and tsunami in November 1755 in Morocco: a different reading of contemporaneous documentary sources. *Nat. Hazards Earth Syst. Sci.* 9: 725-738

Brill D., May S.M., Mhammdi N., King G., Burow C., Wolf D. ... & H. Brückner. 2020. OSL rock surface exposure dating as a novel approach for reconstructing transport histories of coastal boulders over decadal to centennial timescales. *Earth Surface Dynamics Discussions* 1-44.

Castelle B., Marieu V., Bujan S., Splinter K. D., Robinet A., Sénéchal N. and S. Ferreira. 2015. Impact of the winter 2013–2014 series of severe Western Europe storms on a double-barred sandy coast: Beach and dune erosion and megacusp embayments. *Geomorphology 238*: 135-148.

Chahid D., Lenoble A., Boudad L. and B.V. Vliet-Lanoë. 2016. Enregistrements sédimentaires d'événements de haute énergie, exemples de la côte atlantique de Rabat-Skhirat (Maroc). *Quaternaire. Revue de l'Association française pour l'étude du Quaternaire 27*(2): 155-169.

Chakroun A., Chahid D., Boudad L., Lenoble A., Lamothe M., Falguères C. and R. Nespoulet. 2017. Les paléo-rivages des formations littorales atlantiques du Pléistocène moyen – supérieur de Rabat-Témara (Maroc), *L'Anthropologie* 121 (1–2): 122-132

Cherkaoui T.E. 1988. Fichier des séismes du Maroc et des régions limitrophes: 1901-1984. Rabat: *Trav. Inst. Sci., série Géol. & Géogr. phys.* 17: 158 p. + carte h. t

Cherkaoui T.E. and L. Asebriy. 2003. Le risque sismique dans le Nord du Maroc. *Trav. Inst. Sci., sér. Géol.& Géogr. phys.* 21: 225-232.

Cherkaoui T.E. and A. El Hassani. 2012. Seismicity and seismic hazard in Morocco 1901-2010. *Bulletin de l'Institut Scientifique, Rabat, section Sciences de la Terre 34*: 45-55.

Costa P.J., Andrade C., Freitas M.C., Oliveira M.A., da Silva C. M., Omira R. ... & A.G. Dawson. 2011. Boulder deposition during major tsunami events. *Earth Surface Processes and Landforms 36*(15): 2054-2068.

Dasgupta S., Laplante B., Meisner C., Wheeler D. and J. Yan. 2009. The impact of sea level rise on developing countries: a comparative analysis. *Climatic change 93*(3-4): 379-388.

Dawson A.G., Hindson H., Andrade C., Freitas C., Parish R. and M. Bateman. 1995. Tsunami sedimentation associated with the Lisbon earthquake of 1 November AD 1755: Boca do Rio, Algarve, Portugal. *The Holocene 5*(2): 209-215.

Debrach J. 1946. Raz de marée d'origine séismique enregistré sur le littoral atlantique du Maroc. *Annales SPGM 1946*: 59-71.

De Vicente G. and R. Vegas. 2009. Large-scale distributed deformation controlled topography along the western Africa–Eurasia limit: Tectonic constraints. *Tectonophysics 474*(1-2): 124-143.

El Messaoudi B., Ait Laamel M., El Hou M. and H. Bouksim . 2016 : Situations des fortes houles sur les côtes atlantiques marocaines. *Actes Session Plénière Acad. Hassan II des Sciences & Techniques*, Rabat, 79-105.

El Mrabet T. 1991. La sismicité historique du Maroc (en arabe), Thèse de 3eme cycle, Faculté des lettres et des sciences humaines, Université Mohammed V. Rabat, 291 pp., 1991 (in arabic).

El Mrabet T. 2005 : Les grands seismes dans la région maghrébine, Thèse d'état, Faculté des lettres et des sciences humaines, Université Mohammed V. Rabat, 435 pp., 2005 (in arabic)

Feist L., Frank S., Bellanova P., Laermanns H., Cämmerer C., Mathes-Schmidt M. ... & K. Reicherter. 2019. The sedimentological and environmental footprint of extreme wave events in Boca do Rio, Algarve coast, Portugal. *Sedimentary geology 389*: 147-160.

Gazeta de Lisboa, 25 de Janeiro de 1756. (in Portuguese).

Gazette de Cologne, Africa De Ceuta, le 20 Novembre 1756.

Gazette Française d'Amsterdam, Suite des Nouvelles d'Amsterdam du 26 Decembre 1755, 1756

Gjevik B., Pedersen G., Dybesland E., Harbitz C.B, Miranda P., Baptista M.A., Mendes-Victor L., Heinrich Ph., Roche R. and M. Guesima. 1997. Modelling tsunamis from earthquake sources near Gorringe Bank southwest of Portugal, *J. Geophys Res. Atmosph., 102*, C13: 27931–27950.

Hamoumi N. 2012. Le complexe lagunaire de Nador (Maroc) : fonctionnement, contrôle naturel et provoqué, scenarii d'évolution future. *Revue Paralia 5*: 5-1.

Heinrich Ph., Baptista M.A. and P. Miranda. 1994: Numerical simulations of the 1969 tsunami along the Portuguese coasts. Preliminary Results. *Sc. of Tsunami Hazards, 12*, 1: 3–25.

Hindson R.A., and C. Andrade. 1999. Sedimentation and hydrodynamic processes associated with the tsunami generated by the 1755 Lisbon earthquake. *Quaternary International 56*(1): 27-38.

Judd K., Chagué-Goff C., Goff J., Gadd P., Zawadzki A. and D. Fierro. 2017. Multi-proxy evidence for small historical tsunamis leaving little or no sedimentary record. *Marine Geology 385*: 204-215.

Kaabouben F., Iben Brahim A., Toto E., Baptista M.A., Miranda J.M., Soares P. and J.F. Luis. 2008. On the focal mechanism of the 26 May 1975 North Atlantic event: Contribution from

tsunami modeling, *J. Seismol. 12* (4): 575–583.

Kaabouben F., Baptista M.A., Iben Brahim A., El Mouraouah A. and A. Toto. 2009. On the Moroccan tsunami catalogue. *Nat. Hazards & Earth System Sci. 9*(4): 1227-1236.

Khouakhi A. 2008. Evaluation des impacts de l'EANM sur le littoral de Mohammedia : Terres à risque d'inondation et impacts socio-économiques. Mémoire de Master Sciences de la Terre, de la Mer et de l'Environnement, Univ. Mohammed V, Fac. des Sciences, Agdal, Rabat, 97 p.

Klein R.J. and R.J. Nicholls. 1999. Assessment of coastal vulnerability to climate change. *Ambio* 182-187.

Lario J., Zazo C., Goy J.L., Silva P.G., Bardaji T., Cabero A. and C.J. Dabrio. 2011. Holocene palaeotsunami catalogue of SW Iberia. *Quaternary International 242*(1): 196-200.

Mastere M. 2011. La susceptibilité aux mouvements de terrain dans la province de Chefchaouen (Rif Central, Maroc). Thèse de doctorat. Université de Bretagne occidentale,Brest, 319 p.

May S.M., Vött A., Brückner H. and A. Smedile. 2012. The Gyra washover fan in Lefkada Lagoon, NW Greece - possible evidence of the 365 AD Crete earthquake and tsunami. *Earth, planets & space* 64(10): 859-874.

Suárez P.M. 1999. Un siglo de temporales en la prensa de Gran Canaria. *Vegueta* 4: 267-282.

Medina F., Mhammdi N., Chiguer A., Akil M. and E.B. Jaaidi. 2011. The Rabat and Larache boulder fields; new examples of high-energy deposits related to storms and tsunami waves in north-western Morocco. *Natural Hazards* 59: 725-747.

Mhammdi N., Medina F., Kelletat D., Ahmamou M. and L. Aloussi. 2008. Large boulders along the Rabat coast (Morocco); possible emplacement for the 1st Nov. 1755 AD tsunami. *Science of Tsunami Hazards 27*(1): 17-30.

Mhammdi N., Medina F., Trentesaux A., Font E., Belkhayat Z. and M.A. Geawhari. 2015. Sedimentary evidence of palaeo-tsunami deposits along the Loukkos estuary (Moroccan Atlantic coast). *Science of Tsunami Hazards* 34(2): 83-100.

Mhammdi N., Medina F., Belkhayat Z., El Aoula R., Geawahri M.A. and A. Chiguer. 2020. Marine storms along the Moroccan Atlantic coast: an underrated natural hazard? *J. African Earth Sciences* 163: 103730.

Moreira V.S. 1968. Tsunamis observados em Portugal. Publ. Service Meteorologico National, GEOl34, Lisbon.

Morton R.A., Gelfenbaum G., Jaffe B. E., (2007). Physical criteria for distinguishing sandy tsunami and storm deposits using modern examples. *Sedimentary Geology*, Volume 200, Issues 3–4, Pages 184-207,

Muñoz-Martín A., De Vicente G., Fernández-Lozano J., Cloetingh S., Willingshofer E., Sokoutis D. and F. Beekman. 2010. Spectral analysis of the gravity and elevation along the western Africa–Eurasia plate tectonic limit: continental versus oceanic lithospheric folding signals. *Tectonophysics* 495: 298-314. doi:10.1016/j.tecto.2010.09.036

Niazi S. 2007. Evaluation des impacts des changements climatiques et de l'élévation du niveau de la mer sur le littoral de Tétouan (Méditerranée occidentale du Maroc): vulnérabilité et adaptation. Thèse de Doctorat, Univ. Mohammed V-Agdal, Fac. Sci. Rabat, 230 p.

Ponce de León S. and C. Guedes Soares. 2015. Hindcast of extreme sea states in North Atlantic extratropical storms. *Ocean Dynamics* 65: 241-254.

Rabinovich A.B., Miranda P. and M.A. Baptista. 1998. Analysis of the 1969 and 1975 tsunamis at the Atlantic coast of Portugal and Spain. *Oceanology* 38(4): 463–469.

Raji O., Niazi S., Snoussi M., Dezileau L. and A. Khouakhi. 2013. Vulnerability assessment of a lagoon to sea level rise and storm events: Nador lagoon (NE Morocco). *J. Coastal Research* 65: 802-807.

Raji O., Dezileau L., Von Grafenstein U., Niazi S., Snoussi M. and P. Martinez. 2015. Extreme sea events during the last millennium in the northeast of Morocco. *Nat. Hazards & Earth System Sci.* 15(2): 203-211.

Renou C., Lesne O., Mangin A., Rouffi F., Atillah A., El Hadani D. and H. Moudni. 2011. Évaluation de l'aléa tsunami dans la zone côtière de Rabat et Salé, Maroc, *Nat. Hazards & Earth System Sci.* 11: 2181–2191, https://doi.org/10.5194/nhess-11-2181-2191.

Ribera P., Gallego D., Pena-Ortiz C., Del Rio L., Plomaritis T.A. and J. Benavente. 2011. Reconstruction des tempêtes côtières hivernales historiques de l'Atlantique sur les côtes espagnoles du golfe de Cadix, 1929-2005, *Nat. Hazards & Earth System. Sci.* 11: 1715-1722, https://doi.org/10.5194/nhess-11-1715-2011.

Saidi M.E., Daoudi L., El Hassane Aresmouk M., Fniguire F. and S. Boukrim. 2010. Les crues de l'oued Ourika (Haut Atlas, Maroc): Événements extrêmes en contexte montagnard semi-aride. *Comunicaçoes Geologicas* 97(1): 113-128.

Sallarès V. and C.R. Ranero. 2019. Upper-plate rigidity determines depth-varying rupture behaviour of megathrust earthquakes. *Nature* 576 (7785): 96-101.

Satta A., Snoussi M., Puddu M., Flayou L. and R Hout. 2016. An index-based method to assess risks of climate-related hazards in coastal zones: the case of Tetouan. *Estuarine, Coastal & Shelf Science* 175: 93-105.

Shaw B., Ambraseys N.N., England P.C., Floyd M.A., Gorman, G.J., T.F. Higham ... and M.D. Piggott. 2008. Eastern Mediterranean tectonics and tsunami hazard inferred from the AD 365 earthquake. *Nature Geoscience* 1(4): 268-276.

Simonet R. and R. Tanguy. 1956. Etude statistique de la houle dans les différents ports marocains pour la période 1928–1952. *Ann. Serv. Phys. Globe Meteorol., Inst Sci. Chérifien* 16: 109-130.

Snoussi M., Ouchani T. and S. Niazi. 2008. Vulnerability assessment of the impact of sea-level rise and flooding on the Moroccan coast: the case of the Mediterranean eastern zone. *Estuarine, Coastal & Shelf Science* 77(2), 206-213.

Snoussi M., Ouchani T., Khouakhi A. and I. Niang-diop. 2009. Impacts of sea-level rise on the Moroccan coastal zone: quantifying coastal erosion and flooding in Tangier Bay. *Geomorphology* 107 (1-2): 32-40.

Soloviev S. 1990. Tsunamigenic zones in the Mediterranean sea, *Nat. Hazards* 3: 183–202.

Sousa Manuel de Faria. 1678. Europa portuguesa. 2nda edicion corretaprinted by A. Craesbeeck de Mello, 1678–1680, Biblioteca Nacional de Lisboa, Portugal (in Portuguese).

Tel E., Gonzalez M.J., Ruiz C. and M.J. Garcia. 2004. Sea level data archaeology: tsunamis and seiches and other phenomena. 4a Assembleia Luso Espanhola de Geodesia e Geofisica Figueirada Foz, Portugal.

Tinti S., Armigliato A., Pagnoni G. and F. Zaniboni. 2005. Scenarios of giant tsunamis of tectonic origin in the Mediterranean. *ISET Journal of Earthquake Technology* 42(4): 171-188.

Tous M. and R. Romero. 2011. Medicanes: cataloguing criteria and exploration of meteorological environments. *Tethys* 8: 53-61.

World Bank. 2011. North Africa Coastal Cities Address Natural Disasters and Climate Change. Washington, DC. http://hdl.handle.net/10986/18708 License: CC BY 3.0 IGO.

Yanes A. and V. Marzol. 2009. Los temporales marinos como episodios de riesgo en Tenerife a través de la prensa (1985-2003). *Rev. Soc. Geol. España 22* (1–2): 95–104.

Yelles-Chaouche A.K. 1991. Coastal Algerian earthquakes: a potential risk of tsunamis in western Mediterranean? Preliminary investigations. *Science Tsunami. Hazards* 9(1): 47–54.

Exceptionally high sea levels in the northern Adriatic Sea

Iva Međugorac and Miroslava Pasarić

ivamed@gfz.hr, mpasaric@gfz.hr

Department of Geophysics, Faculty of Science, University of Zagreb, Croatia

Abstract

This paper reviews exceptionally high sea levels recorded at the tide-gauge station Bakar (northeastern Adriatic) from 1929 to 2022. Events were analyzed considering five sea-level components, from regional seiches to multidecadal changes, as well as their synoptic backgrounds over the Mediterranean (mean sea-level pressure and 10-m wind). When approaching the end of the period studied, the intensity and frequency of extremes became stronger. Since 2018, there has not been a single year without an extreme event, and the six most intense events occurred in the last 15 years. The synoptic sea-level component was dominant in forming these extreme sea levels, while tide and planetary-scale variability played a secondary role. Slow sea-level processes played a lesser role than planetary-scale variability, with larger contributions at the period's end. The local sea-level component had the slightest effect on events, although its contribution on some occasions was notable. Atmospheric conditions causing a strong sea-level response at Bakar were characterized by a pressure gradient over the Adriatic and non-uniform southeasterly Sirocco wind with maximum speeds closer to the eastern coastline.

1. Introduction

Exceptionally high sea levels (EHSLs) in the northern Adriatic usually occur during late autumn and winter due to storm surges superimposed on other processes. They cause flooding and material damage to coastal cities, infrastructure, roads and interrupt ferry lines and land transport (see Fig. 1). Besides storm surges, sea-level processes contributing more to EHSLs are tides, planetary-scale variability, and pre-existing Adriatic-wide seiches (Šepić *et al*. 2022). Meteorological conditions that induce the Adriatic storm surges are driven by cyclones formed in the western Mediterranean traveling over the Adriatic, generating an air-pressure gradient and consequently Sirocco wind over it, both causing accumulated water in the Basin's closed end (Lionello *et al*. 2012; Međugorac *et al*. 2018). Usually, under such a situation, a Basin-wide seiche is triggered as the cyclone leaves the area, and Sirocco suddenly changes to Bora wind. These long-lasting oscillations have a period of around 22 hours and may, on occasions, considerably reinforce an upcoming storm surge (Šepić *et al*. 2022). The Adriatic tide is of mixed type. It mainly consists of three diurnal and four semidiurnal constituents (K1, O1, P1, K2, S2, M2, N2) and reaches its largest range in the northern shallow part of approximately 150 cm (Janeković & Kuzmić 2005). Planetary sea-level component is a process at temporal scales 10–100 d, controlled mainly by atmospheric planetary waves, i.e., actions of air pressure and the related wind at these frequencies (Pasarić *et al*. 2000). In addition, other processes may contribute to flooding events. These are local processes (e.g., local and regional seiches) and slow sea-level changes (e.g., seasonal cycle, (bi)decadal variability, long-term trend). The latter process is critical considering that the sea level in Bakar has been increasing markedly, rising 3.1 mm/year from 1984 to 2014 (Međugorac *et al.* 2021).

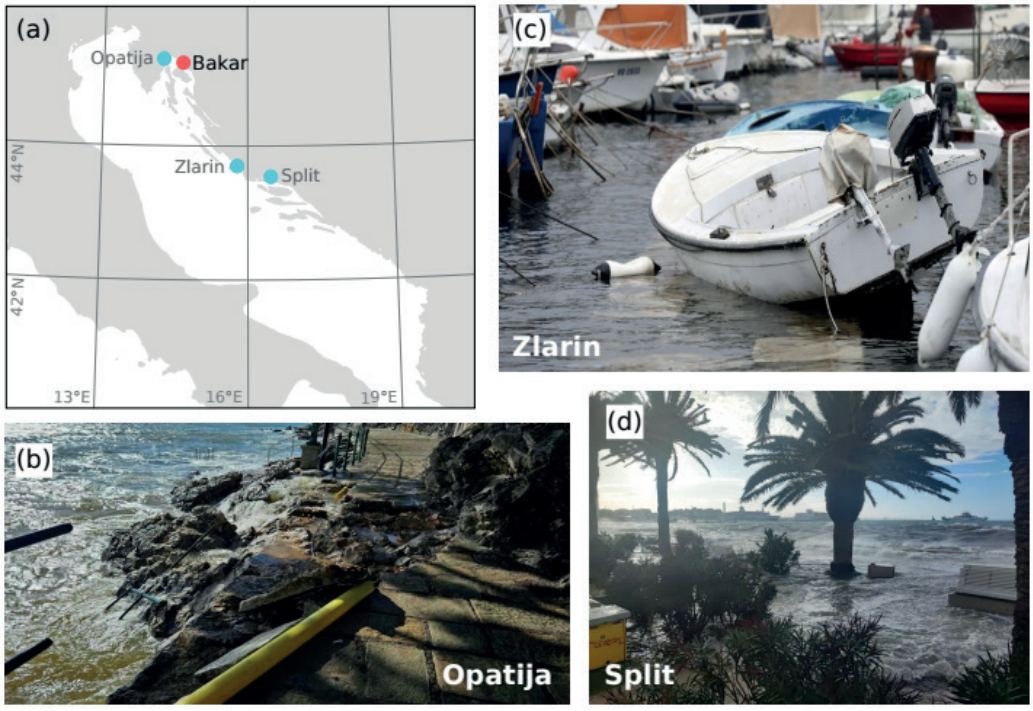

Figure 1. (a) Map of the Adriatic Sea. The red circle marks the position of the tide-gauge station Bakar, while other circles mark locations flooded during an extreme flooding event in November 2023 (shown in other subplots). (b) Damaged Lungomare sea promenade in Opatija. (c) Damaged boats in a harbor on the Island of Zlarin. (d) The city of Split during a flood in November 2023. [Pictures are taken from the Croatian online portal INDEXHR (www.index.hr).]

In the last 15 years, the eastern Adriatic coastline has been hit by severe flooding on several occasions (Međugorac *et al*. 2015; 2016; Bajo *et al*. 2019). These events have become even more frequent since 2017, culminating in October/ November 2023 with four subsequent episodes during 11 days (public reports on the official web page of the Department of Geophysics, University of Zagreb; https://www.pmf.unizg.hr/geof#).

This paper reviews and discusses EHSLs recorded at the oldest Croatian tide-gauge station Bakar (Međugorac *et al.* 2022), from 1929 to 2022. EHSLs were extracted from hourly sea levels and decomposed into five processes. Contributions of all involved processes to EHSLs were estimated and discussed. The average atmospheric background preceding the episodes was analyzed as these events resulted dominantly from storm surges.

2. Data and methods

The analysis is based on hourly sea levels measured at the tide-gauge station Bakar (Figure 1a; Međugorac *et al.* 2022; 2023) in the period 1929-2022, and on the ERA5 global reanalysis dataset (C3S 2017; Hersbach *et al.* 2020).

EHSLs were defined as occasions when sea levels exceeded the 99.99th percentile (90 cm for 1929–2022). On these occasions, flooding of a large part of the eastern Adriatic coastline

was noted and documented. Therefore, these events can be considered as floods. Consecutive hourly sea levels that surpassed a given threshold were merged into one event represented by the maximum sea level reached during that event. All values were recorded above the mean sea level in Bakar (73.8 cm) calculated over the 18.6 years centered around 1971.5 (1962–1980; HVRS71 National Geodetic System; Rožić 2009).

Total sea level was decomposed into five components: (i) local variability (T<10 h), (ii) tide, (iii) synoptic component (10 h<T<10 d), (iv) planetary-scale variability (10 d<T< 100 d) and (v) slow sea-level changes (T>100 d). The components were defined considering their drivers, spectral properties, and established methodologies (e.g., Šepić *et al.* 2022). First, the tide was calculated using harmonic analysis considering the seven major constituents with the most considerable impact on the Adriatic tide (MATLAB T_tide software; Pawlowicz *et al.* 2002). Then, using de-tided sea level, other components were estimated by applying Kaiser filters and going from longer to shorter scales. The presence of pre-existing basin-wide seiches (a process that, with storm surges, forms the synoptic sea-level component) was also estimated by visual inspection of residual sea-level series. This process was considered active during the flood if apparent oscillations (T around 22 h) were present in the basin up to three days before an event. Sea-level components defined in this way include the following processes. The local variability consists of oscillations of Kvarner Bay (T = 6 h), Rijeka Bay (T = 2h) and long ocean waves. The synoptic component consists of storm surges and the Adriatic-wide seiches. The planetary component is a sea-level response to atmospheric Rossby waves and other drivers on these temporal scales. Slow sea-level changes include seasonal cycle, interannual variability, (multi) decadal variability, and sea-level trend. The analysis carried out here assumes that the sea-level processes involved linearly interact in the Adriatic since their amplitudes are significantly smaller than the basin's depths over which they are formed (e.g., Marcos *et al*. 2009).

3. Results and discussion

Using the methodology just described, we extracted 27 EHSLs in the 1929–2022 interval. The temporal distribution of EHSLs is shown in Figure 2. Floods appear nonuniformly in time and more frequently at the end of the period studied: no less than twelve episodes occurred in the last 15 years. It should be noted that the station was not operational from 1939 to 1949 (Međugorac *et al*. 2022), and it is possible that EHSLs occurred in that period. From Figure 2, it is not clear whether the EHSLs intensity is getting stronger, but Table 1 shows that the six most decisive events occurred in the last 15 years. This intensification is in line with Šepić *et al*. (2022), who showed that the strengthening of positive sea-level extremes is significant at several Adriatic stations (Venice, Trieste, Rovinj, Bakar, Split, Dubrovnik) in the period 1956–2020.

The highest hourly sea level at the Bakar station was recorded on 1 November 2012 (Table 1) when sea level exceeded the mean by 113 cm. The list of the most intense events in Bakar differs from the one for station Venice (Lionello *et al*. 2021), due to the incoherent behavior of the northern Adriatic during intense storms. Međugorac *et al.* (2018) showed, comparing residual sea levels (1984–2014) at stations Venice and Bakar, that intense storm surges can have pronounced spatial structure, which is conditioned by bathymetry and spatial distribution of the wind field, which ultimately affects which coast will be exposed to stronger flooding.

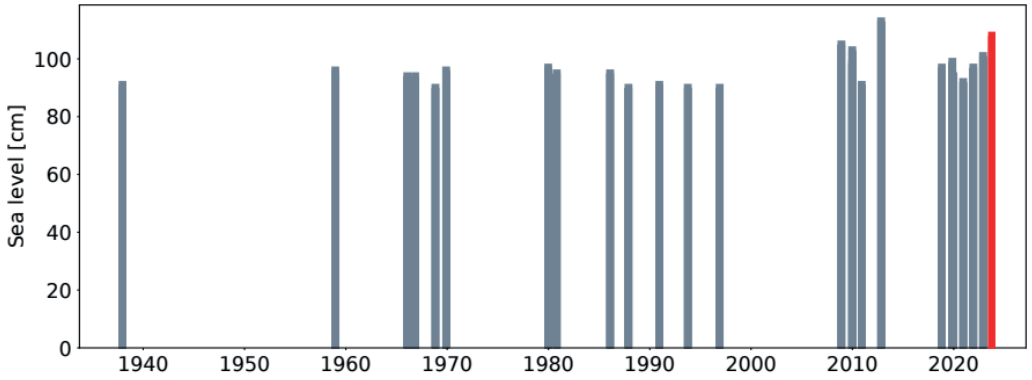

Figure 2. Temporal distribution of EHSLs at the station Bakar in the northern Adriatic. The bars represent sea heights above the long-term mean (Z0 = 73.8 cm). Grey bars are for events recorded in the period studied (1929-2022), while the red bar includes the latest four events observed in October/November 2023.

Table 1: The six most intense sea levels recorded at station Bakar (1929–2022): order according to intensity (1st column), date of the episode (2nd column), time of the maximum sea level (3rd column), highest sea level reached during the episode (4th column), presence of the Adriatic-wide oscillations prior to the event (5th column) and papers that studied the events (6th column).

Intensity	Date	Time (UTC)	Max sea level (cm)	Pre-existing seiche	Bibliography
1	1 November 2012	06	113	No	Međugorac *et al*. (2016)
2	1 December 2008	07	105	Yes	Lionello *et al*. (2021) Bajo *et al*. (2019) Međugorac *et al*. (2015) Bertotti *et al*. (2011)
3	25 December 2009	01	103	Yes	Bajo *et al.* (2019)
4	22 November 2022	06	101	No	
5	13 November 2019	06	99	No	Ferrarin *et al.* (2021) Lionello *et al*. (2021) Cavaleri *et al.* (2020)
6	23 December 2009	02	98	Yes	

The seasonal distribution of EHSLs is shown in Figure 3 below: these episodes occur mainly in the cold part of the year, with a maximum in December, while none of the high sea levels were recorded in Spring or Summer. This seasonality is due to the frequent passage of Mediterranean cyclones over the northern Adriatic in late Autumn and Winter (Trigo and Davies 2002; Lionello *et al*. 2012).

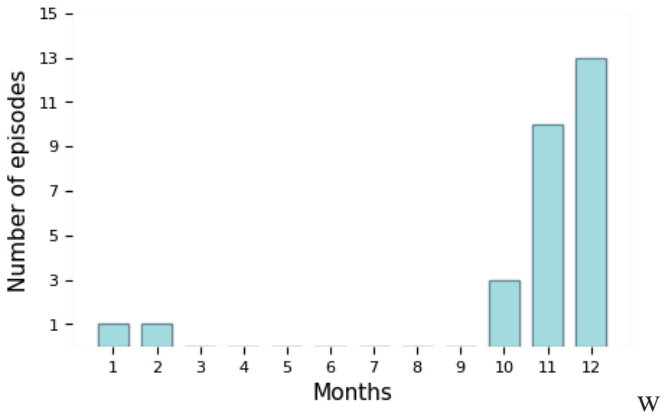

Figure 3. Seasonal distribution of 27 EHSLs extracted from hourly sea levels at station Bakar (1929–2022).

The decomposition of the EHSLs into tidal and residual (de-tided) sea levels is shown in Figure 4, where the tide mostly plays a positive role in forming the northern Adriatic maxima, as there were only three occasions (4 November 1966, 29 October 2018, and 8 December 2020) when it was in a negative phase during a flooding event. However, this negative effect was compensated by the stronger resultant of other processes: clearly the three strongest residuals were precisely those on these three occasions. The 1966 and 2018 episodes would have had a far worse impact if the atmospheric fronts had passed several hours earlier, during the peaks of the tidal signal (Figure 5).

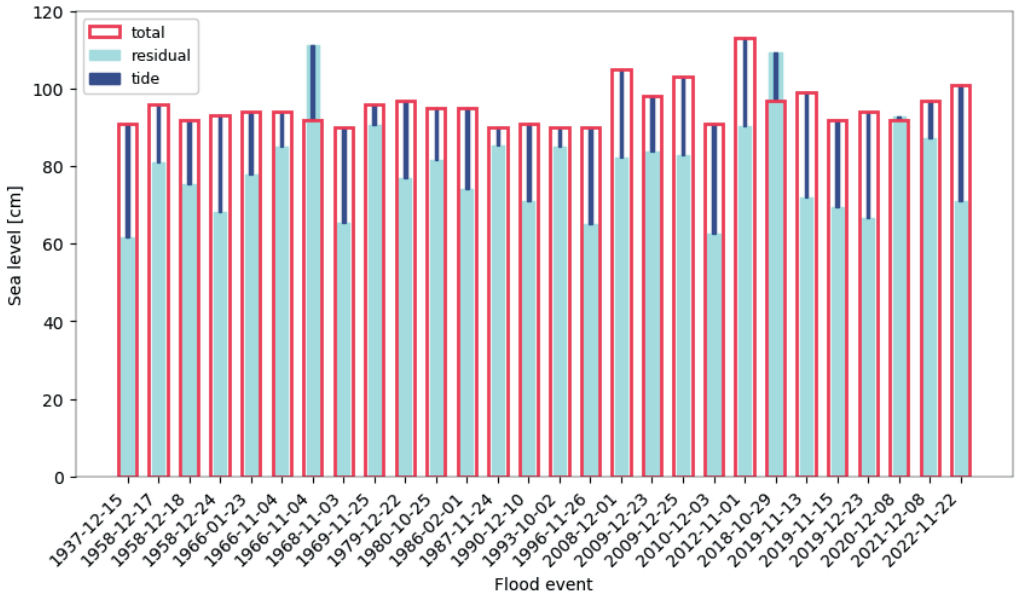

Figure 4. Maximum sea levels recorded during EHSLs decomposed into tidal (dark blue) and residual (turquoise) components.

The contributions of the five components are illustrated in Figure 5. Since extreme sea-level phenomena are formed as a positive superposition of all the involved processes, all components

are expected to be positive during most extracted events. Generally, local sea-level changes contribute the least to the observed EHSLs, while synoptic processes are, in most cases, the dominant contributor (Figure 5). Local processes were usually in the positive phase during the EHSLs; their contribution was between -2.35 cm and 20.29 cm and was generally limited (on average 5.48 cm). A maximum of 20.29 cm was reached during the 1993 episode when the high-amplitude Kvarner Bay seiche was triggered before the episode and was active during the event. Tidal oscillations played a considerable part in EHSL formation. They contributed, on average, 15.80 cm, between -19.29 cm (the 1966 event) and 29.97 cm (the 2022 event).

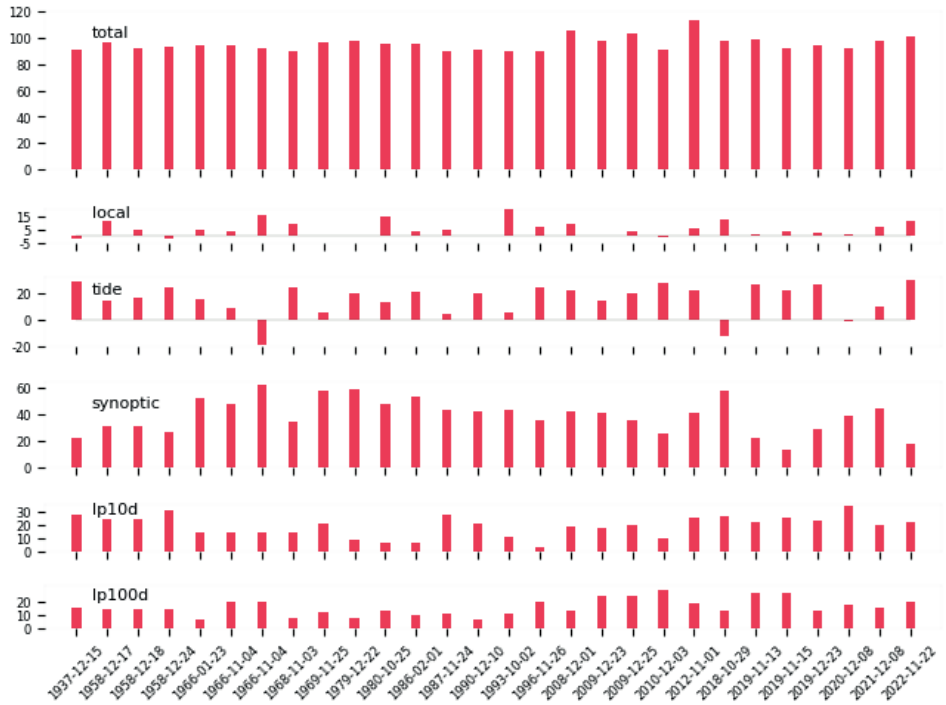

Figure 5. EHSLs recorded at station Bakar (top panel) decomposed into five processes: local variability (T<10 h), tide, synoptic component (storm surge and the Adriatic-wide seiche), planetary component (10 d<T<100 d) and slow sea-level changes (T>100 d).

Synoptic processes - the combined effect of storm surges and pre-existing seiche - frequently had the dominant role. They contributed on average 39.26 cm, ranging between 13.28 cm and 62.31 cm. However, there were two occasions, on 15 November 2019 and 22 November 2022, when these processes were extremely low. These floods formed due to the tide maxima (during the syzygy) and significant contributions of planetary and slow sea-level processes. This indicates that, while storm surges dominate in forming extreme sea levels, other processes can play an important and sometimes decisive role. The planetary component was positive during all extreme events. It contributed to EHSLs on average with 18.80 cm, ranging between 3.34 cm and 34.43 cm, and its influence on late events was mostly high. A similar behavior is noted in slow sea-level changes, i.e., their impact is more substantial as we approach the end of the period studied. However, they contributed with somewhat smaller amounts - on average with 15.91 cm, ranging between 6.59 and 28.53 cm.

As extreme sea levels were predominantly induced by the synoptic component (i.e., processes on time scales 10 h – 10 d), it is plausible to analyse their atmospheric forcing from the mean atmospheric fields. Composite fields of mean sea-level pressure (mslp) and 10-m wind preceding the episodes are shown in Figure 6. The atmospheric situation that favors flooding of the eastern Adriatic coastline is characterized by an air-pressure depression (~995 hPa) located west of the Adriatic, accompanied by westerly winds over the western Mediterranean and southerly winds over the central Mediterranean. This meteorological setup causes an air-pressure gradient over the Adriatic, laid along the basin's main axis with values over the northern sector ~15 hPa lower than over the southern sector, and southeasterly wind Sirocco. In these situations the Sirocco exhibits a nonuniform structure: along the western coastline and over the southern Adriatic, it has south/southeasterly directions, while it becomes more southeasterly along the northeastern Adriatic. Maximum wind speeds are reached closer to the eastern shore (~16 m/s). The described atmospheric situation favors water accumulation mostly along the northeastern Adriatic coastline.

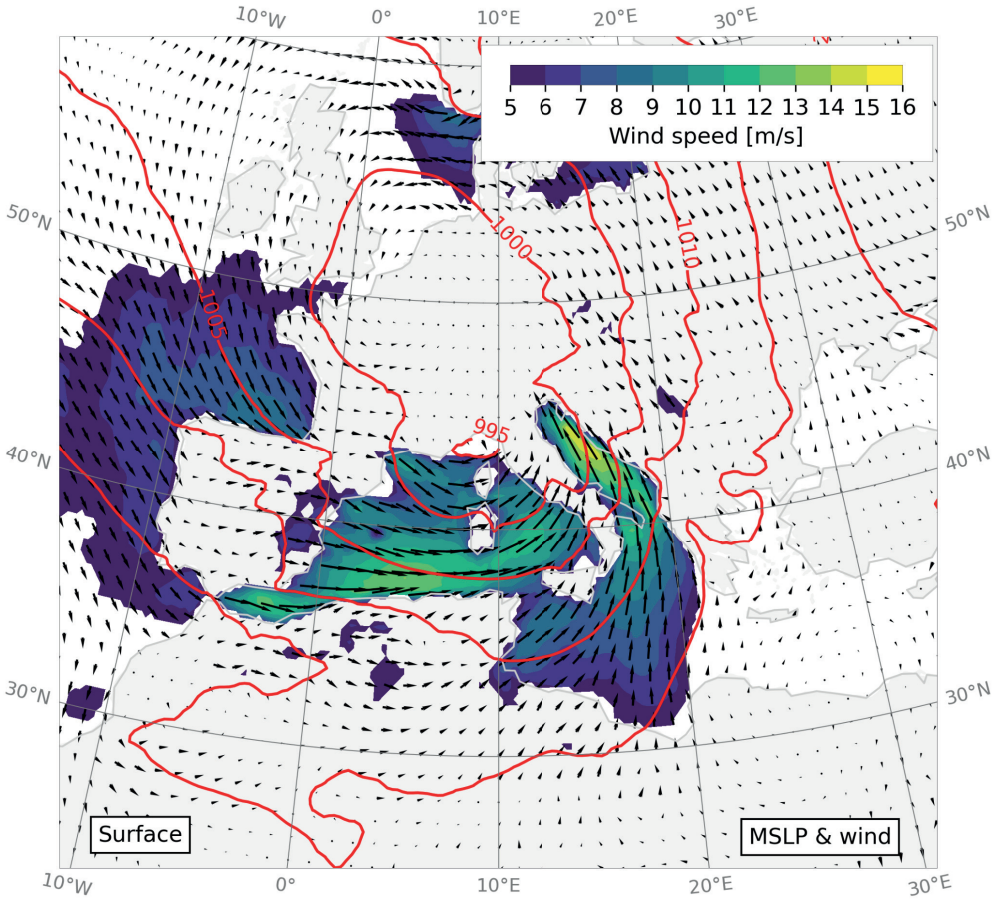

Figure 6. Meteorological background of EHSLs: average fields of mslp and 10-m wind over the Mediterranean and Europe calculated from fields preceding each flooding event (3 h prior to an event). EHSLs were considered only after 1940 since ERA5 data were unavailable for older cases.

The effects of Adriatic storms and accompanying processes (high sea levels, heavy precipitation, strong wind) on Croatian cities are illustrated in Figure 7. During stormy events, drinking water sources may be contaminated due to heavy rain, as was the case in 2009 in the Rijeka area: authorities recommended boiling the water because of the contamination of springs (Figure 7a).

The low-laying parts of some Adriatic cities get flooded frequently during extreme sea-level episodes, e.g., the Rijeka market (Figure 7b). Ferry lines between the mainland and many Croatian islands usually get interrupted due to strong wind and rough sea - Figure 7d reports on Sirocco speeds of 100 km/h during the 1987 event, due to which ferry lines from Split were first rerouted and then suspended. In the absence of a systematic solution to the problems related to flooding, citizens manage themselves and find ways to protect their properties - an example is a cafe on the Island of Cres, whose owners responded to a series of floods with a wall made of sandbags (Figure 7c).

Figure 7. (a) Pages from the newspaper *Novi list* after the flood on 23 December 2009. (b) Pages from the newspaper *Jutarnji list* after the flood on 1 December 2008. (c) Photo taken in Cres (Island of Cres) in December 2023 after a series of floods in October/November 2023. (d) Pages from the newspaper *Slobodna Dalmacija* after the flood on 24 November 1987.

4. Conclusions

Upon analysis the 27 episodes of EHSLs extracted between 1929 and 2022 from hourly sea levels recorded at the tide-gauge station Bakar show a non-uniform frequency and intensity, becoming higher in the past 15 years. The synoptic sea-level component was found to be dominant in forming these extreme sea levels, while tide and planetary-scale variability played a secondary role. While this conclusion holds generally true, each episode is a unique outcome of the interplay between all the involved processes, which may result in a different combination of contributors. Analysis of the synoptic situation showed that storm surges in the northeastern Adriatic were induced by the air-pressure gradient (the difference between northern and southern Adriatic being usually ~15 hPa) and nonuniform Sirocco wind with maximum speed closer to the eastern shore.

Acknowledgments

Many thanks to the personnel of the Department of Geophysics, Faculty of Science, University of Zagreb, for their maintenance of the Bakar tide-gauge station and instruments and continuous digitization and quality check of sea-level data. This research has been supported by the Croatian Science Foundation project StVar-Adri (IP-2019-04-5875).

To be cited as:

I. Međugorac and M.Pasarić. 2024. Exceptionally high sea levels in the northern Adriatic Sea. p 155- 166. In CIESM Monograph 52 [F. Briand, Ed.] Marine hazards, coastal vulnerability, risk (mis)perceptions – a Mediterranean perspective. CIESM Publisher, Paris, Monaco, 182 p.

References

Bajo M., Međugorac I., Umgiesser G. and M. Orlić. 2019. Storm surge and seiche modelling in the Adriatic Sea and the impact of data assimilation. *Quarterly Journal of the Royal Meteorological Society* 145: 2070–2084. https://doi.org/10.1002/qj.3544

Bertotti L., Bidlot J.R., Buizza R., Cavaleri L. and M. Janousek. 2011. Deterministic and ensemble-based prediction of Adriatic Sea sirocco storms leading to 'acqua alta' in Venice. *Quarterly Journal of the Royal Meteorological Society* 137:1446–1466. https://doi.org/10.1002/qj.861

Cavaleri L., Bajo M., Barbariol F., Bastianini M., Benetazzo A., Bertotti L., Chiggiato J., Ferrarin C., Umgiesser G.and F. Trincardi. 2020. The 2019 flooding of Venice and its implications for future predictions. *Oceanography* 33: 42–49. https://doi.org/10.5670/oceanog.2020.105

Copernicus Climate Change Service [dataset]. 2017. ERA5: Fifth generation of ECMWF atmospheric reanalyses of the global climate. *Copernicus Climate Change Service Climate Data Store (CDS)*, date of access: 30 October 2023. https://cds.climate.copernicus.eu/cdsapp#!/home

Ferrarin C., Bajo M., Benetazzo A., Cavaleri L., Chiggiato J., Davison S., Davolio S., Lionello P., Orlić M.and G. Umgiesser. 2021. Local and large-scale controls of the exceptional Venice floods of November 2019. *Progress in Oceanography* 197, 102628, https://doi.org/10.1016/j.pocean.2021.102628

Hersbach H., Bell B., Berrisford P. *et al*. 2020. The ERA5 global reanalysis. *Quarterly Journal of the Royal Meteorological Society* 146: 1999– 2049. https://doi.org/10.1002/qj.3803

Janeković I. and M. Kuzmić. 2005. Numerical simulation of the Adriatic Sea principal tidal constituents. *Annales Geophysicae* 23: 3207–3218. https://doi.org/10.5194/angeo-23-3207-2005

Lionello P., Barriopedro D., Ferrarin C., Nicholls R.J., Orlić M., Raicich F., Reale M., Umgiesser G., Vousdoukas M. and D. Zanchettin. 2021. Extreme floods of Venice: characteristics, dynamics, past and future evolution (review article). *Natural Hazards and Earth System Sciences* 21: 2705–2731. https://doi.org/10.5194/nhess-21-2705-2021

Lionello P., Cavaleri L., Nissen K.M., Pino C., Raicich F. and U. Ulbrich. 2012. Severe marine storms in the Northern Adriatic: Characteristics and trends. *Physics and Chemistry of the Earth, Parts A/B/C*, 40–41: 93–105. https://doi.org/10.1016/j.pce.2010.10.002

Marcos M., Tsimplis M.N.and A.G.P. Shaw. 2009. Sea level extremes in southern Europe. *Journal of Geophysical Research* 114, C01007. http://dx.doi.org/10.1029/2008JC004912.

Međugorac I., Pasarić M. and M. Orlić. 2015. Severe flooding along the eastern Adriatic coast: the case of 1 December 2008. *Ocean Dynamics* 65: 817–830. https://doi.org/10.1007/s10236-015-0835-9

Međugorac I., Pasarić M., Pasarić Z.and M. Orlić. 2016. Two recent storm-surge episodes in the Adriatic. *International Journal of Safety and Security Engineering* 6: 589–596. https://doi.org/10.2495/SAFE-V6-N3-589-596

Međugorac I., Orlić M., Janeković I., Pasarić Z.and M. Pasarić. 2018. Adriatic storm surges and related cross-basin sea-level slope. *Journal of Marine Systems* 181: 79–90. https://doi.org/10.1016/j.jmarsys.2018.02.005

Međugorac I., Pasarić M. and I. Guttler. 2021. Will the wind associated with the Adriatic storm surges change in future climate?. *Theoretical and Applied Climatology* 143(1-2): 1-18. https://doi.org/10.1007/s00704-020-03379-x

Međugorac I., Pasarić M. and M. Orlić. 2022. Long-term measurements at Bakar tide-gauge station (east Adriatic). *Geofizika* 39 (1): 1-16. https://doi.org/10.15233/gfz.2022.39.8

Međugorac I., Pasarić M. and M. Orlić [dataset]. 2023. Historical sea-level measurements at Bakar (east Adriatic). *SEANOE*. https://doi.org/10.17882/85171

Pasarić M., Pasarić Z. and M. Orlić. 2000. Response of the Adriatic sea level to the air pressure and wind forcing at low frequencies (0.01 – 0.1 cpd). *Journal of Geophysical Research* 105: 11423–11439. https://doi.org/10.1029/2000JC900023

Pawlowicz R., Beardsley B. and S. Lentz. 2002. Classical tidal harmonic analysis including error estimates in MATLAB using T_TIDE. *Computers & Geosciences* 28: 929–937. https://doi.org/10.1016/S0098-3004(02)00013-4

Rožić N. 2009. Hrvatski transformacijski model visina, Geodetski fakultet, Sveučilište u Zagrebu (in Croatian).

Šepić J., Pasarić M., Međugorac I., Vilibić I., Karlović M. and M. Mlinar. 2022. Climatology and process-oriented analysis of the Adriatic sea level extremes. *Progress in Oceanography* 209: 102908. https://doi.org/10.1016/j.pocean.2022.102908

Trigo I.F. and T.D. Davies. 2002. Meteorological conditions associated with sea surges in Venice: a 40 year climatology. *International Journal of Climatology* 22, 787–803. https://doi.org/10.1002/joc.719

Psychosocial factors around coastal risk management

Raquel Bertoldo

Université Aix-Marseille, Laboratoire de Psychologie Sociale, France

Abstract

Coastlines are under the pressing stress posed by human occupation and climate changes. The risks presented by these evolving coastal systems are highly dependent on how coastal communities perceive them. This chapter reviews the variables that influence and modulate risk perception: place attachment, trust, risk normalisation, and social representations. However comparable in their overall dynamics, local knowledge about coastal risks and how to mitigate them are highly *contextual*: they depend on past experiences of a risk, national and regional policies for risk mitigation and climate change adaptation.

Keywords: *coastal risks, risk perception, trust, place attachment, social representations.*

Introduction

Female named hurricanes are deadlier than male named hurricanes (Jung *et al.* 2014). Even though male and female names have been alternatively attributed to hurricanes since the 1970s in the USA, gender-based expectations linked to the name of the hurricane significantly influence catastrophe preparedness, and therefore, human lives. Gender based expectations integrate a wider array of social biases in risk perception, understanding and protection that motivated the development of a field of studies: risk perception (Joffe 2003). This approach to risk management concerns a wide range of industrial and natural risks, including the perception of risks related to the coast.

Climate change already drives an increase in coastal storms' frequency and their power. In this sense climate change adaptation efforts must be particularly attentive to build coastal adaptation and resilience in the face of stronger storms, coastal floods, and sea level rise (Poumadère *et al.* 2015). Communities dwelling in Mediterranean regions have been familiar with coastal floods for generations, a knowledge that is shared as part of a local social memory. Climate change does however expose the limits of a local knowledge that becomes less suitable to a changing environment.

Past natural risk experiences have been previously described as contributing to improve present risk preparedness (Demski *et al.* 2017). Yet the constant exposure to threatening environmental elements has also been described as leading to natural risk 'normalization' (Luís *et al.* 2016) – a process that helps individuals build and maintain positive emotional bounds to their local environments (Bonaiuto *et al.* 2016; Krien & Michel-Guillou 2014).

These past studies show how the past risk experiences of coastal communities might either support or hamper situated risk response.

In this chapter I will analyse the paradox faced by coastal inhabitants (Meur-Ferec and Guillou 2020): the desire to stay close to the coastline despite the growing danger they present. I will do so by reviewing some of the key concepts that can support the understanding of these human-environment dynamics: risk perception, trust, place attachment and risk normalisation.

Finally, I will describe how cultural processes (i.e. social representations) are capable of conveying meaning to these biases, therefore contributing to preserving and reproducing them through generations.

Perceiving coastal risks

Risks can be characterized as the probability of a particular adverse event occurring during a particular period (Breakwell, 2014). Modern societies have grown profoundly organized around the definition, prediction, and control of potentially harmful natural risks. The risks that are manageable by science and governance contain an *epistemological* dimension – i.e. once hazards are known, a great deal of uncertainty still exists in relation to when, where, or how intensely they will hit (Rosa 2003).

It is precisely because this epistemological dimension is paramount to understanding how populations react to risks that social psychologists have become interested in the analysis of the variables explaining risk perception by the lay public. If the public does not understand the science behind the risks they face, then what explains how it perceives risks? The psychometric approach developed by Slovic (1987, 2000) proposes a response to this question by considering – other than scientific information – judgements about self-control (how risk exposure is under the individuals' control), timescale of consequences (immediate or cumulative), how well known is the risk (risks known to science vs. unknown to science). Slovic (1987) demonstrated that the perception of a wide range of natural or technological risks could be organised along two main dimensions: one that describes risk *dreadfulness*, or their catastrophic potential (e.g. nuclear weapons vs. caffeine); and another one that describes how *known* the risk is (e.g. genetic therapy vs. handguns).

The question of how 'natural' and 'human-made' risks are perceived – even if this distinction can be questioned – was addressed by an international comparison that underlines the importance of contextual factors (Bodas *et al.* 2022). With a sample of over 4,000 respondents distributed across Italy, Romania, Spain, France, Sweden, Norway, Israel and Japan, the study illustrates a general trend to perceive natural hazards (catastrophes and extreme weather) as *less risky* in relation to pandemics, critical infrastructure failure (e.g. water and energy) and social disruptions (e.g. war). The exception to this trend is Japan, where critical infrastructure failure is regarded as equally risky as natural hazards – yet less risky than extreme weather.

Even if this international study was carried out during the COVID pandemic, its findings are consistent with IPSOS longitudinal track of the key issues concerning the British public (Fig. 1). This analysis situates environmental issues (including climate change) as continuously behind other concerns regarded as 'closer' to the individuals: the state of the economy, inflation, immigration, health issues, and only then the environment. The only time environmental issues surpassed other individual concerns was just after the summer where mega forest fires were observed worldwide (Woodyatt 2021).

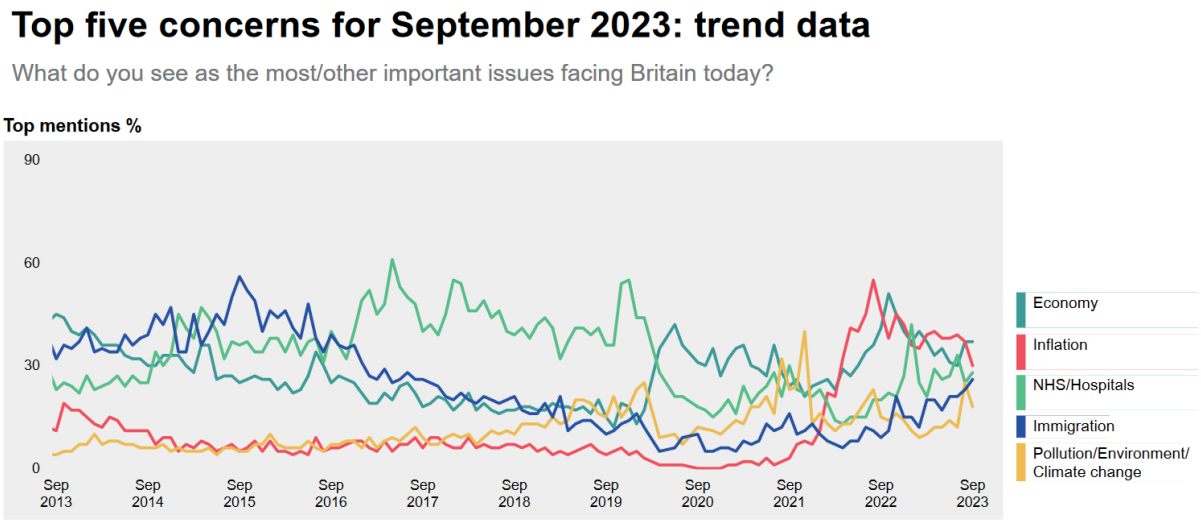

Figure 1. Longitudinal representation of the most important issues for the British population

The longitudinal of social issues by IPSOS MORI (Fig.1) is important to situate perceived risks in their *zeitgeist*, their spirit of time. The analysis of human induced risk perception carried out by Bodas *et al*. (2022) describes more stable and culture-dependent trends in risk perception. Religion for instance has been associated with higher perceived risks (except in Israel, where it is negatively associated with risk perception). Generational differences have also been identified: Millennials view the risk posed by natural hazards and extreme weather more seriously than Generation Z and boomers.

In brief, the international published record shows that natural hazards are in general seen as less risky in comparison to individual, immediate risks. Given the importance of risk perception as a key indicator of risk preparedness, which other variables explain the when and how of public preparedness to coastal risks? Considering that coastal risks are manageable to a lesser extent through individual actions, and rely more directly on local and regional decisions made by representatives, trust in government is a key moderating variable of coastal risk perception.

Trust and coastal risk perception

Despite divergent understandings about trust and why is trusting important, scholars from different disciplines agree that "trust is a psychological state comprising the intention to *accept vulnerability* based upon positive expectations of the intentions or behaviours of another" (Rousseau *et al.* 1998, p. 395, italics added). In other words, people must first be aware that they are exposed to a hazard and that they cannot manage it on their own, to trust – otherwise they would not need to delegate the management of this risk to someone else.

Communities rarely approach environmental risks rationally (Wynne 1992). Relational aspects come strongly into play as communities trust local authorities with their safety. The fact that local authorities are (1) knowledgeable of these risks and (2) have the ability to cope with it are also part of how a community feels more or less exposed to a risk (Engdahl & Lidskog 2014).

This two-level approach can be illustrated by a comparative study between France and the Caribbean (Lemée *et al.* 2018). This study found that coastal risks perception is informed by (1) risk knowledge; (2) risk augmentation – i.e. the impression that coastal risks will get worse in time; (3) risk dreadfulness – or the perception that it is dangerous; and (4) collective vulnerability – or the degree to which a coastal community is prepared (or not) to deal with it. This last dimension taps into how an individual accepts that (i) a coastal risk exists and (ii) that his/her community is capable of dealing with it. It is precisely this latter dimension that was the strongest predictor of coastal risk perception.

A recent Portuguese study endeavoured to understand how different coastal communities perceive coastal risks, and also what type of risk management they would prefer for the coast (Areia *et al.* 2023). Through a sample of 3028 participants (320 of whom were interviewed as well) from all over the country, results show that citizens prioritize "the intrinsic value of coastal systems when favouring a risk adaptation strategy". In other words, coastal communities prefer ecosystem-based adaptation measures rather than hard defences. But also, because high levels of distrust were identified, participatory actions for coastal risk management are preferred in relation to top-down, techno-scientific decisions.

Community relocation is another issue in coastal risk management where trust in authorities will play a key role. Past studies analysing this issue indicate that retreating is only a last resort solution (Poumadère *et al.* 2008; Tol *et al.* 2006), a finding that is also confirmed by Areia *et al*. (2023). Because trust conditions how the public will follow the instructions from authorities – particularly in relation to indirectly experienced threats such as the coast – we may already anticipate important issues arising from a situation where relocation plans are necessary and imposed instead of an option.

But more than an individual level variable, trust is part of how a culture conceives of power relations and private-public decisions, or control over the risk situation. As part of an international comparison between seismic regions with radically different cultural understandings of seismic risk (Japan, Turkey, USA) Joffe *et al*. (2013) found that the uptake of seismic preventive behaviours in the household is higher in the US, where individual-level agency is promoted (e.g. private insurance and house retrofitting). Turkey is where this study found protective behaviours are less frequent, and emotions related to stress and control over an earthquake the most extreme due to "an *untrustworthy* government and corrupt construction industry" (p. 390, italics added). This view that authorities are untrustworthy increases fatalism – the feeling that nothing the individual can do will change the situation – and reduces the probability that individuals take action to reduce their risk exposure (Joffe *et al.* 2013).

If trust in authorities constitutes an important part of how individuals assume responsibility for risks presented by their households – as is the case with earthquakes – this is even more the case in relation to coastal risks, where it is the coast at large that presents threats to the communities.

Place attachment and the coast: the perception-action paradox

A variety of studies engaged in coastal risk perception, worry and risk mitigation behaviours on the Atlantic (Michel-Guillou *et al.* 2015; Michel-Guillou and Meur-Ferec 2017) and Mediterranean (Durand *et al.* 2018) French coasts have shown that while local inhabitants *are aware* about their exposure to coastal flooding, they are *not worried* or ready to present mitigation behaviours (Meur-Ferec and Guillou 2020; Michel-Guillou *et al.* 2015, 2016).) This apparent carelessness of coastal communities can be described from a strictly informational, cognitivist perspective as a "poor risk culture" (Durand *et al.* 2018. p. 10). Other studies have framed the issue as based on logical 'paradoxes' that take their meaning from contextually situated practices, which justify the use of constructivist approaches such as the social representations theory.

Based on a series of studies in risk-prone coastal French communities, Meur-Ferec and Guillou (2020) describe local coastal response as paradoxical: (a) local people are aware of risks but are not worried; (b) local people are aware of risks and are still attached to their location; and (c) local people are willing to act but resist adaptation strategies. Points (a) and (b) are based on the common observation that coastal communities are aware of coastal risks (Doue *et al*. 2020; Michel-Guillou *et al.* 2015; Michel-Guillou and Meur-Ferec 2017); yet, because of a strong attachment to socially valued real state by the sea, these threats are downplayed (Bonaiuto *et al.* 2016; Michel-Guillou *et al.* 2016). The last-mentioned paradox (c) underlines another real threat posed by local authorities when applying their coastal risk management plans, namely to limit real estate development or even enforce evictions. The economic value of coastal properties means that owners will inevitably lose money if they accept coastal risk mitigation measures: the loss in value of their property when risks are acknowledged, or the possibility of an eviction and property loss.

Risk normalisation

The risk perception paradox described by Meur-Ferec and Guillou (2020) can also be seen as a risk normalisation effect: the fact that when individuals are exposed to a risk which they cannot control, they will normalise it as part of a coping strategy. This assumption, already demonstrated by Lima (2004) and Lima *et al.* (2005) in the context of industrial risks was tested by Luís *et al.* (2016) in the context of coastal risks.

More precisely, Luís *et al*. (2016) explored the assumption that because coastal populations are more informed, they will present a greater deal of protective behaviour – intending to leave in case of alert, building protections against a second flood. Results are counter-intuitive, showing that the relation between coastal risk awareness and coastal risk perception is actually *negative*. In other words, the more individuals are informed about coastal risks, the less risks they perceive. This relationship was described as even stronger for risks with a higher probability of occurrence for a specific location. This effect is explained as a coping mechanism through which individuals rationalise the risks they face through a stronger reliance on already existing safety and emergency preparedness dispositions.

The particularity of natural risks in relation to other individual risks or industrial risks is that vulnerability depends a great deal on geographical and on risk management choices (Poumadère *et al.* 2015). This is one of the reasons why it is so difficult to predict actual risk exposure and vulnerability based solely on individual-level information about risk perception, knowledge, and behaviour. Therefore, more complex approaches that are equipped to deal with the local collective response to political choices are needed to understand people-place dynamics around coastal risk management.

Social representations and coastal risk perception

Attempts to make the public aware of a risk are common in risk management policy (Renn 2008). This vision of environment and risks departs from a 'deficit model' where the public is regarded as naïve in the face of an environment that holds secrets only decipherable by specialists (Wynne, 1992). Traditional communities have learned over generations local adaptation strategies and have built practical knowledge embedded in meanings and tradition. These locally embedded knowledge are very different from the scientific exercise: they organise and convey meaning to contextualised social practices (e.g. Wagner *et al.* 1999).
The social representations approach is interested in describing how new knowledge emanating mainly (but not exclusively) from scientific spheres is appropriated across different social groups and integrates shared social knowledge (Moscovici 1961, 2001). This diffusion process involves sharing new information and new meanings (Joffe 2003): lay people then resort to metaphors and images to translate these yet novel ideas into familiar ones (Wagner and Hayes 2005).

The importance of insisting on 'social knowledge' as meaning rather than information is particularly important when such knowledge concerns risks. The concept of 'risk perception' presented above and often used in risk literature refers to the individual processing of cognitive, sensorial input. "While perception is based upon sensorial knowledge, representation is concerned with symbols, social reality and social knowledge" (Joffe 2003, p. 60). Because environmental events involve different sorts of sensorial information, we consider here risk representation as an overarching shared knowledge structure that conveys risk perception in its meaning, which might under different circumstances be exaggerated or made completely invisible.

The shared meanings associated with coastal risks are *inevitably* local. They depend on shared memories and social constructions that are specific to a place and time. The research I will present below follows a storm (Xynthia) that, for its strength and consequences, pushed the French government to elaborate a national frame for the development of local coastal management plans (PPRI). This storm was paramount for coastal management in the region because if reminded the national Authorities of the increasing strength that these events will have in the future, and the need to prepare the coast for them.

The PPRI is a public document that depicts a variety of risks, including coastal floods. While local inhabitants have access to this type of information, it is their *experience* with floods that remains the strongest predictor of how seriously they will prepare for future risks (Demski *et al.* 2017). While research shows that risk experience does increase awareness and preparedness namely through more effective coping strategies, other studies show that long continuous risk exposure might also contribute to risk 'normalization' (Luís *et al.* 2016), where local inhabitants become accustomed to the idea that they are exposed but also convinced they can cope. This latter point where a risk becomes progressively invisible and underwhelming has been described as 'social attenuation of risk' (Burgess 2012; Kasperson *et al.* 1988).

Consequently Bertoldo *et al*. (2021) have adopted a constructivist approach to understand the risk practices of local communities from their own perspective, and which are the elements from their environment that they regard as risky or not. This duality between (1) the risks that are represented - thus seen and managed - and (2) the risks that may exist for scientists but that are not echoed yet by the experience of local communities reveals an inconsistency between risks that are represented (Moscovici 2001) and others that only exist as a possibility but are not yet based on shared experience. The latter risks are still invisible, therefore attenuated (Pidgeon *et al.* 2003).

This qualitative study explored through interviews the paradoxical relationship that coastal communities have with coastal risks: despite their knowledge of coastal risks, inhabitants are not drawn to risk mitigation behaviours (Meur-Ferec and Guillou 2020). The two localities in the south of France chosen for this study have a different connection to the coast: Port-Saint-Louis-du-Rhône (PSLR), a small town, isolated at the entrance of the Camargue delta; and Fréjus, a mid-sized city on the French Riviera with a booming real estate market for new retirees (Bertoldo *et al*. 2021). How do coastal cities like Fréjus and PSLR, constantly exposed to the risk of marine submersion, construct meaning in the face of this risk?

The contents of the interviews carried out with 40 people (21 in Fréjus and 20 in PSLR) were entirely transcribed and analysed (Bertoldo *et al*. 2021). They illustrate how local people react to coastal risks largely based on psychosocial comparative processes allowing local communities to cope with a potential threat. The four meta-categories identified in this study are described in the Table below.

Table 1. Coastal risk perception by the local population of two coastal towns in southern France.

Meta-category	Categories	Sample discourse
1. Knowledge of coastal flood risk exposure	Climate change, risk entanglement, dikes, erosion, vulnerability, soil tightness, information, floods, prevention, humidity, industrial risk, scientific knowledge, storm, marine submersion.	In fact, here when it's flooded, it's pretty strange there have to be two things mixed together. There must be floods from the Rhone, and at the same time, there must be the storm of the sea wind which prevents the Rhone from flowing.
2. Emotional ties to the coast	Animism, place attachment, shed (cabanon), destruction of nature, social ties, nostalgia, observing nature, biophilia.	In fact, I often have fun saying,"I know the waves by their first name" but we're negotiating. […] Our boats are not so strong that they would pass anyway, we must negotiate with the waves. But this can be learned.
3. Argumentative strategies contributing to risk attenuation	Categorical differentiation, risk differentiation, fatalism.	I wouldn't go live in Bangladesh! But the region here, that's not something that hangs in my face, if I may say so. That's not the problem.
4. Role of past risk events in risk amplification	Community history, lack of risk experience, environmental memory, role of disasters.	What can happen is something similar to what we experienced in 2010, where [the flood] took everything in its path. There were gas canisters in the middle of the bay of Saint Aygulf. 27 dead, I believe, there were in the county. It's huge.

Knowledge of coastal flood risk exposure. Local inhabitants show a greater concern and knowledge about the river in relation to coastal flooding. In the absence of risk events related to coastal floods, the French collective memory about river flooding is mentioned. These two risks correspond however to distinct categories in the local flood risk prevention plan (PPRI). Participants also made extensive use of expert concepts when referring to the coastline, seawalls, and hydrodynamics typical of the region.

Emotional ties to the coast. Coastal communities share a specific relationship with their territory, marked by maritime culture and the strong attraction of the seaside in recent decades. More precisely, the inhabitants of PSLR are geographically isolated and surrounded by salt marshes, which is associated with an island identity with activities often linked to the environment. The 'shed' (cabanon) is described here as a bridge between the social space of the community and the natural space- an environment presented as part of themselves. The risk associated with coastal flooding that hits the coast each winter is therefore described as an inherent part of nature, a nature that participants/ citizens respect and feel well adapted to. The inhabitants of

Fréjus praise the beauties of their coast, which motivated many of them to settle there. Yet, due to the absence of a major coastal flooding event in both PSLR and Fréjus, they are hesitant to articulate how they might be affected by coastal flooding during their lifetime.

Argumentative strategies contributing to risk mitigation. Individuals compensate for this inconsistency with rationalizations (Breakwell 2014) which allow residents to continue to enjoy the pleasures of life by the sea. These rationalizations have been identified in the form of argumentative strategies: social comparison, comparison of risks and fatalism. These strategies allow individuals to put the risk into perspective and then justify both individual and collective apathy when facing the absence of protective actions. Together, such argumentative strategies contribute to social mitigation (Kasperson *et al.* 2003).

Social role of disasters. This collective effort to mitigate the risk of coastal flooding would end, according to the participants' analysis, the day 'something' happens. According to them, the absence of social memory on coastal risks contributes to political inertia and, consequently, to the passivity of citizens in the face of this risk. The public record shows, for example, that human casualties are an important factor in the search for responsibility and changes in risk management – e.g., the Xynthia storm in France (Lelaurain *et al.* 2021).

Conclusion

Coastlines are under the combined stress posed by dense human occupation and climate changes. Risks associated with sea level rise, coastal erosion and the increasing strength of storms impact the way of life and security of coastal communities. However comparable in their overall dynamics, local knowledge about coastal risks and how to mitigate them are highly *contextual*: they depend on past experiences with a risk, on national and regional policies for risk mitigation and on climate change adaptation.
This chapter endeavoured to analyse an array of concepts that can help to understand broad dimensions of how humans perceive coastal risks, prepare for them and trust authorities with their management. In this paper we reviewed contextual concepts that are specific to national or regional communities, their shared memories, and representations through the case of two French mediterranean communities.

While these concepts are varied in their nature and scope, we found that risk management cannot rely on scientific information of environmental systems alone. Populations are not convinced solely by scientific and technical information: they need shared experiences, memories, and real encounters to be able to apprehend, talk about and take action to protect their communities. The examples of how French society accepted the development of risk preparedness plans for heatwaves (Poumadère *et al.* 2005) or coastal risks (Lelaurain *et al.* 2021) only after catastrophes took human lives are a good reminder of how our societies can react on shared experiences, but less so when these catastrophes are scientifically predicted. Such experienced knowledge of risk indicates how and when communities are better equipped to act and be actor of more participative risk management strategies (Areia *et al.* 2023).

To be cited as:

R. Bertoldo. 2024. Psychosocial factors around coastal risk management. p 167- 177. In CIESM Monograph 52 [F. Briand, Ed.] Marine hazards, coastal vulnerability, risk (mis)perceptions – a Mediterranean perspective. CIESM Publisher, Paris, Monaco, 182 p.

References

Areia N.P., Tavares A.O. and P. J.M. Costa. 2023. Public perception and preferences for coastal risk management: Evidence from a convergent parallel mixed-methods study. *Science Total Environt.* 882: 163440.

Bertoldo R., Lelaurain S., Guignard S., and A. Schleyer-Lindenmann. 2021. From Risk to Legislative Innovation: the Trajectory of Marine Submersion through the French Media. *Environmental Communication*, https://doi.org/10.1080/17524032.2021.1954538

Bodas M., Peleg K., Stolero N. and B. Adini. 2022. Risk perception of natural and human-made disasters—cross sectional study in eight countries in Europe and beyond. *Frontiers in Public Health 10*: 1–9. https://doi.org/10.3389/fpubh.2022.825985

Bonaiuto M., Alves S., De Dominicis S. and I. Petruccelli. 2016. Place attachment and natural environmental risk: Research review and agenda. *Journal of Environmental Psychology 48*, 33–53. https://doi.org/10.1016/j.jenvp.2016.07.007

Breakwell G.M. 2014. *The Psychology of Risk*. Cambridge, UK: Cambridge University Press.

Burgess A. 2012. Media, risk, and absence of blame for "acts of God": Attenuation of the European volcanic ash cloud of 2010. *Risk Analysis 32*(10): 1693–1702. https://doi.org/10.1111/j.1539-6924.2012.01803.x

Demski C., Capstick S., Pidgeon N., Sposato R.G. and A. Spence. 2017. Experience of extreme weather affects climate change mitigation and adaptation responses. *Climatic Change* 149–164. https://doi.org/10.1007/s10584-016-1837-4

Doue C.M., Navarro O., Restrepo D., Krien N., Rommel D., Lemée C., Coquet M., Mercier D. and G. Fleury-Bahi. 2020. The social representations of climate change: comparison of two territories exposed to the coastal flooding risk. *International Journal of Climate Change Strategies and Management 12*(3): 389–406. https://doi.org/10.1108/IJCCSM-11-2019-0064

Durand P., Anselme B., Defossez S., Elineau S., Gherardi M., Goeldner-Gianella L., Longépée, E. and A. Nicolae-Lerma. 2018. Coastal flood risk: Improving operational response, a case study on the municipality of Leucate, Languedoc, France. *Geoenvironmental Disasters 1*: 5–19. https://doi.org/ https://doi.org/10.1186/s40677-018-0109-1

Engdahl, E. and R. Lidskog. 2014. Risk, communication and trust: Towards an emotional understanding of trust. *Public Understanding of Science 23*(6), 703–717. https://doi.org/10.1177/0963662512460953

Joffe H. 2003. Risk: From perception to social representation. *British Journal of Social Psychology 42:* 55–73. https://doi.org/10.1348/014466603763276126

Joffe H, Rossetto T., Solberg C., and C. O'Connor. 2013. Social Representations of Earthquakes: A Study of People Living in Three Highly Seismic Areas. *Earthquake Spectra 29*(2): 367–397. https://doi.org/10.1193/1.4000138

Jung K., Shavitt S., Viswanathan M. and J.M. Hilbe. 2014. Female hurricanes are deadlier than male hurricanes. *Proc. Nat. Acad. Sciences USA 111*(24): 8782–8787. https://doi.org/10.1073/pnas.1402786111

Kasperson R.E., Renn O., Slovic P., Brown H.S., Emel J., Goble R., Kasperson, J.X. and S. Ratick. 1988. The Social Amplification of Risk: A Conceptual Framework. *Risk Analysis 8*(2): 177–187. https://doi.org/10.1111/j.1539-6924.1988.tb01168.x

Krien N. and E. Michel-Guillou. 2014. Place des risques côtiers dans les représentations sociales du cadre de vie d'habitants de communes littorales. *Les Cahiers Internationaux de Psychologie Sociale 101*(101–122).

Lelaurain S., Guignard S., Schleyer-Lindenmann A. and R. Bertoldo. 2021. From Risk to Legislative Innovation: the Trajectory of Marine Submersion through the French Media. *Environmental Communication,* https://doi.org/10.1080/17524032.2021.1954538

Lemée C., Fleury-Bahi G., Krien N., Deledalle A., Mercier D., Coquet M., Rommel D. and O. Navarro. 2018. Factorial structure of the coastal flooding risk perception and validation of a French coastal flooding risk evaluation scale (CFRES) for non-experts. *Ocean and Coastal Management 155*: 68–75. https://doi.org/10.1016/j.ocecoaman.2018.01.030

Lima M.L. 2004. On the influence of risk perception on mental health: Living near an incinerator. *Journal of Environmental Psychology 24*(1): 71–84. https://doi.org/10.1016/S0272-4944(03)00026-4

Lima M.L., Barnett J. and J. Vala. 2005. Risk perception and technological development at a societal level. *Risk Analysis 25*(5): 1229-1239. https://doi.org/10.1111/j.1539-6924.2005.00664.x

Luís S., Pinho L., Lima M.L., Roseta-Palma C., Pinho L., Martins F. C. and A.Betâmio de Almeida. 2016. Is it all about awareness? The normalization of coastal risk. *Journal of Risk Research 19*(6): 810–826. https://doi.org/10.1080/13669877.2015.1042507

Meur-Ferec C. and E. Guillou. 2020. Interest of Social Representations Theory to grasp coastal vulnerability and to enhance coastal risk management. *PsyEcology 11*(1): 78–89. https://doi.org/10.1080/21711976.2019.1644003

Michel-Guillou E., Lalanne P.-A. and N. Krien. 2015. Hommes et aléas : appréhension des risques côtiers par des usagers et des gestionnaires de communes littorales. *Pratiques Psychologiques 21*(1): 35–53. https://doi.org/10.1016/j.prps.2014.12.001

Michel-Guillou E., Krien N. and C. Meur-Ferec. 2016. Inhabitants of coastal municipalities facing coastal risks: Understanding the desire to stay. *Papers on Social Representations 25*(1): 8.1-8.21.

Michel-Guillou E. and C. Meur-Ferec. 2017. Representations of coastal risk (erosion and marine flooding) among inhabitants of at-risk municipalities. *Journal of Risk Research 20*(6): 776–799. https://doi.org/10.1080/13669877.2015.1119181

Moscovici S. 1961 /1976. *La psychanalyse, son image et son public*. Presses Univers. de France, Paris.

Moscovici S. 2001. Why a theory of social representations? pp. 8-35 In *Representations of the Social* [K. Deaux & G. Philogène, Eds.]. Blackwell, Oxford.

Pidgeon N., Kasperson R.E. and P. Slovic. 2003. *The Social Amplification of Risk*. Cambridge University Press, Cambridge.

Poumadère M., Mays C., Le Mer S. and R. Blong. 2005. The 2003 heat wave in France: Dangerous climate change here and now. *Risk Analysis 25*(6): 1483–1494. https://doi.org/10.1111/j.1539-6924.2005.00694.x

Poumadère M., Mays C., Pfeifle G. and A.T. Vafeidis. 2008. Worst case scenario as stakeholder decision support: a 5- to 6-m sea level rise in the Rhone delta, France. *Climatic Change 91*(1–2): 123–143. https://doi.org/10.1007/s10584-008-9446-5

Poumadère M., Bertoldo R., Idier D., Mallet C., Oliveros C. and M. Robin. 2015. Coastal vulnerabilities under the deliberation of stakeholders: The case of two French sandy beaches. *Ocean and Coastal Management 105*. https://doi.org/10.1016/j.ocecoaman.2014.12.024

Renn O. 2008. *Risk governance: Coping with uncertainty in a complex world*. Earthscan, London.

Rosa E. 2003. The logical structure of the social amplification of risk framework (SARF): Metatheoretical foundations and policy implications. pp. 47- 79 In *The Social Amplification of Risk* [N. Pidgeon, R.E. Kasperson, P. Slovic, Eds.]. Cambridge University Press, Cambridge.

Rousseau D.M., Sitkin S. B., Burt R. S. and C. Camerer. 1998. Not so different after all: A. Perception of risk. *Science1 236*(4799): 280–285. https://doi.org/10.1126/science.3563507

Slovic P. 1987. Perception of risk. *Science 236*(4799): 280–285. https://doi.org/10.1126/science.3563507

Slovic P. 2000. *The Perception of Risk*. Routledge, London.

Tol R.S.J., Bohn M., Downing T. E., Guillerminet M., Hizsnyik E., Kasperson R., Lonsdale K., Mays C., Nicholls R. J., Olsthoorn A., Pfeifle G., Poumadere M., Toth F. L., Vafeidis A.T., van der Werff P.E. and I.H. Yetkiner. 2006. Adaptation to Five Metres of Sea Level Rise. *Journal of Risk Research 9*(5): 467–482. https://doi.org/10.1080/13669870600717632

Wagner W., Duveen G., Themel M. and J. Verma. 1999. The Modernization of Tradition: Thinking about madness in Patna, India. *Culture & Psychology 5*(4): 413–445. https://doi.org/10.1177/1354067X9954003

Wagner W. and N. Hayes. 2005. *Everyday discourse and common sense: The theory of social representations*. Palgrave-Macmillan, Basingstoke.

Woodyatt A. 2021, November 21. *British people are more concerned than ever about climate, ahead of Covid and Brexit, poll shows*. CNN. https://edition.cnn.com/2021/11/23/uk/climate-uk-concern-poll-ipsos-mori-gbr-intl/index.html

Wynne, B. 1992. Risk and social learning: Reification to engagement. In *Social Theories of Risk*. [Krimsky S. and D. Golding, eds.]. Praeger, Westport, CT, USA.

LIST OF PARTICIPANTS

Maria-Ana Baptista
IPMA
Lisbon, Portugal
mavbaptista@gmail.com

Raquel Bertoldo
Univ. Aix-Marseille
France
raquel.bohn-bertoldo@univ-amu.fr

Frédéric Briand
CIESM Headquarters
fbriand@ciesm.org

Helmut Brückner
Univ. Köln,
Germany
h.brueckner@uni-koeln.de

Francesco Chiocci
Univ. La Sapienza,
Italy
francesco.chiocci@uniroma1.it

Laura Giuliano
CIESM Headquarters
lgiuliano@ciesm.org

Hakan Kuslaroglu
Director Turkish Hydro & Oceano
Istanbul
director@shodb.gov.tr

Iva Međugorac
Univ. Zagreb
Croatia
ivamed.geof@pmf.hr

Nadia Mhammdi
Univ. Mohamed V,
Rabat, Morocco
nmhammdif@yahoo.com

Rania Mohamed
Univ. Alexandria
Alexandria, Egypt
rania_mohamed@alexu.edu.eg

Isavela Monioudi
Univ. Aegean,
Greece
imonioudi@marine.aegean.gr

Sinan Özeren
Istanbul Tech. Univ.,
Turkey
ozerens@itu.edu.tr

Luis Pinheiro
Chair, CIESM Commitee on Marine Geophysics
Univ. Aveiro,
Portugal
lmp@ua.pt

Kaveh Rassoulzadegan
CIESM Headquarters
kvr@ciesm.org

Roger Urgeles
ICM,
Barcelona, Spain
urgeles@icm.csic.es

Printed by

IMPRIM'VERT®

MULTIPRINT
MONACO

FOURNISSEUR BREVETÉ DE S.A.S. LE PRINCE DE MONACO